REFERENCE ONLY

UNIVERSITY OF LONDON THESIS

Degree PhD Year 2005 Name of Author BOUCHER C.P

COPYRIGHT

This is a thesis accepted for a Higher Degree of the University of London. It is an unpublished typescript and the copyright is held by the author. All persons consulting the thesis must read and abide by the Copyright Declaration below.

COPYRIGHT DECLARATION

I recognise that the copyright of the above-described thesis rests with the author and that no quotation from it or information derived from it may be published without the prior written consent of the author.

LOAN

Theses may not be lent to individuals, but the University Library may lend a copy to approved libraries within the United Kingdom, for consultation solely on the premises of those libraries. Application should be made to: The Theses Section, University of London Library, Senate House, Malet Street, London WC1E 7HU.

REPRODUCTION

University of London theses may not be reproduced without explicit written permission from the University of London Library. Enquiries should be addressed to the Theses Section of the Library. Regulations concerning reproduction vary according to the date of acceptance of the thesis and are listed below as guidelines.

A. Before 1962. Permission granted only upon the prior written consent of the author. (The University Library will provide addresses where possible).

B. 1962 - 1974. In many cases the author has agreed to permit copying upon completion of a Copyright Declaration.

C. 1975 - 1988. Most theses may be copied upon completion of a Copyright Declaration.

D. 1989 onwards. Most theses may be copied.

This thesis comes within category D.

☑ This copy has been deposited in the Library of UCL.

☐ This copy has been deposited in the University of London Library, Senate House, Malet Street, London WC1E 7HU.

Development of an automated ~~procedure for the selection and design under uncertainty of chemical reactors in the~~ REACTOR SELECTION AND DESIGN PROCEDURE IN THE pharmaceutical industry

Cyrille P. Bouché

February 14, 2005

ProQuest LLC
789 East Eisenhower Parkway
P.O. Box 1346
Ann Arbor, MI 48106-1346

ABSTRACT

The drug market has become very competitive with the development of existing companies and the emergence of new companies. The emergence on the market of so-called generic drugs makes the speed of development of new drugs a prime target. The pharmaceutical industry has until now focused on speeding-up drug development by focusing on the chemistry aspects with very little attention given to potential engineering solutions.

When looking at the engineering side of the pharmaceutical industry, and more particularly to the design side of equipment like chemical reactors, the pharmaceutical industry has restricted itself to using stirred tank reactors to analyse, develop and produce products. This type of reactor is perceived as flexible and easy to operate for batch operations. Chemical engineering research has opened up the route for new potential reactor designs, which can offer effective solutions to the problems of reaction scale-up.

This work aims to develop an automated comparison of different types of chemical reactors in accordance with their ability to scale-up bulk pharmaceutical products. It looks at the engineering side of drug scale-up in order to provide a reliable and fast evaluation procedure for the selection of a reactor which facilitates reaction scale-up. In this piece of research, indicators of success in the scale-up and assessment of quality of process design is centred around yields (or selectivity), capital expenditures and costs and regulatory compliance.

Due to the complexity of the reactions i.e. the number of components or the number of steps involved in the synthesis of a compound, side reactions occur undermining the production of a targeted compound. This problem can be solved in some cases by changing the chemistry of the synthesis of the product. This procedure tends to be very time consuming as each possible route has to be first developed at bench scale. Then each promising route is scaled-up over increasing sizes of stirred tank reactor. The different engineering factors involved within the reaction are commonly neglected, so is the possibility of using different types of reactor. In this study, the level of selectivity achieved, i.e. how much product is generated for the amount of reactant used, is simulated by mathematical models. Selectivity is then used to evaluate profit generated or cost (capital or running) endorsed and reflect on the efficiency of the process design. Regulatory compliance is also looked at through the impact that parameter uncertainty can have on the process design.

The influence of mixing on product selectivity is shown in this work as being critical. A comparison of the mixing efficiency of various types of reactors is studied through the influence of mixing on selectivity. Mass transfer is also of prime importance in organic synthesis with the emergence of catalysts. This aspect has also been given particular attention in this work, and various types of reactor have been evaluated against their potential to scale-up a mass transfer sensitive reaction.

The comparison of the different types of chemical reactor is carried out through the use of an optimisation procedure. The optimisation is done over the different variables which represent inherent characteristics of each reactor type e.g. energy dissipation rate, mass transfer achievable in a reactor. Uncertainty analysis is also used through the Fourier Amplitude Sensitiv-

ity Test (FAST), a global sensitivity analysis method, to evaluate the impact that parameter uncertainty or parameter tolerance has on the process design. The FAST method is a global sensitivity analysis method which offers the advantage that a limited number of sampling points are necessary to evaluate the parameter sensitivity analysis of a model. The selection is then based on a multi-objective optimisation procedures. This allows us to trade-off uncertainty and annualised costs. The advantages of this methodology are the speed of evaluation, the ease of use as well as the versatility and generic aspect. It permits to evaluate the impact that parameter uncertainty has on each type of reactor as well as the identify the equipment which generate the best profit.

The mathematical model is able to incorporate dynamic behaviour without having to resort to the level of detail required for computational fluid dynamics (CFD) and have been implemented in gPROMS.

Acknowledgments

Among the people who, throughout the last four years, have contributed to the creation of this work, I would particularly like to thank my supervisor, Professor Eric Fraga, for his constant guidance and intellectual input as well as for his support and help during difficult periods.

I would like to thank also Dr Georges Manos for his explanation, thoughtfulness and advice during the completion of this thesis.

The work described in this thesis was supported by the Engineering and Physical Science Research Council (EPSRC) as well as by the Centre for Process Systems Engineering (CPSE) and I would like to thank them both for their financial support.

Several people have helped considerably with the nuts and bolts of the project. I would like to thank Dr Graham Caygill for his support and for his ability to communicate his knowledge and enjoyment of science and engineering. I would also like to thank Dr Asterios Gavriilidis and Dr Monica Zanfir for their much appreciated guidance and advice as well as for their industrial connections.

I must, of course, thank all my friends and colleagues in the Chemical Engineering Department and especially the people of the CAPE Room.

Finally, I would like to thank my family and friends for putting up with me through what has been a very challenging period of my life, with a special thought for Austen, without whose encouragement this work would not have been finished. I particularly wish to thank my wife, Jessica, for her support throughout the writing of my thesis.

CONTENTS

1. SCALE-UP IN THE PHARMACEUTICAL INDUSTRY

1.1 Introduction

Predictable scale-up in the pharmaceutical industry is a challenge. The current methodology adopted is time and resource consuming. A chemical reaction is studied considering only one type of reactor, typically a stirred tank. In practice, the scale-up methodology is to study a chemical reaction over a range of reactor sizes so as to predict the behaviour of the reaction at plant scale. This ad hoc procedure is the result of a lack of suitable scale-up models.

In the industry numerous difficulties, which can lead to the early termination of promising projects, are encountered during the scale-up of particular reaction systems. For instance, side reactions often undermine the production of targeted compounds and reduce the selectivity of the reaction system. This impacts on the profitability of the project and ruin the projects economic viability. In the following the pharmaceutical industry development method is look at and analysed. The pharmaceutical industry process development requirements, demands, and hurdles are identified and explained. The traditional approach to overcoming difficulties during scale-up is to change the chemistry of the system and to find a new route for the organic synthesis of the compound.

In this study a different approach is considered. The equipment used for

the scale-up of a chemical reaction i.e. the chemical reactor is considered as a fundamental element to the scale-up of a chemical reaction. It is considered that different types of chemical reactor are better suited to some reaction systems than others [87]. Also we will be looking at comparing the impact that different types of reactor have on the scale-up of a typical reaction system. The aim of the project is to obtain an automated selection procedure which will consider and gauge the different factors impacting the scale-up of a reaction system at the equipment level and will guide the engineer in determining the equipment most suited to the scale-up of a particular reaction system.

1.2 Cost and development time of new medicines

It has been established that the time for the development of a new drug from the moment a patent is filed to the approval for releasing to the market by the U.S. Food and Drug Administration (FDA) or its European counterpart the European Medicine Evaluation Agency is on average 12 years [61]. A new drug remains protected by a patent for 20 years with a possibility for extension of certain pharmaceutical patents for up to a further 5 years (cf. EU Regulation 1768/92). This means that a pharmaceutical company has, if looking at an optimistic situation, around 13 years to recover the cost of the development of the new medicines. The development cost for a medicine has been evaluated at around £350m [30], a list of R&D cost for different pharmaceutical companies is also listed in table 1.1.

Biotech top 10 : Celltech, British Biotech, Oxford Glycosciences, Powderject Pharmaceuticals, Vernalis, Cambridge Antibody Technology, Cantab Pharmaceuticals (now part of Xenova), Acambis, CeNeS Pharmaceuticals, Xenova, Antisoma

Key : UK = spend in UK; g = global R&D spend (Data from Department of Trade &

Tab. 1.1: 2000/2001 R&D expenditure of selected biotechnology and pharmaceutical companies with a significant R&D presence in the UK [30]

Companies	2000/01 R&D spend
	(£millions)
GlaxoSmithKline	2,526 $^{(g)}$
AstraZeneca	1,936.7$^{(g)}$
Pfizer	373.2$^{(UK)}$
Roche	92.0$^{(UK)}$
Eli Lilly	77.9$^{(UK)}$
Aventis	57.8$^{(UK)}$
Shire	47.5$^{(g)}$
Novartis	40.4$^{(UK)}$
Bristol-Meyers Squibb	37.8$^{(UK)}$
Johnson & Johnson	9.8$^{(UK)}$
Biotech sector (top 10)	221.7$^{(UK)}$
GRAND TOTAL	5,196.1$^{(g)}$

Industry (DTI) *'Research and Development Scoreboard'*)

In order to recover these costs and develop profits the pharmaceutical industry has reduced time to market. As it is shown in figure 1.1, some stages can be reduced, for example the chemistry and process development stages. If combinatorial chemistry has helped in the number of new medicines developed in the last 20 years [172], this new technology has not helped in reducing the development time of drugs, as figure 1.2 shows.

Also the process development of new medicines can been identified as carrying potential for reducing time to market, as various studies of performance suggest that a significant portion (as much as 80%) of manufacturing process quality is rooted in the product and process design phase [36, 208, 197], particularly when considering the issue link to 'Scale-up' i.e. developing a drug from the tube test size to the production plant size. We define these issues in section 1.6.

1.3 Structure and methodology of the development of a drug

The traditional pathway of pharmaceutical drug development is shown in figure 1.3 [147].

Graph 1.4 summarises the different steps involved in the development of a pharmaceutical drug [147]:

The development of generic drugs as shortened the return on investment period for pharmaceutical companies, forcing these companies to reduce the time-to-market in order to carry on sustaining their income. Process development within the pharmaceutical industry as been identified as a potential strong element in achieving this reduction of the time to market for new pharmaceutical drugs [147]:

Data have shown that greater emphasis on early problem solving through

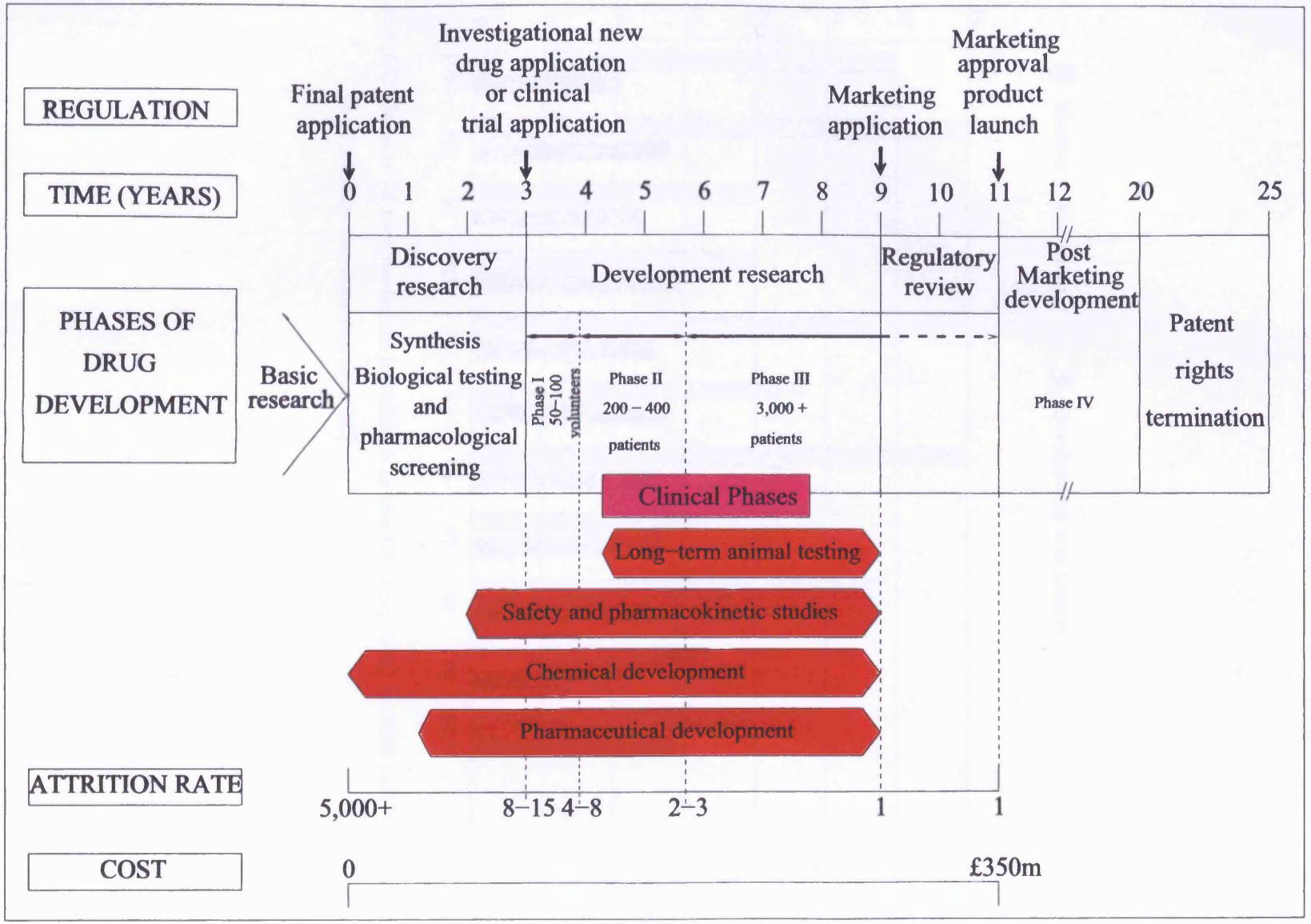

Fig. 1.1: Stages in the discovery and development of a new medicine [30]

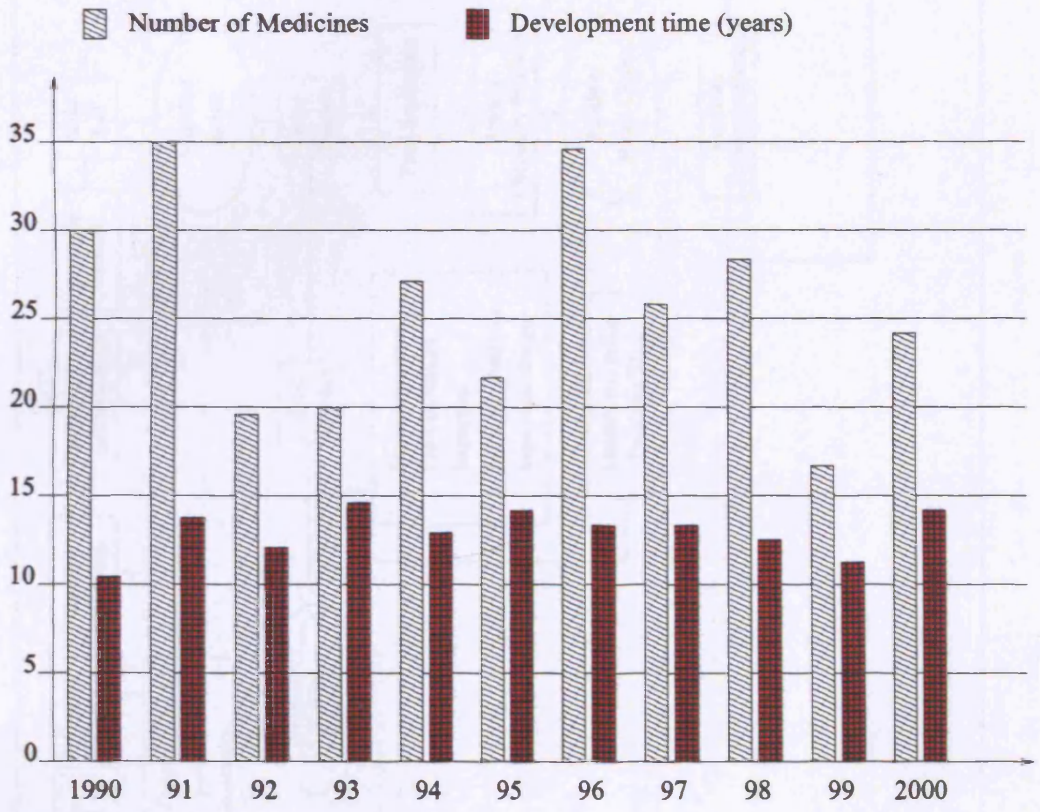

Fig. 1.2: Number of new medicines introduced in the UK from 1990 to 2000 and their average development time [30]

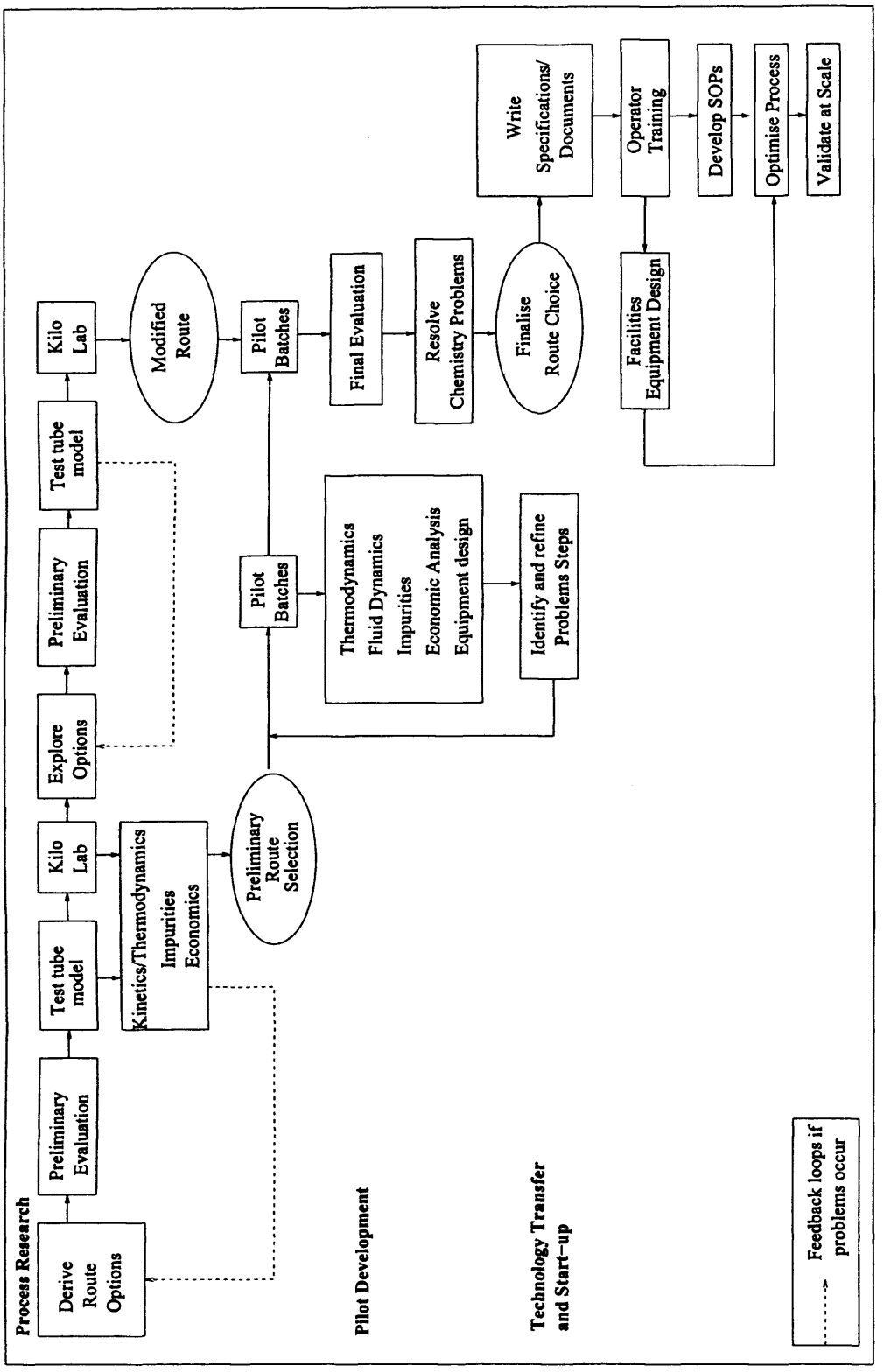

Fig. 1.3: The process R&D cycle for a chemically synthesised drug

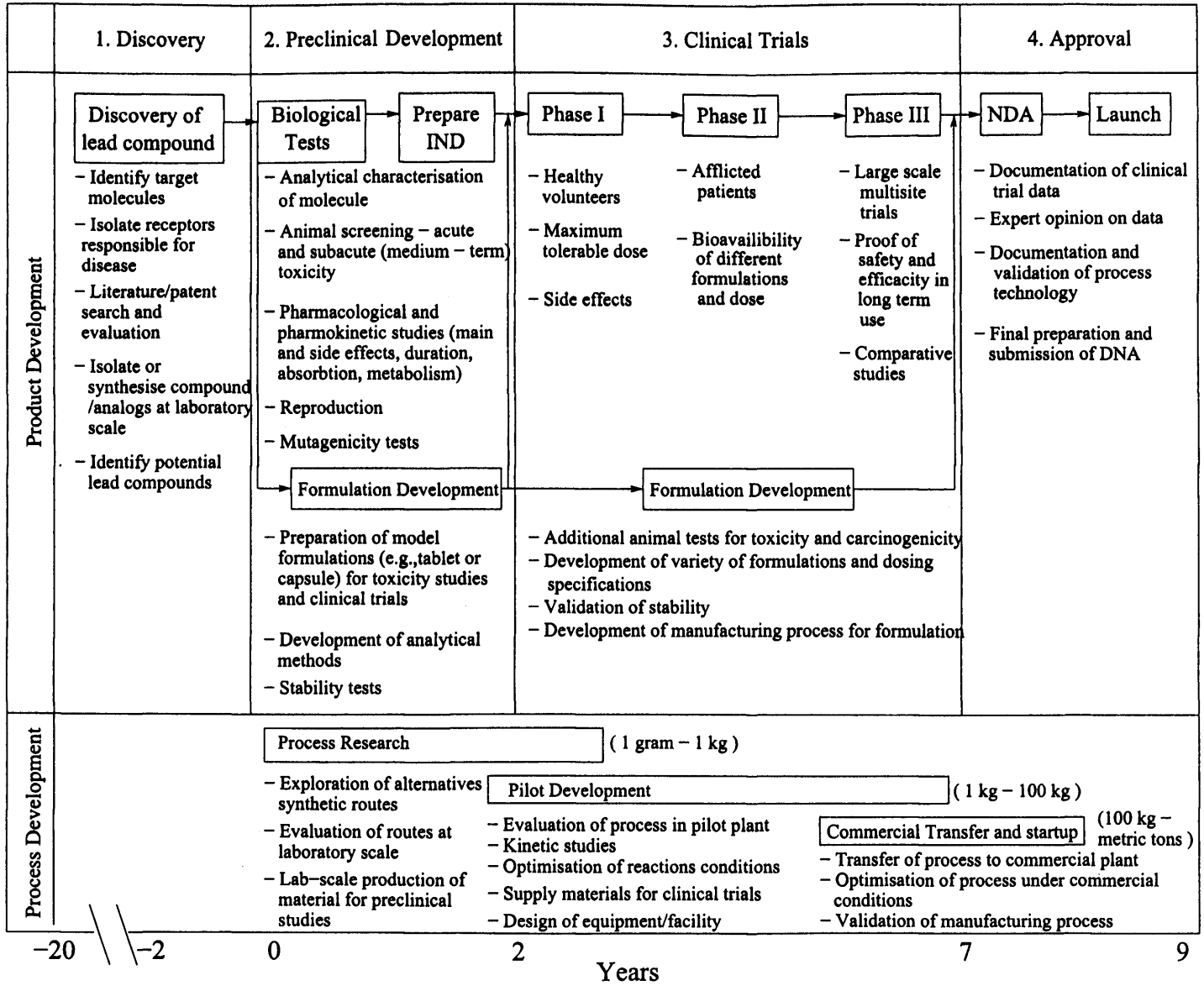

Fig. 1.4: Time line for discovery and development of a new chemical entity

	Driving Forces		
	Growing Technological Parrity	Product Complexity	Shorter Product Life Cycles
Competitive Implications	Difficult to sustain advantage on product functionality or performance alone	Costly/Uncertain development	Rapid obsolescence of physical and intellectual capita
Source of Advantage	First to market; rapid market penetration; barrier to imitation/entry	Sophisticated technical problem–solving capability to push the envelope of both product and process technology	Short development lead time; rapid market penetration; lower fixed development and manufacturing cost
Potential Strategic Contibution of Process Development Capabilities	Rapid process development increases time to market; fast manufacturing ramp–up supports market penetration; process technology enhances customer acceptance; proprietary process technology used as barrier to imitation	Rapid process development reduces risk and complexity of development by allowing later start; Strong problem–solving capabilities provide technical degrees of freedom for product design	Rapid process development facilitates quick time to market; rapid manufacturing ramp–up supports market penetration; Efficient process development increases returns to R&D; Development of processes that econo––mise on capita expenditure increase return on net assets

Fig. 1.5: Process Development Capabilities : Driving Forces and Competitive Implications

intense process research - that is, doing it right the first time - helps reduce overall development lead time [147]. Lead time, is of course an important indicator of quality in the development process; failure to identify design problems early on leads to rework, which can in turn extend project time lines and consume resources. The ability for efficient and rapid process development is increasingly important in shaping pharmaceutical companies competitive advantages.

However, lead-time and efficiency are not the only critical dimensions of development performance. The output of the development process - in this case, the manufacturing process itself - must also be of high quality. It will do a firm little good to be fast and efficient at developing complex, costly process technologies that are difficult to implement. Thus the challenge facing most companies is to create a development process that is fast, efficient, and capable of generating high quality process designs [147]. Quality, of course, is a multidimensional concept, taking on different meanings in different context. In the pharmaceutical industry, a high quality process design can be measured by such indicators as yields, capital expenditures, costs, batch-to-batch consistency and regulatory compliance [147]. Batch-to-batch consistency will not be considered in this work due to the lack of data and as it is more a constituent of the production of the drug rather than a part of the development work see 1.6 [160].

The goal of process development is to find the process parameters (the sequence, timing, and specification of process steps; equipment design and settings; and materials handling procedures) that either optimise performance or achieve a satisfactory target level when operated under actual production conditions [147].

In a competitive environment, development goals should include finding

this process as quickly and efficiently as possible [6]. Process development is a technical problem-solving process, and problem-solving is triggered by gaps between desired and actual performance. In the context of process development, this gap can be framed in terms of differences between what existing process technology can achieve (for instance, yields and costs) and what is required to achieve success in the market [91, 184].

The other characteristic of problem solving is that it generally takes place through iterative cycles of search and selection [133]. Over a number of cycles, the gap between actual and desired performance becomes progressively narrower, as technical solutions are identified and tested and a subset of solutions is selected. At the heart of this learning process are experiments (both physical and conceptual) that provide feedback about gaps between current and target performance levels [146]. The quality of this feedback plays a critical role in determining development performance. Experiments can take many forms and be conducted under a variety of conditions. Although the traditional image of an experiment, particularly in the pharmaceutical industry, is a laboratory-based analysis of product samples or physical prototypes, advances in technology mean that some product and process designs can be run, tested, and analysed using computer-aided simulation, as it has been the case in the pharmaceutical industry with the very rapid expansion in the last few years of combinatorial chemistry and the emergence of numerous chemistry/molecular simulation software and have allowed to reduce research time in product development [192].The availability of software in process development targeted to the pharmaceutical industry is still limited [147], to the difference of other industry e.g., Petrochemical industry where process simulation and optimisation tools have a track record of success e.g., [83].

Because experimental conditions affect experimental outcomes, estimates of process performance achieved under laboratory conditions are not always representative of a full-scale run in an actual factory [6]. Very often, the technology developed and tested in the laboratory is replicated nearly perfectly in the plant the problem is that specific elements of the plant environment (such as equipment configurations) can cause a deterioration in process performance [147]. Also the issue of scale-up in the pharmaceutical industry can be analysed not as a technology transfer but as a technology development matter. Also the idea of learning before doing rather than learning by doing through computer modeling and simulation can bring a solution to process development issues and more particularly scale-up difficulties faced in the development of a new drug [146].

1.4 Consistency, robustness and regulatory compliance

Delays in new product introductions and the market value of the firm have been proven to have very drastic consequences in the well being of a pharmaceutical companies [86]. The main cause of delays in the production of most pharmaceutical and medical products is the results of problems in getting approvals from government regulatory agencies such as the Food and Drug Administration (FDA) [86]. In another way the U.S. FDA and its European counterpart the European Medicine Evaluation Agency (EMEA) have the power to stop the sale of any pharmaceutical drug if it considers it unsafe, unreliable or defective. A very important stage in the development of a drug manufacturing process is the so-called process validation in which a report is issued showing that the process meets the FDA inspection guideline [92]. The FDA's guidelines on process validation define process validation as "*establishing documented evidence that provides a high degree of assurance that a*

specific process will consistently produce a product meeting its predetermined specification and quality attributes [70]". Nevertheless *documenting* that a process "*consistently*" meets "*specifications*" is exactly what process validation is not, because using quality controls to prove reproducibility is exactly what the FDA does not consider sufficient (according to FDA speakers at meetings with the industry)[160]. Instead one must build in quality and assurance of reproducibility up front, i.e., with process development [160]. During process optimisation, the process chemist would typically vary the reaction temperature, the process chemist would typically vary the reaction temperature in several experiments and look at the resulting stereoselectivity [6]. Process validation, on the other hand, is the opposite activity [160]. Process optimisation, by the narrow definition, means finding the values for which the process runs at its optimum conditions. Process validation is taking the process apart and stressing the process until its edges are found. The two activities are thus opposing, but good process development would contain both process validation and process optimisation, as such information is valuable to the plants [160]. Process validation is thus defined as *finding the limits of process variables* and is only a part of process development. Process development consists of process optimisation plus process validation plus scale-ups plus proving reproducibility moving from the R&D side of process development to the production side of process development as summarised in scheme 1.6. All these nuances in drugs process development have to considered when developing process development tools for the pharmaceutical industry.

The FDA would like to see written evidence that the process is well understood and under control, because it believes that a well-developed process ensures a reproducible quality of the drug substance. The development re-

port is the backbone for this written evidence and is just a summary of the history of process development, both in the laboratories and in the plants. A typical development report for example contains the following sections [160]:

- Process scheme
- Comparison of development processes
- Comparison of development and production batches
- Comparison of production batches
- Explanation of each operation in the NDA (New Drug Application) process
- Development history
- Process validation

In the light of the list above, the use of a mathematical model based computer program to help on the selection of equipment becomes more apparent and fundamental. In particular, when considering: comparison of

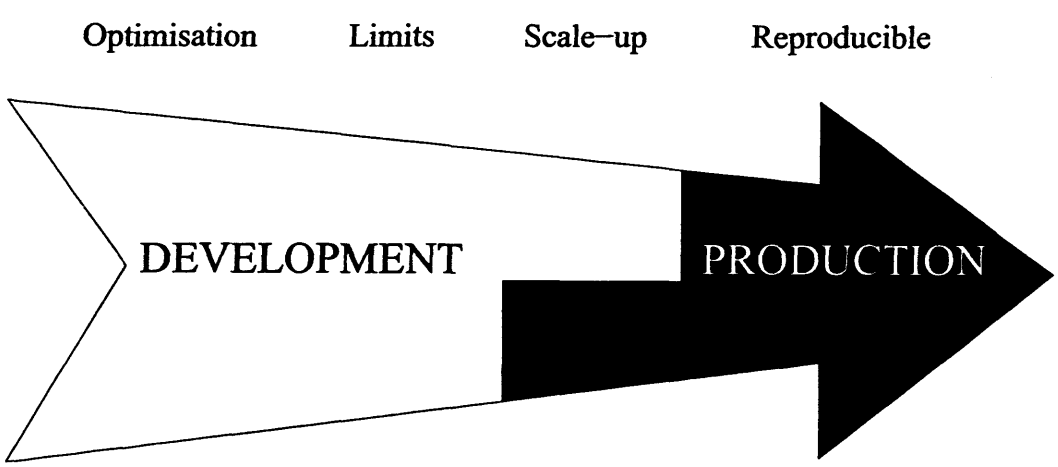

Fig. 1.6: Component of process development

development processes; comparison of development and production batches; explanation of each operation in the NDA (New Drug Application) processes, development history and process validation; as the program will allow testing of the equipment selection through simulation and help in refining backing reports and justifying choices.

1.5 Product development, new technology and uncertainty

The product development of a drug is a matter which is nowadays followed very closely by investors. For instance delays in the launch of AstraZenecca's cholesterol-busting drug Crestor and cancer drug Iressa, have shown that the stock market reacts to delayed announcements and that the reaction is strongly negative. On average, delayed announcements decrease the market value of the firm by 5.25% [86]. Nevertheless time-to-market is a fundamental objective in the pharmaceutical industry [181].

Three reasons why speed and quality are two important factor in product development are given as follow [99]:

1. First, faster development tends to be associated with higher rates of employee learning and the construction of relevant competencies

2. Second, speed improves the accuracy of forecasting because firms are required to project environmental and technological forces into a shorter time period, thus making for a better customer fit.

3. Third, reduced time-to-market allows more advanced components to be incorporated and faster products can, thus, be perceived as more current (i.e., cutting edge) than competitor products. In the pharmaceutical industry, reducing time to market also means that the return-on-investment will be much larger given the fact that drugs are protected

by patents which are themselves fixed in time i.e. 20 years extendable to 25 years (cf. EU Regulation 1768/92)

Also, in order to achieve high quality products at a fast development pace, the level of uncertainty in the drug development process must be reduced to its bare minimum. Kessler et al. found that although speed is generally good, it is most functional under low uncertainty, and recommends that managers should pursue speed most vigorously when they have a 'clear target', that is, when the technology is known and markets can be forecast, therefore minimising uncertainty [99, 100].

A proven method for speeding up new product development and reducing its cost is the use of Computer Aided Design (CAD) software. CAD offers nowadays a variety of possibilities like modeling and simulation or analysis and data mining. CAD usages can reduce expenditure by limiting the man-hours required in early development stages as well as the time taken to communicate information from one stage to another [98]. CAD through computer simulation can also help to understand and learn about the process before doing [146], it can therefore help to reduce cost which should be attacked at its roots - the design stage, and that company should seek to do it right the first time instead of the costly making and correcting of mistakes [126].

Nevertheless CAD misused can also have a counter effect if CAD system direct activities towards automating well-known calculations and facilitating reuse of old designs; that is, they may be poorly suited for the creation of new designs and testing them [100]. These issues have been addressed in the reactor selection procedure developed in this work by :

1. taking account and giving measure of technical uncertainty which refers to difficulty in determining the precision, reliability and capacity of new

processes [74] - a different level of uncertainty in the reaction system studied generates different answers and therefore does not facilitate the reuse of old design

2. Based on case-by-case mathematical models that address the issue of one 'old'-model-fits-all

3. Fast in comparison of pilot plant experiences - allowing the study of the impact of the design at very early stages of project through the study of different scenarios

4. Generic and adaptable - allows the selection to have very low levels of maintenance and minimise the need of constant adjustment to match various cases

1.6 Definition of scale-up

Pharmaceutical Process Scale-up is defined as the procedure of transferring results of R&D obtained at laboratory scale to the pilot plant and finally to production scale [114]. It is also defined as the process of increasing the batch size [114]. The current practice in the pharmaceutical industry is to carry out a reaction at increasing volume levels, in order to define the best operation parameter(s) for its production at industrial level. Scale-up of a process is also viewed in the pharmaceutical industry as a procedure for applying the same process to different output volume [114]. A subtle difference between these two definitions exists, in the fact that batch size enlargement does not always translate into a size increase of the processing volume, as enlargement can be also be achieved through changing the processing form e.g. batch to continuous processing [136, 87]. The scale-up of a pharmaceutical drug has

been described as striking the right balance between different criteria such as economics of the process, quality of the product, environmental impact of the waste streams, safety of the reactor operation [191].

Table 1.2 summarises what scale-up involves from a quality and a quantity point of view within the pharmaceutical industry [147].

Tab. 1.2: Initial discovery versus full-scale commercial production

	Initial discovery process	Final commercial production process
Number of chemical steps	25	7
Equipment	Test tubes 1-liter flasks	$2,000 - 4,000$ gallon Stainless steel vessels
Batch size (output)	$\sim 1gram$	$100 - 200$ kg
Operators	PhD Chemists	Technicians; semiskilled plant workers
Purity	$1\% - 10\%$	99.9%
Cost per kilogram	$\sim \$20,000 - \$50,000/kg$	$\sim \$3,500/kg$
Criteria for process design	Biological activity of molecule ; patent issues	Cost; quality (purity); conformance to drug and environmental protection regulations; operability

Although scale-up is commonly viewed as a critical problem in chemical projects, there are no quantity or scale variables in chemistry. That is, simply scaling up does not by definition, change a process's chemistry. Scale can, however, have important second-order effects. Scale can influence such process parameters as pressure, temperature, and sheer forces; these may in turn

influence the performance of the process [147]. For example, at larger scale, heat may not be uniformly distributed throughout a reaction vessel. Thus the chemical reactions taking place within the vessel may vary: a reaction may fail to take place in those areas where the temperature has fallen below a predetermined threshold, thereby reducing yields or increasing the number of impurities caused by for example side reactions. All these aspects of the scale-up of drugs can be partially or even totally summarised in a mathematical model or models. These models can then allow us through computer simulation, to foresee the outcome for various mild or extreme changes in the process design.

1.7 Reactor selection: existing work

In the following, work done on chemical reactor selection procedure has been looked at in order to define the state-of-the-art procedure in the area and identify potential novel approaches to match the pharmaceutical industry demands, the hurdles and needs which have been identified in the previous chapter.

A few computerised reactor selection methodologies can be found in literature. This selection uses different programming methods or mathematical tools to carry out the evaluation of different types of reactors.

The synthesis approaches for reactor selection were first originated by Aris [10, 11] using dynamic programming. More recently, selection procedures of the heuristic-numeric type based on expert systems have been developed, e.g. READPERT [175], through the use of a consulting system that creates a dialogue between the engineer and the computer. The engineer provides the computer with data, which is treated by the latter via numeric calculation, included in advance. The program is set-up as a succession of modules

and the information treated from one module is thereafter fed to the following module through this step by step dialogue with the engineer. This type of selection is based on rule-based programming which is one of the most commonly used techniques for developing expert systems. This type of programming involves rules, which are used to represent heuristics, or 'rules of thumb', which specify a set of actions to be performed for a given situation. A rule is composed of an *if* portion and a *then* portion. The *if* portion of a rule is a series of patterns that specify the facts (or data) which cause the rule to be applicable. The process of matching facts to patterns is called pattern matching.

The expert system tool provides a mechanism, called the inference engine, which automatically matches facts against patterns and determines which rules are applicable. The *if* portion of a rule can actually be thought of as the *whenever* portion of a rule since pattern matching always occurs whenever changes are made to facts. The *then* portion of a rule is the set of actions to be executed when the rule is applicable. The actions of applicable rules are executed when the inference engine is instructed to begin execution. The inference engine selects a rule and then the actions of the selected rule are executed.

This may affect the list of applicable rules by adding or removing facts. The inference engine then selects another rule and executes its actions. This process continues until no applicable rules remain. A variant of this type of reactor selection can also be found in literature as knowledge-based systems [93]. In order to reduce the impact of the *if-then* type of rule mentioned above and try to obtain a less directed selection, decision making techniques were introduced within the reactor selection such as the Analytic Hierarchy Process [167, 82, 81].

In this case a branch-and-bound chart of decision hierarchy is created, by breaking down the decision problem into a hierarchy of inter-related elements. A pairwise comparison of the different decision elements is then carried out through the input data fed to the computer. A method using eigenvalue is used to estimate the relative weights of the decision elements from the weights which is attributed originally by the program user. The relative weights of the decision elements are then aggregated to arrive at a set of ratings for the decision alternatives. This methodology permits the normalisation of the different weights attributed to the different decision elements. Nevertheless, in the expert system the weights of the different decision elements are attributed by a biased external intervention. In order to reduce external intervention artificial neural networks have been used within an expert system to create the knowledge acquisition and storage of the expert system [43]. Feed-forward neural networks have the capability to learn heuristics from given examples. Also a neural network is trained to carry out a reactor selection expert system.

Other reactor selections focus on the optimisation of reactor networks where all the structural and operational alternatives of the process are combined in an integrated scheme. The early work used mathematical programming techniques to rich superstructures of reactor models. The first work was done by using an extended version of an axial dispersion model [1, 2], other work focused on using compartment mixing models [15, 134]. Optimisation techniques have been used to solve stagewise models in terms of super structure schemes [103, 104]. In a different approach the concept of attainable region has been developed to solve the problem from a geometrical point of view [76, 77], and it has also been integrated to mathematical programming [109]. Reactor networks have been used also to develop a new generation

of novel reactor types and designs for multiphase reaction systems[121, 122]. And it has been extended to the synthesis of reaction/separation systems [117] and has been used to target specific issues e.g. mixing [215]

Other automated reactor selections use pure mathematical tools and modeling. For example an automated reactor selection uses Sensitivity Analysis [96]. Rabitz et al. started using Sensitivity Analysis in chemical kinetics modeling [155] as a mathematical tool to quantify the importance and impact on the modeling endeavour of the parameters included in a mathematical model. Sensitivity Analysis (SA) is the study of how the variation in the output of a model (numerical or otherwise) can be apportioned, qualitatively or quantitatively, to different sources of variation, and of how the given model depends upon the information fed into it. A generic reactor model based on a reactor network model is generated complying performance index, which is generated through the help of a heuristic. A sensitivity analysis is carried out over the different parameters that define the reactor network. Each parameter being representative of an inherent characteristic of a type of reactor, the parameters which have the biggest impact on the model output towards the performance index are recorded and a type of reactor which matches the input parameter values can then be selected.

Another automated reactor design selection is based on mathematical expression of mixing [171]. This reactor selection is limited to the design selection of stirred tank reactors. The selection uses a mathematical model representing the influence of mixing on the selectivity, a selection of reactors attributes and operating conditions is carried out for liquid-phase agitated reactor. First the reactor performance are estimated in various operating regimes then the reactors attribute i.e. the feed addition time, number of feed ports, agitator speed, agitator type and reactor geometry, feed location

are defined. The reactor selection is completed by an automated selection of heat transfer equipment, which is based this time on an heuristic, if the reacting mixture requires it.

A literature research was done to acknowledge the different selection of chemical reactors existing. This has underline the limited amount of work produced on the field of reactor selection procedure. Furthermore only a couple of these reactor selection procedures have a focus on the scale up of chemical reactions. The different chemical reactor selection procedures presented above can be classified in two different types. One type uses heuristics and rules-of-thumb, this leads to simplistic automation of the type *if-then*. The other type based on reactor network configuration uses mathematical tools that create better comparison, as the evaluation of the different solutions is not restrictive and directed by heuristic rules. It is noticeable that no chemical reactor selection offers the advantage of using non-heuristic mathematical tools.

The automated chemical reactor selection which is proposed in this study is based on the optimisation of the parameters which define the design and the intrinsic characteristics of different types of reactor. This optimisation is articulated around a mathematical model that reflects the type of chemical reaction occurring. The selection of chemical reactor is therefore directly linked to the chemistry (nanoscale) of the reaction studied. Also the chemical reactor selection presented in this study, presents the advantage of using a mathematical optimisation tool to define the best feature for a industrial scale reactor to produce the chemical reaction studied.

1.8 Aim of the project

The aim of the project is to look at developing a computer tool that the engineer/chemist can use to help his/her work in the development of a new drug. The chemistry side of scale-up has been for many years the focus of drug development departments. Nowadays with an increasing demand from the market either for reduction of time to market due to the development of 'generic' drugs, or for the reduction of cost or again for better production quality, the process side of drug development is the focus for better selection and understanding of processes. The stirred tank reactor has ever been the main and almost only development and production process mean used by the pharmaceutical industry [87]. This is mainly due to its low cost and versatility. Many more reactor types are available for the production of pharmaceutical products e.g. loop reactor, Jet-loop reactor, plate reactor, tube reactor ... as well as the possibility to develop specific types of reactors which match reaction requirements and/or specific type of production mode e.g. continuous, semi-batch, batch [87]. Also, this project aims at developing a computerised automated selection of reactor for the scale-up of pharmaceutical products. The selection will have to address the pharmaceutical industry's needs of efficiency, safety and environmental concerns of this industry which can be summarised as such:

- Selection of the reactor(s) which offers the potential of rapid and safe scale-up of the chemical development process
- Estimation of loss/Benefit of implementing techniques or controls to minimise waste and maximise yield

The way this problem has been tackled is to create an automated reactor selection procedure to optimise scale-up of homogeneous reactions. The aim

is to compare over a common goal, the achievement of different types of reactors having themselves different possible designs. The problem becomes then to compare the best reactor design for each type of reactor and then compare each type of reactor against another over sets of targets i.e. yields (or selectivity), capital expenditures and costs. The selection procedure should not only be constrained to the design of the reactor, but also to the way the reactors operate e.g. continuous operation versus batch operation [89].

Another fundamental aspect in the development of drugs is that technical uncertainties must be totally handled. The production of drugs cannot accommodate any type of approximation as already mentioned in section 1.4 and 1.5. The FDA guidelines for process validation are as follow :*in assessing the suitability of a given piece of equipment, it is usually insufficient to rely solely upon the representations of the equipment supplier, or upon experience in producing some other product. Sound theoretical and practical engineering principles and considerations are a first step in the assessment [70].* Also a prime aspect of the development of a process in the pharmaceutical industry will be to determine and understand the limits of the process to variation e.g. temperature, pressure, reaction kinetics, ... [6]. The chemist/engineer needs to take account and give measure of technical uncertainty which refers to difficulty in determining the precision, reliability and capacity of new processes [74]. The need is then to compare a series of parameters, defining a reaction-reactor system, and evaluate the best suited to achieve an equal target and therefore reduce the uncertainty carried by the process.

One can say that this selection is based on a multi-objective optimisation procedure. Where on one side the cost aspect of the scale-up of a particular drug plays its traditional and fundamental role in the survival of the project i.e. is the project commercially viable ? But where the uncertainty aspect

of drug development is also taken into account as a fundamental aspect in the viability of the drug development project. Amongst advantages emerging from this methodology are the speed of evaluation and the possibility of identification of process and operating design at a very early stage of a project, which presents multi-advantages e.g. environmental advantages like waste minimisation [201]. The tackling of uncertainty and the evaluation of its impact on a drug development project, feeding back commercial and time information, presents a direct and useful information in drug development.

1.8.1 Computer aided reactor selection

In this part of the project we will be looking at the architecture of the chemical reactor selection procedure which is developed in this work.

Rational scale-up procedures have been developed over the years to increase the chance of success in the development of a drug e.g. figure 1.7 [194].

The novel scale-up procedure presented in this thesis is also based on the same type of rational procedure. As a novel feature the procedure is automated and includes the evaluation of the impact of parameter uncertainty, through the use of sensitivity analysis.
The reactor selection procedure is constituted by three different steps:

1. Mathematical Modeling
2. Sensitivity Analysis
3. Multi-Objective Optimisation

A mathematical model describes a system by means of variables. The values of the variables can be practically anything; real or integer numbers,

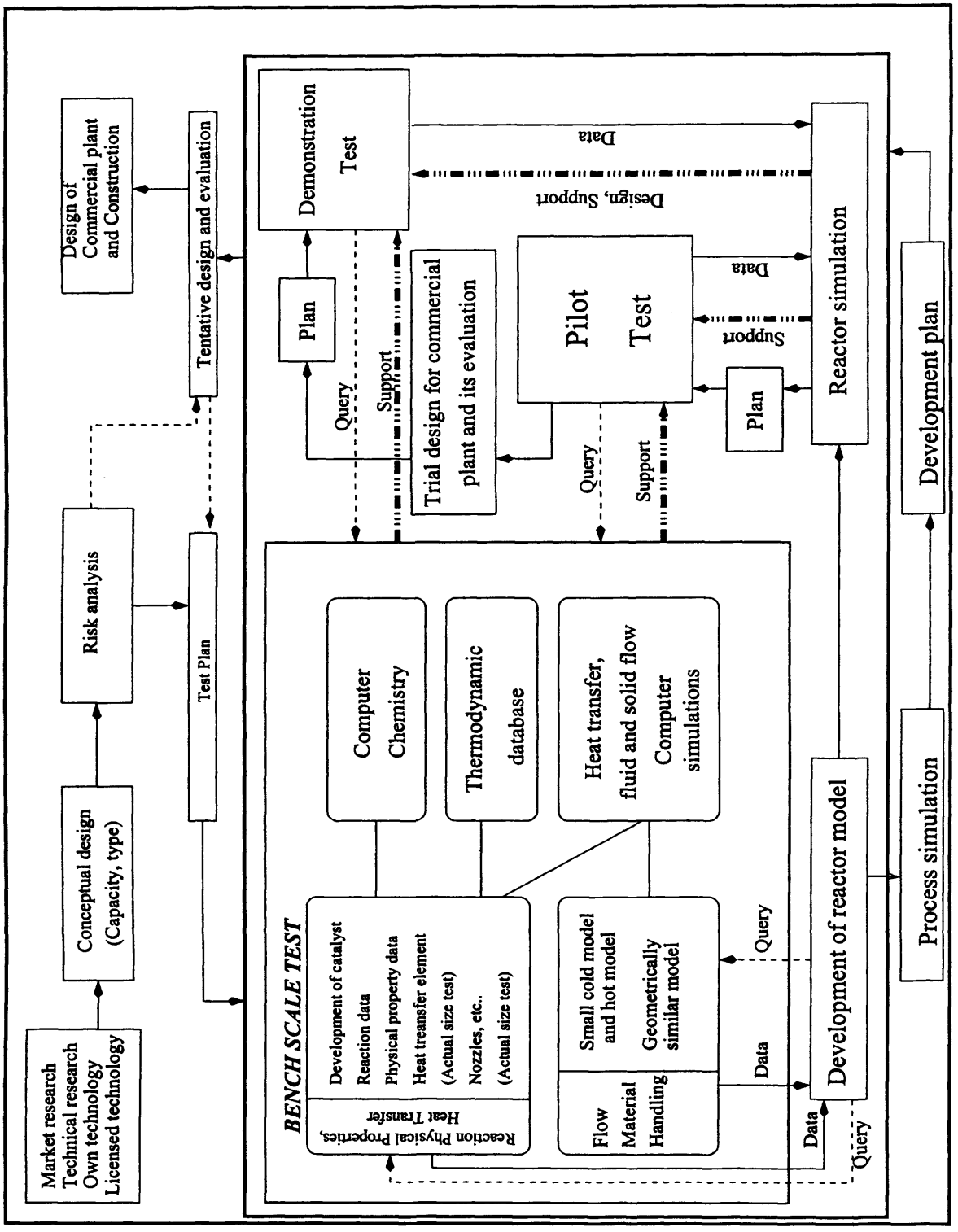

Fig. 1.7: Example of rational scale-up procedure [194]

boolean values or strings, for example. The variables represent some properties of the system, for example, measured system outputs often in the form of signals, timing data, counters, event occurrence (yes/no). Mathematical models have been used in this study to look at the difficulties that the scale-up of a chemical reaction can present. A mathematical model of a physical system is simplifying formal abstraction of reality through mathematical equations. In our case, these equations are Ordinary Differential Equations (ODE) and Algebraic equations, this type of system is called Differential Algebraic equation or DAE. When solved this system of equation returns a prediction y (y may be a vector) for any physically achievable values of the parameters k and constants c, and over any physically meaningful range of values of the design variables x see figure 1.8.

The actual model is the set of functions that describe the relations between the different variables. The simulation of models constitutes the first step of the selection procedure. The simulation allows the simulation of various phenomena developing during reaction occurrence and provides the evaluation of various indicators, as variables. The model provides output values for each variable (set of variables) values fed to it. These output values can then be compare and analyse and constitute the basic of the decision making process. The output values provided by the model are specific to a certain set of input variables values. These input variables values are used to determine the type of reactor and its design. This underlines the importance of the model and the choice of the input variables. The model has to describe the physical phenomena. The input variables have to relate to the design of the reactor and have to be selective enough with regard to the type of reactor.

The second stage of the selection procedure is constituted by a sensitivity

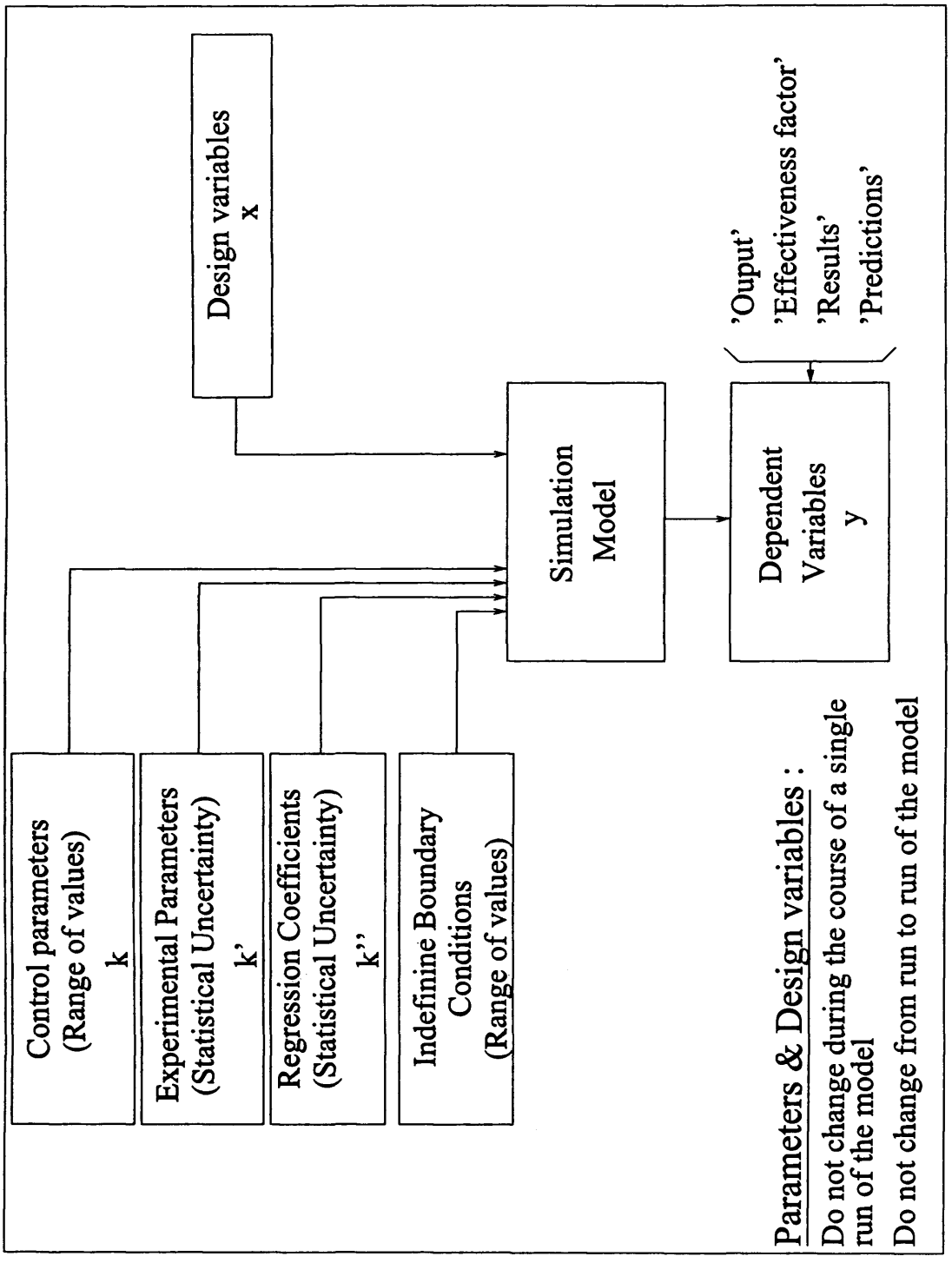

Fig. 1.8: Inputs and Outputs of the simulation model

analysis. The sensitivity analysis allows to evaluate each set of input variables the variance that the model output carries when the parameters of the mathematical model are varied within a range of values. A model typically is characterised or controlled by *parameters*. The parameters have unique values during the course of a single evaluation of the model, although it may be necessary to vary these values from one evaluation to the next. The need for such variation may rise from any of several possible sources, several of which are indicated in figure 1.8.

For example, a physical parameter certainly has a unique value, but this exact value may not be known because of limitation of information and only a range or distribution of values may be known. As another example, a parameter may be controllable in a particular physical circumstances only to within some range. This represents an expression of the uncertainty carried by the scale-up of one or another type of reactor. During scale-up, parameter values are distorted [6] and the sensitivity analysis reflects this distortion by varying parameters values within a range.

The fact that the parameter(s) can take on a range of values suggests that instead of considering the effect on the output functions of a particular value of the parameter(s) for a particular set of values for the design variables, the uncertainty of the model will be represented by measuring the influence of the parameter range of values for each set of values assigned to the design variables during the optimisation. Therefore at first a sensitivity analysis is carried out on a set of parameters then the second step is constituted by the optimisation of the set of design variables see figure 1.9

The Multi-objective optimisation constitutes therefore the third and last step of the computerised selection. It allows the comparison of different reactor types and designs. The objectives taken are to compare the reactors

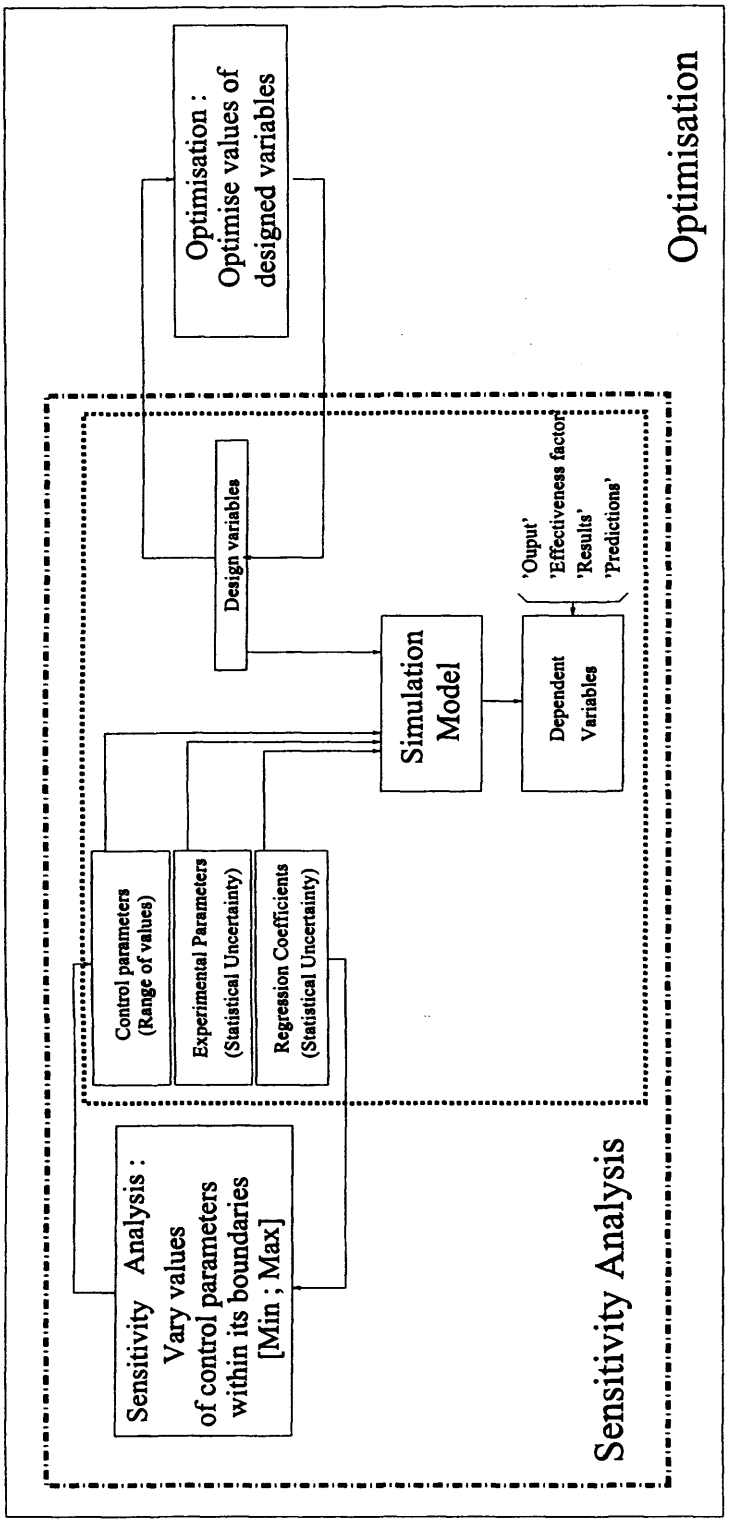

Fig. 1.9: Identification of optimal design variable values and measure of uncertainty

on the profit made per year and the level of uncertainty carried by a particular type of reactor and design. The purpose of the multi-objective optimisation is therefore to maximise profit and minimise the level of uncertainty by using various combinations for the values of the different parameters selected for optimisation.

Another advantage of this reactor selection is that it will be based on algorithms, as opposed to heuristics which contain general recommendations based on statistical evidence or theoretical reasoning. Algorithms are completely defined, finite sets of steps, operations or procedures that will produce a particular outcome.

1.9 Conclusion

In this chapter the structure type of the reactor selection procedure that is being developed has been presented. The automation and the inclusion of parameter uncertainty have been introduced as novelty factors. We then looked at the different elements i.e. catalyst design, mixing, heat transfer and multiple phase system which can undermine the scale-up of a reaction system. The focus in the scale-up of a targeted compound is the amount of product achieved. The emergence of by-products can counteract the production of the targeted compound. Side reactions occur frequently as a direct effect of the complexity of organic synthesis reactions undertaken in the production of a pharmaceutical compounds. The effect is further aggravated by the number of reactions necessary. The aim of the reaction scale-up is to eliminate or contain this problem to allow the project to remain economically viable.

A chemical reaction can also be visualised as the contact between different compounds. Mixing in the chemical industry is the operation that describes the way different compounds are put in contact with each other.

When studying pharmaceutical reactions it becomes apparent that mixing at molecular level also called micromixing was an influential factor on product distribution i.e. ratio targeted compounds produced over reactant reacted of the reaction system. Also a micromixing model was selected regarding the parameter used within the model. The purpose of the project is to compare different type of chemical reactors, also the mathematical model had to gather all the components defining a chemical reactor but also parameters which are intrinsic to each type of chemical reactor. This allows the comparison of one type to another.

2. MODELING

In this chapter the mathematical models that have been used in the development of the reactor selection are presented. These models are the core of the reactor selection. The models are used to provide values to the reactor selection. The values represent the physical behaviour of particular phenomena that develop when a reaction(s) occurs in the reactor 2.1.2. Two types of phenomena have been considered in this study, micromixing and mass transfer. A micromixing model and a mass transfer model are explained and implemented using the mathematical model solver/simulator gPROMS. The two models formulation are described as well the assumptions and limitations of use.

2.1 Factors influencing Scalability

The selectivity achieved is crucial to the feasibility of the scale-up of a reaction-reactor system. Due to the complexity of the reaction network e.g. number of components and very often also the number of reaction steps involved in the synthesis of a drug, side reactions occur undermining the production of the targeted compound. The custom in the pharmaceutical industry has been to study this factor by producing the product in reactor of increasing size, using a multiplying factor not greater than twenty from size to size. This procedure led to abandoning projects when the selectivity achieved at lab level was not matched in larger scale reactors [191].

Differences in scale cause differences in the performance of the same process. The amount of wall surface area per volume available to a process is much greater on small scale processes than on large scale ones. Wall and end effects are area based phenomena [189]. If a process is dependent on surface area, the additional surface area on scale-up is needed. For example, heat transfer is an area dependent process. The amount of volume per surface area is much greater on the large scale than on the small scale. Tank wall surface area becomes much less important. End and wall effects become much less important. Because of the large volumes involved and the limitations which volume impose on the process, some processes become impossible to accomplish on the larger scale. For example exothermic reactions with large heat release in large tanks cannot be easily accomplished on a large scale since the heat generated cannot be removed fast enough for safe operation. Phase changes and product degradation are also more likely to occur on larger scale.

In the case of a catalytic reaction, the effect of internal diffusion within a catalyst can have a very strong influence on a reaction selectivity. The internal diffusion within a catalyst particle influences the product made in the case of multiple reactions e.g. in the case : A $\longrightarrow$ B $\longrightarrow$ C reaction occurring through the use of a porous catalyst and B is the desired product. If the reaction is carried out with a catalyst which offers high diffusion resistance, and if the movement of B out of the solid is slowed by diffusional resistance, then B will accumulate inside the catalyst and the system will be driven towards C. Whereas if a catalyst with low diffusion resistance is used, a higher concentration of species B will be achieved. The selectivity in the case of irreversible reactions has been expressed [206]as function of a Thiele modulus for the three following reaction types as independent reactions, parallel reactions and consecutive reactions.

The scales of the process should be matched to scales of the equipment. An example of scale mismatch is where a fast chemical reaction occurs in a slow-mixing device. Mixing occurring around the feed point then controls the reaction rate. Potentially, since the chemical reaction is fast, production could be substantially increased if the mixing is improved.

2.1.1 Mixing

Mixing is one of the main factors impacting on the selectivity reached during the scale-up of a chemical reaction [142, 190, 161].The analysis of mixing can be also expressed by the level of power put in the system to make the reactants in contact with each other and induce a chemical reaction [190]. Power input is energy used over time. Sufficient power input is needed to obtain the desired process result. Better results are often obtained with an increase in power. For other processes, the results are worse. In those situations it is fundamental to determine the best power input. In comparing reactors, the parameter of power input times working volume can be an important quantity. Performances have been found to be a function of this quantity for an individual reactor and for the spectrum of reactor used by industry for a desired processing result [190].

Often enough, scale-up difficulties have been identified as due to insufficient mixing efficiency [189], especially in the case of stirred tank reactors (STR) [210], where it is often stated that matching the quality of mixing given at lab scale is generally impossible at plant scale [191], and also potentially at pilot scale [191]. It has been noticed that at commercial size, available agitators, in the case of batch and semi-batch stirred tank reactor, cannot deliver the power required to perfectly mix a reaction solution, enhancing the formation of by-products [210]. By-products are generally

generated where, in the case for example of fast reactions or viscous fluids, mixing is often slow relative to the reaction rate, desired reactions are slowed down and stopped before reaching completion, while undesirable reactions are enhanced and product selectivity is lowered [142]. In the case of fast competing reactions large Stirred Tank Reactors have been seen as poorly suited as their mixing times are described as being in the order of minute [64]. The product distribution is strongly dependent on mixing and requires that homogeneity be achieved rapidly, particularly in the case of viscous material it is understood that the key to success is matching the type of mixing with the reaction chemistry and physical properties of the constituents. Also a continuous process prevents afore mentioned difficulties linked to start-up and prompts the reach of homogeneity. This is favoured as it also removes the generation of wastes linked to start-up and shutdown and equipment cleaning. Even if it is understood that the feasibility of this way of operating might be forbidden by other intervening factors, such as production scale, production scheduling, segregation of production [143].

The process of turbulent mixing is very complex, in this complex process, one can distinguish and describe some simpler stages of mixing i.e. macromixing, mesomixing and micromixing [202]. The process of mixing on the scale of the whole vessel is called macromixing and refers to those large scale flow processes that cause the realisation of large scale distribution like for example the residence time distribution. Hence macromixing determines the environment concentrations for mesomixing and micromixing through environments where properties such as the rate of energy dissipation, the kinetic energy of turbulence, the scale of turbulence vary. Mesomixing reflects the coarse-scale turbulent exchange between the fresh feed and its surroundings; a fast chemical reaction is usually localised near the feed point forming a plume of

fresh feed. This plume is of coarse scale relative to the micromixing scales but is of fine scale relative to the scale of the system. Micromixing consists in liquids of the viscous-convective deformation of fluid elements, followed by molecular diffusion. The effect of acceleration of the molecular diffusion by the viscous-convective process is considered to be the important feature of micromixing. Micromixing is the type of mixing which governs the reaction occurrence in an agitated reactor with turbulent mixing. Mesomixing and macromixing have no direct effect on the reaction itself, though they still determine the type of mixing, e.g. turbulent, occurring.

2.1.2 Micromixing, selectivity and reaction

Many desirable organic reactions are accompanied by side reactions and undesired by-products, which waste raw materials and complicate product work-up and isolation. By enhancing the competition between reactions to obtain more selective syntheses, ecological, and economic benefits may be expected. Recently, however, more has been learned about the role of *'reactive mixing'*, which refers here to bringing reagents together on the molecular scale [38].

Micromixing, contrary to macro-mixing (contacting pattern), describes the macroscopic mixing-effects in the reaction vessel as it can be physically seen. Micromixing is a feature of the fluid : the fluid can either be mixed in a molecular dispersed manner (microfluid, e.g. salt solution, sugar solution) or on the other hand it can be totally segregated.

In liquid-phase chemical reactors operated under turbulent flow conditions different length scales are involved in the mixing process that have to precede and direct the chemical reactions. The macro-scale is of the order of the size of the reactor itself. Macromixing is the turbulent dispersion

from the inlet throughout the reactor. In a parallel way micromixing occurs at scales much smaller than this scale, the laminar scale. At these micro-scales diffusion and reaction take place. This means that the models for this micromixing are important for predicting the yield of a specific reaction products within a complex reaction system. The parameter that determines the microscale i.e. the kinetic energy dissipation rate, has to be known to calculate the behaviour of the micromixing locally. By tracking elementary microstructure the yield of a chemical reaction in these microstructure can be determined.

Bourne was one of the pioneers who first carried out this research and demonstrated the importance of micromixing within a reaction system [41, 37]. Bourne described micromixing as proceeding by molecular diffusion in small fluid elements that are being gradually strained. In the case of two miscible solutions A and B, B being much more concentrated than A, which are to be mixed in a turbulent flow. Bourne et al. define mixing as consisting initially of convective processes, namely distribution and turbulent dispersion [41, 37]. Whereby fresh B-rich fluid elements are deformed until their scale of segregation is comparable to the Kolmogorov velocity microscale. Mixing continues below this scale by molecular diffusion, which reduces the intensity of segregation, and also by laminar strain, which reduces the scale further and accelerates diffusion. The modeling consists of the unsteady state diffusion equation with a convective term for the simultaneous shrinkage of the fluid element. Where they determined that first estimates of the initial size and the rate of deformation could be obtained from the energy dissipation rate and the kinematic viscosity. Bourne et al. relates as well that fast multiple reactions, whose product distribution have been shown to depend on the level of micromixing reached within the reaction system [8, 7, 9].

In order to model the effect of micromixing on the selectivity of a reaction, a simplified version of the Engulfment-Deformation-Diffusion (EDD) model presented by Bourne and Baldyga was used for, where only engulfment is considered as it is the rate for controlling for liquids [19]. This model is defined and explained in section 2.1.4.

Reaction zone

In order to target the key product and enhance the selectivity of the system, the reaction zone of the system must also be considered and defined. The area where the reaction takes place, which in most cases is very small compared to the volume of the entire system, defines the reaction zone. In the case that we considered, where a small amount of incoming fluid is injected into large excess of bulk fluid and mixes into it, three stages are generally identified [204] :

1. Distribution of one fluid through the other and uniformisation of average composition without decreasing local concentration or mesomixing
2. Reduction of size of the region of uniform composition and increase of contact between regions of different composition or mesomixing
3. Mixing by molecular diffusion or Micromixing

Many models of different types have been proposed to describe the mixing of two reactive fluids :

Phenomenological models : Based on segregated zones, exchange zones, exchange fluxes, a typical example is the Interaction by Exchange with the Mean (IEM)[202]. This model assumes a reversible exchange between segregated regions and their environment through a single time

constant. The main disadvantage of phenomenological models is that they are not able to yield a priori predictions or scale-up rules [204].

Physical models : Based as closely as possible on flow and diffusion processes taking place in the mixing region. These models, for example, the engulfment model or E-model [19], use only parameters which can be independently determined from fluid dynamics or laboratory measurements. The huge advantage of this type of mixing modeling is that they allow a priori predictions.

Detailed analytical models : based on a comprehensive description of the fluid dynamics in the mixing region, which is now more possible with Computer Fluid Dynamics (CFD). The disadvantage of these models is that they require huge computation power and tend to be applicable on a one to one basis [71, 205].

The aim of our project is as defined previously, see section 1.8, to develop an automated reactor selection procedure to facilitate scale-up of drugs in the pharmaceutical industry. Also towards the arguments afore mentioned regarding the pros and cons of the different types of model available it becomes apparent that phenomenological models are not suited for scale-up rules, and that detailed analytical models, being case specific, do not permit to compare reactors, and would not suit our study.

In this part of the study it has been decided to concentrate on the use of physical mixing models to evaluate via dynamic computer simulation i.e. gPROMS [140, 31](see 2.3), the possibilities of a priori prediction of reaction selectivity [171]. The determination of the mixing operating regime, which affects the selectivity of the reaction, will allow us to determine which reactor enhances the selectivity achieved for a particular reaction system, thanks to

the reactor inherent characteristics, such as the energy dissipation rate. The energy dissipation rate of each type of reactor is an inherent characteristic of each type of reactor and its design parameters e.g. feed location, impeller characteristics, pump power, number of feed point.

Micromixing model

Chemical reaction is a molecular-level process and only mixing on the molecular scale can affect its course directly. Micromixing theory is concerned with those features of mixing which cause theattainment of homogeneity on the molecular level, i.e. with the reduction of the scale of unmixed blobs of fluid by breakage and deformation, and with final mixing by molecular diffusion. The chemical reaction kinetic equations can be incorporated into mixing models only locally; this can be achieved by using micromixing models.

In this section a micromixing model is explained and implemented using the mathematical model solver/simulator gPROMS. The model formulation is described as well the assumptions and limitations of use.

2.1.3 Micromixing

The process of turbulent mixing is very complex. In this complex process, one can distinguish and describe some simpler stages of mixing [20], macromixing, mesomixing and micromixing. The process of mixing on the scale of the whole vessel is called *macromixing*. This determines the environment concentrations for mesomixing and micromixing, and conveys fluids that are undergoing meso- and micromixing through environments where turbulence properties vary.

Mesomixing reflects the coarse scale turbulent exchange between fresh feed and its surroundings; a fast chemical reaction is usually localised near

the feed point, forming a plume of fresh feed. This plume is of a coarse scale in comparison to the micromixing scales but is of a fine scale in comparison to the scale of the system. Spatial evolution of the plume can be identified with the process of turbulent diffusion [20].

The process of mixing can be observed and described from Eulerian or lagrangian perspectives. With regards to the Lagrangian approach, the concepts of residence time distribution and micromixing have been introduced and developed using the Lagrangian or material frame approach. Using the Lagrangian frame perspective, one can follow the history of a fluid element, describing the elementary processes that form the overall micromixing or mesomixing process: disintegration of eddies, engulfing, deformation, molecular diffusion, etc. Using residence time distribution functions together with suitable multi-environment models, one is able to make predictions for a certain fluid element distinguishedamong others present in the system, or at least to find limits for various environments in the system. However, such an approach does not permit the prediction of spatial distributions in the system [204].

Another possibility is to link the eulerian coordinate system (x,y,z) for u(x,y,z) and ϵ(x,y,z) to the lagrangian framework for micromixing [18]. When the turbulent dispersion- especially in the direction of flow - can be neglected, the streamlines of a steady state flow determine the trajectories of fluid elements such that:

$$\frac{dx}{u_x(x,y,z)} = \frac{dy}{u_y(x,y,z)} = \frac{dz}{u_z(x,y,z)} = dt \tag{2.1}$$

Solutions of equation 2.1 for any element whose initial position was (x_0, y_0, z_0) give the following: its position $x(t, x_0, y_0, z_0)$ and similarly for y and z; its velocity $u_x(t, x_0, y_0, z_0)$ and similarly for u_y and u_z; its energy dissi-

pation $\epsilon(t, x_0, y_0, z_0)$. The full mechanism of micromixing, included in the engulfment-deformation-diffusion (EDD) model [17] can be applied.

When engulfment controls the micromixing process,the diffusion step can be neglected and the chemical kinetics can be introduced directly into the engulfment equations. Taking into account slowing down of the reaction zone growth by engulfment of the same fluid (self-engulfment), Baldyga and Bourne gave the general E-model equations [19]:

$$\frac{dV_i}{dt} = \langle E \rangle V_i (1 - X_i) \tag{2.2}$$

$$\frac{dc_i}{dt} = \langle E \rangle (1 - X_i) [\langle c_i \rangle - c_i] + R_i \tag{2.3}$$

Equation 2.3 shows how the processes of mesomixing and micromixing interact. Mesomixing determines the local composition of the environment for any fluid element in the system, i.e. the local average concentrations $\langle c_i \rangle$ of species in the environment and the local volumetric distribution X_i of fluids containing these species.

The micromixing parameter E determines the intensity of mass exchange between the relevant fluid element of concentration c_i and its surroundings of concentration $\langle c_i \rangle$. Mesomixing controls the process when a fluid element is surrounded by the fluid elements of the same composition ($X_i \approx 1, c_i = \langle c_i \rangle$), micromixing is most important when the fluid element is surrounded by the fluid elements of the different composition ($X_i \approx 0, c_i \neq \langle c_i \rangle$) and both mechanisms affect the process when these conditions are not fulfilled.

In contrast to a macromixing model where one assumes that distinct subvolumes exist in the reactor with different mean concentrations (i.e. 'zones'), in a well-macromixed micromixing model one assumes spatial homogeneity (mean concentration the same everywhere). The condition of spatial homo-

geneity does not imply that the concentration is the same at every point in the reactor (i.e. a well-micromixed reactor). Concentration fluctuations about the mean concentration may still exist and can have a significant influence on the rate of fast chemical reactions [205]. In Lagrangian micromixing models, concentration fluctuations are assumed to be generated by initial conditions (e.g. non premixed feed), or backmixing of fluid particles with different ages. Lagrangian description: The concentration inside a fluid particle following the flow can be computed in a Lagrangian formulation using a mass-balance equation written in terms of a convected derivative [149]:

$$\frac{D\phi}{Dt} = \text{Micromixing} + S(\phi) \tag{2.4}$$

where the chemical source term $S(\phi)$ is a closed function of the Lagrangian concentration ϕ. The Lagrangian micromixing term on the right-hand side models interactions between fluid particles at the same spatial location in the flow. In most applications of Lagrangian micromixing models, simple flows are considered wherein the histories of other fluid particles present at the same physical location are known. For example, if one assumes that a stirred reactor is well macromixed, the age distribution inside the reactor is known to be the exponential with mean equal to the reactor residence time.

In summary, a micromixing model attempts to describe the evolution of concentration fluctuations in a spatially homogeneous reactor by following Lagrangian fluid particles as they move through the system. In general, a complete description of the full range of concentration fluctuations is not attempted. Instead 'concentration space' is divided into environments', each represented by a single concentration, and the interactions between environments are modeled in terms of mixing times.

Reactive mixing between two feed streams can be described in terms of

four environments [204] as shown in figures 2.1 & 2.2:

Environment V_1 as erosion of fresh fluid. It contains fluid entering the system through the first feed stream. The concentration remains constant (equal to the feed concentration), and the volume fraction diminishes due to mixing to form environment 2. Typically no chemical reactions take place in Environment 1.

Environment V_{31} as dilution of eroded material into the reacting cloud (Total V_3). Part of the cloud (volume V_{31} is made of eroded material from the fresh fluid. In summary it contains partially-mixed fluid, but is rich in fluid from the first feed stream. It interacts due to mixing with environments 1 and 3. Chemical reactions can occur in Environment 2.

Environment V_{32} In corporation of fluid from the bulk (or second stream) into the reacting clouds. This forms the second part (volume V_{32} of the reacting clouds. In summary it contains partially mixed fluid, but is rich in fluid from the second feed stream. It interacts due to mixing with environments 2 and 4. Chemical reactions can occur in environment 3.

Environment V_4 contains fluid entering the system through the second feed stream. The concentration remains constant (equal to the feed concentration), and the volume fraction diminishes due to mixing to form environment 3. Typically no chemical reactions take place in environment 4.

It is to be noted that from the reactor inlet, Environment 1 and 4 are depleted and the model is reduce to only two environment. Also the the two environment model developed by Bourne and Baldyga and used in the work result from an appropriate choice of the mixing time constants [204]

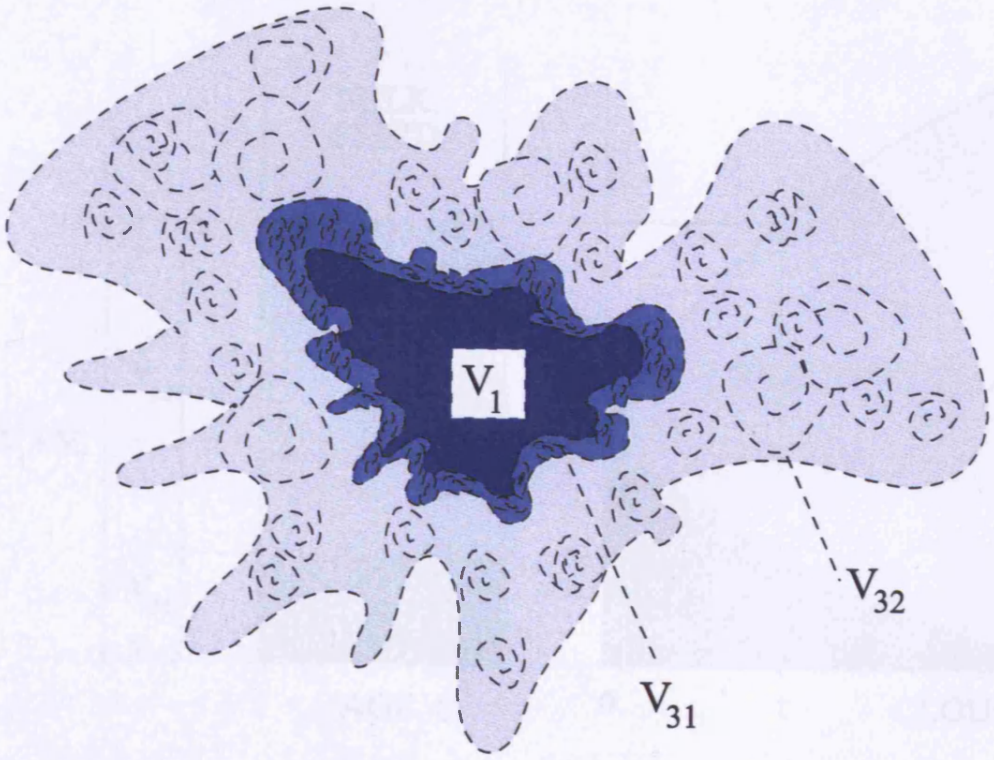

Fig. 2.1: Sketch of the model: various zones and reacting clouds [204]

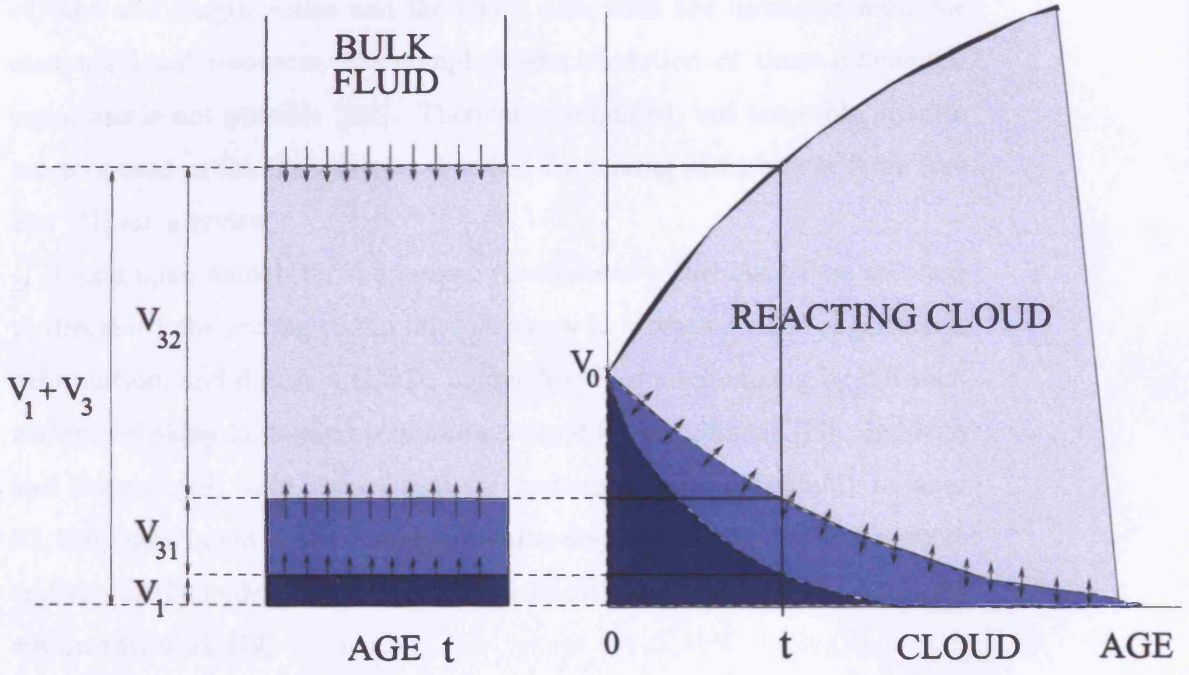

Fig. 2.2: Sketch of the model: Evolution of zones according to the cloud's age [204]

2.1.4 Micromixing model description

Because mixing has a large influence on the product quality of a mixing sensitive reaction, a model for the mixing of reacting flows is a helpful tool in the design of a chemical reactor. In principle, the mixing of fluids is completely described by the partial differential equations describing the momentum, mass and species balances. However, turbulent flows contain a wide range of time and length scales and therefore, even with the nowadays-available computational resources, the complete exact solution of these differential equations is not possible [186]. Therefore, simplified, but tractable, models are proposed in the literature to describe the mixing in turbulent flows (see Fox [71] for a review).

Lagrangian models for the mixing processes in a turbulent flow are used to described the mixing of the fluid elements in a reactor. The engulfment, deformation, and diffusion (EDD) model describes micromixing by diffusion within shrinking laminated structures formed by engulfment [17]. Baldyga and Bourne [19] have shown that for systems having a Schmidt number $ll4,000$, engulfment is the rate-determining step of the micromixing process and the EDD-model is simplified to the engulfment model (E-model) used within this work [19].

The growth of the micromixed volume according to the E-model is:

$$\frac{dV_{mi}}{dt} = EV_{mi} \tag{2.5}$$

$$E = 0.058\sqrt{\frac{\epsilon}{\nu}} \tag{2.6}$$

with

V_{mi} : the volume mixed on a molecular scale

E : the engulfment rate

ϵ : Energy dissipation rate (m^2/s^3)

ν : Kinematic viscosity (m_2/s)

Mixing of micromixed fluid with micromixed fluid will not lead to growth to the total micromixed volume. The probability of this so-called self-engulfment depends on the volume fraction of micromixed fluid inside the spreaded feedstream. The growth of the micromixed volume taking into account possible self-engulfment [19] is:

$$\frac{dV_{mi}}{dt} = EV_{mi}\left(1 - \frac{V_{mi}}{V_{dt}}\right) \tag{2.7}$$

Where,

V_{dt} : is the volume of the dispersed feedstream

The spreading of the feedstream is characterized by a turbulent dispersion coefficient D_t [128].

In liquids, micromixing takes place by molecular diffusion, laminar deformation of striations below the kolmogorov scale (Kolmogorov scale = smallest scale in a turbulent flow) and the mutual engulfment of regions having different compositions leading to growth of the micromixed volume. Under frequently occurring conditions engulfment is the limiting one of these three mechanisms [19]. The time constant defining the engulfment mechanism is τ_e :

Characteristic time for micromixing by engulfment

$$\tau_e = 17.3\left(\frac{\lambda}{\nu}\right)^{\left(\frac{1}{2}\right)} \qquad (s) \tag{2.8}$$

with,

ν : Kinematic viscosity (m_2/s)

ϵ : Energy dissipation rate (m^2/s^3)

In the case of fast reactions, the reaction often take place where the reacting compounds are originally contacted i.e. at the feed entrance. While micromixing favour the reaction, as it represents the mixing at molecular scale. Mesomixing has been observed as being, in some cases, the dominating mixing mechanism [16, 20].
Mesomixing happens through two different mechanisms [23].

1. Turbulent dispersion.
2. Initial convective disintegration of large eddies.

Turbulent dispersion : This mechanism represents the transversal spreading of a feed stream from its original stream line when introduced in the mixing environment. The time constant defining the turbulent dispersion mechanism is τ_d :

Characteristic mesomixing time for transverse turbulent dispersion

$$\tau_d = \frac{Q_B}{uD_t} \qquad (s) \tag{2.9}$$

with,

Q_B : Flow rate of B-solutions (m_3/s)

u : Liquid velocity (m/s)

D_t : Turbulent diffusivity (m^2/s)

Initial convective disintegration of large eddies : This mechanism represents the disappearance of large eddies in the course of dispersion by inertial

action from the integral scale of concentration fluctuations, Λ_c, towards the kolmogorov scale. Kolmogorov length scale is the smallest length scale that can be found in a turbulent flow. When a spot of a passive scalar is mixed by a turbulent flow, the velocity fluctuations of slightly smaller scale distort this spot, thus producing concentration fluctuations of smaller scale. This phenomenon can be interpreted either as break-up of blobs of a pure, unmixed solution resulting in the erosive diminishing of these regions or as formation of smaller eddies within the large eddies. In this work the formation of smaller eddies within the large eddies is only retained as the reason for the erosive diminishing of the reaction regions, which are defined as the areas/eddies where the different reacting compounds are present. The time constant defining the initial convective disintegration of large eddies mechanism is τ_s [113]:

Characteristic mesomixing time for dissipation of segregation in inertial-convective subrange

$$\tau_s = A\left(\frac{\Lambda_c^2}{\epsilon}\right)^{(1/3)} \qquad (s^{-1}) \tag{2.10}$$

where,

A : $A = 1.2$ [25] - A is roughly 1-2 e.g. for fully developed turbulence in liquids A = 2 [53]

Λ_c : Integral concentration scale (m)

ϵ : Turbulent energy dissipation rate (m^2/s^{-3})

This description of the mechanisms allow to compare the time constants i.e. τ_d and τ_s in order to identify the controlling mechanism within the mixing environment.

The mathematical model which has been used in this study couple micromixing and reaction to eddy break-up by inertial forces. Homogeneous turbulence is assumed : for reactors with large ϵ gradient, equations developed may be applied locally.

Various studies have shown that the energy dissipation rate and the feed rate have strong influence in controlling mechanism from micro- to mesomixing [40, 21, 22]. We will be looking at these two parameters and their influence on the model further along in this study. Particularly when studies show that scale-up causes shift from micromixing to mesomixing controlling mixing mechanism [40, 39].

2.1.5 Mathematical formulation

In the following section the formulation of the mathematical model is shown, it is based on the explanation given by Baldyga et al. (1997) [23].

Figure 2.3 represents the structure of a partially segregated fluid as islands. X_u represents the volume fraction of these islands and X_B^e is the composition of these islands i.e. the volume fraction of substance B undergoing mixing. These islands are about to develop by eddy dissipation contained in a surrounding which does not yet contain substance B. Following this description, three regions can be described :

Region a/ : Substance B absent between islands

Region b/ : Substance B present on coarse scale within the islands

Region c/ : Substance B mixed on molecular scale - phenomenological *points* within the islands

Let's consider,

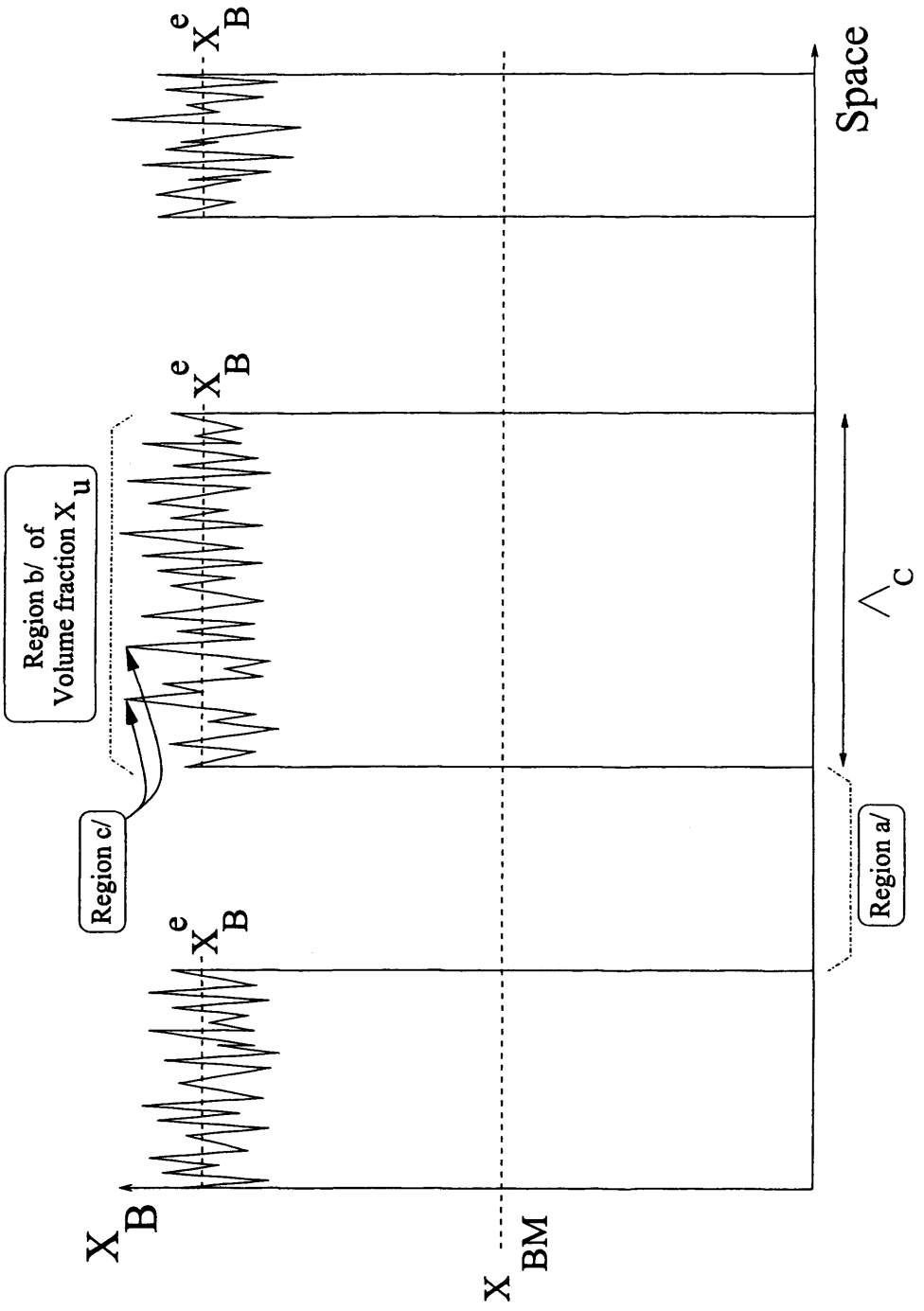

Fig. 2.3: Structure of partially segregated islands where - Region a/ : B absent - Region b/ : B present on coarse scale - Region c/ : B mixed on molecular scale

X_{BM} = Volume fraction of B within the whole structure
then

$$X_{BM} = X_u X_B^e \tag{2.11}$$

A good macro-mixed environment indicates that X_BM is the same throughout the environment as indicated in figure 2.3. The structure changes with time as eddies are broken up, so that X_u and X_B^e increase and decrease, respectively.
The rate of mesomixing can be derived as follow :
The variance of composition of the structure given in figure 2.3 is :

$$\begin{aligned} \sigma^2 &= X_u \left(X_B^e - X_{BM}\right)^2 + \left(1 - X_u\right)\left(0 - X_{BM}\right)^2 \\ \sigma^2 &= X_{BM}\left(X_B^e - X_{BM}\right) \end{aligned} \tag{2.12}$$

Corrsin and Rosensweig defined the rate of decay of variance in the inertial-convective subrange of the concentration spectrum as [53, 164]:

$$\frac{d\sigma^2}{dt} = \frac{-\sigma^2}{\tau_s} \tag{2.13}$$

from equations 2.12 and 2.13,

$$\frac{dX_B^e}{dt} = \frac{-\left(X_B^e - X_{BM}\right)}{\tau_s} \tag{2.14}$$

Substituting this into equation 2.11 gives :

$$\frac{dX_u}{dt} = \frac{X_u\left(1 - X_u\right)}{\tau_s} \tag{2.15}$$

The initial volume fraction of the system where B is present is X_0. For $\tau_s = Const.$, the solution of equation 2.15 becomes :

$$X_u = \frac{X_0}{X_0 + (1 - X_0)\, exp\left(\frac{-t}{\tau_s}\right)} \tag{2.16}$$

In equation 2.16, as $t \ll \tau_s$, X_u tends to 1, which indicates that B is present everywhere although not micromixed.

The micromixing model needs to take account of the so-called 'self-engulfment' mechanism [19]. Self-engulfment occurs when B-rich fluid is engulfed with B-rich fluid. This mechanism does not participate to the growth of the micromixed volume, but tends to slow down the increase of the micromixed volume V_B. Taking into account the self-engulfment phenomena, the rate of growth of the micromixed volume V_B can be expressed by :

$$\frac{dV_B}{dt} = EV_B\,(1 - X_{Bu}) \tag{2.17}$$

with,

V_B : Volume of micromixed fluid

E : $E = \tau_e^{-1}$ Engulfment rate

X_{Bu} : The volume fraction of micromixed B-rich fluid in the islands

The notation V_B refers to the micromixed volume in a batch or semibatch reactor. In a plug-flow reactor it denotes the flow rate of micromixed fluid, which increases with t, i.e. along the flow.

X_Bu, the volume fraction of micromixed B-rich fluid in the islands of partially segregated fluid, can be expressed as follow :

$$X_{Bu} = \frac{V_B}{V_u}$$

$$X_{Bu} = \frac{V_B}{V}\frac{V}{V_u}$$

$$X_{Bu} = \frac{X_B}{X_u} \tag{2.18}$$

with,

V : Total volume of fluid in the reactor

V_B : Volume of micromixed fluid in the reactor

V_u : Volume of B-rich islands in the reactor

X_B : The volume of micromixed fluid relative to the whole fluid contained in the reactor

X_{Bu} : The volume fraction of micromixed B-rich fluid in the islands

Replacing equation 2.18 transformation in equation 2.17 gives :

$$\frac{dX_B}{dt} = EX_B\left(1 - \frac{X_B}{X_u}\right) \tag{2.19}$$

Initial conditions : $X_{B_{(t=0)}} = X_0$; $X_{u_{(t=0)}} = X_0$

The initial condition i.e. flowrate, operating mode define X_0.

Equation 2.19 models the mechanisms of eddy breakage i.e. increase of X_u values which ease the constraint of self-engulfment in equation 2.19 and leads to the start of the micromixing mechanism.

2.1.6 Description

The mixing model chosen for this study is the simplified version of the engulfment model [17] defined by Bourne and Baldyga [19]. The prime advantage of this expression of the engulfment model, also called E-model, is that it allows us to compare the production rate of the different components of the reaction system considered. In our case the reaction system that we consider

is expressed by the reaction equations 2.46 and 2.47 78, this reaction system is typical of the difficulties encountered during scale-up in the pharmaceutical industry [44, 142]. The aim of the scale-up is to produce a targeted product but very often the selectivity obtained for this targeted product is undermined by the production of unwanted by-products. The product targeted here is C of which the selectivity is undermined by the production of D. The aim will then be to enhance the production of C against D.

Another of the advantages offered by the E-model is that the viscosity of the solution is taken into account, which is an important factor when dealing with organic products. The E-model presents also the advantage to have been studied for three phase reactions and was extended to incorporate mass transfer [42]. This would allow in the future to further extend the content of this work for multiphase reaction systems. In the same way a laminar model has also been developed which would allow micro reactors to be included in the scope of this work.

The scale-up of a chemical reactor is difficult as it involves changes in the surface to volume ratio [189]. The amount of wall surface area per volume available to a process, is much greater on a small scale, than on a large scale. The concept developed in this study does not take into account the size of the equipment directly.

A mass balance on substance i in this growing reaction zone is :

$$\frac{d}{dt}\left(V_i c_i\right) = E V_i \left\langle c_i \right\rangle + R_i V_i \tag{2.20}$$

$\langle c_i \rangle$, is defined by Baldyga and Bourne [19], as the concentration of i in the local environment of the growing eddy. The first term on the right-hand side of 2.20 is the rate of addition of i by engulfment, the second term is the production of i by reaction. Given that equation 2.48 is verified i.e. Sc

<< 4000 diffusion is rapid compare to engulfment, the reaction zone can be considered as only composed of a uniform concentration.

The model simulates engulfment by a large number of eddy generation, where mixing by engulfment is formulated by the growth of a succession of eddies, and where engulfment takes place between equal volumes of fluid. Eddies start their growth at different times, and averaging over all these generations gives a continuous growth law. Eddies of substance i grow exponentially, which can be represented by the following :

$$\frac{dV_i}{dt} = EV_i \tag{2.21}$$

Introducing equation 2.21 in equation 2.20 gives :

$$\frac{dc_i}{dt} = E\ (\langle c_i \rangle - c_i) + R_i \tag{2.22}$$

$\langle c_i \rangle$ which is, as previously quoted, the concentration of the environment, changes over time in relation to the changes occurring within the reaction zone. The feed as reactant B that is added to the reactor is discretised in the computation of the model. Each part of the feed is reacted in the reaction zone, which then grows for each feed part addition following equation 2.21. This occurs before another part of the feed is added to the reactor. While changes occur within the reaction zone the environment zone remains unchanged. From one feed addition part to the next the environment zone, $\langle c_i \rangle$, is updated by adding or subtracting, with regard to the compound considered, the amount generated or consumed in the reaction zone to the environment zone. The environment zone being a *sum* of the successive reactions occurring in the reaction zone. At this stage, we assume that the fluid remains perfectly mixed because the rate of addition of B is slow relative to the homogenisation of the surrounding. The environment zone as sum of

all the reaction zone which have occurred over a certain feed addition time can be expressed as :

$$\frac{d\langle c_i \rangle}{dt} = \sum \frac{dc_i}{dt} \tag{2.23}$$

The assumption just mentioned previously regarding the homogenisation of the surrounding has been further developed by Baldyga et al. [23]. A self-engulfment factor is added to the original model. The self-engulfment models the engulfment within the fluid element or self-engulfment that does not contribute to the growth of the volume of the micromixed region.

This factor is expressed as follows :

$$f = 1 - \frac{V}{V0} exp\left(\frac{-t}{t_s}\right) \tag{2.24}$$

and equation 2.21 then becomes

$$\frac{dV}{dt} = EVf \qquad V(t=0) = V0 \tag{2.25}$$

t_s is the characteristic time scale of mesomixing (s) which can be expressed for agitated reactors as [171] :

$$t_s = 2\left(\frac{F}{\pi u \epsilon N_f}\right) \tag{2.26}$$

where,

F : Feed rate (m^3/s)

u : Velocity of fluid within the reactor (m/s)

ϵ : Energy dissipation rate (m^2/s^3)

N_f : Number of feed port (-)

From equation 2.20, it can be shown that :

$$\frac{dN_i}{dt} = \frac{d(c_i V)}{dt} \tag{2.27}$$

$$\frac{dN_i}{dt} = \langle c_i \rangle \frac{dV}{dt} + N_T \sum_{j=1}^{r} \nu_{i,j} R_j \tag{2.28}$$

From 2.28 and 2.25 the two previous equations it can be shown that rate of change of composition of component i in the growing fluid elements can be expressed in mole fraction as follow [171].

In the engulfment model, the balance equation for the growing fluid elements are described by 2.25 and 2.28 N_i and N_T are the number f moles of component i and total number of moles, respectively, in the growing fluidelements. $< c_i >$ is the concentration of component i in the environment. A summation of 2.28 over all components gives :

$$\frac{dN_T}{dt} = \left(\sum_{i=1}^{c} \langle c_i \rangle \right) \frac{dV}{dt} + N_T \sum_{j=1}^{r} \nu_{i,j} R_j \tag{2.29}$$

Also, by differentiating $x_i = N_i / N_T$, we get,

$$\frac{dx_i}{dt} = \frac{1}{N_T} \frac{dN_i}{dt} - \frac{x_i}{N_T} \frac{dN_T}{dt} \tag{2.30}$$

Substituting 2.28 and 2.29 into 2.30, we get:

$$\frac{dx_i}{dt} = \left[\frac{\langle c_i \rangle}{N_T} - \frac{x_i \sum_{i=1}^{c} \langle c_i \rangle}{N_T} \right] \frac{dV}{dt} + \sum_{j=1}^{r} \left(\nu_{i,j} - x_i \nu_{TOT,j} \right) R_j \tag{2.31}$$

By using 2.25, $N_T = V \sum_{i=1}^{c} c_i$, and $y_i =< c_i > / \sum_{i=1}^{c} < c_i >$, the first term on the right-hand side of 2.31 can be written as

$$\left[\frac{\langle c_i \rangle}{N_T} - \frac{x_i \sum_{i=1}^{c} \langle c_i \rangle}{N_T} \right] EVf = \frac{\sum_{i=1}^{c} \langle c_i \rangle}{\sum_{i=1}^{c} c_i} \left[y_i - x_i \right] Ef \tag{2.32}$$

Here, the concentration term are :

$$\sum_{i=1}^{c} = \rho_x / M_x \tag{2.33}$$

$$\sum_{i=1}^{c} = \rho_y / M_y \tag{2.34}$$

It is reasonable to assume the mass density of the single-phase liquid mixture to be constant irrespective of it composition. Hence, we get :

$$\rho_x = \rho_y \tag{2.35}$$

$$\frac{\sum_{i=1}^{c} \langle c_i \rangle}{\sum_{i=1}^{c} c_i} = \frac{M_x}{M_y} \tag{2.36}$$

Using the above developments, we get :

$$\frac{dx_i}{dt} = \frac{M_x}{M_y} (y_i - x_i) Ef + \sum_{j=1}^{r} (\nu_{i,j} - x_i \nu_{TOT,j}) R_j \tag{2.37}$$

Substituting t_m for E as :

$$t_m = E^{-1} = \frac{12}{ln2} \left(\frac{\nu}{\epsilon}\right)^{1/2} \tag{2.38}$$

and equation 2.24 for f, we get :

$$\frac{dx_i}{dt} = \frac{1}{t_m} \frac{M_x}{M_y} (y_i - x_i) \left[1 - \varphi e^{\left(\frac{-t_d}{t_s}\right)}\right] + \sum_{j=1}^{r} (\nu_{i,j} - x_i \nu_{Tot,j}) R_j \tag{2.39}$$

with the initial condition :

$$x_i(t = 0) = x_i^F \tag{2.40}$$

The scale-up of the chemical reaction is more successful when micromixing is reached within the reactor. This is due to the fact that micromixing

enhances selectivity. Therefore the design of the reactor is articulated around achieving micromixing. As shown in figure 2.4, (see [171]), two parameters, the Damköler number for micromixing (Da_m) and mixing index (Q) are the determinant factors of the type of mixing achieved within a reactor (see [171]). These two parameters are defined as follows:

Damköler number for micromixing

$$Dam = \frac{t_m}{t_r} \qquad (-) \tag{2.41}$$

Reaction time

$$t_r = \frac{1}{k_{max}} \qquad (s) \tag{2.42}$$

Mixing index

$$Q = \frac{t_m}{t_s} \qquad (-) \tag{2.43}$$

Characteristic micromixing time

$$t_m = \left(\frac{12}{log(2)}\right)\left(\frac{\nu}{\epsilon}\right)^{0.5} \qquad (s) \tag{2.44}$$

Characteristic mesomixing time

$$t_s = 2\left(\frac{Q_f}{\pi u \epsilon N_f}\right) \qquad (s) \tag{2.45}$$

see Appendix A.1 and Appendix A.2 for the full description of the parameters involved and the equations involved.

It then becomes apparent that the micromixing regime, assuming a single feed port i.e. $N_f = 1$, is dependent on the energy dissipation rate ϵ, the viscosity ν, the feed rate F and the velocity u of the fluid within the reactor. Figures 2.5 and 2.6, (see [171]), show the reactor performance for various operating regimes. The product distribution is defined as the amount of target product produced over the amount of limiting reactant reacted. Figure

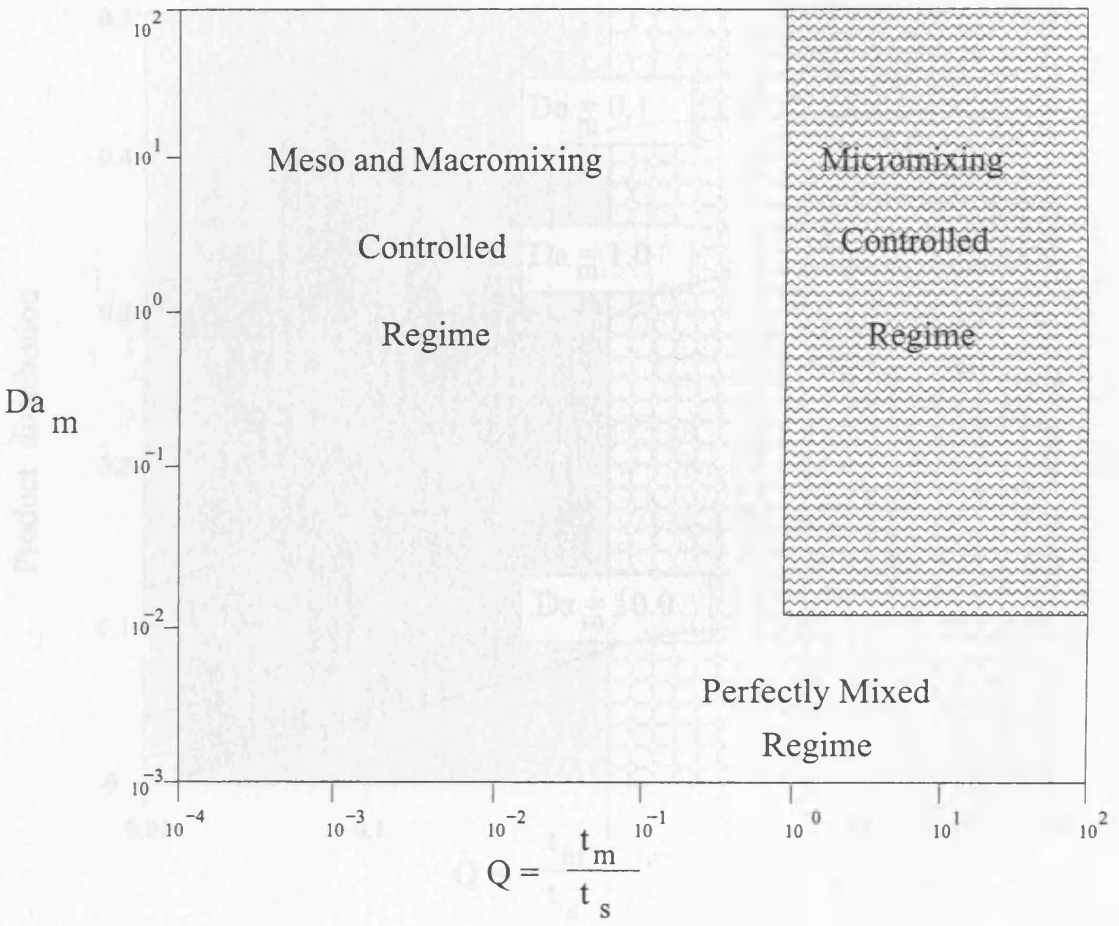

Fig. 2.4: Operating regimes as functions of Damköler number for micromixing (Da_m) and mixing index (Q)

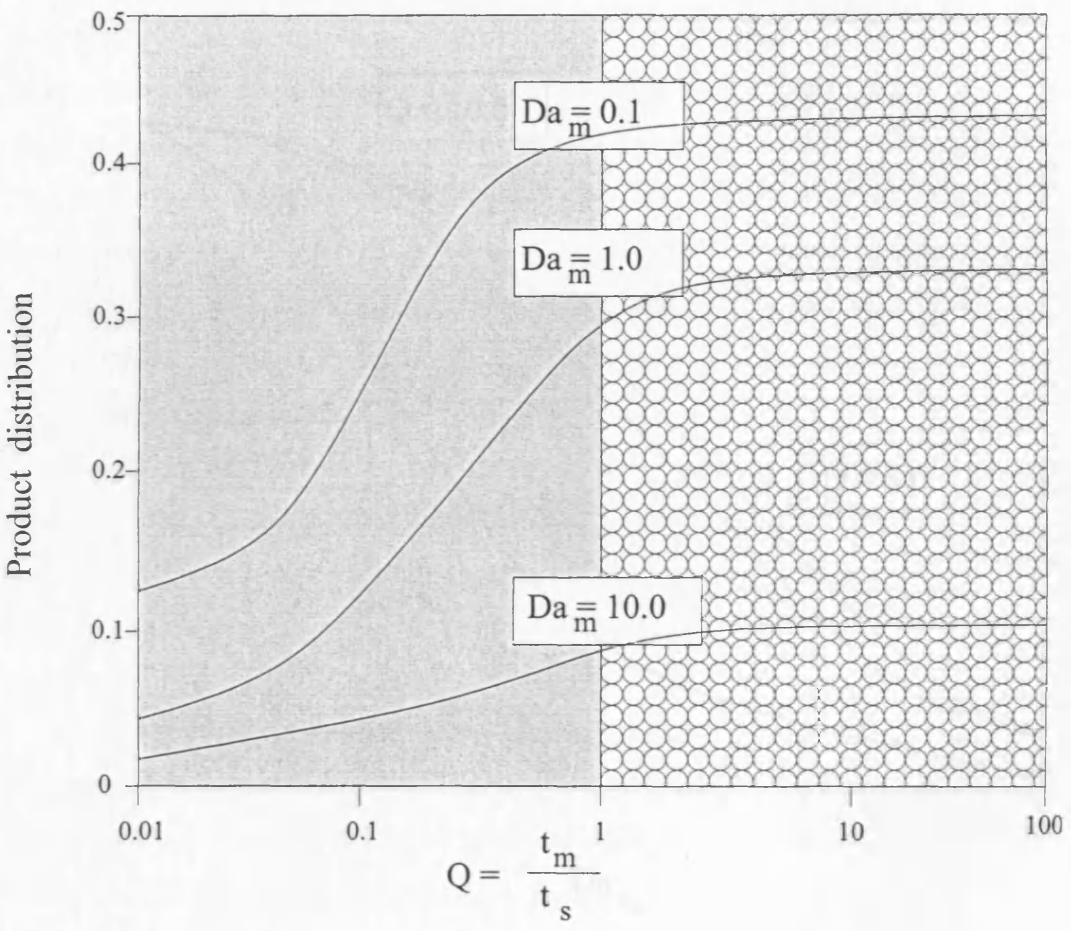

Fig. 2.5: Reactor performance in various operating regimes for $k_1 = k_2 = 250\ s^{-1}$, $V = 1\ m^3$, feed addition time =6000 s and $\epsilon = 2{,}000\ W/kg$

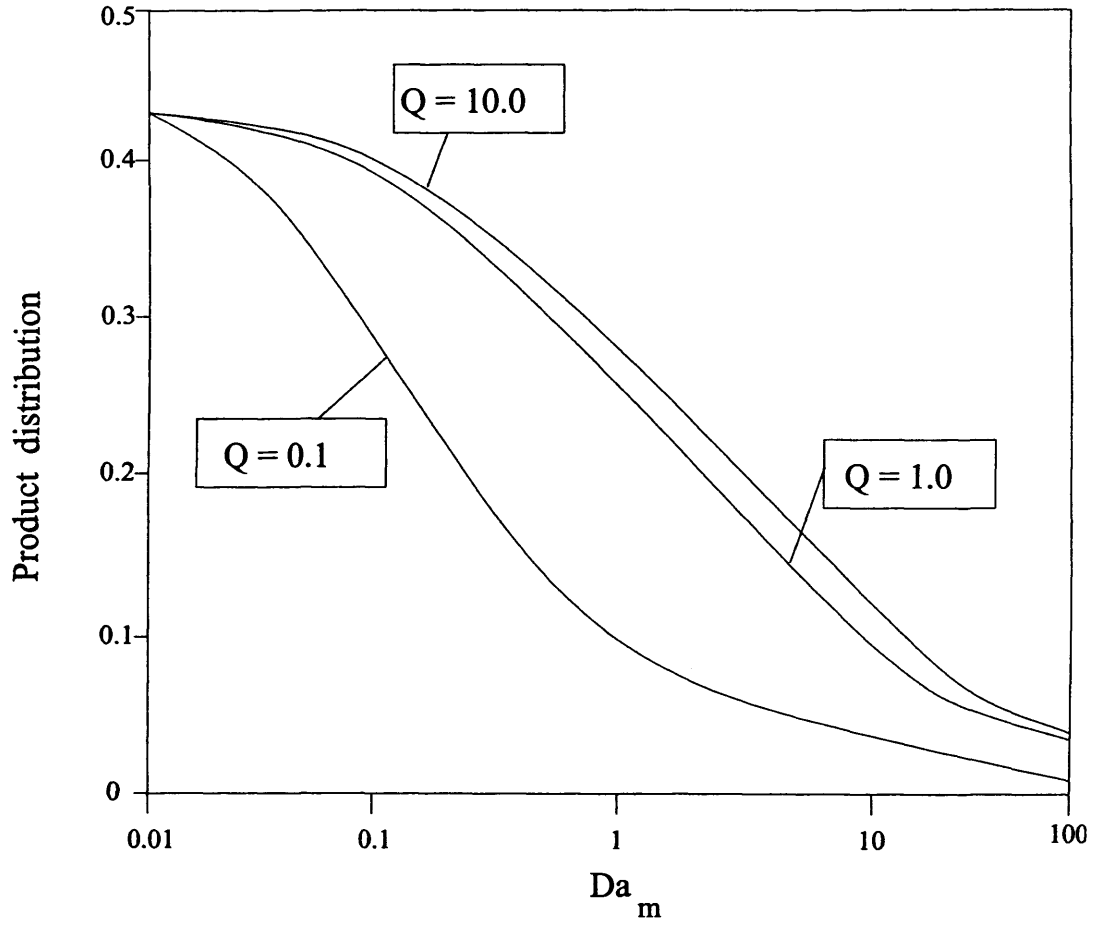

Fig. 2.6: Reactor performance in various operating regimes for $k_1 = k_2 = 250\ s^{-}1$, V = 1 m^3, feed addition time =6000 s and ϵ = 2,000 W/kg

2.5 shows that in the micromixing controlled regime enhanced the production of the targeted product.

The design of the reactor to scale-up a reaction system, is therefore to find the right combination of the parameters ϵ, F and u for which a micromixing controlled regime is achieved. The velocity within the reactor, u, can be used to calculate the different features of the design of a reactor, like size, impeller type or jet type for example to achieve a particular fluid velocity. This can also mean pump for a jet loop or motor size for an impeller. The type of reactor itself is directly given by the level of energy dissipation rate necessary. The maximum energy dissipation rate achievable within each type of reactor is an inherent characteristic of each type of reactor. This can also lead to the design of a novel type of reactor.

It is to be noted that a very similar type of model has been used to model laminar micromixing [26]. This presents an interest for future development, in cases where very high viscosity compounds are used, or more notably in cases where reactors only operate under laminar conditions like microreactors.

The model used is defined over a certain number of assumptions and conditions [17]. One of the first conditions is that it is defined for liquid phase reactions for which physical properties like density and viscosity as well as chemical rate constants are not influenced by the reactions.
A reaction is said to be slow or fast when the time required for the micromixing step is, respectively, shorter or longer than the time required for a chemical reaction. Thus in the slow regime, mixing on the molecular scale precedes reaction, whilst with fast reactions concentration gradients are formed and reaction proceeds in an inhomogeneous solution, which only becomes fully homogeneous after the reaction has been completed. The in-

homogeneity retards the rate of a fast, second order reaction, whose reagents are initially present in separate streams, whilst the relative rates of certain multiple reactions are influenced by the mixing conditions. Let us consider the competitive, consecutive reactions :

$$A + B \xrightarrow{k_1} C \tag{2.46}$$

$$B + C \xrightarrow{k_2} D \tag{2.47}$$

The afore described reaction system is an interesting example of such sensitivity : it is highest in the slow reaction mode and zero in the instantaneous regime [17] . In the fast reaction mode, the reaction zone shrinks to the plane where A and B meet, whilst in the slow regime it is intermediate and influenced by chemical and physical factors.

Turbulent flow is described as rotational and dissipative, and is said to be characterised by high level of fluctuating vorticity - vorticity is the curl or rotation of the velocity vector. The case we considered is for $Sc \ll 4000$ where Sc is defined as the Schmidt number:

$$Sc = \frac{\mu}{\rho D_V} \tag{2.48}$$

with,

μ : Kinetic viscosity (Pa/s)

ρ : Density (kg/m^3)

D_V : Molecular diffusivity (m^2/s)

The model simulates engulfment by a large number of eddy generations, where mixing by engulfment is formulated by the growth of a succession of

eddies, and where engulfment takes place between equal volumes of fluid. Eddies start their growth at different times, and averaging over all these generations give a continuous growth law.

The case of a semi-batch reactor is typical of the pharmaceutical industry [62]. This type of reactor allows the control of a potential runaway by controlling the reaction through the addition of a reagent [183], it thereby offering a safety related advantage over its direct competitor, the batch stirred tank reactor, which is also widely used in the pharmaceutical industry [111]. The semi-batch reactor offers also the advantage to be able to be easily converted to carry out continuous operation.

There are three approaches to processing operations: batch, continuous, and semi-batch or semicontinuous. Each option has its own scale-up advantages presented in table 2.1 and table 2.2 [6].

While batch and semi-batch remain the traditional way of producing pharmaceutical products [12], cost [105], product quality [142] and environmental incentives [200, 143, 64, 176], or even safety [209] have driven the pharmaceutical industry towards automated and continuous mode of operation [136]. Nevertheless there are number of drawbacks to using continuous processes. Resources are needed to develop the process: the appropriate residence time to reach a level of suitable completion must be determined under desired conditions of temperature, flow rate, and any other critical parameters. The reaction system may have limited flexibility for running other reactions [6]. Also it is with these type of difficulties that 'learning before doing' can become an important factor in achieving the best process intensification in the minimum time possible [147, 80, 136].

Also in our study we consider the case of a semi-batch reactor and the case of a continuous reactor e.g. in-line mixer, static mixer, tubular reactor in

Tab. 2.1: Characteristics of semi-batch and continuous operations

Features	General-purpose reactor	Continuous-flow reactor
Typical industrial use:		
Laboratory	General approach for scale-up	Rarely used
Pilot Plant	Most often used	Rarely used
Manufacturing	Often used for bulk chemicals & fine chemicals; rarely used for bulk chemicals	Often used for agricultural chemicals; rarely used for Pharmaceutical & fine Chemicals
Pharmaceutical		
Temperature response	Slower in larger vessels	Response can be very rapid
Localisation of physical effects contents	Macromixing and micromixing always considerations	Equipment can be selected for excellent micromixing and localised physical effects
Reaction times for	Reactions with relatively long reaction times or short reaction times generating products stable under the reaction conditions	Reactions with a short residence time or those with products stable while recycling through reactor; also unstable products
Useful for	Most reactions	Reactions where relative stoichiometry of reactants and products is critical; reverse quenches; tight temperature controls; efficient mixing of heterogeneous streams; localisation of catalysts and physical effects

Tab. 2.2: Characteristics of semi-batch and continuous operations

Features	General-purpose reactor	Continuous-flow reactor
Cost for reactor	\$50,000 (50 gal reactor) and more	Under \$1,000 for static mixer for pilot plant; specialised reactors more costly
Additional equipment needed	Equipment traditionally available in most pilot plants and manufacturing plants	Pumps and heat exchangers in addition to receiving vessels and traditional vessels
Relative operating safety	Good	Very good, as only a small portion of batch is subjected to processing at any moment
Utility demand	Must transfer heat from entire batch and large reactor	Transfer heat from part of batch and small reactor
Additional development	Some time may be needed to optimise processing if labile compounds are produced	Need to determine reaction time for suitable residence time in reactor, or recycle stream through reactor

which B is slowly added to reagent A, present in the reactor. Slow addition of B means that B mixes and reacts slowly and the concentration averages over the whole reactor slowly. Each new fresh feed of B is integrated within the reactor by eddies which incorporate and react by engulfment within the eddy environment (as described in A.3). The eddy environment is constituted by, originally solely A, and then C and D according to equations 2.46 and 2.47 in section 2.1.6.

The expression of the rate of reaction j is expressed as rate of reaction j per mole of reacting mixture of composition x i.e. [171]:

$$R_j = \frac{\text{Fraction of reaction mixture reacting in reaction j}}{second} \tag{2.49}$$

This expression of the engulfment model, or E-model, presents the advantage of expressing the rate change of each product through molar fraction, which is unit independent.

Figure 2.7 show how the model allows to follow the molar fraction evolution of the different components, constituents of the reaction system, over a certain period of time. The period of time for which the reactions occur is called the feed addition time (fat), in these cases 600s. The feed addition time is the length of time for which a reactant, in our case reactant B is fed to the reactor. The flow rate at which reactant B is added to the reaction is considered as constant. As can be seen in 2.7, the Molar fraction of B remains at zero as the reactant B is assumed to be totally reacted for each addition. The molar fraction of each component changes during the reaction, the volume of solution B added to the semi-batch reactor is discretised (see 2.3) into σ equal parts, each of volume V_B and concentration c_{B0}. When any part has been added, the volume of the reaction zone grows according to equation A.3. Engulfment take place independently with the same environment, and

it is assumed that during application of equation A.1 to any part of the feed, the molar fraction remains constant.

The performance objective is to maximise the product distribution, P_dc, of the desired product in our case C. The product distribution of C, P_dc, is defined as :

$$\text{Product Distribution} = \frac{\text{C produced}}{\text{B fed}} \tag{2.50}$$

The evolution of the product distribution of C is shown in 2.8 and 2.9

All the equations for the micromixing model are described in appendix A for the semi-batch operation and in appendix B.2 for the continuous operation.

Assumptions for micromixing model for semi-batch and continuous operation

The following assumptions have been made for the application of the mathematical model described in this chapter 2.1.4. Assumptions are made at two different levels, the first level refers to the application of the model itself, and the second level refers to the process itself.

Model assumptions:

1. Molecular diffusion does not to influence reaction rate. Therefore we only consider systems with a Schmidt Number : Sc$\ll$ 4000

2. The reactant is integrated within the fluid on the reactor by being rolled up by turbulent vorticity thereby creating multiple layers or slabs of fresh liquid and liquid already reacted

3. The system is a liquid phase system with only one liquid phase present

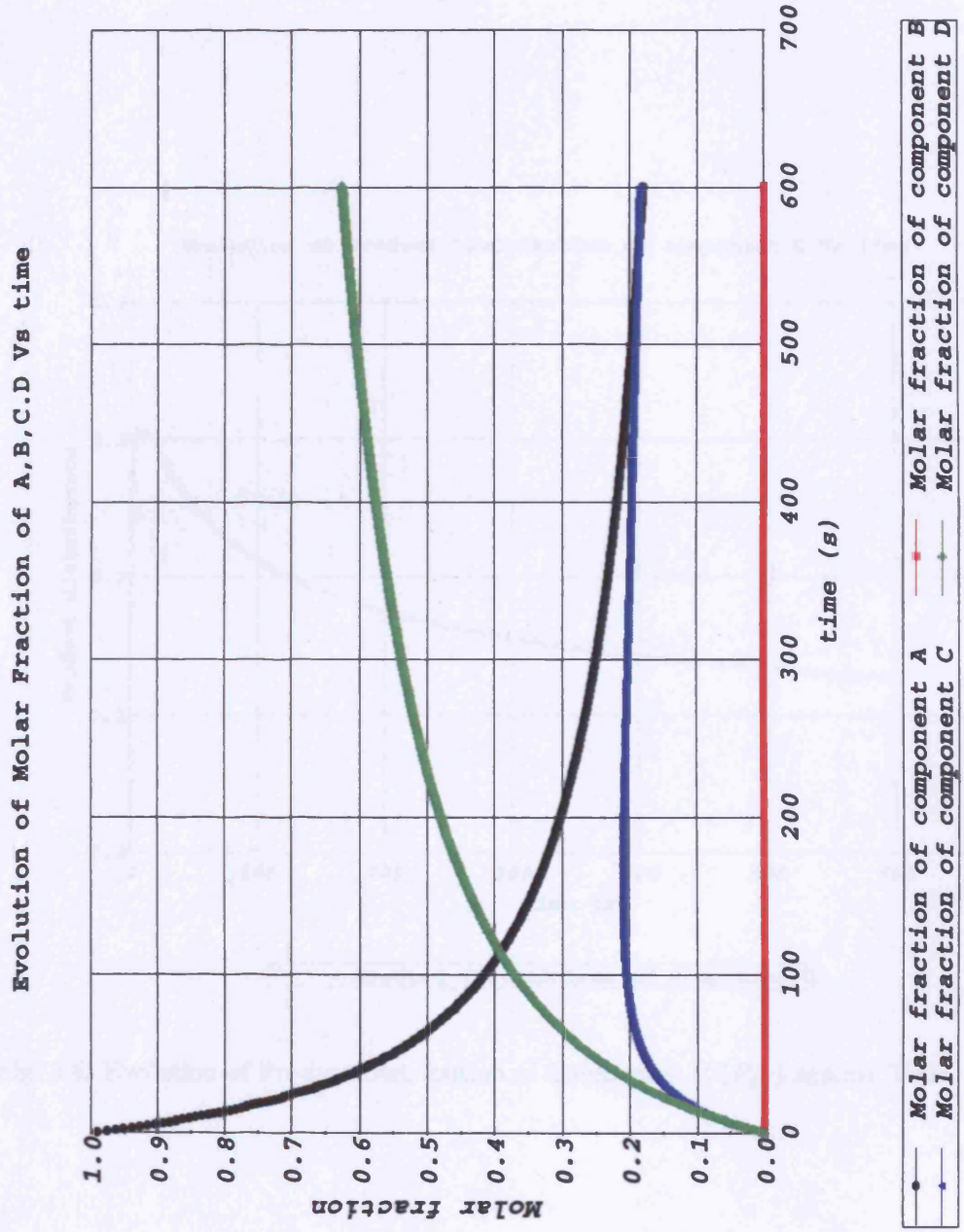

Fig. 2.7: Evolution of Molar Fraction of Component A,B,C,D against Time

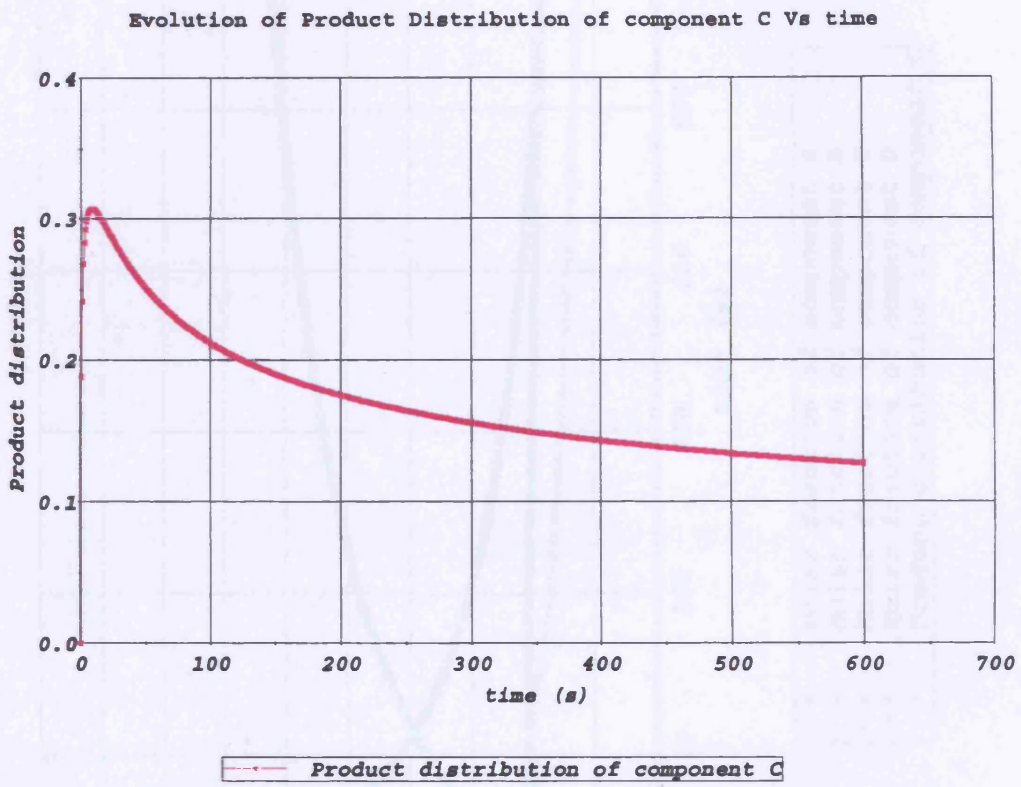

Fig. 2.8: Evolution of Product Distribution of Component C (P_{dC}) against Time

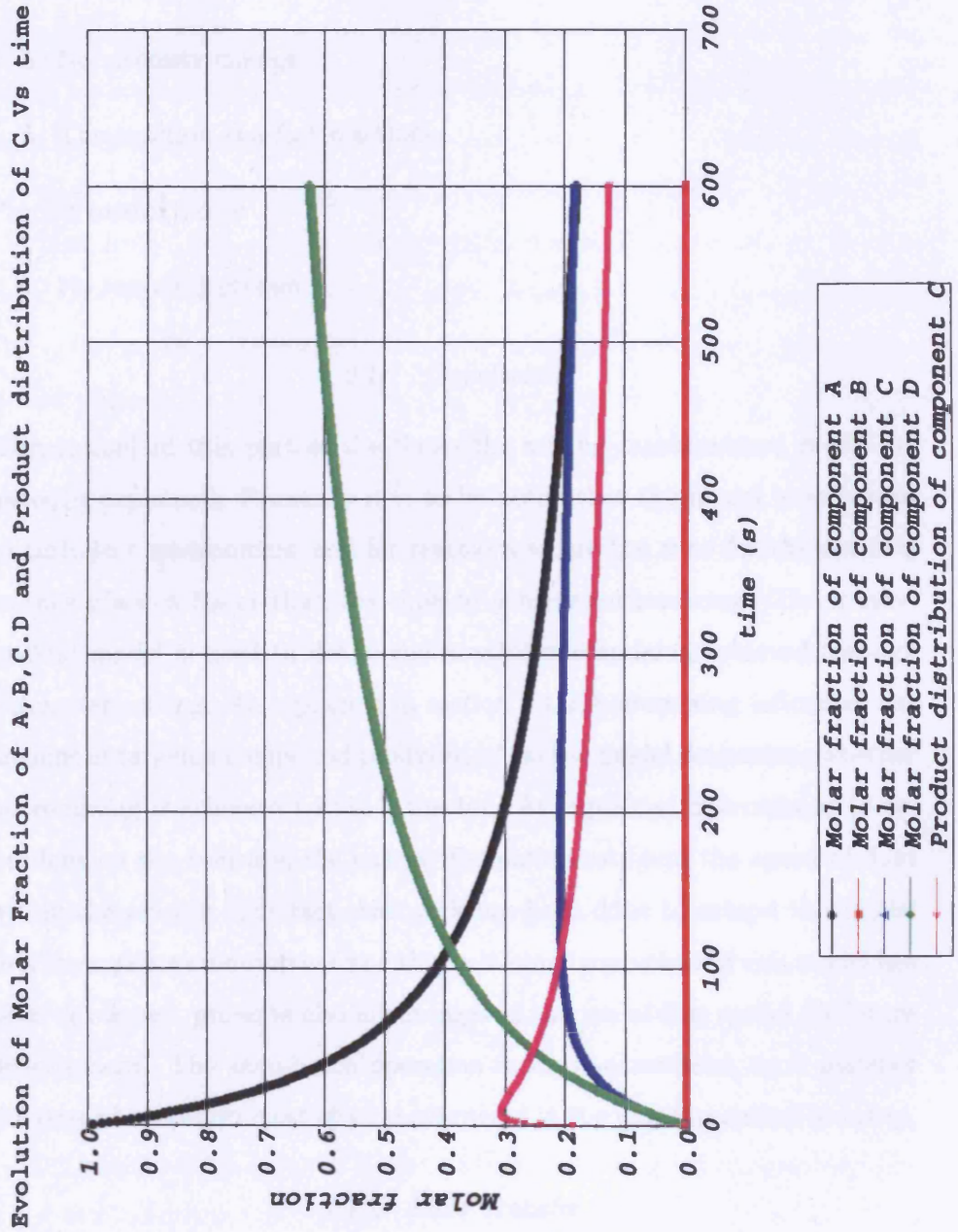

Fig. 2.9: Evolution of Molar Fraction of All the components and Product Distribution of Component C (P_{dC}) against Time

4. No phase change

5. No viscosity change

6. The reaction is a fast reaction

Process assumptions:

1. No recycling stream

2.1.7 Conclusion

[Conclusion] In this part of the thesis the mixing mathematical model selected is explained. Primarily it is to be noted that the model is restricted to turbulent environment and for reactions where the time for the reaction to take place is faster than the time to achieve micromixing. The mathematical model is used to define the level of micromixing achieved through parameter setting. As explained in section 2.1.2 micromixing influences the amount of targeted compound produced. Also the model determines whether micromixing is achieved within a reactor. As explained micromixing is dependent on the feedrate, the energy dissipation rate and the speed of fluid within the reactor. The fact that work has been done to extend this model to a three phase environment and that a laminar equivalent of this model has been developed, presents also advantages in the use of this model for future development. The semi-batch operation mode is considered, as it matches the type of operation most often encountered in the pharmaceutical industry.

2.1.8 Mass Transfer

The organic synthesis of various pharmaceutical compounds can often involve heterogeneous reactions [62]. The more intense use of catalysts has

also driven the pharmaceutical industry to face more often heterogeneous reactions i.e. Solid-Liquid, Gas-Liquid and Solid-Liquid-Gas. For example, when looking at the importance that asymmetric synthesis occupies nowadays in organic synthesis [34, 62], one can understand the increasing interest in mastering the scale-up of heterogeneous reaction systems.

Mass transfer in a heterogeneous reaction system can be one of the most influential factors for the scale-up, as the catalytic reaction process through the mass transfer of the reactant to the catalyst sites is the driving factor to the occurrence of the reaction [32]. This involves not only the transfer within the bulk fluid phase, but also the transport within the structure of the catalyst. The actual transport in the fluid phase can be slow, and thus the observed reaction rate is in fact affected by - and may indeed be dominated by - the mass transfer process [32]. In the case of a first order reaction, diffusion and kinetic rates have the exact same dependency on concentration. Also it is difficult experimentally to decouple the transport and kinetic processes. The case of diffusion and mass transfer is different as these two parameters have lower dependency on temperature, and therefore mass transfer-inhibited rates are characterised by an artificially depressed value of the activation energy (and the Arrhenius plot may yield a curve rather than a straight line) [32].

The mass transfer in a reactor occurs on several different scales:

1. Turbulent mass transfer from the bulk fluid to near the catalyst surface (1 - 100 mm)

2. Laminar mass transfer in the fluid boundary layer (or mass transfer film) about the catalyst particle (0.01 - 1 mm)

3. Diffusion within the porous structure of the catalyst (0.2 - 3 mm)

Aspects 1. and 2. above are largely dependent on the fluid properties (den-

sity,viscosity), the fluid velocity relative to the solid, and the size of channel in which the fluid is flowing.

A further complication can arise in liquid phase reactions involving a gaseous reactant, such as hydrogenation and oxidation. Commercially, these reactions are typically carried out in sparged stirred tanks or trickle beds. In this case, there is the added step of the gaseous reactant transferring into the liquid phase, en route to the catalyst surface. This opens up an additional area of mass transport in chemical reactors that depends critically on the inter-dispersion of the phases and the reactor hydrodynamics [32].

It has been reported that the mass transfer rate can be enhanced either by increasing the surface area between the gas and the liquid and/or by increasing the intensity of mass transfer fluxes through increasing the intensity of turbulence [73]. This requires the dissipation of additional mechanical energy. High performance gas-liquid contactors with high mass transfer rates are usually high consumers of mechanical energy [73]. Also while a sufficiently high mass transfer value is desirable, as not to limit the intrinsic rate, it may not be economic. Furthermore, the conversion of the key reactant may not be linearly proportional to the mass transfer coefficient ($k_l a$); thus, the return from increasing $k_l a$ may diminish beyond a certain level [112]. Gas/Liquid (G/L) mixing intensity is customarisedly quantified by a $k_l a$ or a value. The overall mass-transfer coefficient, k_l, is based on the liquid side concentration differential as the driving force for the mass transfer. The unit of k_l is $m.s^{-1}$ or equivalent. The G/L interfacial area per unit volume of the dispersion, a, has the unit of m^2/m^3 or equivalent. It is much easier to measure the product of k_l and a than the individual terms. The value of k_l depends upon the diffusivity of the dissolved gas in the liquid and the relative velocities between the gas bubbles and the liquid [57]. The typical value

range of $k_l a$ or a is a feature of G/L contactors and the power input. The energy dissipation rate rises with increasing power input into the contactor, resulting in greater turbulence, which is a major driving force for boosting a. A higher $k_l a$ can cut capital costs, because the same mixing duty can be achieved in a smaller device, or in a shorter batch time for a batch process or at a higher throughput rate for a continuous process [112].

The energy dissipation rate has been related over different studies to the mass transfer process [203, 129]. These studies concluded that power dissipation must be coupled to the transfer or mixing process and appear physically as its driving force. Villermaux offers some suggestions for the search of new scaling factors for the volumetric mass transfer coefficient $k_l a$ and for the specific power dissipation ϵ. Villermaux introduces the idea of developing a universal diagram for the comparison of different contactor [203]. This point of view is further developed with diagrams that allow to compare the mass transfer performance for gas-liquid contactors [73]. In these diagrams (see [73, 203]) it is noticeable that each type of reactor is defined by a specific range of achievable energy dissipation rates and a specific range of achievable mass-transfer coefficient, $k_l a$.

Mass transfer and energy dissipation rate have been correlated by mathematical expressions in the past [110, 28, 153, 58, 115]. The Eddy Cell model [110] for mass transfer in a turbulent fluid presents good results when compared to experimental cases [151, 154, 152, 123, 129]. In the Eddy Cell model, the mass transfer occurring into a single idealised eddy located near the interface is calculated. The overall effect of the turbulence, on the macroscopic mass transfer rate, is determined from a consideration of eddies of all sizes and energies, according to a proposed structure of the turbulent field. This model is considered to be applicable not only to bubbles in concurrent

turbulent flow, but equally also to any phase contacting situation in which fluctuating turbulent velocities make up the dominating velocity field [110]. The view adopted by Lamont and Scott [110], is that the small scale motions may be more efficient for interphase transfer, in spite of their low energy, because they cause mixing within the very surface of a large eddy. Lamont and Scott found that for well-developed turbulence, there exists a range of small scales of motion that are isotropic and dominated by inertial forces [110]. The expression that they developed for the overall transfer rate k_l is defined as follow :

$$k_l = 0.4 \left(\frac{\nu}{D_V}\right)^{(-1/2)} (\epsilon\nu)^{(1/4)} \quad (m/s) \tag{2.51}$$

with,

k_l : Liquid-phase controlled mass transfer coefficient (m/s)

D_V : Molecular diffusivity (m^2/s)

ϵ : Energy dissipation rate per unit mass (m^2/s^3)

ν : Kinetic viscosity (m^2/s)

The mathematical expression allows us to relate the overall mass transfer coefficient to the energy dissipation rate that is, as explained above, one of the main characteristics of a chemical reactor. Nevertheless the type of mass transfer sensitive reaction in this work are considered as non mixing sensitive. Also for the selection of reactor, the value of k_l will only be used to identified the type of reactor through table presented in the literature [112].

The choice of a suitable reactor for scale-up of a chemical reaction is the question of matching the reaction kinetics with the capabilities of the pro-

posed reactor [46]. The mass transfer model developed in this work includes the reaction kinetics see appendix C.2.

2.1.9 CASE STUDY: Mass transfer - Reactor selection

In the following a case study for the selection of a reactor for a mass transfer sensitive reaction is presented. The reaction system studied is given and then the modeling of the system is presented.

Reaction system description

The fundamentals of the mass transfer model are given in this part of the project - further details are provided in appendix C.2.

In order to present an up-to-date and interesting case for the scale-up of a mass transfer sensitive reaction, a reaction being studied by the group of Professor Gavriilidis at the Department of Chemical Engineering at University College London is hereby presented [185]. The reaction describes an asymmetric hydrogenation reaction known as the CATHy reaction (CATHy : catalytic asymetric transfer hydrogenation) is taken as a case study to evaluate mass transfer phenomena (see also [135]). Thanks to experimental results obtained on this particular reaction by the research group of Professor Gavriilidis [185], we were also able to compare experimental results to results obtained by modeling and verify the authenticity of the mathematical model developed.

The reaction system is described by the reaction system 2.52: [185]:
CATHy Reaction:

$$1 + \left(\frac{1}{2}\right) 2 \underset{k2}{\overset{k_1}{\rightleftharpoons}} 3 + \mathrm{HCl} \quad \text{(step1)}$$

$$\mathrm{HCl} + \text{sodium isopropoxide} \underset{k4}{\overset{k_3}{\rightleftharpoons}} \mathrm{NaCl} + IPA \quad \text{(step2)}$$

$$3 + \text{sodium isopropoxide} \underset{k_6}{\overset{k_5}{\rightleftharpoons}} 4 + \text{NaCl} \quad \text{(step3)} \tag{2.52}$$

And the reaction mechanism is described by scheme 2.10

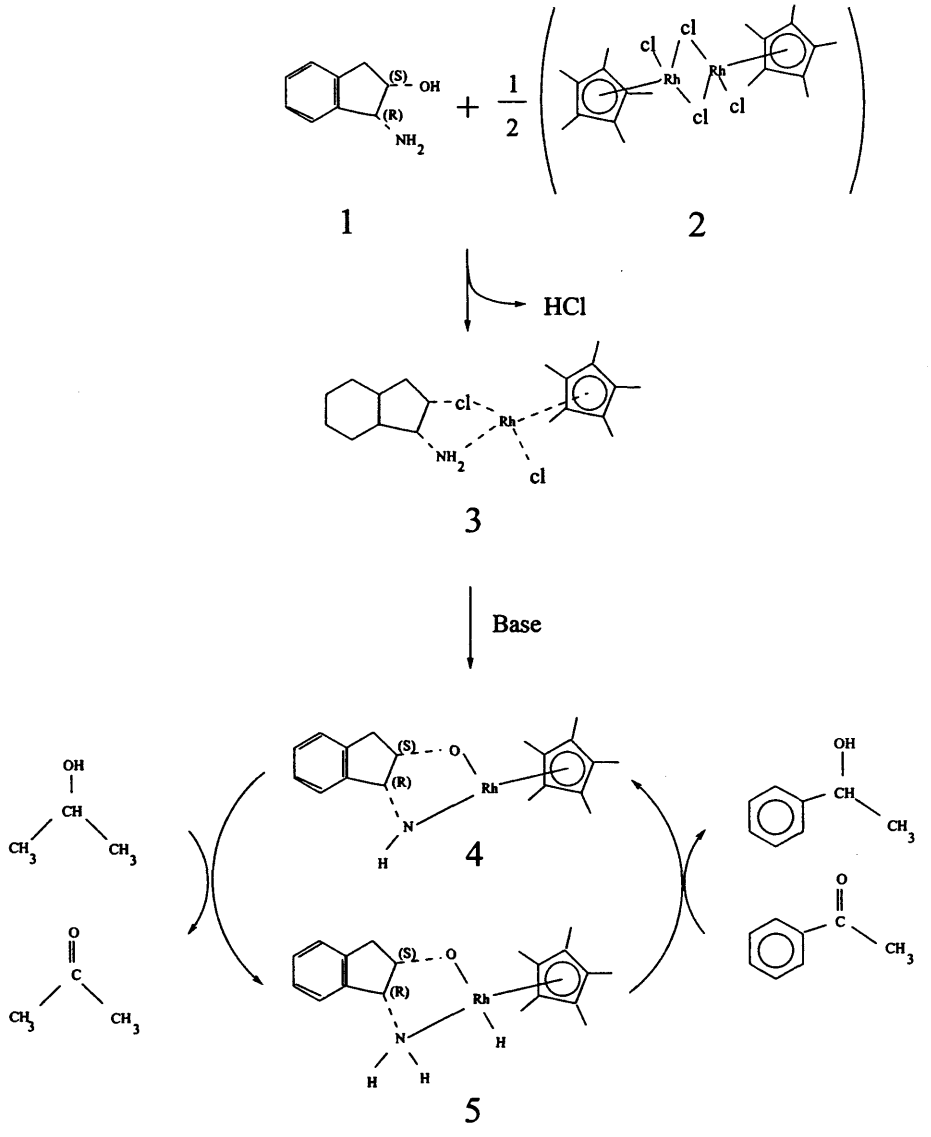

Fig. 2.10: Metal-Ligand bifunctional catalysis mechanism [185]

All the reactions in this reaction system occur in the liquid phase of the

system. No reaction occurs in the gas phase or in between the two phases involved as gas and liquid.

In the reaction system, see equation system 2.52, mass transfer of acetone occurs at the interphase of the gas and the liquid phase. The rate of mass transfer is proportional to the interstitial area and the concentration driving force. Acetone is being transferred from its liquid to its gas phase. The concentration of acetone in the gas phase is $C_{g(acetone)}$ and in the liquid phase is $C_{l(acetone)}$. The conversion of the liquid equivalence values from the liquid phase to the gas phase is carried out using the equilibrium relationship between the gas and liquid phase concentrations. In our case this is done by assuming Henry's law. Thus the gas phase concentration which is equivalent to $C_{l(acetone)}$ is $K_H C_{l(acetone)}$ where K_H is Henry's law constant. The overall driving force for mass transfer is $\left(C_{l(acetone)} - K_H C_{g(acetone)}\right)$, also the rate of mass transfer across the interface can be expressed by :

$$\text{Mass transfer rate} = k_l a V \left(C_{g(actone)} - K_H C_{l(actone)}\right) \tag{2.53}$$

as by assumption $Cg = K_H C_{l(acetone)}$, another expression is :

$$\text{Mass transfer rate} = k_l a V \left(\frac{C_{g(acetone)}}{K_H} - C_{l(acetone)}\right) \tag{2.54}$$

$k_1 = 25s^{-1}$ and $k_2 = 25s^{-1}$

Equations C.20 and equations C.30 represent the mass transfer for acetone between the liquid phase and the gas phase. The acetone gas-liquid as shown is equation 2.53, is influenced by factor $k_l a$, which is the mass transfer coefficient between the two phases.

Also in equation C.20 the change of concentration of acetone is expressed by the mass transfer occurring between the gas and the liquid phase in the gas phase minus the quantity of acetone removed from the gas phase by the

nitrogen .

All the equations for the mass transfer model are described in appendix C.2

Operation mode

In order to compare with the operation mode used in the development of the CATHy reaction [185], a batch operation was modeled. The reactor is considered as being loaded with an original amount of solution and catalyst. Nitrogen is assumed being bubbled perfectly through the reaction (i.e. no preferential path) following flowrates indicated by Professor Gavriilidis team [185] and is used as such to create an inert blanket over the reaction. The reactant is fed to the catalytic solution in one injection and the operating conditions are the one specified by Professor Gavriilidis research group [185].

Experimental results Versus mathematical model results

In this section the experimental results obtained for this reaction are compared to results obtained with the mathematical model.

The operatus modi was as follow:

Model validation:

This experimental data were obtained by the research group of Professor Gavriilidis in a simple batch laboratory reactor consisting of a round bottom flask operated at constant temperature [185]. A continuous nitrogen flow was used to ensure inert atmosphere and to strip acetone. The reaction network and the kinetic mechanism with the values of the rate constants at $30°C$ is described below with the initial conditions in terms of volume of the liquid phase, concentration of reactants and catalyst. Also, recorded concentration of acetophenone [Sub] as main reactant, acetone [$acetone$] as by-product and

the enantiomeric products $[R - Prod]$ and $[S - Prod]$ are given in order to compare the model prediction with the recorded experimental data as function of time [185].

The experimental set-up is described as follow:

A simple batch laboratory reactor consisting of a round bottom flask is operated at constant temperature. A continuous nitrogen flow is used to ensure inert atmosphere and to strip acetone. The reaction is run at a constant temperature of $30°C$. The initial conditions in terms of volume of the liquid phase, concentrations of reactants and catalysts is given as such by table 2.3 :

Tab. 2.3: Initial conditions for the Mass-transfer limited reaction

Initial conditions	Value
Liquid phase volume	257 ml
N_2 flowrate	890 ml/min
Sub concentration	0.144 mol/l
$RhL*$ concentration	$0.144.10^{-3}$ mol/l
Temperature	$30°C$
Pressure	1 bar

The rate constants were provided by Prof. Gavriilidis F-Team and are presented in table 2.4 [185].

The results obtained are listed in table 2.5 and the comparisons of the results obtained experimentally and through the mathematical model developed in 2.1.9 are listed in table 2.6

As shown in table 2.6 the percentage of error between the experimental results and the results achieved with the mathematical for the percentage of Conversion obtained versus time are small for conversion over 85% i.e.

$TIME > 30min$. The error can be considered negligible for $conversion >$ 92% as the % error is then less than 1%.

Assumptions for mass transfer model

The following assumptions have been made for the application of the mathematical model described in this chapter. Assumptions are made at two different levels, the first level refers to the application of the model itself, and the second level refers to the process itself.
Model assumptions:

1. Raoult's law is followed by the reaction system i.e. that the gas mixture in equilibrium with an ideal liquid solution also follows the ideal-gas law

2. Perfect mixing is assumed and the reaction is not considered as mixing

Tab. 2.4: Rate constant for mass transfer limited reaction [185]

Rate constant		Units
k_1	37.5	l/(mol.min)
k_2	3677.5	l/(mol.min)
k_3	15162.7	l/(mol.min)
k_4	27.7	min^{-1}
k_5	5478.0	l/(mol.min)
k_6	511.5	min^{-1}l
k_7	655.9	min^{-1}
k_8	80390.8	l/(mol.min)
k_9	114.4	min^{-1}
k_{10}	3430.9	l/(mol.min)

Tab. 2.5: Summary of experimental results achieved for the Mass-transfer limited reaction (CATHY reaction)

TIME (min)	Sub	Acetone	R-prod	S-Prod
min	mol/l	mol/l	mol/l	mol/l
0	0.1452	0	0	0
2	0.1101	0.0315	0.0023	0.031
4	0.0887	0.055	0.0036	0.05
6	0.0732	0.068	0.0047	0.064
8	0.0621	0.075	0.0054	0.0744
10	0.053	0.0779	0.006	0.0812
15	0.04	0.092	0.0071	0.0952
20	0.0322	0.0962	0.0078	0.01025
30	0.0244	0.0936	0.0084	0.1106
40	0.0215	0.0872	0.0087	0.1127
60	0.0174	0.0732	0.0094	0.1202
90	0.0143	0.058	0.01	0.1262
120	0.0118	0.0457	0.00105	0.1323
180	0.089	0.0266	0.0116	0.1429
240	0.0067	0.0165	0.01256	0.15421

Tab. 2.6: Comparison between Conversion versus Time obtained with the mathematical model and the experiment

TIME (min)	Conv	Conv.	% ERROR
min	Exp.	Model	Conv.
0	0	0	0
2	0.2593	0.2226	16.5
4	0.4119	0.3421	20.4
6	0.5202	0.4302	20.9
8	0.5978	0.5333	12.1
10	0.6556	0.5582	17.5
15	0.7476	0.6659	12.3
20	0.7983	0.7375	8.2
30	0.8495	0.8162	4.1
40	0.8671	0.8509	1.9
60	0.8962	0.8812	1.7
90	0.9168	0.9085	0.91
120	0.9327	0.9293	0.36
180	0.9526	0.9580	0.57
240	0.9667	0.9751	0.85

sensitive

3. The conversion of the liquid equivalence values from the liquid phase to the gas phase is carried out using the equilibrium relationship between the gas and liquid phase concentrations. In our case this is done by assuming Henry's law

4. The system is constituted by two phases, a liquid phase and a gas phase. The reaction only occurs in the liquid phase of the reaction system

5. No phase change

6. No viscosity change

Process assumptions:

1. No recycling stream

2. Batch operation

2.2 Other factors influencing Scalability

2.2.1 Heat transfer

The process objectives in heat transfer are varied. It is important to determine what is to be accomplished and the process equipment needed to handle the requirements Heating, melting, cooling, freezing, crystallisation, etc... Low heat removal may cause the product to burn. High heat removal rates may not permit the reaction to 'kick off'. If the process becomes very hot safety issues arise; Most reactions are exothermic and require heat removal to prevent runaway and side reactions. Runaway reactions are undesirable. Side reactions cause separation problems in downstream processing.

Heat transfer in reactors can be carried out in several ways, external heat exchanger, internal heat exchanger, coil, tubes, jacket... The rate of heat transfer is directly proportional to the surface area [144], and for vessels cooled externally the rate of heat transfer decreases as the volume increases, indicative of the fact that the ratio surface area over volume reduces as the volume increase in size. The cooling rates attainable in scale-up vessels will be considerably slower than those of small laboratory vessels. Efficient stirring allows for improved heat transfer and minimises impurity formation from any localised hot spots with in the vessel and permits to be maintained the desired temperature profile in the reactor [12]. Typically, in heat transfer processes in chemical reaction engineering, there are two engineering objectives [6]:

- To have a good fluid circulation in the bulk of the tank
- To have good fluid exchange and circulation to and from the heating and/or cooling element. Often, the elimination of local hot spots becomes a primary objective since hotspots can cause loss of product quality [6].

Heat transfer becomes an important objective in larger processes and may become limiting factor on the size of the process. Some volume processes, such as exothermic reactions, release significant amounts of heat. Heating and cooling jackets are not effective on volume processes [51]. Extensive heat and cooling coils are after added to obtain the area necessary for heat transfer in large-volume systems such as reacting and cooking processes [51].

On scale-up from a small-scale process with no internals to a large-scale process with massive internal, circulation patterns are altered and prediction of heat-transfer coefficients using an appropriate correlation becomes difficult

[29]. Often, dead zones can form and effectively lower heat-transfer areas. The reduction in heat transfer is not due to fouling [51]. In design of a heat transfer process, there are usually [51]:

- An anticipated heat transfer coefficient
- A known fixed heat transfer area
- A known fixed temperature difference

The amount of transfer is a process result that can be used to determine whether the anticipated transfer is actually occurring. Often, the anticipated heat-transfer coefficient is higher than the 'delivered' coefficient. This difference can be due to a reduction in flow circulation over the heat-transfer surface. In these cases, calculations can be done to determine the effective impeller Reynolds number that the heat transfer senses. These calculations should be done with heat-transfer data in which fouling has not yet occurred [51].

The addition of another phase such as a gas complicates matters even further. In this situation, gas will lower the heat transfer coefficient and adversely affect the liquid circulation. Bubbles can become attached to heat transfer areas. Gas pockets can also form over heat-transfer surfaces [95, 60]. Heat transfer also becomes a major problem under laminar flow situations. Without good circulation materials may burn on the heating element, or the heating element may overheat and be destroyed. Laminar flow mixing is notorious for not having good circulation, particularly for viscoelastics fluids [51].

2.2.2 Multiphase system impact

Good contacting between phase in multiphase reactors is essential to promote interphase transport of species and energy. However, in many circumstances this is hard to achieve, as the state of uniform spatial distribution of the various phases is unstable and gives way to nonuniform structures, spanning a wide range of length and time scales [186]. Macro-scale coherent structures, and which are responsible for large-scale coherent structures, which are responsible for large-scale mixing, are commonly observed [3]. Their formation, growth, and propagation are influenced by reactor size, as well as reactor inlet and outlet configurations; this relationship is poorly understood. Consequently, the chemical industry continues to rely on expensive pilot-scale cold flow experiments and remain unsure of the effects of heat transfer, operating pressure, and temperature [213, 4, 68]. In the absence of generic mathematical models modeling multiphase system impact, is done with continuum hydrodynamic models which have been formulated by averaging over details at the length scale of few particles or bubbles will have to be used [42], while models that match the macro-structure are developed [186].

2.3 Discretisation and computer implementation

A fundamental aspect of computers is the fact that all computers are limited in their resources. No computer has unlimited memory and unlimited speed. Thus, in order to make the best use of the resources they can provide, and solve the mathematical equation system faced, for example, in the case of a differential equation, the solution will be only represented at a limited number of values of the independent variable(s). Because solving a continuous

function will require infinite memory. This process is called discretisation, and is fundamental to all numerical analysis. The differential equations employed in process modeling are continuous approximations to nature's phenomena, which are discontinuous at the atomic level. The mathematical model described in this chapter has been solved with the software gPROMS - general PROcess Modeling System [140]. gPROMS is a general-purpose process modeling and simulation software package. It allows the modeling and the simulation of combined discrete and continuous processing system of arbitrary complexity. One of the key concept in gPROMS is that of the process entity combining a continuous model entity with a set of task entities describing external actions. It can also simulate multiple interacted process entities which also presents a very useful asset [140].

2.4 Conclusion

In this part of the project we presented the mathematical models used to evaluate mixing and mass transfer occurring in a chemical reaction.

The mixing mathematical model selected is detailed and explained and its simulation features are given. Primarily it is to be noted that the model is restricted to turbulent environment and for reactions where the time for the reaction to take place is faster than the time to achieve micromixing. The mathematical model is used to define the level of micromixing achieved through parameter setting. As explained in section 2.1.2 micromixing influences the amount of targeted compound produced. Also the model determines whether micromixing is achieved within a reactor. As explained micromixing is dependent on the energy dissipation rate and the speed of fluid within the reactor, and the feedrate in the case of the semi-batch reactor. The fact that work has been done to extend this model to a three phase en-

vironment and that a laminar equivalent of this model has been developed, presents also advantages in the use of this model for future development. Semi-batch and continuous operation mode is considered, as it matches the type of operation most often encountered in the pharmaceutical industry. Also two micromixing models have been implemented with gPROMS i.e. a semi-batch micromixing model and a continuous micromixing model.

The mass transfer mathematical model selected is detailed and explained. The model presented is a generic model. The assumptions made are that the model follows Raoult's law, that the reaction is not mixing sensitive, that the system is constituted by two phases a gas and a liquid phase and that the reaction occurs in the liquid phase. It is also assumed that there is no phase change and no viscosity change and finally Henry's law is also assumed. The operating mode considered is a batch system. The level of mass transfer achieved being related to the value of the mass transfer coefficient and is specific to each type of reactor. This permits the best reactor to be identified by linking the value found through optimisation to values found in the literature. The mass transfer model selected in this thesis has been developed and has been implemented with gPROMS. This model has been validated with experimental results.

Finally we also looked at other potential factors which could influence scaleability i.e. heat transfer and multiphase reaction systems. These two factors are not investigated further in this work but are nevertheless considered when looking at improvement that could be brought to this work.

3. DEFINITION OF UNCERTAINTY

As shown in the previous chapter, the optimisation of the set of parameters defines the type of reactor and its design. This optimisation provides the optimum solution(s) to achieve the lowest loss for the synthesis of a compound through a particular reaction system. The scaling up of a system is dependent on uncertain data. Evaluating the impact that the uncertainty of these data has on the results would refine further the choice of the best reactor. The purpose of the project is to reduce the degree of failure occurring during scale-up. Also understanding the impact that some uncertain data carry through the models and the optimisation allows to reduce or eliminate certain reactor options. The modeling of uncertain data can be done via various mathematical tools e.g. Sensitivity Analysis, Interval Mathematics, Bayesien Statistics, Fuzzy Data Analysis [27]. It has been underlined that amongst these different possible methods to represent model uncertainty, the chosen approach depends essentially on the knowledge or preference of the practitioner and not on the specificity of the given problem [27]. In this study, besides the expression of uncertainty, there is an interest in studying the sensitivity of the models used to the different parameters involved i.e. to identify the parameters that have the biggest impact on models output. Following this interest, sensitivity analysis was considered as the best mathematical tool to carry out this type of evaluation.

3.1 Evaluation of uncertainty by sensitivity analysis

Sensitivity analysis is described as the study of how the variation in the output of a model can be apportioned [169], qualitatively or quantitatively, to different sources of variations, and of how the given model depends upon the information fed into it. A large number of methods exist to carry out a sensitivity analysis on a particular model [169, 141]. Also to define the best sensitivity analysis method to characterise the impact of model parameter uncertainty on the results, we looked at the different parameters involved in the mathematical models used(see section 2.1.4). Thus we identified the parameters for which a degree of uncertainty exists in their determination. The parameters carrying uncertainty are the parameters which are experimentally determined and which are part of the input of the models. These parameters are listed below :

For the micromixing model - semi-batch and continuous

ν :Kinematic viscosity (m^2/s)

k_j:Reaction constant ($\frac{m^3}{mol.s}$)

For the mass transfer model

K_H :Henry's constant (-)

In the case of the micromixing model, the reaction rates of a chemical reaction system have traditionally been difficult to determine, due to the fact that the kinetic rates can be influenced by various factors like the nature of the ions being used, the concentration of the reactants, the temperature increase and decrease, catalysts and the surface area. Due to all the different factors it is difficult to obtain precise data for the scale-up of a reaction. More

fundamentally, the making of some drugs requires more than one organic reaction steps. Therefore the understanding of the impact of the uncertainty carried by the different kinetic rates involved in the different steps, would be beneficial to this study. It will allow us to determine which reaction steps could most undermine the production of the targeted compound. The case of the mass transfer model is similar to the micromixing model though the parameter considered here is the Henry's constant. Henry's constant is a parameter specific to each type of reaction system and differs widely from one reaction to another. It is also a parameter which is difficult to identify experimentally. It is usually done through the use of solubility curve and the accuracy achieved can be limited. Also looking at the impact that uncertainty within this parameter (K_H)has on the reactor selection was considered of interest.

It is understood and assumed that the reaction is not temperature sensitive to a level high enough to create reason for concern, in the case of slight temperature variation [185]. Also the uncertainty carried by temperature variation was not studied. In the case of the different rate constants we assume that the uncertainty attached to there determination is low. The reaction rate constants were determine with purpose built instrumentation and they have been shown as robust [35, 33]

It is to be noted that the selection of reactor in this reactor selection procedure does not depend on the parameters chosen nor on the number of parameter chosen. The number of parameters chosen will nevertheless have an impact on the speed at which a solution will be found.

It will also allow further study of the organic reaction step(s) identified as having a strong impact on the reactor-reaction system in the case of the micromixing model. It will allow us to evaluate the importance of the Henry's

constant identification accuracy in the case of the mass transfer model.

Also having identified which parameter(s) will impact the most the scale-up of a reaction system, further experimental work could reduce the uncertainty carried by the parameter and make scale-up more straight forward.

The aim of this part of the project then becomes to express the uncertainty carried by the various parameters and evaluate their influence on the mathematical model output e.g. the product distribution (see equation 2.50 page 83) of the targeted product.

To illustrate the following we take the case of the micromixing model. Also if we consider the same reaction system as in section 2.1.6 i.e.:

$$A + B \xrightarrow{k_1} C \tag{3.1}$$

$$B + C \xrightarrow{k_2} D \tag{3.2}$$

which can be considered as a simple reaction system with regard to some drug organic synthesis. Reaction rate k_1 influences the production of compound C. k_2 influences the production of compound D through the consumption of the targeted product C. Therefore these two parameters have both a impact on the production of the targeted compound C. Also the impact of uncertainty on these two parameters has to be considered simultaneously on both. This type of study is called global sensitivity. It provides information about the behaviour of each dependent variables k_i in response to simultaneous, large variations in all the input parameters. This method differs from other sensitivity analysis methods called local sensitivity analysis by the fact that in the latter the local response of the output(s), obtained by varying input factors one at a time, is investigated while holding the others fixed to a central (nominal) value. This involves partial derivatives, possibly normalised

by the nominal value of the factor or by its standard deviation. The analysis is run at a given point in the space of the input factors, and the volume of the region explored is nil [169, 199]. In Global sensitivity analysis the space of the input factors is explored within a finite region and the variation of the output induced by a factor is taken globally - that is averaged over the variation of all the factors [169, 199]. This methodology offers the advantage of being faster than local sensitivity analysis as all the parameters are changed one at a time. Given that the number of parameters carrying uncertainty in a model can be larger than two or three, and that the number of function evaluation increases drastically with the number of parameters involved, global sensitivity analysis presents a functional solution to the problem.

Among the different possible global sensitivity analysis methods which can be found [169], modelers conduct sensitivity analysis for a number of reasons including the need to determine :

1. Which input parameters contribute the most to output variability and, possibly, require additional research to strengthen the knowledge by reducing output uncertainty;

2. Which parameters are significant and can be eliminated from the final model;

3. If and which (group of) parameters interact with each other;

4. The optimal regions within the parameters space for use in a subsequent calibration study

There are many different ways to perform sensitivity analysis [169], but just a few are able to tackle the item (1), which would allow to reduce the level of uncertainty carried through the system. This could be done

by either reducing the level of uncertainty carried by the most uncertain parameter. Another possibility would be to choose a solution for which the impact of uncertainty on the parameters is less stringent on the scale-up of the reaction system. We will more specifically be looking at using the variance-based methods [173], in which the variability, or uncertainty, associated with an important input parameter is propagated through the models resulting in a large contribution to the overall output variability. Global sensitivity methods are able to estimate the main effect contribution of each parameter to the output variance [169]. However, it can happen that whether a parameter is influential or not it depends on the interactions and influences of all parameters [188]. This is not always measured by all the global sensitivity analysis methods. We will therefore focus on the sensitivity analysis methods able to provide this type of information, like the Fourier Amplitude Sensitivity Test (FAST) method [54, 120], the Sobol method [179, 180], and the extended FAST and SOBOL methods [170, 168]

3.2 *Fourier Amplitude Sensitivity Index - FAST*

The Fourier Amplitude Sensitivity Test method is a procedure that can be used for both uncertainty and sensitivity analysis [54]. The FAST method is used to estimate the expected value and variance of the output, and the contribution of individual inputs to the variance of the output [54]. The FAST method is independent of any assumptions about the model structure, and works for monotonic and non-monotonic models [169]. The effect of only one input(local sensitivity) or the effect of all inputs varying together can be assessed by FAST. The main feature of the FAST method is a pattern search method that selects points in the input parameter space, and which is reported to be faster than the Monte Carlo method [120].

A transformation function is used to convert values of each model input to values along a search curve. As part of the transformation, a frequency must be specified for each input. By using Fourier coefficients, the variance of the output is evaluated [54]. The contribution of input x_i to the total variance is calculated based on the Fourier coefficients, fundamental frequency ω_i, and higher harmonics of the frequency [55]. The ratio of the contribution of each input to the output is referred to as the first order sensitivity index and can be used to rank the inputs [169]. The first order indices correspond to the contribution of individual inputs and not to the contribution of interactions amongst inputs. To account for the residual variance in the output due to higher order or interaction terms that is not explained by first order indices, the extended FAST method is used [168]. The model needs to be evaluated at sufficient number of points in the input parameter space such that numerical integration can be used to determine the Fourier coefficients [168]. The minimum sample size required to implement FAST is approximatively eight to ten times the maximum frequency used (see appendix D). In the case of discrete inputs, if a sufficiently large sample size is not available, then the output can have frequent discontinuities. In such a case, the Fourier coefficients may not be estimated properly and hence, the reliability of the results can be adversely affected.

The advantages and disadvantages of the FAST method are summarised as follow:

Advantage: The FAST method is superior to local sensitivity methods because it can apportion the output variance in the inputs. It also can be used for local sensitivity analysis with little modification [69]. It is model independent and works for monotonic and non-monotonic models [169]. Furthermore, it can allow arbitrarily large variations in input

parameters. Therefore, the effect of extreme events can be analysed [118]. The evaluation of sensitivity estimates can be carried out independently for each factor using just a single set of runs [168]. The FAST method can be used to determine the difference in sensitivities in terms of the differing amount of variance in the output explained by each input and, thus, can be used to rank order key inputs.

Disadvantage: The FAST method suffers from computational complexity for a large number of inputs [168]. The classical FAST method is applicable to models with no important or significant interaction among inputs [168]. However, the extended FAST method can account for high-order interactions [170]. The reliability of the FAST method can be poor for discrete inputs [169]

It is to be noted that the classical FAST method has been implemented in this work as no interaction among inputs has been assumed from the definition of the parameter selected and that the inputs to FAST are continuous inputs and not discrete inputs.

The mathematical implementation of the FAST method is described in appendix D

3.3 Conclusion

Uncertainty is a very important factor in a process scale-up operation. The pharmaceutical industry favours process equipment that offers the lowest level of uncertainty. The purpose of this part of the project is to evaluate the parameter uncertainty carried out through the model and the objective function in order to estimate their impact on the result of the optimisation i.e. on the selection of a chemical reactor. A method to carry out sensitivity

analysis to evaluate the impact of the different parameters and their respective uncertainties on the mathematical model has been selected. The Fourier Amplitude Sensitivity Index (FAST) carries out *Global Sensitivity Analysis.* Global Sensitivity Analysis describes the effect of simultaneous large variations of all parameters on the dependent variables. FAST is a sensitivity analysis method that is independent of any assumptions about the model structure. The core feature of FAST is that it explores the multidimensional space of the input factors by a search curve that scans the entire input space. The output values allows us a better understanding of the model, like which input parameters, contribute most to the output variability. This can then be used to further refine the model or reduce the uncertainty of the most influential parameters through better lab experiments.

4. OPTIMISATION

4.1 Single objective optimisation

In this part of the project various optimisation techniques have been looked at and evaluated for the case of a single objective optimisation. This allowed us to determine the type of optimisation technique which proved the most effective. Special attention is given to local optimisation techniques. The use of the reactor selection is chosen for the development of conceptual reactor design. And also the reactor selection use is targeted to be used at the very early stage of the process development. Therefore the research of various possibilities of reactor design primes to the selection of the global optimum reactor design. This justifies the use of local optimisation techniques versus global optimisation techniques.

In this chapter, first a summary of the different optimisation methods used is given. The definition of the objective function that characterises our aim i.e. maximise profit, through the optimisation of some selected parameters constituting the objective function. We then describe the different optimisation methods, and an account of the result obtained is given. Though our objective is to maximise the profit made, the different optimisation methods used are minimiser methods. Also in this chapter we will be working on minimising the loss through the optimisation of different selected parameters of the objective function given that we will consider: loss= − Profit

4.1.1 Optimisation using direct search methods

In order to solve the afore mentioned optimisation problem, various optimisation programs have been used. Given that the objective function is highly discontinuous as a result of the nature of the model i.e. due to the discretisation as described in section 2.1.4, the model is therefore not defined by a continuous equation. Also, it was decided to avoid using search methods using gradient, as the derivative of the function cannot be directly explicit but would rather be estimated. Direct search algorithms were favoured and have been used to evaluate the objective function [97]. The aim of the optimisation is to find the maximum of the objective function as defined in section 4.1.1.

Direct search methods are based on using values of the objective function taken from a set of sample points, and use that information to continue the sampling. The problem itself being the adjustment of the variables so that the function becomes least, where each value of the function is returned by a subroutine for each trial vector of variables. The direct search methods can be described as optimisation methods which consists of comparing each trial solution with the best previous solution. Three of these methods were used as the *Nelder-Mead simplex* algorithm, the *Hooke-Jeeves* algorithm and the *multidirectional search* algorithm.

Constraints and penalty function

Penalty function is a technique for introducing constraints into an otherwise unconstrained minimisation problem, the name comes from the idea of adding a penalty for the violation of constraint. The traditional concept is to augment the objective with a function and one positive constant, so that the original mathematical program is replaced by solving a parametric family

of the form $Maxf(x) - uP(x) : xinX^0$. The function, P, is called a penalty function if it satisfies $P(x) > 0$ for x not feasible and $P(x) = 0$ if x is feasible. The set X^0 depends on the type of penalty function, and there are two classical types, each requiring P to be continuous: interior (or barrier) and exterior. A penalty function is exact if there exists a finite parameter value such that its maximum is a solution to the original mathematical program [65].

Direct search methods used for optimisation : Description

In the following section a description of the different direct search methods that have been implemented to solve the optimisation problem is given. An account is given for each method of the way the search algorithm is developed :

Hooke-Jeeves :

In the Hooke-Jeeves algorithm at each iteration, the method first defines a pattern of points by moving each parameter one by one, so as to optimise the current objective function [88]. The entire pattern of points is then shifted or moved to a new location; this new location is determined by extrapolating the line from the old base point in the m (in our case m = 5) dimensional parameter space to the new base point. The step sizes in this process are constantly adjusted to converge intently on the respective optimum. A starting vector of variables x_1 has to be given, and k= 1,2,3,...., the k^{th} iteration derives $x_k + 1$ from x_k in the following way. A non zero search direction d_k is chosen. This move that defines a new base point from the initial point represents what is also called the pattern move [88]. If $f(x_{k+1}) < f(x)$ then a succession of so called exploratory moves are conducted where

the function is sampled at successive perturbations of the base point in the search direction v_j. v_j is the j^{th} column of a direction matrix, i.e. that a single co-ordinate of the point is varied to see whether a successful move can be made by either increasing or decreasing this co-ordinate by a prescribed step size. Then the function of one variable $\phi(\alpha) = F(x_k + \alpha d_k)$, is evaluated, in order to identify a new vector of variables of the form :

$$x_{k+1} = x_k + \alpha d_k \tag{4.1}$$

If $f\left(x_{v_{j+1}}\right) < f\left(x_{v_j}\right)$ then the new point $x_{v_{j+1}}$ is recorded and becomes the new base point. If the new objective function value is not minimised then the previous point co-ordinates are kept and a different exploratory move is made. If the exploratory move is successful then the search direction becomes $d_k = x_{v_{j+1}} - x_{v_j}$. If the exploratory move is successful then another pattern move is performed from $x_{v_{j+1}}$ of length $d_k = x_{v_{j+1}} - x_{v_j}$ which means that the objective function is tested at a new co-ordinate

$$\begin{aligned} x_w &= x_{v_{j+1}} + d_k \\ x_w &= x_k + 2d_k \end{aligned} \tag{4.2}$$

If this second exploratory move fails to minimise the objective function, then an exploratory move with $x_{v_{j+1}}$ as the centre is tried. If this fails then d_k is reduced, and the search process is restarted from the last successful base point. This 'double move' presents the advantage of avoiding to use some of the same points that were evaluated in the previous exploratory move.

The purpose of this methodology is to determine α

It has been expressed that this method, which can give encouraging results [72], presents the disadvantage that points may be sampled more than once which makes the method more time consuming [97].

Nelder-Mead algorithm : This method also called *simplex method* [132], constructs a simplex in d-space, a figure with (d+1) vertices i.e. a simplex is a geometrical figure formed by N+1 points in a N-dimensional space, like a triangle in a plane or a tetrahedron in the three dimension space. The Nelder-Mead simplex finds an approximation of the extremum of a function by considering the worst point of the simplex and forming its symmetrical image through the centre of the opposite (hyper)face, as shown in figure 4.1 :

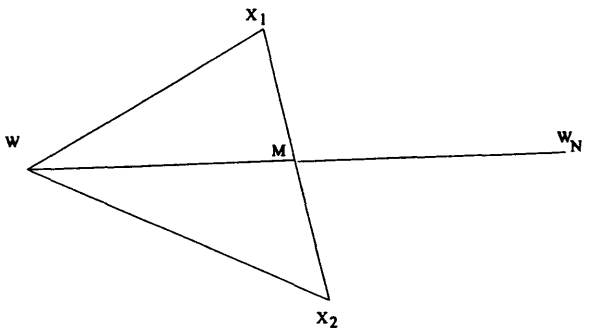

Fig. 4.1: Nelder-Mead simplex creation

At each iteration, the method evaluates the function at one or more trial points whose location depends on the relative values of the function at the vertices and at earlier trial points. The purpose of each iteration is to create a new simplex in which the previous worst vertex, i.e. the vertex with, in our case, the largest value of the objective function has been replaced as our goal is to minimise the objective function.

The Nelder-Mead algorithm is best described geometrically, as follows: For N variables, Nelder-Mead first generates N initial points in addition to the one given by the user, to form an N-dimensional simplex, the geometrical figure consisting of N+1 points (or vertices) and their interconnecting line segments. In two dimensions, a simplex is a triangle. The N initial points are generated by keeping the initial point given by the user as a base, and varying each variable at a time by randomly either adding or subtracting the initial value, by the amount in between the initial value to either the minimum or maximum value specified, whichever allows to keep the value within the range in which the initial point is bounded by. After the initial simplex has been generated, Nelder-Mead takes a series of steps, most steps just moving the point of the simplex where the function is largest ('highest point') through the opposite face of the simplex to a lower point, as previously illustrated. These steps are called reflections, and the relative step length is determined by an argument. After a successful reflection, the method tries to expand the simplex in the same direction to take larger steps. The optimisation process terminates if:

1. The largest relative change in the objective function is smaller than a given tolerance value e.g. in our case the tolerance value - l = 1E-6
2. The largest relative change of the optimisation variables is smaller than a given tolerance value (not specified in our case)
3. The optimisation specifications are met e.g. budget = maximum number of iteration, not specified in our case

It has been found that this method is not guaranteed to converge [97,

119].

Multi-Directional Search : The Multi-Directional Search (MDS) method is based on the algorithm first developed by Torczon et al. [195] for execution on a multi processor machine. The main difference between the MDS and other simplex searches is that, during a reflection step, rather than simply reflecting the vertex with, as in our case, the greatest function value through the centroid of the other vertices. The MDS method instead, reflects all vertices through the best vertex, V_0^k. As a result, each iteration of the MDS algorithm involves two simplices : a primary simplex and its reflection through the current best minimiser, V_0^k. The algorithm uses a 'greedy' approach to function sampling : function values are calculated only until a new minimiser is found. If a new minimiser is identified in the reflection simplex, see figure 4.2:

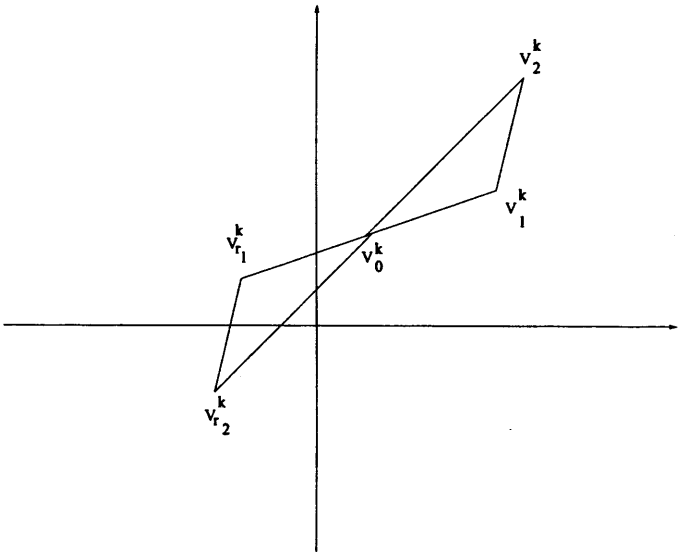

Fig. 4.2: Multidirectional reflection move

the reflection simplex $V_0^k, V_{r1}^k V_{r2}^k$ becomes the new primary simplex with

the newly identified minimiser as its new starting point, also called basepoint, and a new reflection simplex is constructed. Supposing that one of the new vertices does satisfy the acceptance criteria, in our case minimising the objective function, the algorithm then tries to see if further improvement could be found by considering an even longer step size. Also the algorithm takes a step from the best vertex, V_0^k, in each of the original n search directions, but now each step is twice as long as the algorithm *expands* the trial simplex by doubling the length of every edge in the reflected simplex to give the new simplex $V_0^k, V_{e1}^k V_{e2}^k$ see figure 4.3

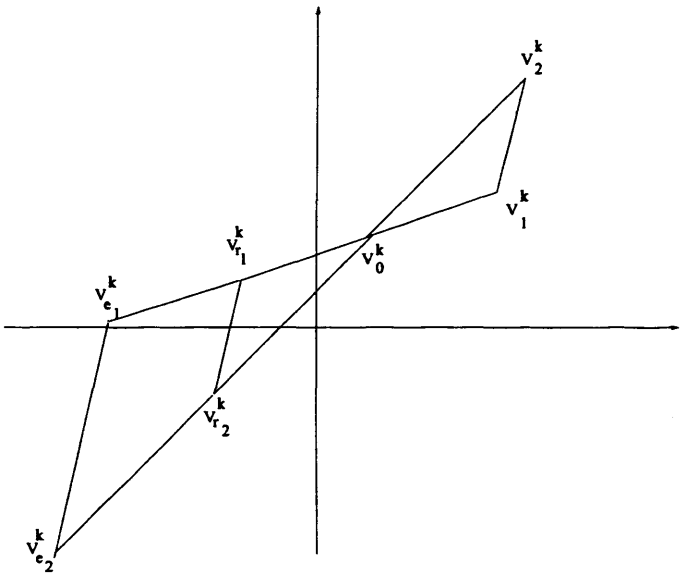

Fig. 4.3: Multidirectional reflection and expansion move

If all 2n+1 points in both primary and reflection simplices have been evaluated with no improvement found, the primary simplex shrinks around the basepoint V_0^k and creates the new simplex $V_0^k, V_{c1}^k V_{c2}^k$, and a new iteration is begun, with a smaller simplex, this move is also called

the contraction, see figure 4.4.

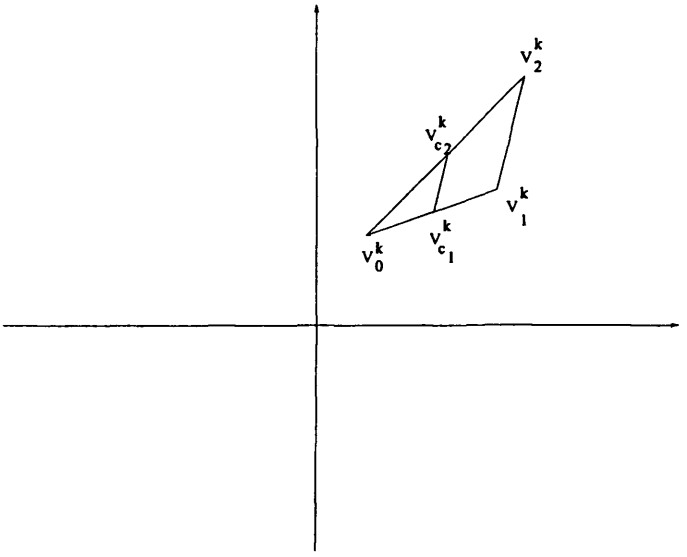

Fig. 4.4: Multidirectional contraction move

The major difference between this method and the Nelder-Mead optimisation method, is that in the Multi-Directional Search method each new simplex created is made congruent to the previous one as shown in figure 4.5.

It is to be noted that unlike the simplex methods discussed above as the Nelder-Mead optimisation method, the multidirectional search method is also a pattern search method [196]. It is also said that a great advantage of the multidirectional search method is its strong convergence properties [211]. It is to be noted that alike the Hooke and Jeeves pattern search method, this method, presents also the disadvantage that points may be sampled more than once, making the method more time consuming [97].

Objective function definition

The objective function is

Profit per year = Sales of product - (Capital cost + Operating cost + Cost of A + Cost of B) (£)

Sales of product = $P\ P_{dc}\ F\ t\ B\ p$

Capital cost = $\frac{C}{A}$

Operating cost = $P_u\ e\ t\ B\ p$

Cost of B = $R_B\ F\ t\ B\ p$

Cost of A = $R_A\ V_a\ B\ p$

Tab. 4.1: Summary of the objective function parameters

Profit per year =	+ Sales	- Cost			
=	Product C	Capital	Operating	Reactant A	Reactant B
=	$P\ P_{dc}\ F\ t\ B\ p$	$\frac{C}{A}$	$P_u\ e\ t\ B\ p$	$R_B\ F\ t\ B\ p$	$R_A\ V_a\ B\ p$

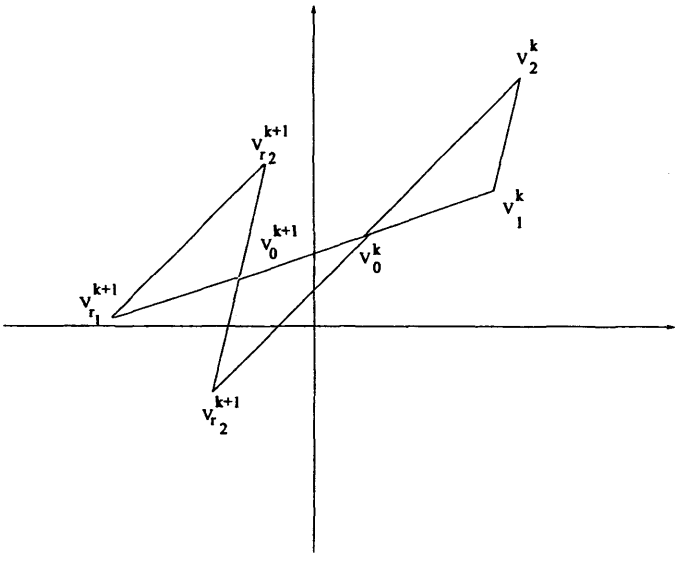

Fig. 4.5: Multidirectional - The next Iteration - with new search directions

The cost of the reactant A and B is expressed by the cost of each raw constituent multiplied by the amount of material fed to the reactor. In other term the cost of reactant A and B is the cost of the amount of material fed to the reactor, as we have assumed that no recycle would be present in the process (see 2.1.6).
see pages 225 and 227 for the full description of the parameters involved and the equations involved.

Optimisation problem

max Profit per Year

s.t.

$10 > u > 1.10^{-2}$ $(m.s^{-}1)$	:	The speed of the liquid within the reactor cannot exceed 10 $m.s^{-}1$
$N_{Re} > 1.10^{4}$ $(-)$	:	Insures that the impeller Reynolds number defines an agitated flow within the reactor
$36 > F > 3.6.10^{-3}$ (m^3/h)	:	Reflects the type of flowrate encountered in the production of pharmaceutical drugs
$t < W$ $(hours)$	:	t cannot exceed the number of daily working hours
$B > 1$	:	The minimum number of batches per day must be greater than 1
$0 < N < 50$ (rps)	:	The agitator speed cannot exceed 50 rps - the definition of N for a motor is $N = \frac{120\,f}{p}$ with f=frequency and p=number of pole in the motor $p_{min} = 2$ $f = 50$ Hz therefore $N_{max} = 3000\,rpm$ or 50 rps
$0 < a < 1$ $(-)$	:	The ratio of the feed volume over the reactor content is within a 0 to 1 range

Variables selected for optimisation

The following variables have been selected for optimisation :

a : Ratio of the feed volume to the reactor volume

ϵ : Energy dissipation rate (m^2/s^3)

t : Feed addition time (s)

u : Velocity of the fluid within the reactor (m/s)

V : Volume of the reactor content (m^3)

The aim of the optimisation is to define the best reactor and the best reactor design for a given system of reaction. Also the parameters selected for optimisation need to be applicable for any type of reactor. The importance of ϵ, the energy dissipation rate, has already been discussed (see section 2.1.2 and 2.1.4). In our case it will be the parameter which will be used to define the better types of reactor for a particular reaction system, as each type of reactor has a distinctive energy dissipation rate [44]. It also allows us to look at the design of novel types of reactor, for example, the spinning disk reactor [165, 137]. The velocity achieved within some types of reactor is a limiting factor. For example the velocity of the fluid achieved within a reactor using a stirrer will be different to the one achieved with a reactor using a pump as fluid circulation mean. The range of velocity achievable will therefore be a very differentiating factor of the different type of reactors considered. The importance of the velocity can also be seen at a different angle - Consider the jet mixing experiments using very large containers and very small jets; In very large containers with jets with low velocity, mixing times will be longer than in the containers with larger jet and therefore larger velocity. This example also underlines the economic impact of the feed addition time

and the volume of the reactor. It is conventional not to refer to the feed concentration c_{B0} but to the concentration which B would have if it were to mix completely with stream A before that reaction started ($\bar{c}_B$). This explains why an expression using the ratio of the feed volume to the reactant volume is preferred. Defining a by :

$$a = \frac{V_A}{V_B} \qquad (-) \tag{4.3}$$

a simple dilution calculation shows that the concentration of B averaged over the whole reactor can be expressed by

$$\bar{c}_B = \frac{c_{B0}}{(1+a)} \qquad (-) \tag{4.4}$$

The parameters listed above are typical characteristics of any type of reactor and as such can be used to compare different type of reactors.

Difficulties with the objective function discontinuity

In this part we look at the difficulty created by the discontinuity of the objective function. The discontinuity creates an artifact and undermine the search of the optimiser for local minima. This is illustrated with the semi-batch micromixing model.

In order to accommodate the discontinuity of the problem, adjustment had to be made to ensure that the optimiser e.g. direct search methods, find local optima. Figure 4.6 shows the evolution of the product distribution of the component C against the time.

The feed B is being discretised in order to simulate the model see section 2.3. The model simulates B being adding 'drop by drop', as a consequence of the discretisation. As a consequence of each drop of B added, the reaction occurs in the reaction zone, which is then mixed within the reaction

environment zone which is the content of the reactor, e.g. see section 2.1.4.

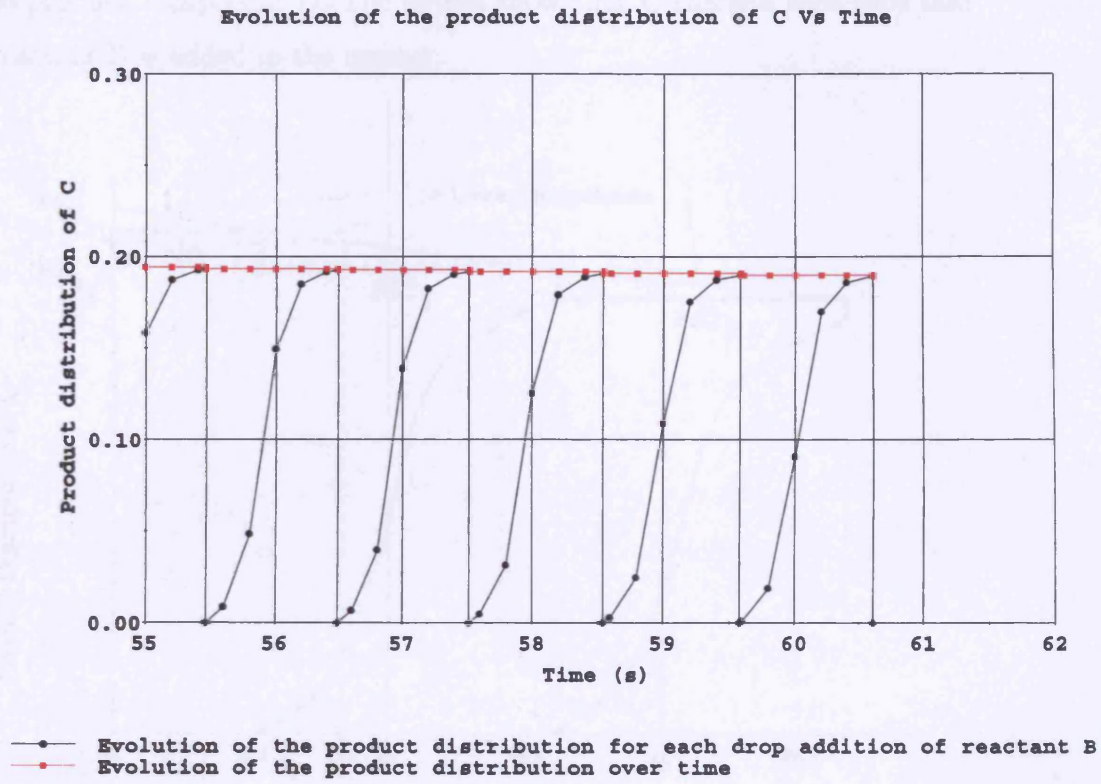

Fig. 4.6: Evolution of Product distribution of Component C for the period 55 - 62 seconds

These figures show that the product distribution (see equation 2.50, page 83) of component C, which represents how much of product C is produced against the amount of B consumed, evolves with the time by reaching a maximum level at the beginning of the reaction and then decreases according to equation 2.50. As the reactions follow the scheme defined in section 2.1.6, for the reaction system defined in equation 2.46 and equation 2.47. First C is the only component in the reactor, then C and B react with each other to produce D. Therefore the product distribution of C reaches a maximum

at the beginning of the reaction and decreases rapidly, as it reacts with B to produce component D. The figures show that C changes each time that reactant B is added to the reactor.

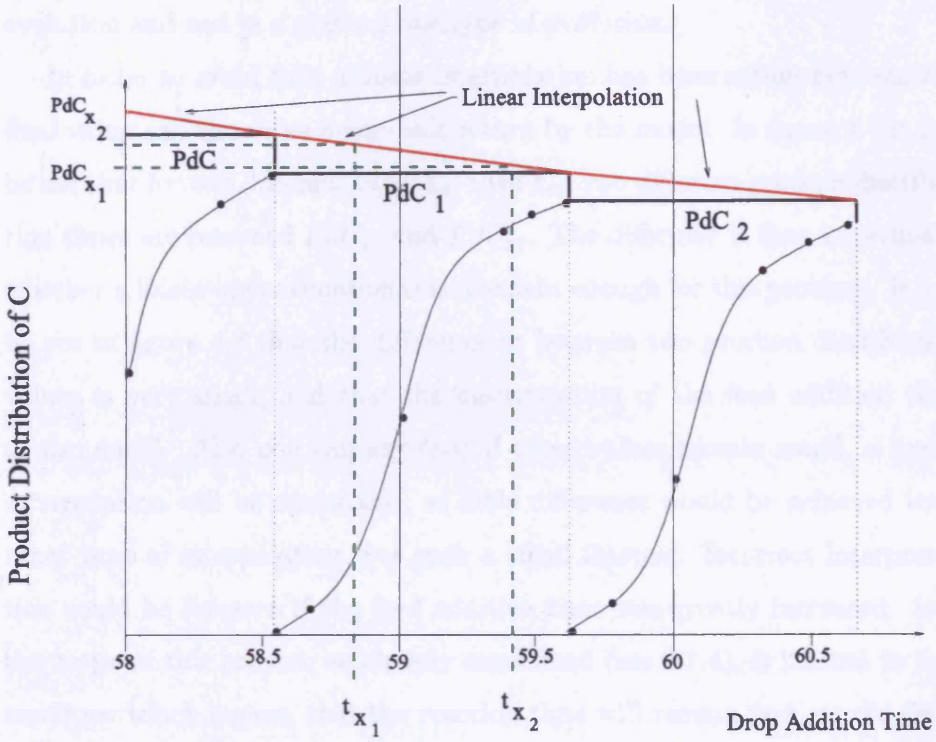

Fig. 4.7: Evolution of Product distribution of Component C against Time

From an optimisation point of view the discretisation creates a difficulty as it makes the system discontinuous. Also due to the discretisation the model is only updated each time that a new drop of reagent is added. Therefore as it is shown in figure 4.7, which is a schematisation of the computer output (see figure 4.6) between 58 and 60 seconds. The product distribution is only updated at time t_d then t_{d+1} then t_{d+2} etc... In between these values it can be easily noticed that the product distribution stays the same i.e. for to different times t_{x_1} and t_{x_2} the same value PdC_x is found. This means that

for different times the optimisation program will return the same product distribution which is not the reality as the reaction occurring within the reactor makes the reactants present in the reactor evolve in a fluid-like type of evolution and not in a plateau-like type of evolution.

In order to avoid this, a linear interpolation has been set-up between the final value and the value before last return by the model. In figure 4.7 it can be see that for two different times t_{x_1} then t_{x_2}, two different product distribution times are returned PdC_{x_1} and PdC_{x_2}. The difficulty is then to estimate whether a linear approximation is convenient enough for this problem. It can be see in figure 4.6 that the difference in between two product distribution values is very small, and that the discretisation of the feed addition time is also small. Also one can say that if these values remain small, a linear interpolation will be reasonable, as little difference would be achieved with other type of interpolation over such a small interval. Incorrect interpretation could be foreseen if the feed addition time was greatly increased. But the scope of this project, as already mentioned (see 2.1.4), is limited to fast reactions which means, that the reaction time will remain fast, so the drop addition time will always be short.

Optimisation results with direct search methods

It is necessary to check that the values returned by the different direct search methods listed above verify the afore mentioned definition of a local minima. A plotting of the different values has been done in order to check their respective positioning against each other. To show in a graph the positioning of the 5 different variables, a 6 dimensional graph would have been necessary : one dimension for each variable and another dimension to represent the objective function values. This is obviously impossible. Also another method

has been used to plot the objective function results towards the variables coordinates. A program that evaluates the objective value at a particular point is first constructed. Two points, which have been returned as local minima by the optimisation program, are then selected. The points, x_i, $i = 1, \ldots, n-1$ on a line connecting the two endpoints, x_a and x_b, in multidimensional space can be defined by:

$$\delta x \equiv \frac{x_b - x_a}{n} \tag{4.5}$$

$$x_i = x_a + i \times \delta x \qquad i = 1, \ldots, n-1 \tag{4.6}$$

where, n is the number of discrete points desired.

The graphs obtained are in 2-dimensions see figures 4.8 and 4.9.

In these figures the two local minima are the starting point and end point of the graph.

In the figure above one can see that the starting point of the curve and the end point of the curve represent two local optima, following the local minima definition.

But some curves of the type shown in figure 4.9 were also obtained.

One can see that the graph in figure 4.9, where the two optimised vector values are the starting point and the end point of the curve, does not corroborate the definition of a local minima as defined above. Consequently one or both of this 2 points are not local optima.

In figure 4.8 it can be seen that a lot of so-called noise is present and this could represent an explanation for not finding local minima. Indeed one can imagine that the direct search algorithm can evaluate one of the noisy deep dent as a local minima and therefore stops the optimisation search at a point which is not a local minima. In order to avoid this type of phenomena it was decided to use new search algorithm based on genetic algorithms [79]

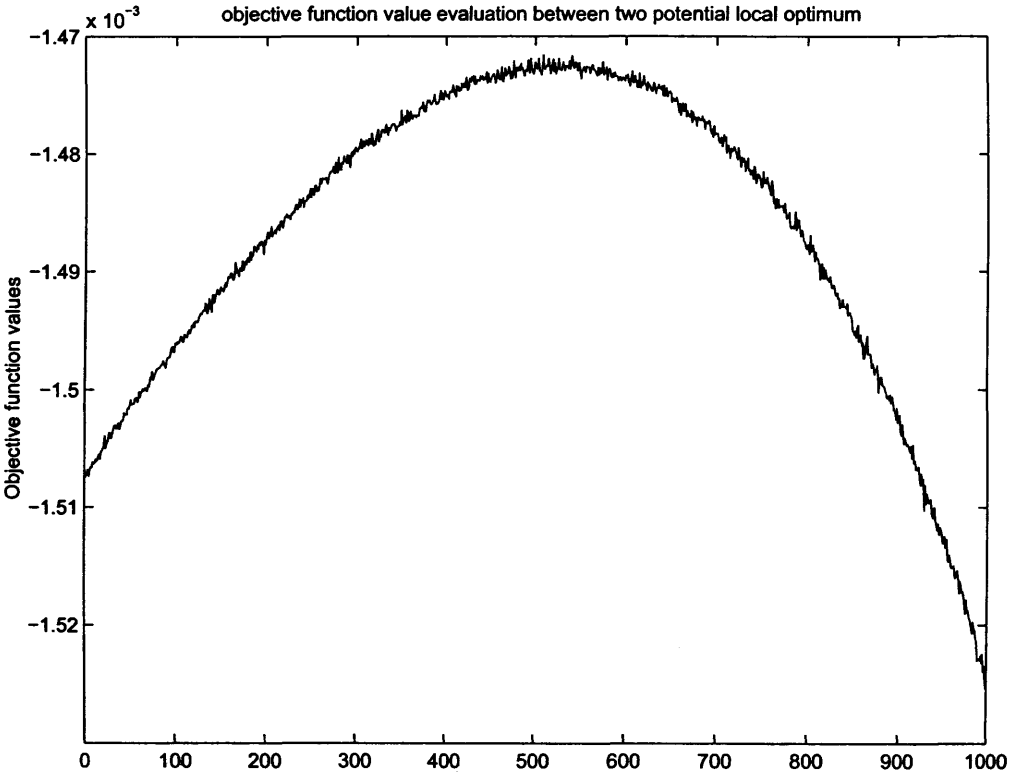

Fig. 4.8: Objective function values between the two local optima

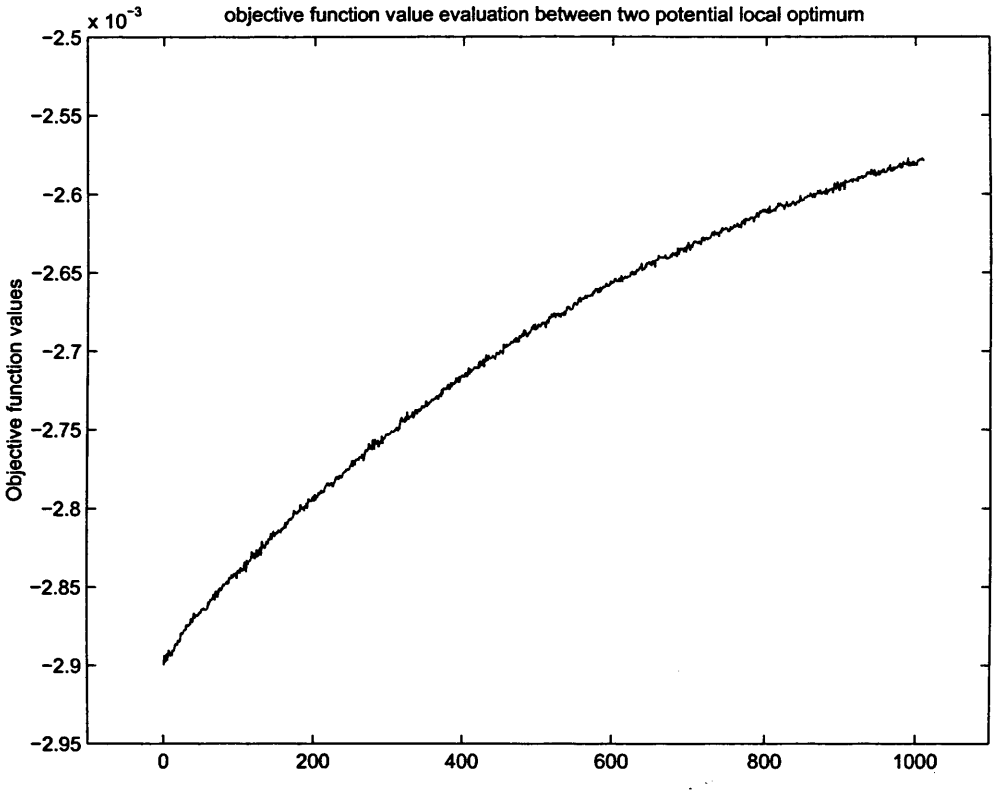

Fig. 4.9: Objective function values between a local optima and a non local optima obtained through the use of direct search optimisation methods

and simulated annealing [102]. Genetic Algorithms (GA) belong to a class of stochastic optimisation methods based on analogies to natural selection strategies from evolution. Simulated Annealing (SA) is another stochastic optimisation method that is based on a thermodynamic process called annealing. Both GA and SA have the property that they allow uphill directions and the iterates will therefore not necessarily decrease monotonically. This property can be exploited to allow the search methods to jump out of local wells by moving uphill. Simulated annealing has been used in this work to solve the optimisation problem. The method and its implementation are described in the following.

4.1.2 Simulated Annealing

In this part of the project, the Simulated Annealing optimisation method was selected, and implemented, as a down-climbing algorithm to optimise i.e. in our case to minimise, the objective function defined previously (see section 4.1.1). In this part of the project the method is described and the results obtained with this optimisation method are explained.

Method theory and description

Simulated annealing is a generalisation of a Monte-Carlo method for examining the equations of state and frozen states of n-body system [124]. Simulated annealing was first introduced in 1983 for optimising functions of many variables [102]. Although this heuristic approach cannot guarantee to produce the optimum, also called global optimum, it is known that an acceptable optimum can be found in a reasonable time [106].

Simulated annealing is based on an analogy to the cooling of heated metals. In any heated metal sample the probability of some clusters of atoms at

a position, r_i, exhibiting a specific energy state, $E(r_i)$, at some temperatures T, is defined by the Boltzmann probability factor :

$$P(E(r_i)) = e^{-\frac{E(r_i)}{k_B T}} \tag{4.7}$$

where k_B is the so called Boltzmann's constant. As a metal is slowly cooled, atoms will fluctuate between relatively higher and lower energy levels and allowed to equilibrate at each temperature T. The material will approach a ground state, a highly ordered form in which there is very little probability for the existence of a high energy state throughout the material. Now if we replace the energy function of this physical system by the objective function we are dealing with, as $f(X)$ (see section 4.1.1) with X being the vector of variable as defined in section 4.1.1, then the slow progression towards an ordered ground state is representative of a progression to a global optimum. To achieve this, a control parameter T, analogous to a temperature, and a constant C, analogous to the Boltzmann's constant , must be specified for the optimisation problem. In standard iterative improvement methods, a series of trial point is generated until an improvement in the objective function is noted in which case the trial points is accepted. It can be understood that this process only allows for downhill movement to be made over the search space. In order to generate the annealing behaviour, a secondary criterion is added to the process. If a trial point generates a large value of the objective function then the probability of accepting the trial point is determined using the Boltzmann probability distribution :

$$P[\text{accept } X_t] = e^{-\frac{f(X_t)-f(X_0)}{C\,T}} \tag{4.8}$$

where X_0 is the initial starting point. This probability is compared against a randomly generated number over the range [0...1]. If $P[\text{accept}X_t] >$

random [0...1] then the trial point is accepted. This dependence on random numbers makes simulated annealing a stochastic method. Various implementations will use various methods of random number generation. Repeating this iterative improvement many times at each value of the control parameter T, the methodical thermal rearrangement of atoms within a metal at a temperature T is simulated [102]. This iterative improvement forms the 'inner' loop of the method. The variation of the control parameter T is contained in an 'outer loop'. The initial value of the control parameter is suitably high and a methodology for decrementing T is applied.

Application of the annealing strategy to any engineering optimisation problem requires definition of four major components :

1. Problem configuration: a definition of the suitable domain over which the optimum can be sought. This knowledge is expressed as the constraint equation and more specifically in our case is dealt by the use of penalty constraints (see section 4.1.1).

2. Neighbourhood configuration: a method of iteratively perturbing the design vector to create new trial points. The type of 'move' use in our case is defined as follow [116]:

$$X^{\text{new}} = X^{\text{old}} + \left(X^{\max} - X^{\text{old}}\right) r^2 \frac{T}{T_0} - \left(X^{\text{old}} - X^{\min}\right) r^2 \frac{T}{T_0} \quad (4.9)$$

where r is a random numbers between 0 and 1, T_0, T are the initial and current system temperature, X_{new}, X_{old} are new and old parameter vectors, and X^{max}, and X^{min} are respectively upper and lower bound of each parameter. The interest of this neighbourhood generation function is that it includes the factor $\frac{T}{T_0}$ within the function. This

means that the neighbourhood search will be restricted after each temperature reduction. The temperature T is constantly reduced after a fixed number of iteration. Also this has for effect to diminish the factor $\frac{T}{T_0}$. As the factor $\frac{T}{T_0}$ diminishes within the range [0,1] it restricts the neighbourhood search range as the algorithm is converging towards the optimum solution.

3. Cooling / Annealing schedule: a procedure for specifying the maximum number of inner loop iterations and the manner in which the control parameter will be decremented in each iteration of the outer loop

In our case the most challenging part was the definition of the annealing process has been to develop an appropriate cooling schedule. Indeed, to ensure the success of the optimisation, the temperature which is one of the control parameter must be controlled so that it is large enough to move off a local minimum, but small enough not to move off a more global minimum. Ideally, the temperature should be lowered slowly enough to ensure that a good minimum is achieved, but also quick enough so that computational time is minimised [75, 106].

Simulated annealing is especially well suited to tackle problems best described as 'dirty', i.e. problems either numerous, contradictory cost constraints or complex, baroque cost functions [166]. The advantages of simulated annealing are that it is not a derivative based method and can handle the discontinuities in the state of large problems much easier than MINLP methods [138]. Simulated annealing works best in situations where the objective function landscape is rough and may have many local optima. In this cases, as we showed it before (see 4.1.1, gradient descent methods often get 'stuck' in a configuration which is not optimal. The probabilistic nature of the configuration changes (move acceptances) in annealing allows the system

to go uphill and to leave the basin of attraction of one relative minimum to go into another, deeper basin. Because of these characteristics, simulated annealing has been proven to be a fairly robust combinatorial optimisation technique, although annealing is by no means a panacea for all combinatorial optimisation problems [139].

4.1.3 *Micromixing model for continuous operation*

Objective function definition

Profit per year = Sales of product - (Cost of A + Cost of B) (£/year)

Sales of product = $P\, P_{dC}\, F_B\, W * 3600\, p$

Cost of B = $R_B\, F_B\, W * 3600\, p$

Cost of A = $R_A\, F_A\, W * 3600\, p$

Tab. 4.2: Summary of the objective function parameters

Profit per year =	+ Sales	- Cost	
=	Product C	Reactant A	Reactant B
=	$P\, P_{dC}\, F_B\, W * 3600\, p$	$R_A\, F_A\, W * 3600\, p$	$R_B\, F_B\, W * 3600\, p$

The cost of the reactant A and B is expressed by the cost of each raw constituent multiplied by the amount of material fed to the reactor. In other term the cost of reactant A and B is the cost of the amount of material fed to the reactor, as we have assumed that no recycle would be present in the process (see 2.1.6).

see appendix B page 233 for the full description of the parameters involved and the equations involved in the continuous micromixing model.

Optimisation problem

max Profit per Year

s.t.

$0 > \epsilon > 5000 \quad (m^2.s^-3)$	:	The energy dissipation rate is limited to these values which includes all the different type of reactor existing reactor [12, 21]
$3 > u > 1.10^{-2} \quad (m.s^-1)$	:	The speed of the liquid within the reactor cannot exceed 3 $m.s^-1$
$N_{Re} > 1.10^4 \quad (-)$	:	Insures that the impeller Reynolds number defines an agitated flow within the reactor
$F = 1 \quad (m^3/h)$	:	Reflects the type of flowrate encountered in the production of pharmaceutical drugs
$t < W \quad (hours)$	:	t cannot exceed the number of daily working hours

Variables selected for optimisation

With reference to a degree of freedom of 2 identified for the continuous micromixing model see B.4. The following variables have been selected for optimisation :

u : Speed within the reactor $(m.s-1)$

ϵ : Mass transfer coefficient (m^2/s^3)

As already discussed and explained in section 4.1.1, the energy dissipation rate is specific and inherent to each type of reactor. Therefore by determining the optimum energy dissipation rate, the optimum type of reactor is also identified. The speed within the reactor is on the other hand providing various information regarding the design itself of the reactor i.e. residence time, diameter, length and therefore volume of the reactor.

loss versus Capital Cost

The objective function used for the optimisation with the continuous micromixing model is based on the loss generating by the different type of reactor and not on the reactors capital cost. This is due to the fact that the capital cost of the different type of reactor e.g. Jet-loop reactor, static mixer, Sulzer mixer, rotor-stator etc... used for continuous operation tend to be similar.

4.1.4 Mass transfer model

The reactors considered in this part of the study are as follow :

1. Mechanically agitated
2. Jet loop
3. Bubble column excluding Jet-loop
4. Packed column counter-current
5. Spray column

The different reactor characteristics are defined following the classification given by Lee and Tsui [112] see table 4.3.

In this study all reactor with $k_l a$ and Gas hold-up values outside the range listed in table 4.3 have been considered as novel reactor type. For example if the result of the optimisation gives $k_l a = 3$ then the type of reactor defined by this result is classified as 'Novel reactor'.

Mathematical formulation

The rate of reaction for the different component is calculated as follow :

$$
\begin{aligned}
r_1 &= k_1\,[\text{RhL*}]\,[\text{IPA}] \qquad (4.10)\\
r_2 &= k_2\,[\text{RhL*H}]\,[\text{Acetone}]]\\
r_3 &= k_3\,[\text{RhL*H}]\,[\text{Sub}]]\\
r_4 &= k_4\,[\text{SIM}]\\
r_5 &= k_5\,[\text{RhL*H}]\,[\text{Sub}]]\\
r_6 &= k_6\,[\text{RIM}]\\
r_7 &= k_7\,[\text{SIM}]\\
r_8 &= k_8\,[\text{RhL*}]\,[\text{S-SubH}]]
\end{aligned}
$$

Tab. 4.3: Mass transfer $k_l a$ and Gas hold-up characteristics of common contactors

Reactor type	$k_l a$	Gas Hold-up
	(1/s)	(-)
Bubble column excluding jet-loop	0.005 - 0.01	< 0.2
Spray Column	0.00007 - 0.015	> 0.8
Packed column counter-current	0.005 - 0.02	> 0.95
Plate column	0.01 - 0.05	> 0.8
Mechanically agitated	0.02 - 0.2	< 0.1
Jet-loop	0.01 - 2.2	< 0.5

$$r_9 = k_9\,[\text{RIM}]$$
$$r_{10} = k_{10}\,[\text{RhL*}]\,[\text{R-SubH}]]$$

All the reactions in this reaction system occur in the liquid phase of the system. No reaction occurs in the gas phase or in between the two phases involved as gas and liquid.

Objective function definition

$$Capital Cost per Unit of production = \frac{Capital cost}{Production} \qquad (£/m^3)$$

A capital cost is attributed to each type of reactor listed above see 4.1.4.

The capital cost attributed to each type of reactor is based on a curve equation obtained by fitting data obtained from Balfour Beaty for the cost of a stirred tank reactor i.e. :

$$Capital cost of Stirred tank reactor(CCSTR) = 14595 + 13418 * V^{0.661}$$

The capital cost for other type of reactor is adjusted by a multiplying factor, x_n, in accordance to the difference between the reactor type and a stirred tank reactor i.e. :

Mechanically Agitated $= CCSTR \qquad (£/year)$

Jet loop $= x_1\,CCSTR \qquad (£/year)$
Bubble column excluding Jet-loop $= x_2\,CCSTR \qquad (£/year)$
Packed column counter-current $= x_3\,CCSTR \qquad (£/year)$
Spray column $= x4\,CCSTR \qquad (£/year)$
Novel reactor $= x5\,CCSTR \qquad (£/year)$

Different results are presented for different value of the multiplying factors x_n.

Production $= (Cr + Cs)\, V\, M\, B\, P \qquad (kg/year)$

where,

Cr : Concentration of product R (mol/m^3)

Cs : Concentration of product S (mol/m^3)

V : (m^3)

B : number of batch per day (-)

M : Molecular weight of R and S (kg/mol)

P : Number of production days per year $(days/year)$

Variables selected for optimisation

The aim of the optimisation is to define the best reactor and the best reactor design for a given system of reaction. Also the parameters selected for optimisation need to be applicable for any type of reactor. kla, the mass transfer coefficient, and the Gas hold-up are specific for each type of reactor [112], this permit the selection of the reactor type. As mentioned before if the value of kla or $Gashold - up$ cannot be reattached to a reactor type e.g. $kla > 2.2$ then reactor type is considered as novel and the design problem then becomes to find the mechanical elements of the reactor which permit to reach the level of mass transfer or gas hold-up defined by the reactor optimisation. The conversion to be achieved has a very important impact within the reaction and more particularly on the reaction time, as the time required

to reach the highest possible conversion i.e. 1 can be double, triple or even more than the amount of time required to reach a conversion of 0.95, and the time loss is not compensated by the quantity of product gained. Nevertheless a conversion target lower than 0.95 can be considered as unrealistic whether from a reactant cost point of view or from a environmental point of view as all the unreacted have to be disposed of. It has also be shown that the level of confidence in the mass transfer model developed is much higher for $conversion > 92\%$ see section 2.1.9. The nitrogen flow introduced within the reactor as explained before (see 2.1.9) help to remove acetone from the reaction system and therefore drive the reaction equilibrium towards the production of the racemique. Also this factor has a direct influence on the reaction system, also it will also be interesting to look at its influence on uncertainty within the reactor system.

Also, the following variables have been selected for optimisation :

$Conversion$: Conversion achieved

kla : Mass transfer coefficient $(1/s)$

$Nitrogenflow$: Feed addition time (m^3/s)

$Vl_{initial}$: Initial liquid volume of the reactants (m^3)

$Gashold - up$: Velocity of the fluid within the reactor (m/s)

Optimisation problem

min *Capital Cost per Unit of production*

s.t.

$t < W \quad (hours)$: t cannot exceed the number of daily working hours i.e. 8 hrs

$B > 1$: The minimum number of batches per day must be greater than 1,

it is assumed that production is done during days and that there is no evening or night shift.

$1 < V < 10$ (rps) : The total volume of the reactor is within the range 1 to 10 m^3 this reflect the most common sizes of pharmaceutical reactors for production. It is also considered as traditional with regards to the different types [51]

$0.95 < X < 1$ $(-)$: The conversion X for the CATHy reaction is within the range [0.95 ; 1] see section 2.1.9
It is also considered that the pharmaceutical industry does not consider profitable any conversion rate ≤ 0.95 [145]

4.2 Multiobjective optimisation

Many real-world decision making problems need to achieve several objectives : minimise risks, maximise reliability, minimum deviations from desired level, minimise cost, etc ... The main goal of single-objective (SO) optimisation is to find the 'best' solution, which correspond to the minimum or maximum value of a single objective function that lumps all different objectives into one. This type of optimisation is useful as a tool which should provide decision makers with insights into the nature of the problem [214, 177]. But this methodology cannot provide a set of alternative solutions that trade different objectives against each other. On the contrary, in a multiobjective optimisation with conflicting objectives, there is no single optimal solutions, largely known as the trade-off, non-dominated, non-inferior or pareto-optimal solutions. Simultaneous optimisation by *mathematical programming* brings promising future for conceptual design. It has also been applied to discrete

optimisation, superstructure optimisation and subsystem synthesis [5]. Furthermore, advances in Multi-Objective Programming permits to cope with bigger and more complex problems [212] and some involving uncertainty [162, 163]. Attractive application of MOP lies in developing a multi-objective process synthesis methodology [182]. However, in its early stage of applications, MOP was only used to solve rather simple and small scale problems because the classical methods are not efficient in searching capability [59, 125]. Due to excellent searching ability and being less susceptible to the shape or continuity of the pareto front, stochastic search algorithms have been introduced into MOP [94, 49].

4.2.1 Objectives and algorithm

In our case, our objective is to assist the decision maker in selecting a reactor(s) which permit the scale-up of a reaction system. The objectives are to compare the ability of different type of reactor against their potential in scaling-up the reaction system and this is assessed through loss and uncertainty. We want to minimise the loss i.e. maximise the profits that the reaction system can generate but at the same time the aim is also to minimise the uncertainty in reactor design.

4.2.2 Evolutionary Multi-Objective Optimisation technique

4.2.3 Pareto-Based approaches

Many real world design problems involve multiple, often conflicting optimisation criteria, in our case uncertainty and cost. It is very difficult to weight the criteria exactly before alternatives are known. Multiobjective evolutionary algorithms based on the principle of pareto optimality are designed to explore the complete set of non-dominated solutions, which then allows the

user to choose among many alternatives Having several objective functions, the notion of 'optimum' changes, because in multi-objective optimisation, the goal is more to find good compromises (or 'trade-offs') rather than a single solution as in global optimisation. The definition of Pareto Optimality is defined to explicit the 'trade-off' between the two objectives.

Definition of Pareto Optimality : We say that a vector of decision $\vec{x} \in F$ is *pareto optimal* if there does not exist another $\vec{x^*} \in F$ such that $f_i(\vec{x}) \leq f_i(\vec{x^*})$ for all $i = 1, \ldots, k$ and $f_j(\vec{x}) \leq f_j(\vec{x^*})$ for at least one j. Here, F denotes the feasible region of the problem.

In words, this definition says that $\vec{x^*}$ is pareto optimal if there exists no feasible vector of decision variables $\vec{x} \in F$ which would decrease some criterion without causing a simultaneous increase in at least on other criterion. Unfortunately, this concept gives rarely one solution, but rather a set of solutions called the *pareto optimal set.* The vectors $\vec{x^*}$ corresponding to the solutions included in the pareto optimal set are called non-dominated. The plot of the objective functions whose non-dominated vectors are in the pareto optimal set is called the *pareto front.* The graph 4.10 summarises this definition.

The idea of using Pareto-Based fitness assignment was first proposed by Goldberg [79] to solve the problems of Schaffer's approach with genetic algorithms. He suggested the use of non-dominated ranking and selection to move a population toward the pareto front in a multiobjective optimisation problem. The basic idea is to find the set of strings in the population that are Pareto non-dominated by the rest of the population. Theses strings are then assigned the highest rank and eliminated from further contention. Another set of pareto non-dominated strings are determined from the remaining population and are assigned the next highest rank. This process continues

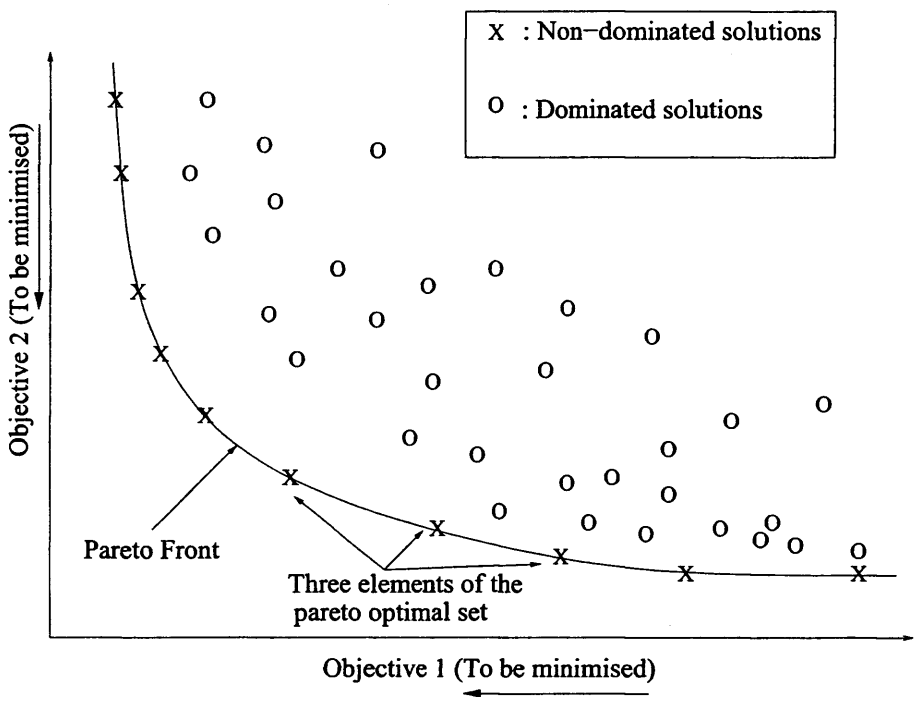

Fig. 4.10: Pareto optimality and pareto front

until the population is suitably ranked.

Currently there are over 30 mathematical programming techniques for multiobjective optimisation [125, 78, 63]. However, these techniques tend to generate elements of the pareto optimal set one at a time. Additionally, most of them are very sensitive to the shape of the pareto front (e.g., they do not work when the pareto front is concave or when the front is disconnected) [50]. Evolutionary algorithms seem particularly suitable to solve multiobjective optimisation problems, because they deal simultaneously with a set of possible solutions (the so-called population). This allows us to find several members of the pareto optimal set in a single run of the algorithm, instead of having to perform a series of separate run as in the case of the traditional mathematical programming techniques. Additionally, evolutionary algorithms are less susceptible to the shape or continuity of the Pareto front (e.g., they can easily deal with discontinuous or concave pareto front), whereas these two issues are a real concern for mathematical programming techniques. Within the Evolutionary algorithm group, metaheuristic algorithms have been proved as very useful tool for tackling multiobjective problems [94].A heuristic is defined by Reeves [158] as a technique which seeks or finds good solutions to a difficult model. A meta-heuristic goes beyond this to draw on ideas and concepts from another discipline to help solve the artificial system being modeled. The most popular meta-heuristics include genetic algorithm [79], which emulate the way species breed and adapt in the field of genetics; simulated annealing, which emulates the way in which a material cools down to its steady state in the field of physics; and tabu search, which draws on the social concept of 'Taboo' in order to provide and effective search technique which avoids local minima. It has been shown that Multi-Objective Simulated Annealing (MOSA) is a clear candidate when

compared to Multi-Objective Genetic Algorithm (MOGA) [198, 193, 66]. In that case MOSA offers better result quality and better speed in convergence [193]. Another disadvantage of MOGA versus MOSA is the fact that MOGA is a evolutionary search with variable size representations. Variable length methods for evolutionary computation can lead to a progressive and mainly unnecessary growth, known as bloat [101]. Also in this work preference was given to MOSA. The method and algorithm are explained in the following

4.2.4 *Multiobjective Simulated Annealing (MOSA)*

The Simulated Annealing algorithm has foundations in the statistical mechanics of annealing in solids see 4.1.2. The algorithm seeks to minimise a given objective, f, by making small random changes to the control variables. If $f$is reduced the changes are accepted with a probability $exp(-\frac{\delta f}{T})$ where T is a control parameter (the 'temperature') which is gradually lowered.

Multiobjective SA (MOSA) uses the domination concept and the annealing scheme for efficient search. The main obstacle for SA in multiobjective optimisation is its ability to find multiple solutions. However, SA can do the same work by repeating the trials as it converges to local optima with a uniform probability distribution in the single objective optimisation. As already presented see 4.1.2, the general SA algorithm involves the following three steps. First, the objective function corresponding to the energy function must be identified. Second, one must select a proper annealing scheme consisting of decreasing temperature with increasing of iterations. Third, a method of generating a neighbour near the current search position is needed. In single objective optimisation problems, the transition probability scheme is generally selected by the metropolis and logistic algorithms [124] [127]. However, the situation is different in multiobjective optimisation and choos-

ing a proper transition probability is difficult and to perform multiobjective optimisation the acceptance probability formulation is changed to [187] [198]:

$$p_{all} = \prod_{i=1}^{N} exp\left[-\frac{f_i(X_{n+1}) - f_i(X_n)}{T_i}\right] \tag{4.11}$$

with a temperature T_i now being associated with each objective f_i.

The key to successful multiobjective optimisation is to record the best solutions encountered during search. This can be done by maintaining an archive of non-dominated solutions (one solution dominates another if it is better on all counts), the principle of which is shown see figures 4.11 for the case of minimisation of 2 objectives.

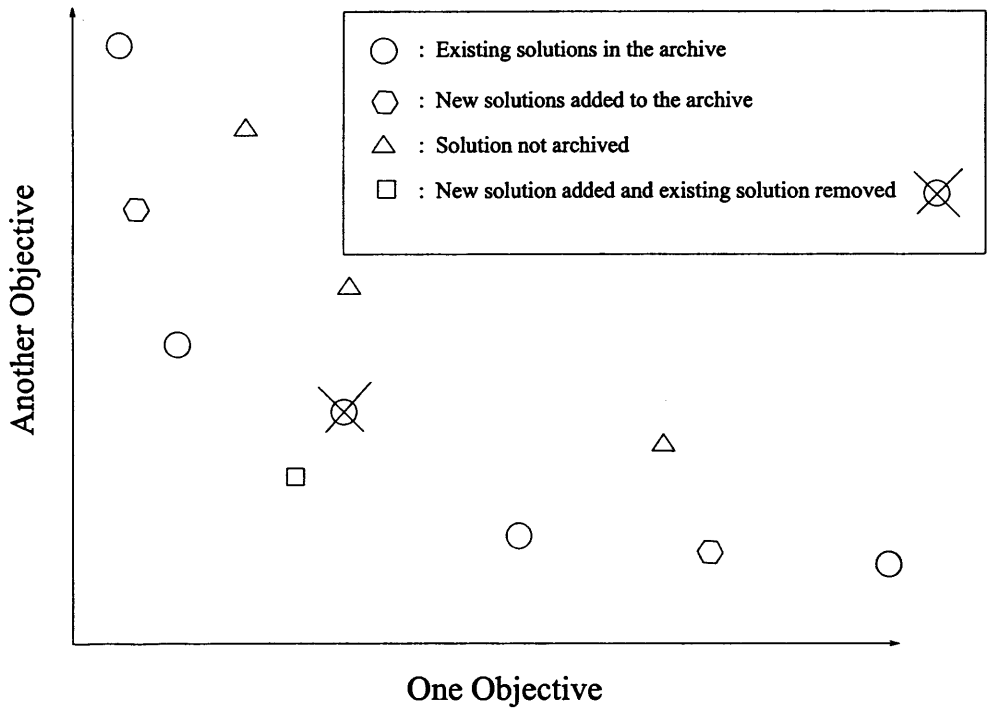

Fig. 4.11: Dominated and non-dominated solutions

MOSA : algorithm

The following diagram, see 4.12, represents the algorithm used for the Multi-Objective Simulated Annealing [187]. X_0 represents the initial vector of variables and X_n represents the current search position (or the current state in a finite state search problem) and T is the temperature parameter, which is gradually decreased as time goes on. A new search position X_{n+1} is generated by the S(X) function, its cost and uncertainty are calculated and compared to the previous cost and uncertainty values achieved. When it is determined to be a good solution by the domination test, the state is accepted. When the new position is dominated by the current state it is accepted with the acceptance probability described earlier see 4.11. When there is no superiority between the current state and the next state, the new state is accepted instead of the current one because moving in the non-dominated situation helps increase the spread performance and evade local optima.

Cooling schedule

As explained previously the simulated annealing technique stems from thermal annealing which aims to obtain perfect crystallisation by a slow enough temperature reduction to give atoms the time to attain the lowest energy state. This search tries to avoid local minima by jumping out of them early in the computation. Towards the end of the computation, when the temperature, or probability of accepting a worse solution, is nearby zero, this simply seeks the bottom of the local minima. The chance of getting a good solution can be traded off with computation time by slowing down the cooling schedule. The slower the cooling, the higher the chance of finding the optimum solution, but the longer the run time. Thus effective use of the simulated annealing optimisation depends on ending a cooling schedule that gets good

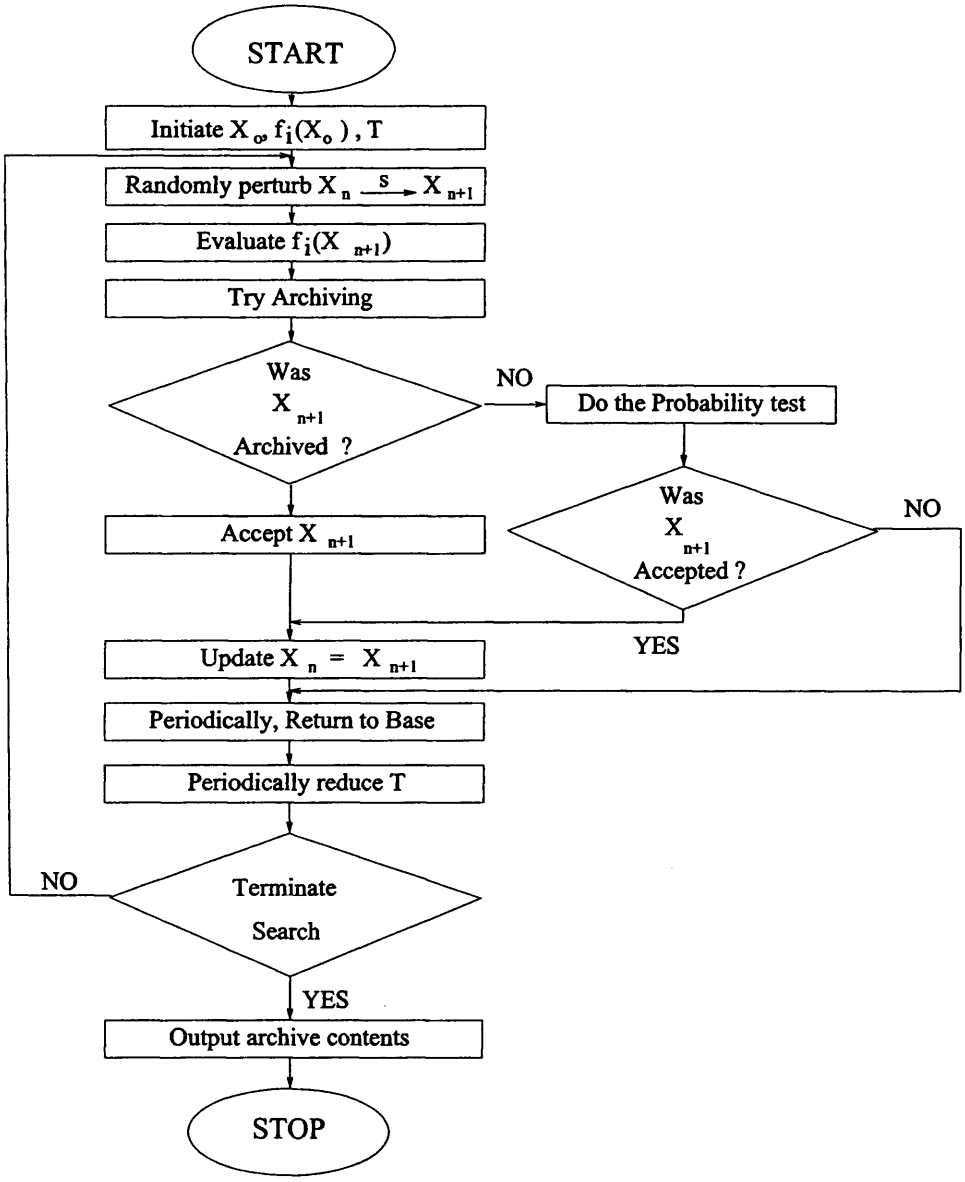

Fig. 4.12: Multi-Objective Simulated Annealing Algorithm

enough solutions without taking too much time.

In remedy of this inefficiency various approaches have been proposed to speed up simulated annealing [207]. One of the best general cooling schedule is proposed by Huang et al. [150]. The advantage of the temperature decrement proposed by Huang et al. [90], based on the standard deviation of the cost distribution at a temperature to determine the next temperature, is that it is dynamically controlled by the system itself and hence is applicable to a variety of problems.

In their approach, the annealing curve - a curve of average cost ¡ C ¿ versus the logarithmic of temperature - is used to guide the temperature decrease. The idea is to control the temperature so that the average cost decreases in a uniform manner. The slope of the annealing curve is :

$$\frac{d < C >}{d\,(ln\,(T))} = T.\frac{d < C >}{dT} \tag{4.12}$$

From the relationship [159] :

$$\frac{d < C >}{d\,(T)} = \frac{\sigma^2}{T^2} \tag{4.13}$$

where, *sigma* : Standard deviation of the cost distribution at the temperature T

It follows that :

$$\frac{d < C >}{d\,(ln\,(T))} = \frac{\sigma^2}{T} \tag{4.14}$$

The slope itself can be approximated by $\Delta C/\,(ln\,(T\prime) - (T))$, where ΔC is the change in the average cost at different temperatures. Hence,

$$\frac{\Delta C}{d\,(ln\,(T))} = \frac{\sigma^2}{T} \tag{4.15}$$

which leads to

$$T\prime = T.exp\left(\frac{T.\Delta C}{\sigma^2}\right) \tag{4.16}$$

To maintain quasi-equilibrium, we require that the expected decrease in the average cost be less than the standard deviation of the cost. For instance, $\Delta C = -\lambda\sigma$ where $\lambda \leq 1$. A typical value for λ is given as 0.7 [90].
and,

$$T\prime = T.exp\left(\frac{\lambda.T}{\sigma}\right) \tag{4.17}$$

In the actual implementation, the ratio $\frac{T\prime}{T}$ is lower bounded by a small number, 0.5 is given by Huang et al., to prevent a drastic decrease in temperature caused by the flat annealing curve at high temperatures.

The frozen condition

Typical stopping criterion for termination of the annealing process found in the literature is when the average cost is unchanged for 3 or 4 consecutive temperatures. The temperature cooling schedule used in our methodology will determinate by itself to stop as the maximum and minimum costs amongst the accepted states are compare through the standard deviation. If the different between the different cost is non existent then the temperature will be set to zero from definition and therefore the algorithm becomes a standard 'greedy' random selection algorithm. An optional exhaustive search follows which ends the optimisation process.

Step change in MOSA

The perturbation move from $X_n \rightarrow X_{n+1}$ (see 4.12) are generated in the same way as previously explained see 4.1.2. Nevertheless in order to respond

to the wide range of values that some of the selected variables can take (see 4.1.4):

Tab. 4.4: Mass transfer $k_l a$ characteristics of common contactors

Reactor type	$k_l a$
	$(1/s)$
Bubble column excluding jet-loop	0.005 - 0.01
Spray Column	0.00007 - 0.015
Packed column counter current	0.005 - 0.02
Plate column	0.01 - 0.05
Mechanically agitated	0.02 - 0.2
Jet-loop	0.01 - 2.2

Tab. 4.5: Nitrogen flowrate

Reactor type	Nitrogen Flowrate $(m3.s)$
	$(m3.s)$
All reactors	0.005 - 0.1

The move has been adapted by taking the logarithm of the value selected before the move change and taking the exponential of the value created through the random perturbation (see 4.1.2). In doing so the full range of value available for the random perturbation can be explored, and avoiding missing as such potential solutions.

Well distributed pareto front

In order to generate a well-distributed set of pareto points, a random selection of a solution from the archive, from which to recommence search is generated [187]. As indicated in the Multi-objective algorithm 4.12, periodically a so

called 'return-to-base' is trigged used to replace the search for pareto points in a different location of the pareto front. In order to fully expose the trade-off, solutions (pareto points) that are more 'isolated' from the rest of the trade-off should be primarily selected in returns-to-base. The extreme solutions, those solutions that correspond to extrema in the trade-off i.e. solutions with the lowest value of each objective, also require special consideration. These solutions are almost invariably only just feasible, which makes the design space around them difficult to search. For these reasons, Suppapitnarm et al. [187] proposed a base set of candidate solutions which consists of a number of the most isolated of those solutions currently held in the archive and the M extreme solutions in the archive. Therefore, when a return-to-base is activated the search diversifies into less well explored regions of the trade-off. To measure of the degree of isolation of a solution, the following definition is introduced :

$$I(X_j) = \sum_{\substack{i=1 \\ i \neq j}}^{A_S} \sum_{k=1}^{M} \left(\frac{[f_k(X_i) - f_k(X_j)]}{[f_{kmax} - f_{kmin}]} \right)^2 \tag{4.18}$$

X_j: denotes the jth archived solution

$I(X_j)$: is the normalised measure of distance in objective space of the jth solution from all other archived solutions

A_s: is the total number of solution stored in the archive

f_{kmax} and f_{kmin}: Maximum and minimum values, respectively, of the k^{th} objective function, f_k.

Each solution - except for the extreme solutions - is then ranked in order of decreasing isolations at its top and the least isolated solutions at the bottom. Suppapitnarm et al. [187] also proposed, that for the ith return-to-base after the start of search, the number of candidate solutions, A_{Ii} (the A_{Ii} - M most isolated solutions and extreme solutions), be some fraction, Φ_{Ii}, of the total

number of solutions in the archive, i.e.,

$$A_{Ii} = \Phi_{Ii} A_s, \qquad i = 1, 2, 3, ... \tag{4.19}$$

with,

$$\Phi_{Ii+1} = r_I \Phi_{Ii}, \qquad i = 1, 2, 3, ... \tag{4.20}$$

where r_I is a parameter of value between 0 and +1. For the first return-to-base,$i = 1$, Φ_{Ii} is set equal to +1 and $A_{Ii} = A_S$. This procedure permit that at the beginning of the program execution, all solutions within the archive are potential return-to-base candidate. Thereafter candidates list becomes increasingly focused on the most isolated and the extreme solutions in the archive. Suppapitnarm and al. found that for $r_i = 0.9$ the algorithm performs well in accordance with some of their previous work - This value was also used in this work as well as $r_i = 0.8$ which proved also to perform well and increase the speed by reducing the number of return to base done.

4.2.5 *Continuous micromixing model :Mathematical model, uncertainty, optimisation and reactor selection*

Continuous micromixing model : Optimisation of cost

In our case the design variables chosen are see 4.1.3: *Energy Dissipation Rate(ϵ), Average speed within the reactor (u)* in agreement with the number of degree of freedom of 2 given by the model see B.4. These design variables allows to define the reactor type i.e. *Energy dissipation rate(ϵ) and the reactor design through the average velocity within the reactor (u)* see 4.1.3

To compare the different type of reactor one to another, simulated annealing optimisations are used to identify the minimum loss $£/yr$, achievable

for each type of reactor design considered. The loss has been chosen to compare the different type of reactor as the selection of processing equipment is generally largely determined by two financial considerations [6]. Nevertheless in the case of reactors used for continuous operation the different of capital cost is minim. Also it was decided to referee to the loss as defined in section 4.1.3.

Continuous micromixing model : measure of uncertainty by sensitivity analysis

The uncertainty in the continuous operation micromixing model is expressed through the impact that changes on the reaction kinetics and the kinematic viscosity have on the loss achieved for the different types of reactor. The reaction system studied is the same as the one described in section 2.1.6 i.e.:

$$A + B \xrightarrow{k_1} C \tag{4.21}$$

$$B + C \xrightarrow{k_2} D \tag{4.22}$$

with, $k_1 = 250s^{-1}$ and $k_2 = 250s^{-1}$

The reaction rate constants $k_1 \& k_2$ are varied within a $\pm 5\%$ range (this figure is based on the fact that the accuracy for delivery of solvents is expected to be $\pm 5\%$ and that processes should tolerate such a range [6]) i.e. $k_1 \in [237.5; 262.5] \& k_2 \in [237.5; 262.5]$. The kinematic viscosity is varied as such : $\nu \in [1.10^{-6}; 3.10^{-6}]$

In the case of the micromixing model from continuous operation, 3 variables are therefore varied and the impact that the variations have on the loss as defined in 4.2 is quantified by a global sensitivity analysis which permit to figure the standard deviation on the cost.

Therefore the optimisation permits to find the minimum loss while the Fourier Amplitude Sensitivity Test (FAST) (global sensitivity analysis method used) permit to give the standard variation on loss for perturbation of reaction constant and kinetic viscosity of up to ±5%.

As explained in section 3.2 the advantage of FAST is its speed in conducted a sensitivity analysis in our case i.e. 3 parameters, the standard deviation is provided after 27 function evaluations see D.1.

4.2.6 Mathematical model, uncertainty, optimisation and reactor selection

Mass transfer model : Optimisation of Capital Cost per Unit of Production (CCUP)

In our case the design variables chosen are see 4.1.4: *Conversion (X), Overall mass transfer coefficient (kla), Gas hold-up (ϵ_G), Initial volume of the reaction ($Vl_i nitial$), flowrate of nitrogen stripping (QgN_2)* in agreement with the number of degree of freedom of 5 see C.4. These variables, also called design variables, allows us to define the reactor type i.e. *Overall mass transfer coefficient (kla), Gas hold-up (ϵ_G)* [112], and the more detailed design of the reactor and some of the operating conditions i.e. *Conversion (X), Initial volume of the reaction ($Vl_i nitial$), flowrate of nitrogen stripping (QgN_2).*

To compare the different type of reactor one to another, simulated annealing optimisations are used to identify the minimum Capital Cost per Unit of Production (CCUP) $£/kg$, achievable for each type of reactor design considered. The Capital Costs per Unit of Production (CCUP) has been chosen to compare the different type of reactor as the selection of processing equipment is generally largely determined by two financial considerations. One is the actual capital costs for equipment, and the other is the cost of building a new plant [6].

The minimum Capital cost per Unit of Production that each type of reactor can achieve :

$$\text{Capital cost per unit operation} = \frac{\text{Capital Cost of Reactor}}{\text{yearly production}} \quad (£/gram/year) \tag{4.23}$$

The capital cost of the different type of reactor is defined as follow :

$$\text{Capital Cost of reactor} = C_F\,(\text{Capital Cost of a Stirred Tank Reactor}) \quad (£) \tag{4.24}$$

where,

C_F : Correction Factor (-)

Capital Cost of a Stirred Tank Reactor $= 14595 + 13418V^{0.661}$ – (Determined via data provided by Pfaudler-Balfour reactor system) where V is the inside volume of the reactor in (m^3)

The correction factor permits the determination of the capital cost of the reactor considered in reference to the capital cost of a stirred tank reactor - different values for the C_F will have to be used to understand further with limitation and impact that this factor has on the reactor selection.

For all the following results, the value of C_F selected is equal to 1 :

$$C_F = 1 \tag{4.25}$$

Though the value 1 is not representative of the difference of capital cost between the different type of reactor, it will nevertheless offer a base of reference from which we will later move away from by using more representative values for C_F.

Mass transfer model : measure of uncertainty by sensitivity analysis

The uncertainty in the mass transfer model is expressed through the uncertainty that Henry's constant as a control parameter can carry through its determination i.e. a isobaric (at 760 mmHg) vapour-liquid equilibrium of the mixture 2-propanone/2-propanol graph was used to determined Henry's constant for the mixture. The data provided on the graph presented few points near the origin which made the drawing of the vapour-liquid equilibrium curve is approximated and therefore the determination of Henry's constant uncertain. The values for the Henry's constant of the mixture 2-propanone/2-propanol were found to be included in the range $10^{-4} and 10^{-1} (dimensionless K_H)$

.

The sensitivity analysis carried on the mass transfer model has been tackled as a 'propagation' of the uncertainty contained in Henry's constant through the model and estimate the uncertainty in the model output. The propagation of the uncertainty contained by Henry's constant in the mass transfer model is done by giving four different values to the K_H parameter i.e. $10^{-4}, 10^{-3}, 10^{-2}, 10^{-1} (dimensionless K_H)$, each of these four values is evaluated for the same set of design variables selected at the time by the optimisation algorithm i.e. only the K_H value is changed four times with all the other parameter and variables remaining the same in the mathematical model. The model output will be a vector of four values reflecting the changes made in the control parameter i.e. K_H.

In the following, for $CCUP$ = Capital Cost per Unit of Production, the expression of uncertainty is as follow :

$$Uncertainty = \frac{CCUP_{maximum}}{CCUP_{minimum}} \tag{4.26}$$

To express uncertainty we had the following various choices i.e.

Absolute uncertainty with an expression of the type

$$Uncertainty = CCUP_{maximum} - CCUPminimum \tag{4.27}$$

Relative uncertainty with an expression of the type

$$Uncertainty = \frac{CCUP_{maximum}}{CCUP_{minimum}} \tag{4.28}$$

Mix absolute and relative uncertainty with an expression of the type

$$Uncertainty = \frac{CCUP_{maximum} - CCUP_{minimum}}{CCUP_{minimum}} \tag{4.29}$$

Also while an absolute expression of uncertainty can appear more transparent , an relative expression provides a direct measure between the best and the worst achievable. It is to be noted that the method introduce in this thesis does not depend on the choice made for the expression of uncertainty. And any type of the three mentioned above is possible.

Also Uncertainty is calculated as such (see 4.26), for each set of design variable selected during the optimisation, four different values of Henry's constant K_H are used (see above part 4.2.6): $10^{-4}, 10^{-3}, 10^{-2}, 10-1(dimensionle$ For each of these values the Capital Cost per Unit of Production (CCUP) is calculated and then the maximum and minimum values are used to calculate the uncertainty linked to the set of design variable used.

4.3 Conclusion

In this part of this thesis the objective functions that have been developed to compare the reactor are given. The purpose of the objective function is to sum up the different economical elements present. Different optimisation methods used are also presented. The optimisation method constitute the basis of the selection procedure. The discontinuous behaviour of the model restricts the type of optimisation potentially useable and the simulated annealing method was successfully used. This optimisation technique was further used and implemented for the case of multi-objective optimisation. The multi-objective optimisation permits to address simulatively two fundamental issues that are the uncertainty carried by the model parameters and the cost.

5. RESULTS

5.1 Optimisation results with a single objective simulated annealing method

In the chapter results are first presented for single objective optimisation for the different models presented in chapter 2.

First results are presented in the case of a single objective optimisation for the micromixing model, various values of the kinetic constants were used. Three cases are studied. For each case the kinetic constants are changed in order to evaluate how the optimisation method adapts and determine different types of reactor for different types of reaction system. First values of $k_1 = 25s^{-1}$ and $k_2 = 25s^{-1}$ are used for the kinetic constant. Then the kinetic constant values are changed to $k_1 = 2.5s^{-1}$ and $k_2 = .25s^{-1}$ and $k_1 = 5s^{-1}$ and $k_2 = 2s^{-1}$. The selection of reactor by the reactor selection for these different cases is presented and discussed.

Second results are presented for the case of the mass transfer sensitive reaction described in chapter 2. In this case the value used for the different kinetic constant are the values determined by the Professor Gavriilidis' F-team [185]. The selection of reactor by the optimisation procedure is presented and discussed

5.1.1 Micromixing

In this part of this work the micromixing model presented in chapter 2 is used along the reaction system described in chapter 2 as a competitive, consecutive reaction system defined by :

$$A + B \xrightarrow{k_1} C \tag{5.1}$$

$$B + C \xrightarrow{k_2} D \tag{5.2}$$

Results for kinetic constant $k_1 = 25s^{-1}$ *and* $k_2 = 25s^{-1}$

The figure 5.1 shows the evolution of the different parameters (see section 4.1.1) in between the parameter boundaries, and also the evolution of the objective function as a function of the different parameter moves. The algorithm is set to minimise the objective function, as it can be seen in the figure 5.1

The graph represents the different solutions accepted by the algorithm and the outcome of the objective function. It can be seen that the simulated annealing procedure accepts a lot of *up-moves* at the beginning of the sequence, this acceptance is reduced as the number of iterations increases, and the algorithm only accepts moves which minimise the objective function towards the end of the optimisation.

The Final value for the objective function and the different parameters is listed in table 5.1:

These results (see table 5.1 show the different types of reactor that the computer has selected. The different type of computer are identified thanks to the different values achieve for the reactor design parameter

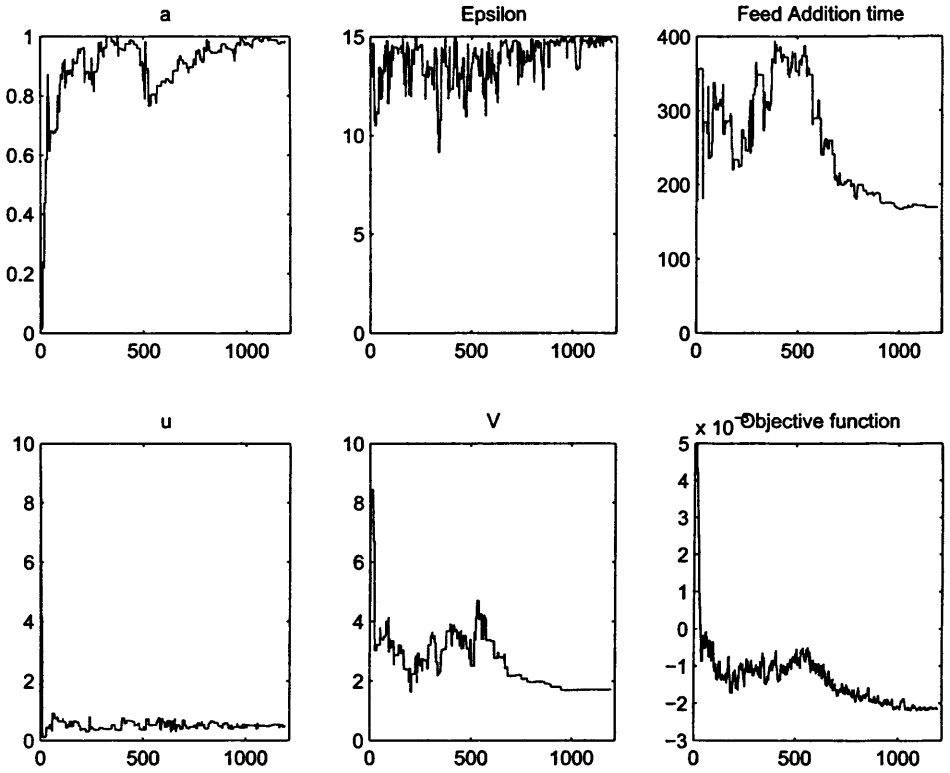

Fig. 5.1: Simulated Annealing Optimisation : Parameters and Objective function evolution

Tab. 5.1: Optimised design parameter values for $k_1 = 25s^{-1}$ and $k_2 = 25s^{-1}$

Variables	Units	Bounds		Optimum	
		Lower	Upper	1	2
a: Ratio of feed volume to reactor volume	(-)	0	1	1	1
ϵ: Energy dissipation rate	$m^2.s^{-3}$	1	15	15	15
t: Feed addition time	s	0.1	400	70	150
u: Fluid velocity within the reactor	m.s	0.01	10	0.4	0.5
V: Reactor Volume	m^3	1E-4	10	0.7	1.5
Profit	£/year			3.2×10^7	2.3×10^7

i.e. The energy dissipation rate, the addition time, the velocity within the reactor, the volume and the ratio of feed volume to reactor volume which correspond Optimum 1 and Optimum 2 represent 2 different solutions found by the automated reactor selection. These two different optima were found for two separate trials. The two optima found are noticeably similar, and they represent the two extreme results obtained over a series of five optimisation trials carried out. The results show that for the particular reaction system studied (see section 2.1.6) with $k_1 = 25s^{-1}$ see equation 2.46 and $k_2 = 25s^{-1}$ see equation 2.47, the types of reactor chosen are similar i.e. that the various optimum dissipation rates are close to each other. In the literature different dissipation rates for different type of reactor can be found [44, 21]. The type which matches this dissipation rate order value (see 5.1) is a Jet-loop reactor [22]. But more importantly this level of energy dissipation rate excludes any stirred tank reactor. The other parameters also give valuable indications of the design like the speed of the fluid for example, which is a fundamental element on the design of a Jet-loop reactor. One can also notice the similar results obtained for the profit generated per year.

Results for kinetic constant $k_1 = 2.5s^{-1}$ *and* $k_2 = .25s^{-1}$

Another case has been looked at. In the following case different rate constants were used to investigate the reactor selection, the first reaction rate constant was given the value, $k_1 = 2.5s^{-1}$, for the second reaction rate constant the value $k_2 = 0.25s^{-1}$ was selected. Table 5.2 gives the summary of the results found.

The energy dissipation rates given as optimum in this example are

smaller to the ones achieved in the previous example. In this case the energy dissipation rate achieved represents a stirred tank reactor with a rushton turbine type of impeller [44]. In this example as the side reaction represented by the second reaction has less importance than in the previous example, and as the first reaction is slower than in the previous example, less energy is necessary to reach the micromixing zone described in 2.4 page 74.

Results for kinetic constant $k_1 = 5s^{-1}$ *and* $k_2 = 2s^{-1}$

In the last case studied, the first reaction rate constant was given the value, $k_1 = 5s^{-1}$, for the second reaction rate constant the value $k_2 = 2s^{-1}$ was selected. Table 5.3 gives the summary of the results achieved for two different optima.

The optimum energy dissipation rate achieved in this case indicates that the reactor selected is a reactor which can deliver a energy dissipation rate smaller than of the one achieved in the first example i.e.

Tab. 5.2: Optimised design parameter values for $k_1 = 2.5s^{-1}$ and $k_2 = 0.25s^{-1}$

Variables	Units	Bounds		Optimum	
		Lower	Upper	1	2
a: Ratio of feed volume to reactor volume	(-)	0	1	0.54	0.57
ϵ: Energy dissipation rate	$m^2.s^-3$	1	15	1.8	1.2
t: Feed addition time	s	0.1	400	280	390
u: Fluid velocity within the reactor	m.s	0.01	10	0.03	0.07
V: Reactor Volume	m^3	1E-4	10	5	7
Profit	£/year			3×10^8	3×10^8

$\epsilon = 15m^2.s^{-3}$ but higher than the energy dissipation rate achieved in the second example i.e. $\epsilon = 1.5m^2.s^{-3}$. In this example the side reaction represented by the second reaction has a higher kinetic constant ($k_2 = 2s^{-1}$) than in the second example ($k_2 = 0.25s^{-1}$). But when compared to the first example, the side reaction represented by the second reaction has a lower kinetic constant ($k_2 = 2s^{-1}$) than in the first example ($k_2 = 25s^{-1}$).

Summary of results

The table 5.4 summarises the results obtained

The three previous examples 5.1, 5.2,5.3 show that for different type of reaction kinetics, different type of reactor design are selected as more economically suitable for the reactions scale-up.

In the literature different dissipation rates for different types of reactor can be found [44, 21]. The following work is focused on using literature results to define which reactors match the results obtained above.

Tab. 5.3: Optimised design parameter values for $k_1 = 5s^{-1}$ and $k_2 = 2s^{-1}$

Variables	Units	Bounds		Optimum	
		Lower	Upper	1	2
a: Ratio of feed volume to reactor volume	(-)	0	1	0.6	0.4
ϵ: Energy dissipation rate	$m^2.s^{-3}$	1	15	11	11
t: Feed addition time	s	0.1	400	150	280
u: Fluid velocity within the reactor	m.s	0.01	10	0.1	0.2
V: Reactor Volume	m^3	1E-4	10	3	8
Profit	£/year			2.2×10^8	2.4×10^8

These results show clearly that for different cases as for different type of reaction sensitivity to mixing, the reactor procedure adapts to the type of reaction system considered and identifies reactor for the scale-up of the reaction that can cater for the need of the reaction from a mixing point of view.

5.1.2 Mass transfer

In this part of the thesis results found for the selection of reactor for the scale-up of the mass transfer sensitive reaction system presented in 2.52 [185]. The values used for the kinetic constant are the values identified by Prof. Gavriilidis' F-Team [185].

In order to carry out the reactor selection for this case study the following procedure was used.

To compare the different types of reactor to one another, simulated annealing optimisations are used to identify the minimum Capital Cost

Tab. 5.4: Optimised design parameter values for different kinetic values k_1 and k_2

Variables	Units	Optimum		
		case 1	case 2	case 3
k_1 & k_2	s^{-1}	$k_1 = 25$ & $k_2 = 25$	$k_1 = 2.5$ & $k_2 = 0.25$	$k_1 = 5$ & $k_2 = 2$
a	(-)	1	0.55	0.6 - 0.4
ϵ	$m^2.s^{-3}$	15	1.5	11
t	s	70 - 150	280 - 390	150 - 280
u	m.s	0.4 - 0.5	0.03 - 0.07	0.1 - 0.2
V	m^3	0.7 - 1.5	5 - 7	3 - 8
Profit	£/year	3.2 - 2.3 $\times$ 10^7	3 $\times$ 10^8	2.2 - 2.4 $\times$ 10^8

per Unit of Production (CCUP) $£/m^3/year$, achievable for each type of reactor considered. This permits us to compare the best minimum cost achievable for each type of reactor regardless of how disparate the minimum achievable Capital Cost per Unit of Production for each type of reactor is. If a simulated annealing was conducted to find the minimum CCUP for all type of reactor, then some reactor types might not be selected i.e. the CCUP achieved is much higher than the CCUP achieved with other reactor types. By using a simulated annealing optimisation per type of reactor then we make sure that a minimum CCUP is achieved for each reactor type. A simulated annealing optimisation will be used for each type of reactor considered. Each simulated annealing optimisation is restricted to the design variables defining the type of reactor i.e. *Overall mass transfer coefficient (k_la), Gas hold-up (ϵ_G)* restrained to values which defined the type of reactor the simulated annealing optimisation is for [112].

Tab. 5.5: Mass transfer k_la and Gas hold-up characteristics of common contactors

Reactor type	k_la	Gas Hold-up ϵ_G
	(1/s)	(-)
Bubble column excluding jet (loop)	0.005 - 0.01	< 0.2
Spray Column	0.00007 - 0.015	> 0.8
Packed column counter current	0.005 - 0.02	> 0.95
Plate column	0.01 - 0.05	> 0.8
Mechanically agitated	0.02 - 0.2	< 0.1
Jet (loop)	0.01 - 2.2	< 0.5

To restrain the design variables to a certain type of reactor the upper-limit and the lower-limit of the design variable are set to fixed bound-

aries, as for example, in the case of a stirred tank reactor (i.e. Reactor Mechanically agitated) : $kla \in [0.02 - 0.2]\,(s^{-1})$ & $\epsilon_G < 0.1(s^{-1})$, also $kla_{upper-limit} = 0.2(s^{-1}) - kla_{lower-limit} = 0.02(s^{-1})$ and, $\epsilon_{G_{upper-limit}} = 0.1(-) - \epsilon_{G_{lower-limit}} = 0(-)$.

In the following we compare 3 different types of reactor like the Stirred Tank Reactor, Bubble Column Reactor and Jet-Loop reactor over the minimum Capital cost per Unit of Production that each type of reactor can achieve :

$$\text{Capital cost per unit operation} = \frac{\text{Capital Cost of Reactor}}{\text{yearly production}} \quad (£/gram/year) \tag{5.3}$$

The capital cost of the different type of reactor is defined as follows :

$$\text{Capital Cost of reactor} = C_F\,(\text{Capital Cost of a Stirred Tank Reactor}) \quad (£) \tag{5.4}$$

where,

C_F : Correction Factor (-)

Capital Cost of a Stirred Tank Reactor $= 14595 + 13418V^{0.661}$ – (Determined via data provided by Pfaudler-Balfour reactor system) where V is the inside volume of the reactor in (m^3)

The correction factor allows us to determine the capital cost of the reactor considered in reference to the capital cost of a stirred tank reactor - different values for the C_F will have to be used to understand

further the limitation and impact that this factor has on the reactor selection.

For all the following results, the value of C_F selected is equal to 1 :

$$C_F = 1 \tag{5.5}$$

Though the value 1 is not representative of the difference of capital cost between the different type of reactors, it will nevertheless offer a base of reference from which we will later move away from by using more representative values for C_F. The minimum Capital Cost per Unit of Production (CCUP) achieved for each type of reactor can be summarised in table 5.6.

Tab. 5.6: Minimum Capital Cost per Unit Operation and design characteristics for three different type of reactors

Reactor type	Minimum Capital Cost per unit operation (£/gram/year)	X (%)	QgN_2 (m^3/s)	$Vl_{initial}$ (m^3)
Bubble column excluding jet (loop)	0.126	96	0.093	1.9
Mechanically agitated	0.059	95.4	0.098	2.5
Jet (loop)	0.053	95	0.099	1.5

The results presented in table 5.6 are the minimum values achieved with 5 simulated annealings for the Bubble column excluding jet(loop) and mechanically agitated reactors and 3 simulated annealing for the Jet (loop) reactor. Table 5.7presents - Mean minimum CCUP - CCUP variance - Standard deviation - achieved for each type of reactor.

The results presented in table 5.7 are the mean results achieved with 5 simulated annealings for the Bubble column excluding jet(loop) and mechanically agitated reactors and 3 simulated annealings for the Jet (loop) reactor.

5.1.3 Discussion

From the above results, the Jet-loop reactor is the reactor which presents out of the three reactors considered the lowest Capital Cost per Unit Operation. More reactor types (Packed Column counter-current, Spray reactor, Plate Column) will be included in the next report to be able to compare the results achieved with the Jet-loop to confirm that the Jet-loop is the most cost effective reactor for the mass transfer model.

5.2 Optimisation results with a Multi Objective Simulated Annealing (MOSA) method

In the chapter results are first presented for Multi Objective Simulated Annealing method (MOSA) for the different models presented in

Tab. 5.7: MEAN min CCUP - Variance - Standard Deviation

Reactor type	MEAN Minimum CCUP (£/gram/year)	Variance	STD (Standard Deviation)
Bubble column excluding jet (loop)	0.14	4.10^{-4}	0.02
Mechanically agitated	0.09	4.10^{-4}	0.02
Jet (loop)	0.059	3.10^{-5}	5.10^{-3}

chapter 2.

First results are presented for the case of a Multi Objective Simulated Annealing optimisation method (MOSA) for the micromixing model, the kinetic constants are varied by *10%* of their original values, $k_1 = 25s^{-1}$ and $k_2 = 25s^{-1}$, to evaluate the impact that uncertainty in the determination of the kinetics constant has on the determination of the reactor the most suited for the scale-up of the mixing sensitive reaction system described in chapter 2 see 2.1.6 page 78. The selection of reactor by the multi optimisation reactor selection procedure is also discussed.

In the second part of this section the results for the selection of reactor for the scale-up of the CATHy reaction [185, 135], shown in chapter 2, is presented. Here again a Multi Objective Simulated annealing Optimisation method is used to find the best reactor for scaling up the CATHy reaction in terms of cost and in term of uncertainty. In this case the uncertainty on the scale-up of the reaction is measured by varying the Henry's constant, determined graphically as 4.210^{-2}, from this original value. The propagation of the uncertainty contained by Henry's constant in the mass transfer model is done by giving four different values to the K_H parameter i.e. $10^{-4}, 10^{-3}, 10^{-2}, 10^{-1}(dimensionless K_H)$. The variation resulting from the changes in the Henry's constant are used in the selection procedure to evaluate which reactor reacts the most to uncertainty and identify reactors which present the most robust behaviour to uncertainty.

5.2.1 Continuous operation Micromixing model : reactor design selection

Results are presented for the case of a Multi Objective Simulated Annealing optimisation method (MOSA) for the micromixing model.

The kinetic constants are varied by *10%* of their original values ,$k_1 = 25s^{-1}$ and $k_2 = 25s^{-1}$, to evaluate the impact that uncertainty in the determination of the kinetics constant has on the determination of the reactor.

The mixing sensitive reaction system studied is shown in chapter 2 see 2.1.6 page 78 and is the same as in the case of the single objective optimisation.

Graph 5.2 shows the evolution of the MOSA search method.

In this graph the bottom left hand corner graph represents all the solution accepted by MOSA while the bottom left hand corner represents only the pareto solutions also called non-dominated solutions (see 4.2.3) as it can be seen in the bottom left hand corner graph of figure 5.2. The pareto solutions are then all selected and each solution is then 'classified' with regards to the design variables which defined each solution.

The reactors are modeled via the same mathematical model - the continuous operation micromixing model that has been implemented see Appendix B . The change of variables is a representation of a change of reactor e.g if $1500 < \epsilon < 2500$ (see table 5.8) then the reactor is a jet-loop reactor.

The graph 5.3 represents the results obtained through the MOSA method

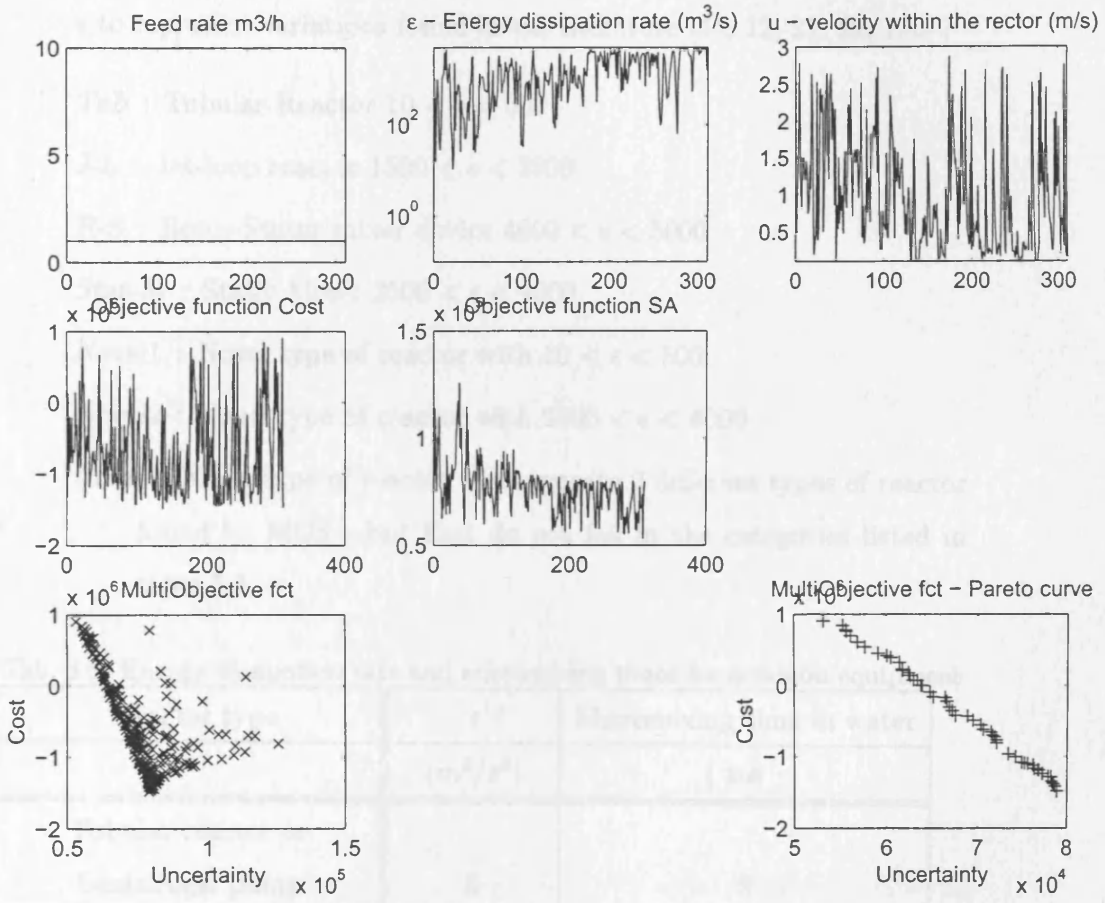

Fig. 5.2: Evolution of the multiobjective search method - MOSA - for the continuous micromixing model

which was described in section 4.2.4, and for which detailed explanation can be found in the following references [187] and [198].

In graph 5.3 the following abbreviations have been used to described the different types of reactor and the following range for the design variable ϵ to represent variations found in the literature [44, 12, 21, 22, 130] :

Tub : Tubular Reactor $10 < \epsilon < 500$

J-L : Jet-loop reactor $1500 < \epsilon < 2500$

R-S : Rotor-Stator mixer device $4000 < \epsilon < 5000$

Stat-M : Static Mixer $2500 < \epsilon < 4000$

Novel1 : Novel type of reactor with $10 < \epsilon < 500$

Novel2 : Novel type of reactor with $2500 < \epsilon < 4000$

Novel : Novel type of reactor - incorporate 2 different types of reactor found by MOSA but that do not fall in the categories listed in table 5.8

Tab. 5.8: Energy dissipation rate and micromixing times for common equipment

Reactor type	ϵ	Micromixing time in water
	(m^2/s^3)	(ms)
Tubular reactor or Centrifugal pump	5	8
Stirred tank reactor	0.2 - 50	40 - 2.4
Static in-line mixer (e.g. Kenics)	1000	0.5
Rotor - Stator mixer device (e.g. Silverson mixer)	5000	0.25
Jet (loop) [21, 22]	1500 - 2500	0.25 - 0.5

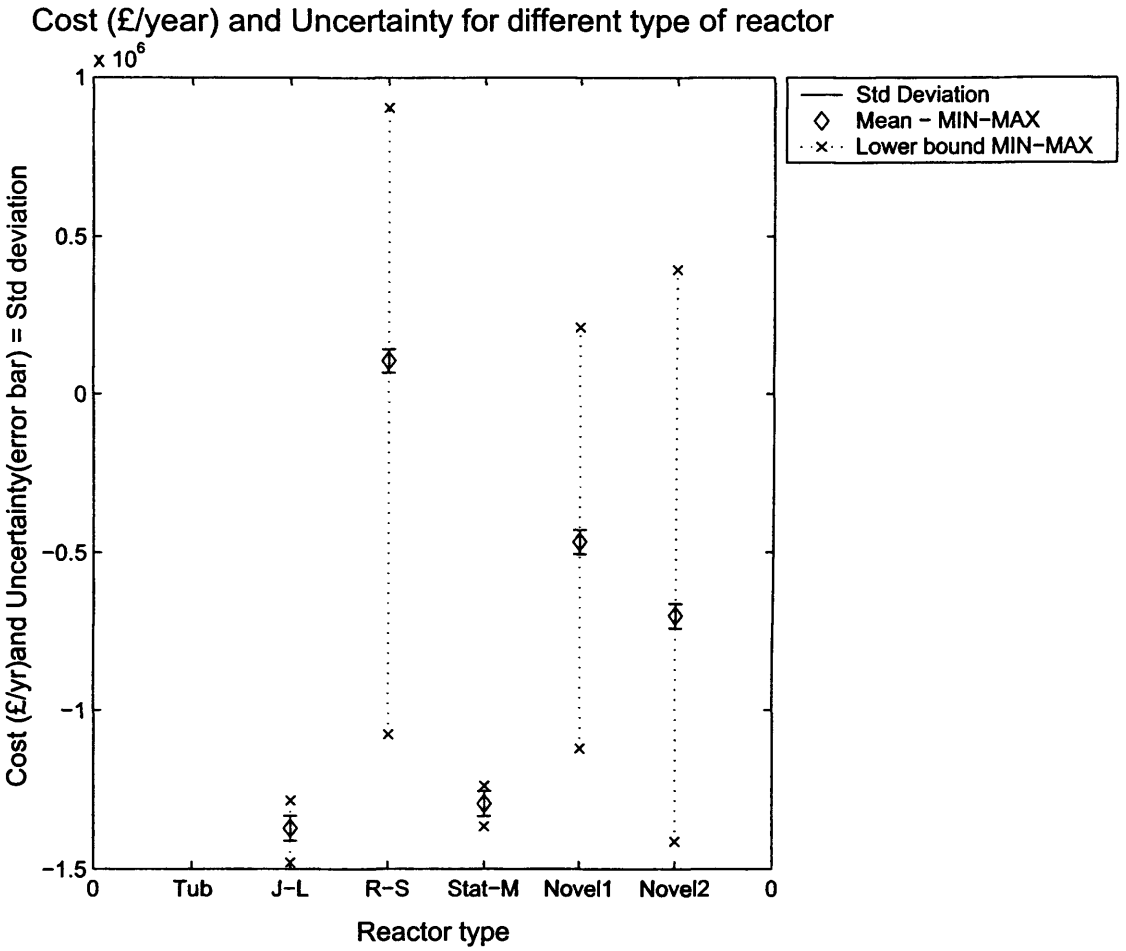

Fig. 5.3: Reactor Selection for the continuous micromixing Model

Graph 5.3 and graph 5.4 present the results obtained for the different types of reactor (see X-axis). The Graphs presents the minimum and the maximum costs achievable per type of reactor and the minimum uncertainty i.e. Standard deviation of cost. In these graphs, the Y-axis represents the loss achieved by each type of reactor - as explained above the non-dominated solutions or pareto front represents the 'BEST' solutions fulfilling both objectives. If within all the solutions constituent

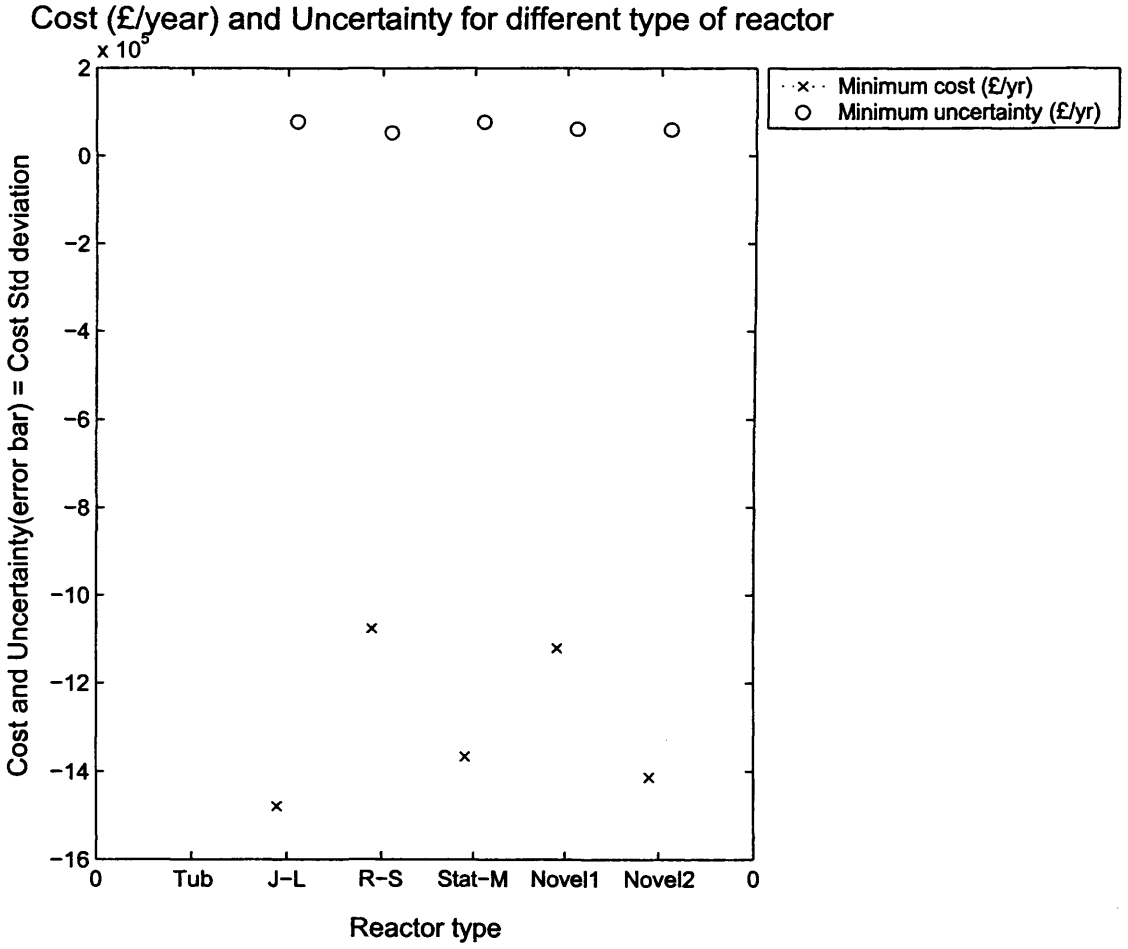

Fig. 5.4: Reactor Selection for the continuous micromixing model

of the pareto front, none with the characteristics as variables values like for example $10 < \epsilon < 500$ then there is no tubular reactors as solutions of the multiobjective optimisation. Also, if there is no symbol for certain types of reactor this means that no solution has been retained for that type of reactor within the non-dominated solution. This means that the type of reactor is not part of the curve that represents the trade-off (pareto front) between the two objectives. The length of the error bar indicates the uncertainty as standard variation in the loss linked to the reactor type. The uncertainty shows how sensitive to the change of parameters values the design of the reactor is. The parameter used are the Reaction rate constant $k_1 \& k_2$ (see 2.1.6) & the kinematic viscosity ν

In graph 5.4 the plots show that the best Loss(£/kg) is achieved for reactor like the static-mixer type of reactor with respectively, $Cost(Jet) = -1.48.10^6 £/yr - CCUP(novel2) = -1.41.10^6 £/yr - Cost(Stat-M) = -1.37.10^6 £/yr$. Let's remember that the objective is to minimise the loss per year and that $Profit = -Cost$, also by minimising the loss we have optimised the profit. In this case like in the previous case (mass transfer model), as it can be seen in graph 5.9, the minimum uncertainty trades against the minimum Loss per year. Also when considering the minimum uncertainty, this is represented by the length of the uncertainty bar (full line) the rotor-stator reactor presents the most robust design, i.e. $StandardVariation = 5.3.10^4 (£/yr)$, with regards to tolerance to parameter variation or rather uncertainty. Though it is also noticeable that the minimum standard variations of loss of the different type of reactor are very close one to another i.e. $CostSTD(Jet) = 7.82.10^4 £/yr - CostSTD(R-S) = 5.3.10^4 £/yr - CostSTD(Stat -$

$M) = 7.7.10^4 £/yr - CostSTD(Novel1) = 6.2.10^4 £/yr - CCUP(novel2) = 6.1.10^4 £/yr$.

Table 5.9summarises the design of the most profitable reactor and the reactor most robust to parameter variation or to uncertainty linked to the determination of the reaction rate constants and the kinematic viscosity parameter.

Tab. 5.9: Comparison between the design of the most profitable reactor and the design of most parameter variation tolerant reactor

Design variables	Jet-loop reactor with lowest CCUP	Rotor-Stator with lowest Uncertainty
Energy dissipation rate - ϵ (m^2/s^3)	1950	4960
Average speed within the reactor - u (m/s)	0.15	2.75
Loss(£/yr)	-1.5E6	9.1E5
Uncertainty (£/yr)	7.9E4	5.3E4

Continuous micromixing model : Results for Upperbound

As for the mass transfer model, the study has also been carried out for the Upperbound level of the parameters.

Graph 5.5 shows the evolution of the MOSA search method.

In this graph the bottom left hand corner graph represents all the solutions accepted by MOSA while the bottom left hand corner represents only the pareto solutions also called non-dominated solutions (see 4.2.3) as it can be seen in the bottom left hand corner graph of figure 5.2. The pareto solutions are then all selected and each solution is

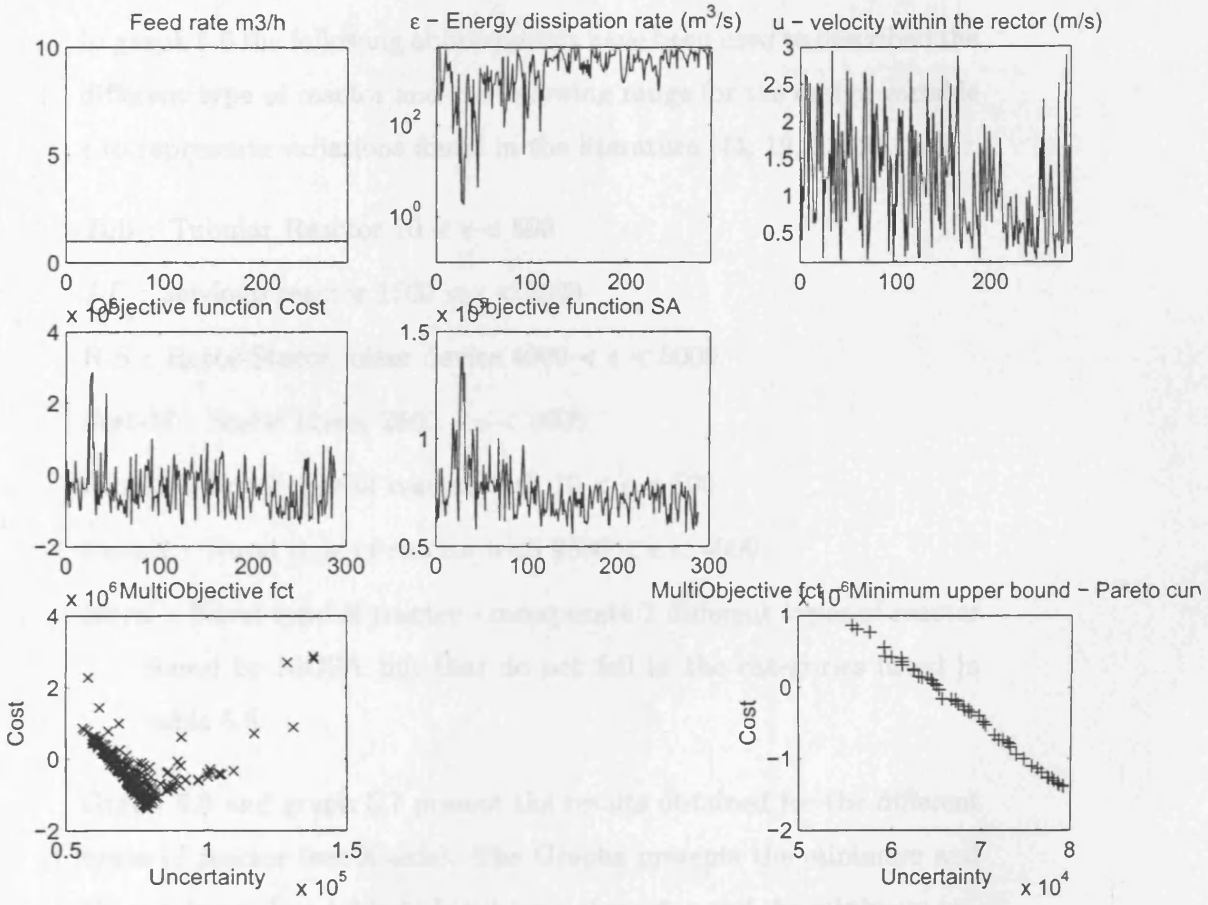

Fig. 5.5: Evolution of the multiobjective search method - MOSA - for the continuous micromixing model

then 'classified' with regards to the design variables which define each solution.

Graph 5.6 represents the results obtained through the MOSA method for the parameter Upperbound.

In graph 5.6 the following abbreviations have been used to described the different type of reactor and the following range for the design variable ϵ to represents variations found in the literature [44, 12, 21, 22, 130] :

Tub : Tubular Reactor $10 < \epsilon < 500$

J-L : Jet-loop reactor $1500 < \epsilon < 2500$

R-S : Rotor-Stator mixer device $4000 < \epsilon < 5000$

Stat-M : Static Mixer $2500 < \epsilon < 4000$

Novel1 : Novel type of reactor with $10 < \epsilon < 500$

Novel2 : Novel type of reactor with $2500 < \epsilon < 4000$

Novel : Novel type of reactor - incorporate 2 different types of reactor found by MOSA but that do not fall in the categories listed in table 5.8

Graph 5.6 and graph 5.7 present the results obtained for the different types of reactor (see X-axis). The Graphs presents the minimum and the maximum loss achievable per type of reactor and the minimum uncertainty i.e. Standard deviation of cost. In these graphs, the Y-axis represents the loss achieved by each type of reactor - as explained above the non-dominated solutions or pareto front represents the 'BEST' solutions fulfilling both objectives. If within all the solutions constituent of the pareto front, none with the characteristics as variables values like for example $10 < \epsilon < 500$ then there is no tubular reactors as a

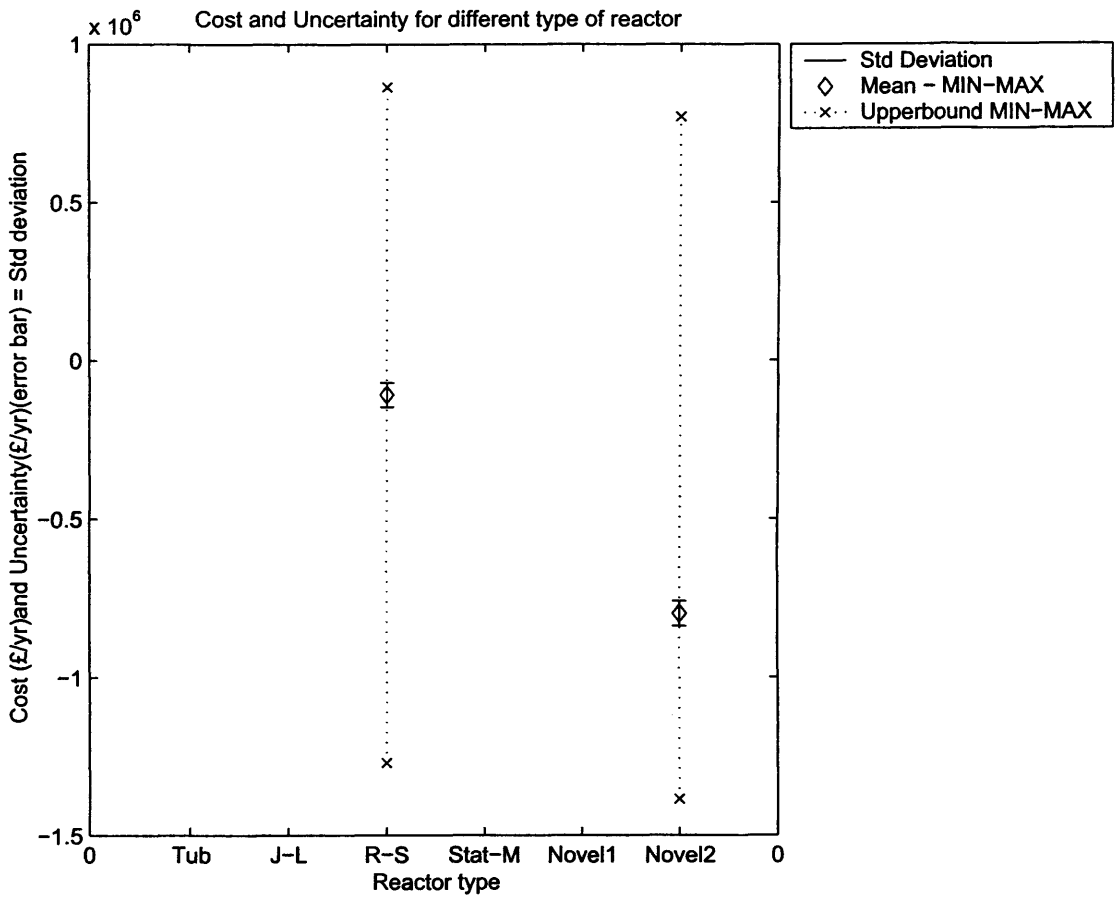

Fig. 5.6: Reactor Selection for the continuous micromixing Model - Upperbound

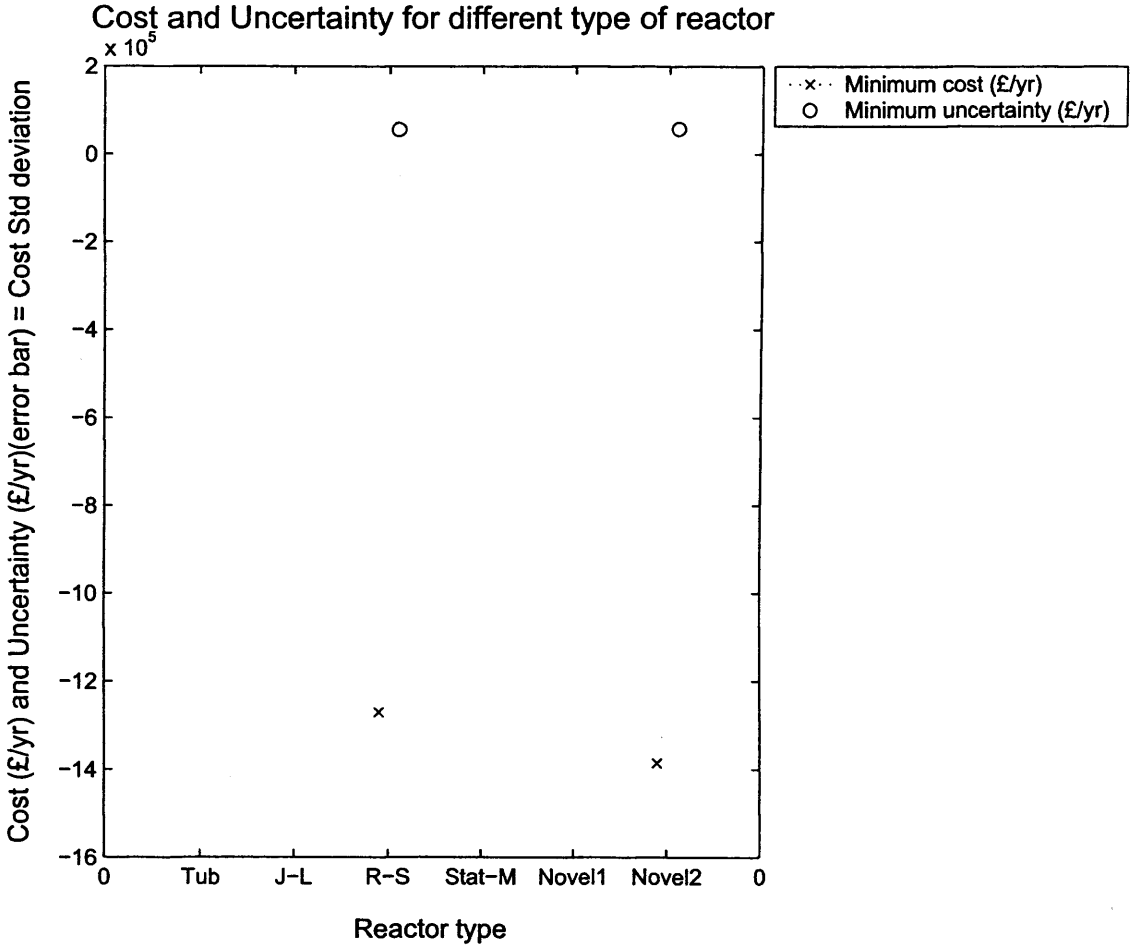

Fig. 5.7: Reactor Selection for the continuous micromixing model - Upperbound

solution of the multiobjective optimisation. Also, if there is no symbol for certain types of reactor this means that no solution has been retained for that type of reactor within the non-dominated solution. This means that type of reactor is not part of the curve that represents the trade-off (pareto front) between the two objectives. The length of the error bar indicates the uncertainty as standard variation in the loss linked to the reactor type. The uncertainty shows how sensitive to the change of parameters (Reaction rate constant k_1&k_2 see 2.1.6 & kinematic viscosity ν)values the design of the reactor is.

In graph 5.7 the plots show that the best Loss(£/kg) is achieved for reactor like the Novel2 type of reactor $Cost(Novel2) = -1.4.10^6(£/yr)$. Also when considering the minimum uncertainty, this is represented by the length of the uncertainty bar (full line) the rotor-stator reactor presents the most robust design, i.e. $StandardVariation = 5.4.10^4(£/yr)$, with regards to tolerance to parameter variation or rather uncertainty.

Table 5.10 summarises the design of the most profitable reactor and the reactor most robust to parameter variation or in uncertainty linked to the determination of the reaction rate constants and the kinematic viscosity parameter.

Like in the previous results, one can notice that the reactor with the lowest uncertainty present a profit at loss, this is because the uncertainty and the loss trade against each other.

Graph 5.8 presents a comparison of the Lowerbound and Upperbound pareto fronts.

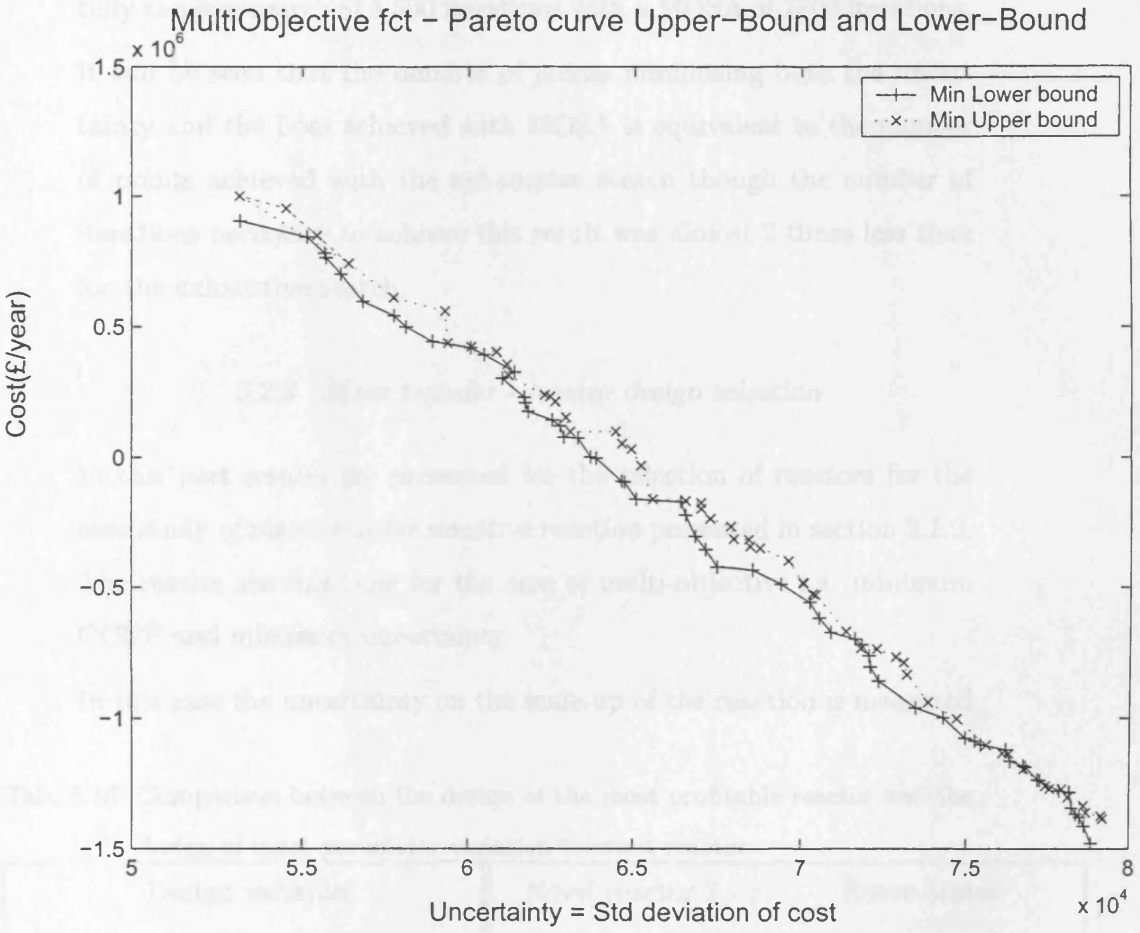

Fig. 5.8: Lowerbound and Upperbound pareto front - Continuous micromixing model

5.2.2 Exhaustive Search (ES) versus Multiobjective Simulated Annealing (MOSA)

Graph 5.9 represents a comparison between an exhaustive search or totally random search of 3,500 iterations with a MOSA of 1800 iterations.

It can be seen that the number of points minimising both the uncertainty and the Loss achieved with MOSA is equivalent to the number of points achieved with the exhaustive search though the number of iterations necessary to achieve this result was almost 2 times less than for the exhaustive search.

5.2.3 Mass transfer - reactor design selection

In this part results are presented for the selection of reactors for the case study of mass transfer sensitive reaction presented in section 2.1.9. The results are this time for the case of multi-objective i.e. minimum CCUP and minimum uncertainty.

In this case the uncertainty on the scale-up of the reaction is measured

Tab. 5.10: Comparison between the design of the most profitable reactor and the design of most parameter variation tolerant reactor

Design variables	Novel reactor 2 with lowest CCUP	Rotor-Stator with lowest Uncertainty
Energy dissipation rate - ϵ (m^2/s^3)	3029	4884
Average speed within the reactor - u (m/s)	0.14	2.8
Loss(£/yr)	-1.4E6	1E6
Uncertainty (£/yr)	7.9E4	5.4E4

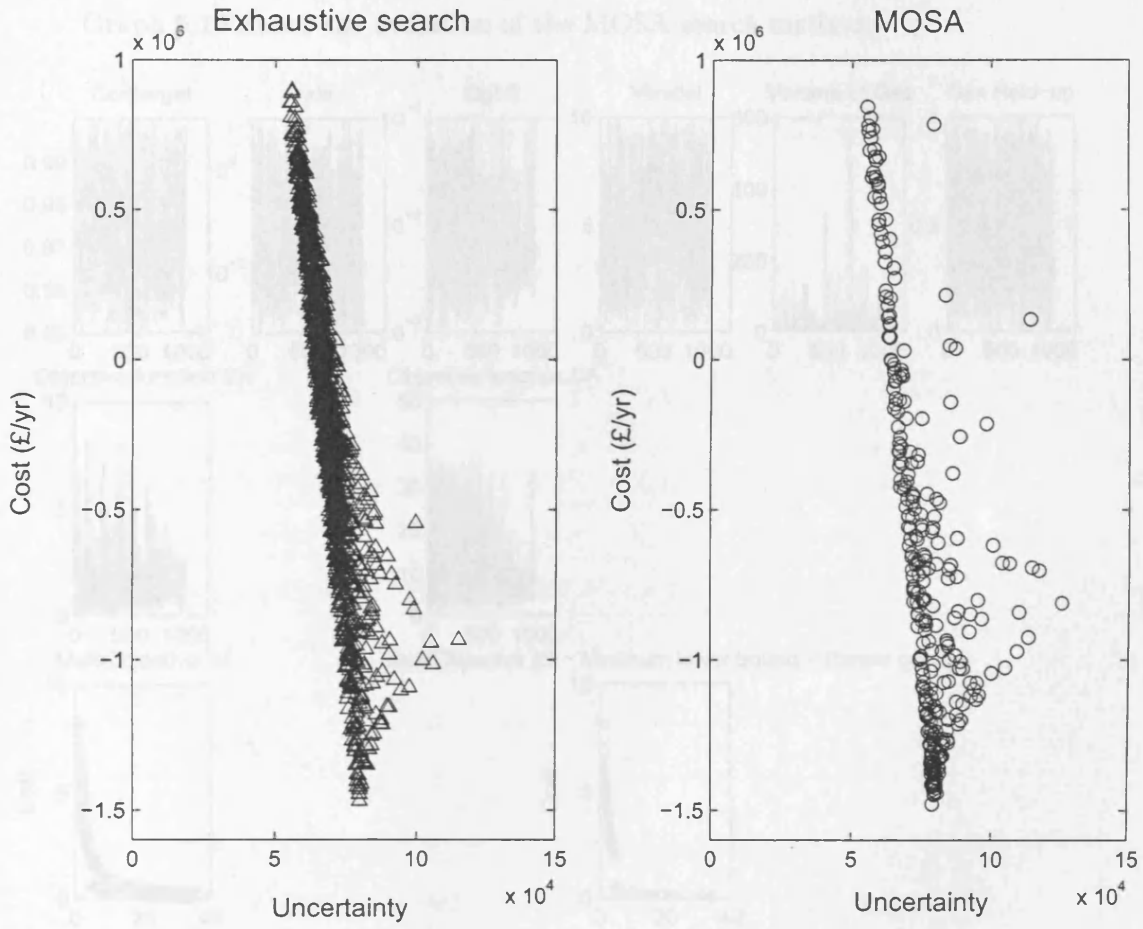

Fig. 5.9: Exhaustive search space Versus MOSA search space

by varying the Henry's constant, determined graphically as 4.210^{-2}, from this original value. The propagation of the uncertainty contained by Henry's constant in the mass transfer model is done by giving four different values to the K_H parameter i.e. $10^{-4}, 10^{-3}, 10^{-2}, 10^{-1}(dimensionless K_H)$.

Graph 5.10 shows the evolution of the MOSA search method.

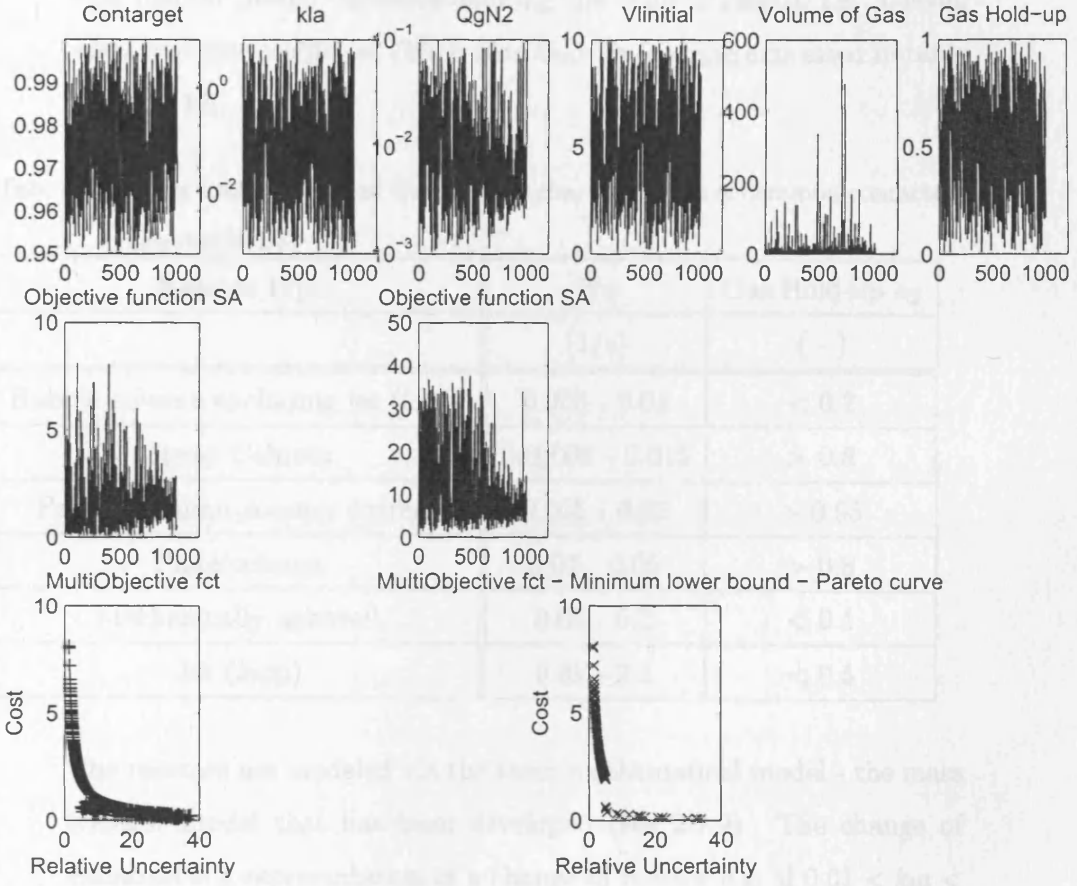

Fig. 5.10: Evolution of the multiobjective search method - MOSA - for the mass transfer model

In this graph the bottom left hand corner graph represents all the solution accepted by MOSA while the bottom left hand corner repre-

sents only the pareto solutions also called non-dominated solutions (see 4.2.3) as it can be see in the bottom left hand corner graph of figure 5.10. The pareto solutions are then all selected and each solution is then 'classified' with regards to the design variables which defined each solution.

The reactor design variables defining the type of reactor i.e. *Overall mass transfer coefficient (kla), Gas hold-up* (ϵ_G) are expressed in table 4.3 see[112].

Tab. 5.11: Mass transfer $k_l a$ and Gas hold-up characteristics of common contactors (see table 4.3)

Reactor type	*kla*	Gas Hold-up ϵ_G
	(1/s)	(-)
Bubble column excluding jet (loop)	0.005 - 0.01	< 0.2
Spray Column	0.00007 - 0.015	> 0.8
Packed column counter current	0.005 - 0.02	> 0.95
Plate column	0.01 - 0.05	> 0.8
Mechanically agitated	0.02 - 0.2	< 0.1
Jet (loop)	0.01 - 2.2	< 0.5

The reactors are modeled via the same mathematical model - the mass transfer model that has been developed (see 2.1.9). The change of variables is a representation of a change of reactor e.g. if $0.01 < k_l a < 2.2 \& 0.55 > Gashold - up > 0.45$ (see table 4.3) then the reactor is a jet-loop reactor.

In graph 5.11, 5.12 and 5.13, the following abbreviations have been used :

STR : Stirred Tank Reactor

Jet : Jet-loop reactor

B-Col : Bubble Column

P-Colcc : Packed Column reactor counter-current

S-Col : Spray Column

Pl-Col : Plate Column

Novel : Novel type of reactor - incorporates all the reactors found by MOSA but that do not fall in the categories listed in table 4.3

Graphs have been used to express the comparison between the different reactors. The type of graphs used is described in figure 5.11 and 5.11. In these graphs it can be seen how the results obtained for the pareto curve are put into the form of bar graph which permits us to compare the different reactors considered one against the other. The pareto curve obtained at the end of the multi-objective optimisation represents all the reactors and all the specific designs attached to each types of reactor. In order to compare the different type of reactor and there specific designs, a clustering is done to regroup the reactor by type according to table 4.3. Once this is done the best reactor of its category is selected regarding the two criteria selected i.e. minimum uncertainty - minimum CCUP.

The maximum uncertainty value shown on the graphs represents the results achieved for the reactor and design identified by MOSA calculated through the formula definition of uncertainty i.e.

$$Uncertainty = \frac{CCUP_{maximum}}{CCUP_{minimum}} \tag{5.6}$$

The multi-objective optimisation presents results for Uncertainty and $CCUP_{minimum}$, therefore:

$$CCUP_{maximum} = UncertaintyxCCUP_{minimum} \tag{5.7}$$

The maximum CCUP value shown on the graphs represents the results achieved for the reactor and design identified by MOSA and is calculated in the same way.

The graph 5.13 represents the results obtained through the MOSA method which was described in section 4.2.4, and for which detailed explanation can be found in the following references [187] and [198].

Graph 5.13 presents the results obtained for the different types of reactor (see X-axis). In this graph, the Y-axis represents the Capital Cost per Unit of Production achieved for each type of reactor - as explained above the non-dominated solutions or pareto front represents the 'BEST' solutions fulfilling both objectives. If within all the solutions constituent of the pareto front, none with the characteristics of variables values for example $0.01 < k_l a < 2.2 \& 0.55 > Gashold - up > 0.45$ then there is no Jet-loop reactors as solutions of the multiobjective optimisation. Also, if there is no symbol for certain types of reactor this means that no solution has been retained for that type of reactor within the non-dominated solution. This means this type of reactor is not part of the curve that represents the trade-off (pareto front) between the two objectives. The length of the error bar indicates the uncertainty linked to the reactor type. The uncertainty shows how sensitive to the change of parameter (Kh - Henry's constant value)values the design of the reactor is.

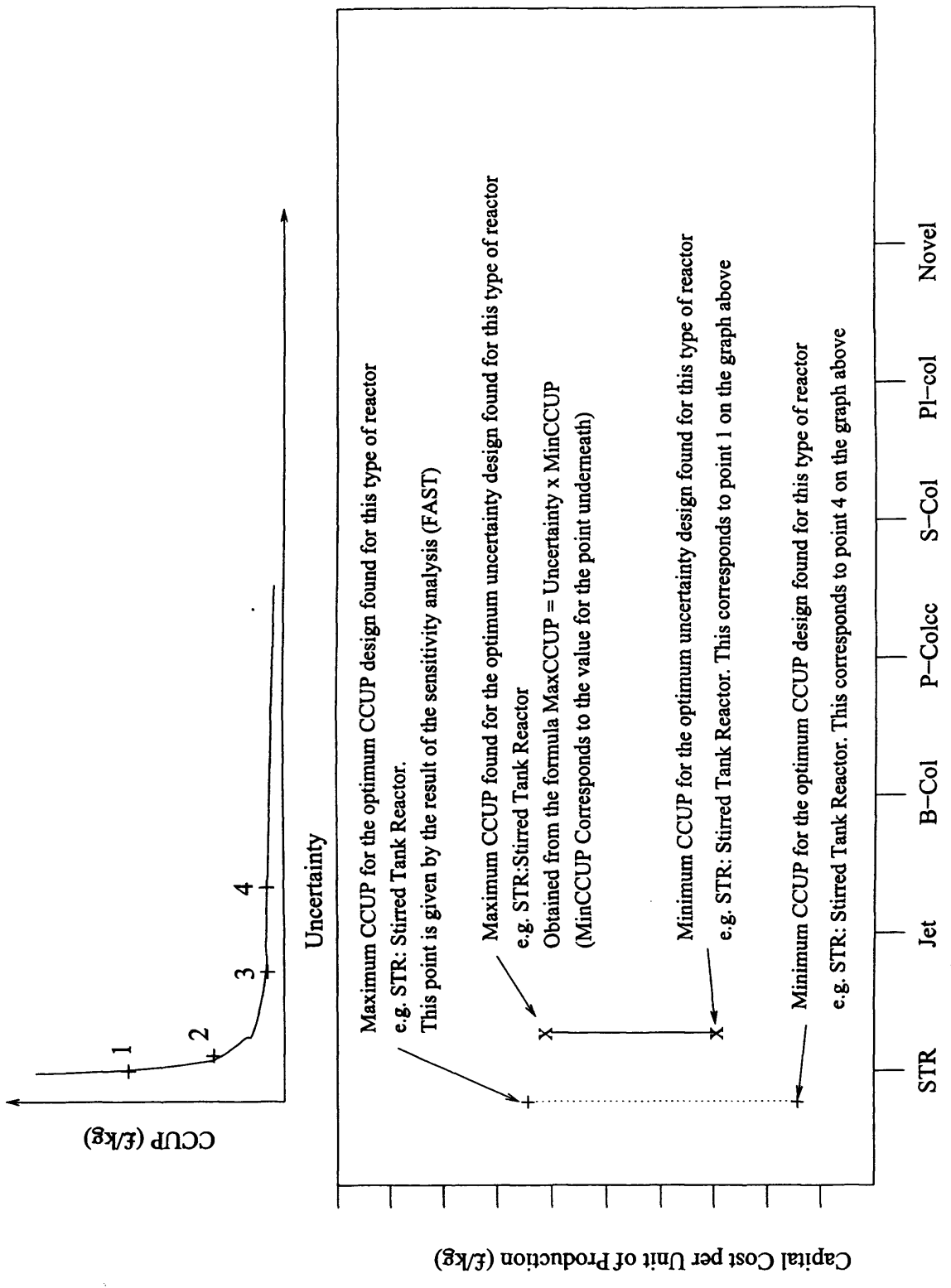

Fig. 5.11: Reactor Selection graph for Stirred Tank Reactor

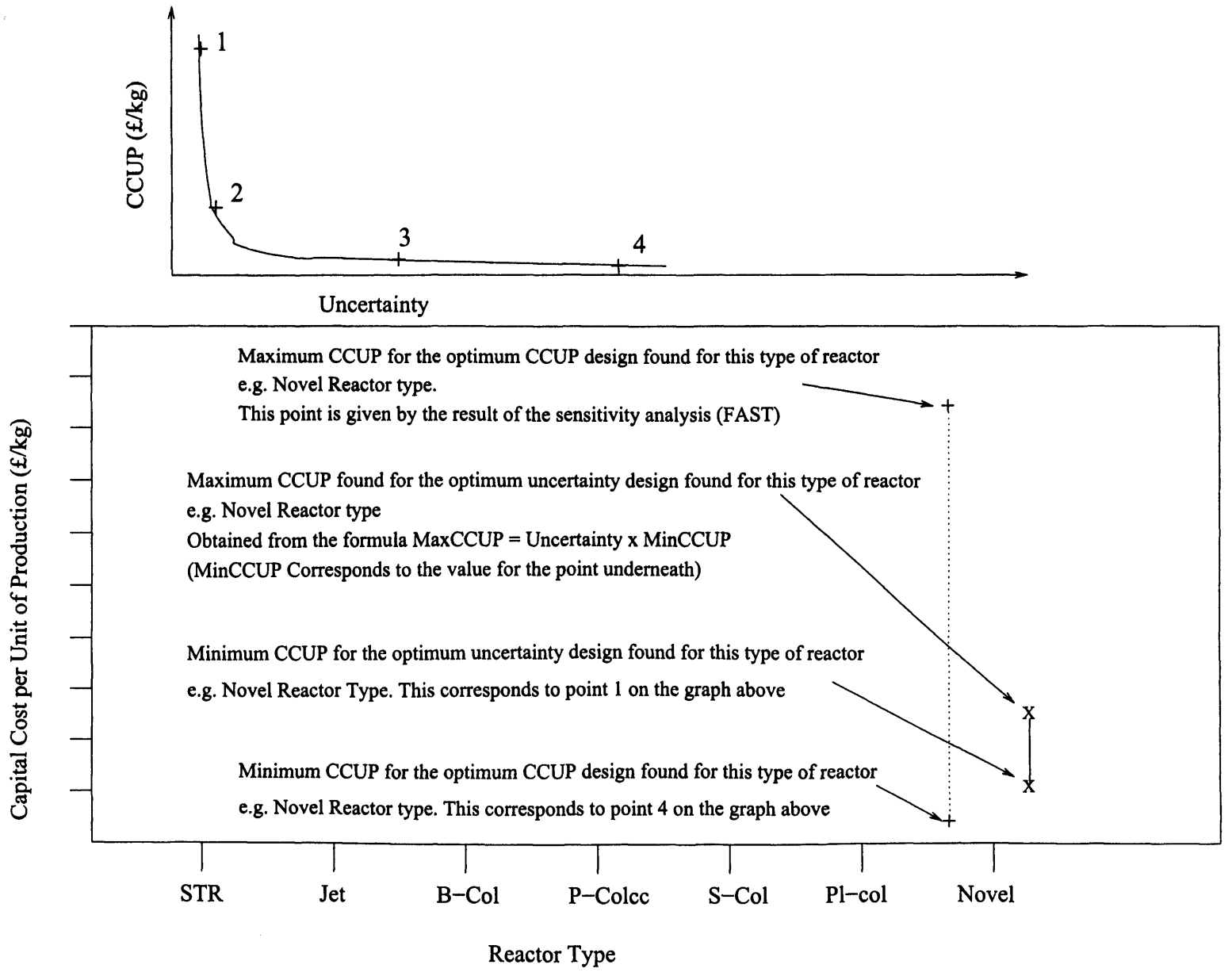

Fig. 5.12: Reactor Selection graph for Novel Reactor

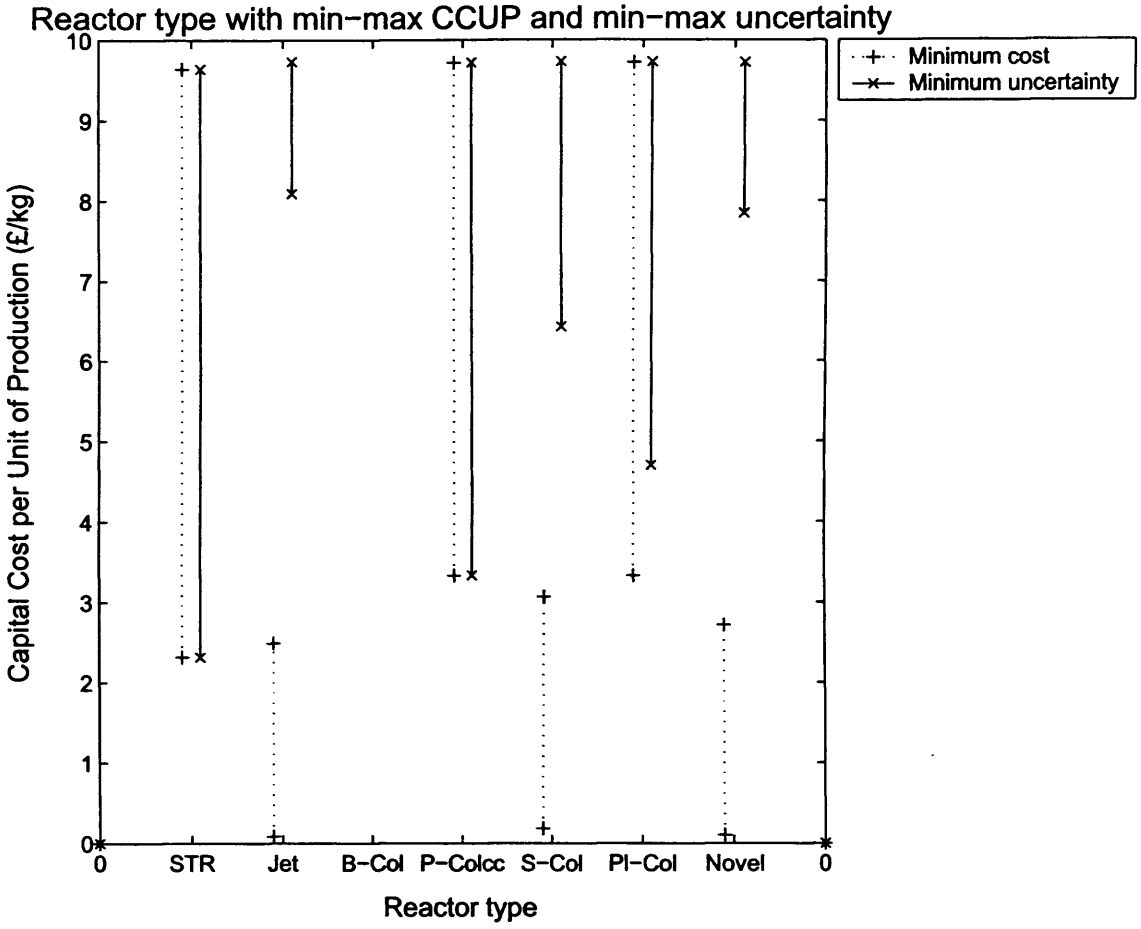

Fig. 5.13: Reactor Selection for Mass Transfer Model

These results show that the best Capital Cost per Unit of Production (£/kg) is achieved for reactor like the jet loop reactor and the novel reactor with $CCUP(Jet) = 0.1£/kg\&CCUP(novel) = 0.09£/kg$. Also reactors presenting the most profitable robust design with regards to their parameter tolerance are the stirred tank reactors (STR) $CCUP(STR) = 2.3£/kg$, the packed column counter current reactor $CCUP(P_Colcc) = 3.3£/kg$ and the plate column reactor $CCUP(STR) = 4.7£/kg$. Nevertheless from the definition of the uncertainty given (see above 4.27) the loss associated with these designs is not the most profitable. As it can also be seen in graph 5.20, the minimum uncertainty trades against the minimum Capital Cost per Unit Operation. When only considering the minimum uncertainty, this is represented by the length of the uncertainty bar (full line), the Jet-loop is the reactor which presents the minimum uncertainty i.e. that particular design of jet-loop reactor is the one for which the value of the CCUP varies the less with regards to variation or rather uncertainty in the determination of the K_H. Nevertheless this particular design of jet loop reactor does not appear to be very profitable see graph 5.13, this is consistent with the trade-off uncertainty versus loss i.e. as one can see in graph 5.20, if a particular reactor design is profitable then it inclines to carry a high(er) level of uncertainty.

Table 5.12 summarises the difference of design between the 2 jet-loop reactor design. One can see that the main difference between the two designs lies in the flowrate of nitrogen stripping. While the nitrogen stripping is important and influence the conversion achieved, it has also an influence on the parameter variation tolerance achievable by the reactor.

This information is useful for the scale-up of the reaction, where the nitrogen flow has to be monitored carefully e.g. accurate process control, and is part of the learning-before doing methodology [146].

Tab. 5.12: Comparison between the design of the most profitable reactor and the design of the most parameter variation tolerant reactor

Design variables	Jet-Loop reactor with lowest CCUP	Jet-loop reactor with lowest Uncertainty
Conversion - (X)	0.98	0.995
Mass transfer coefficient $k_l a$ $(1/s)$	1.9	0.74
flowrate of nitrogen stripping QgN_2 (m^3/h)	0.09	0.0011
Initial volume of the reaction $Vl_initial$ (m^3)	1.75	3
Gas Hold-up - ϵ_G (-)	0.42	0.12
CCUP (£/kg)	0.09	8.09
Uncertainty (-)	29.04	1.2

It can also be noticed that for some of the reactors i.e. the bubble column reactor, the loss and the uncertainty is present, this indicates that this type of reactor is not part of the pareto curve of the trade-off curve between uncertainty and minimum cost, and therefore does not represents an optimum design for the scale-up of the mass transfer sensitive reaction.

Mass transfer model : Lowerbound-Upperbound of Uncertainty measure

The sensitivity analysis carried on the mass transfer model has been tackled as a 'propagation' of the uncertainty contained in Henry's constant through the model and estimate the uncertainty in the model output. The propagation of the uncertainty contained by Henry's constant in the mass transfer model is done by giving four different values to the K_H parameter i.e. $10^{-4}, 10^{-3}, 10^{-2}, 10^{-1}(dimensionless K_H)$. Each of these four values is evaluated for the same set of design variables selected at the time by the optimisation algorithm i.e. only the K_H value is changed four times with all the other parameter and variables remaining the same. The model output will be a vector of four values reflecting the changes made in the control parameter i.e. K_H as shown in figure 5.14.

The Upper bound of the model output represents the maximum value achieved by the model output for a defined set of design variable values. Also the lower bound of the model output represents the minimum value achieved by the model output for a defined set of design variable values. It has to be noticed that as the set of design variable values are changed through the optimisation the lower-bound and Upperbound of the model out will change, as shown in figure 5.15

When comparing these two sets of Lowerbound and Upperbound (Upper bound 1 & Upper bound 2 - Lower bound 1 & Lower Bound 2) will present different values for the minimum Upperbound and its counterpart i.e. the minimum lower bound, see figure 5.16. *Upper bound 1* represents the minimum Upperbound between *Upper bound 1* and *Up-*

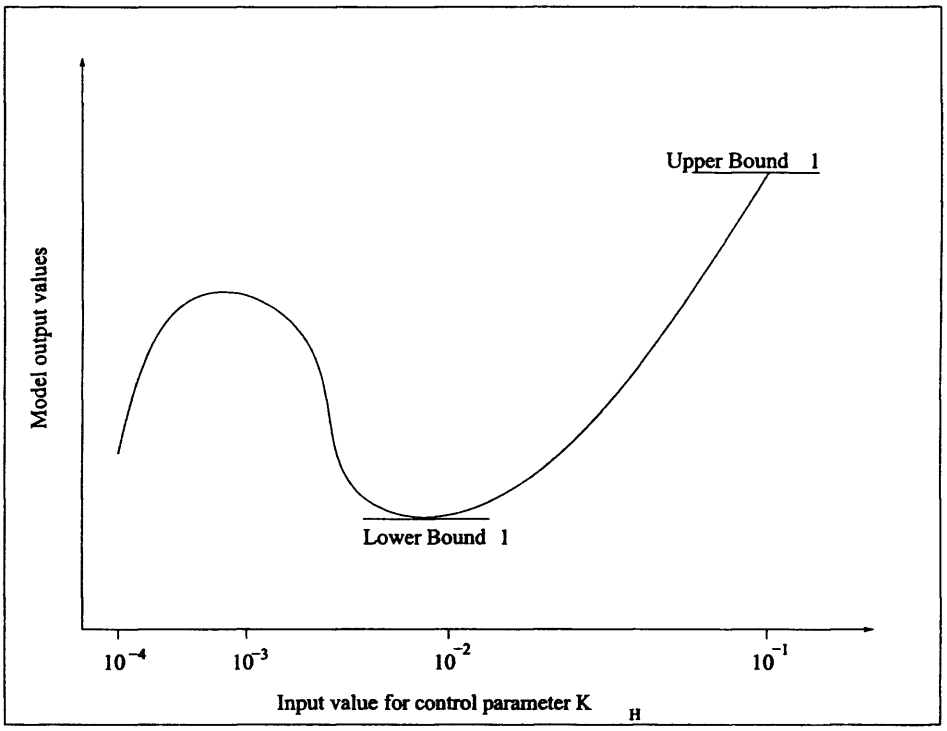

Fig. 5.14: Lowerbound - Upperbound of the model output for a defined set of design variable values

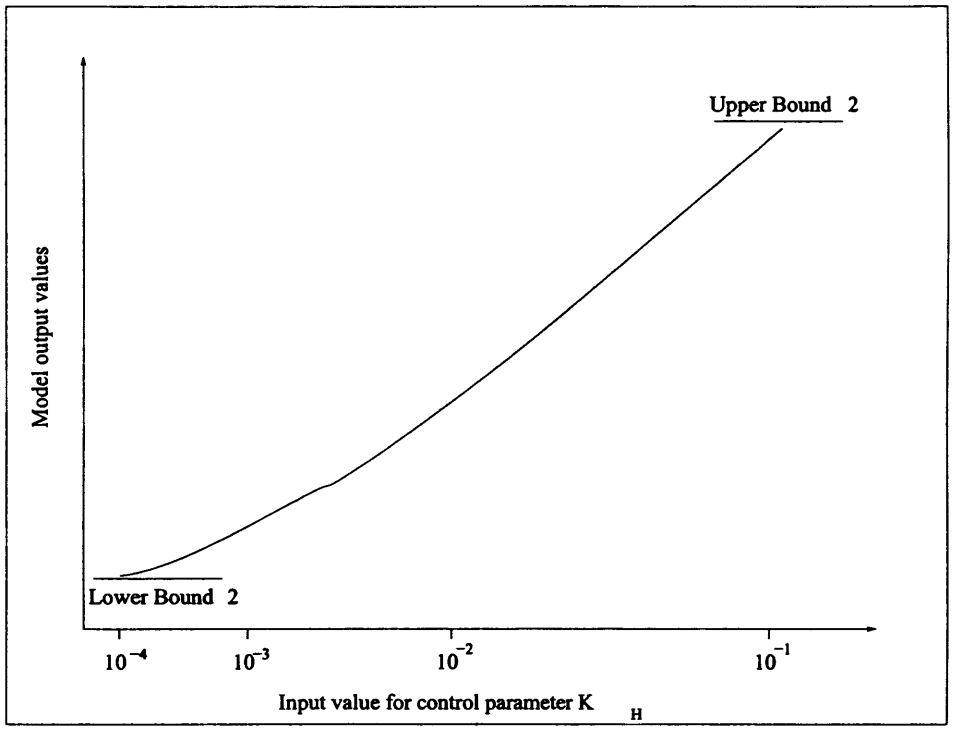

Fig. 5.15: Lowerbound - Upperbound of the model output for a different set of design variable values

per bound 2 while *Lower bound 2* represents the minimum lower bound between *Lower bound 1* and *Lower bound 2.*

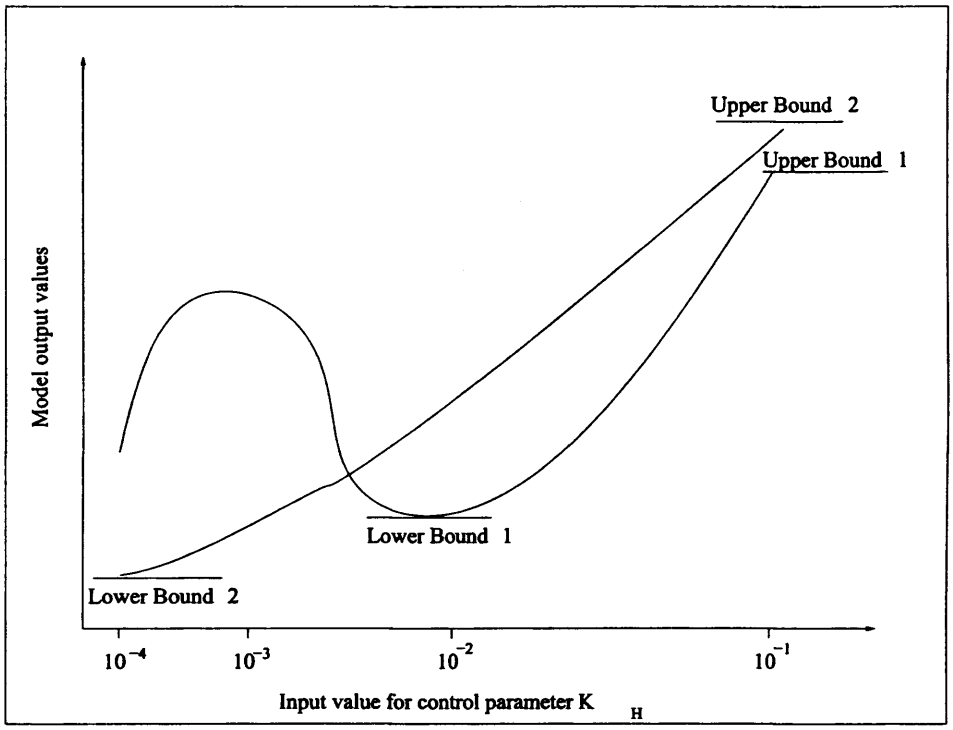

Fig. 5.16: Lowerbound - Upperbound of the model output for a different set of design variable values

The aim of the project is to identify the reactor that presents the minimum uncertainty, also we will have to consider both the minimum lower bound and the minimum upper bound and the aim will be to identify both the minimum lower bound uncertainty and the minimum Upperbound uncertainty.

Mass transfer model : Results for Upperbound

Graph 5.17 shows the evolution of the MOSA search method in the case of the minimisation of the upper bound of the objective function.

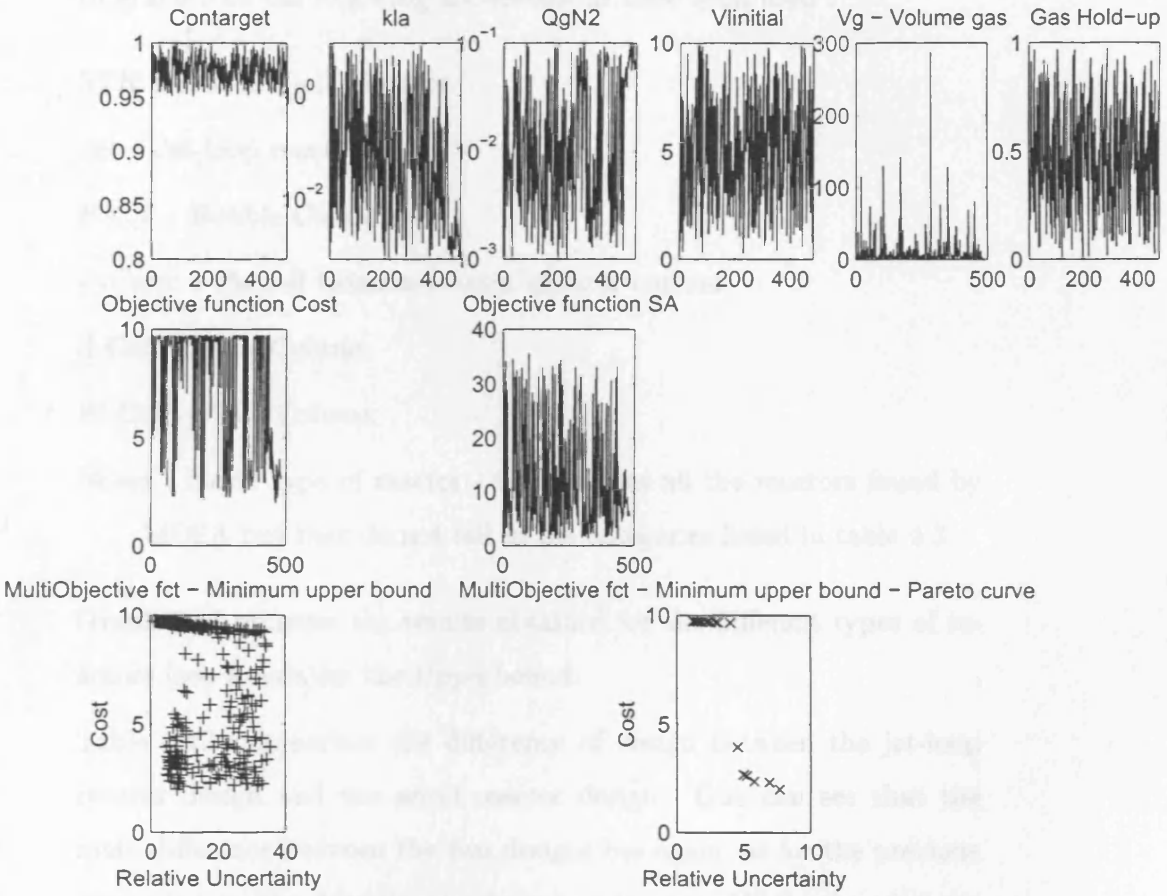

Fig. 5.17: Evolution of the multiobjective search method - MOSA - for the mass transfer model - minimisation of the upper bound of the objective function

In this graph the bottom left hand corner graph represents all the solutions accepted by MOSA while the bottom left hand corner represents only the pareto solutions also called non-dominated solutions (see 4.2.3)

as it can be see in the bottom left hand corner graph of figure 5.10.

The graph 5.18 represents the results obtained through the MOSA method.

In graph 5.18 the following abbreviations have been used :

STR : Stirred Tank Reactor

Jet : Jet-loop reactor

B-Col : Bubble Column

P-Colcc : Packed Column reactor counter-current

S-Col : Spray Column

Pl-Col : Plate Column

Novel : Novel type of reactor - incorporates all the reactors found by MOSA but that do not fall in the categories listed in table 4.3

Graph 5.18 presents the results obtained for the different types of reactors (see X-axis)for the Upperbound.

Table 5.13 summarises the difference of design between the jet-loop reactor design and the novel reactor design. One can see that the main difference between the two designs lies again, as for the previous discussion in the flowrate of nitrogen stripping. While the nitrogen stripping is important and influence the conversion achieved, it has also an influence on the parameter variation tolerance achievable by the reactor.

This information is useful for the scale-up of the reaction, where the nitrogen flow will have to be monitored careful e.g. accurate process control, and is part of the learning-before-doing methodology [146].

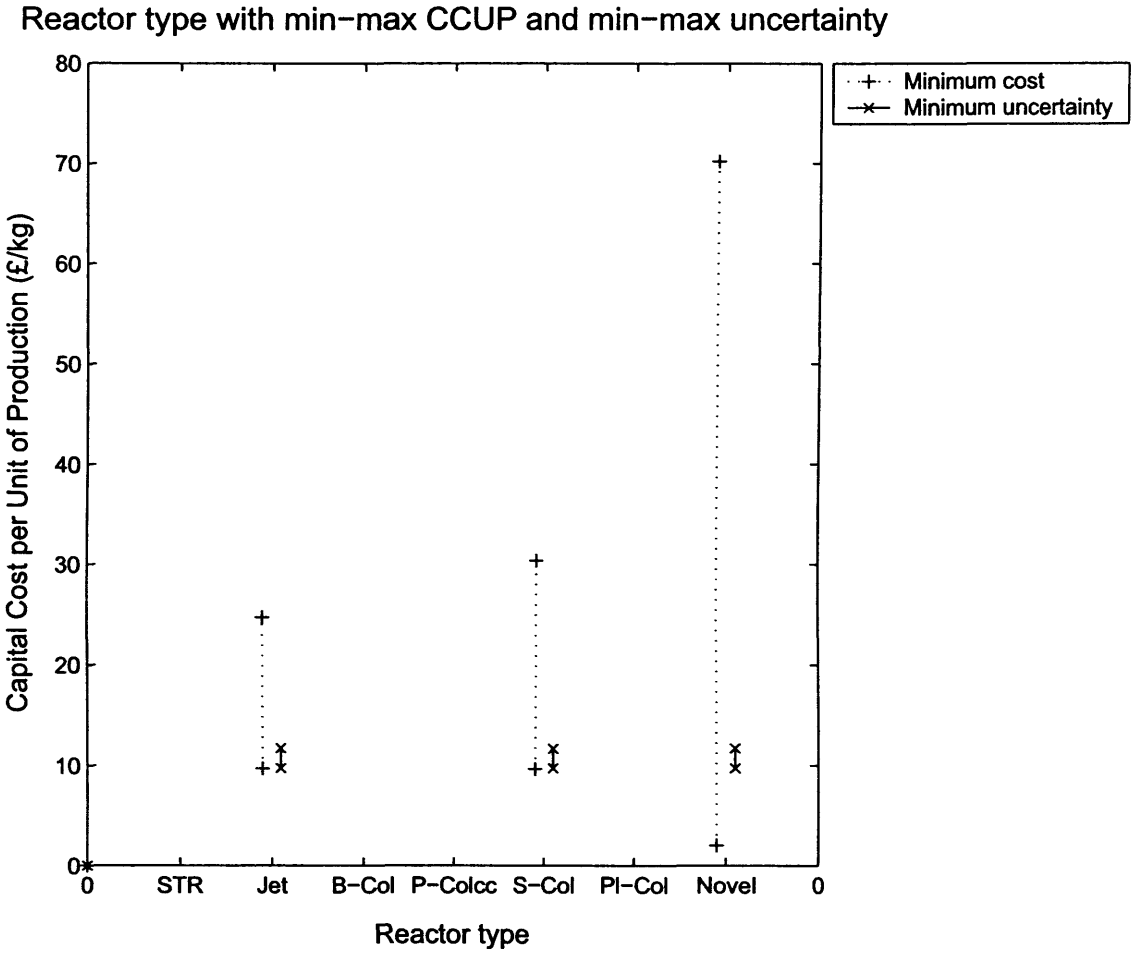

Fig. 5.18: Reactor Selection for Mass Transfer Model - Results for Upperbound

Tab. 5.13: Comparison between the design of the most profitable reactor and the design of the most parameter variation tolerant reactor

Design variables	Novel Reactor with lowest CCUP	Jet-loop reactor with lowest Uncertainty
Conversion - (X)	0.96	0.999
Mass transfer coefficient $k_l a$ $(1/s)$	2	0.002
flowrate of nitrogen stripping QgN_2 (m^3/h)	0.098	0.0011
Initial volume of the reaction $Vl_initial$ (m^3)	3.25	3
Gas Hold-up - ϵ_G (-)	0.71	0.84
CCUP (£/kg)	2	9.7
Uncertainty (-)	34.6	1.2

Finally Graph 5.19 presents a comparison of the Lowerbound and Upperbound pareto fronts.

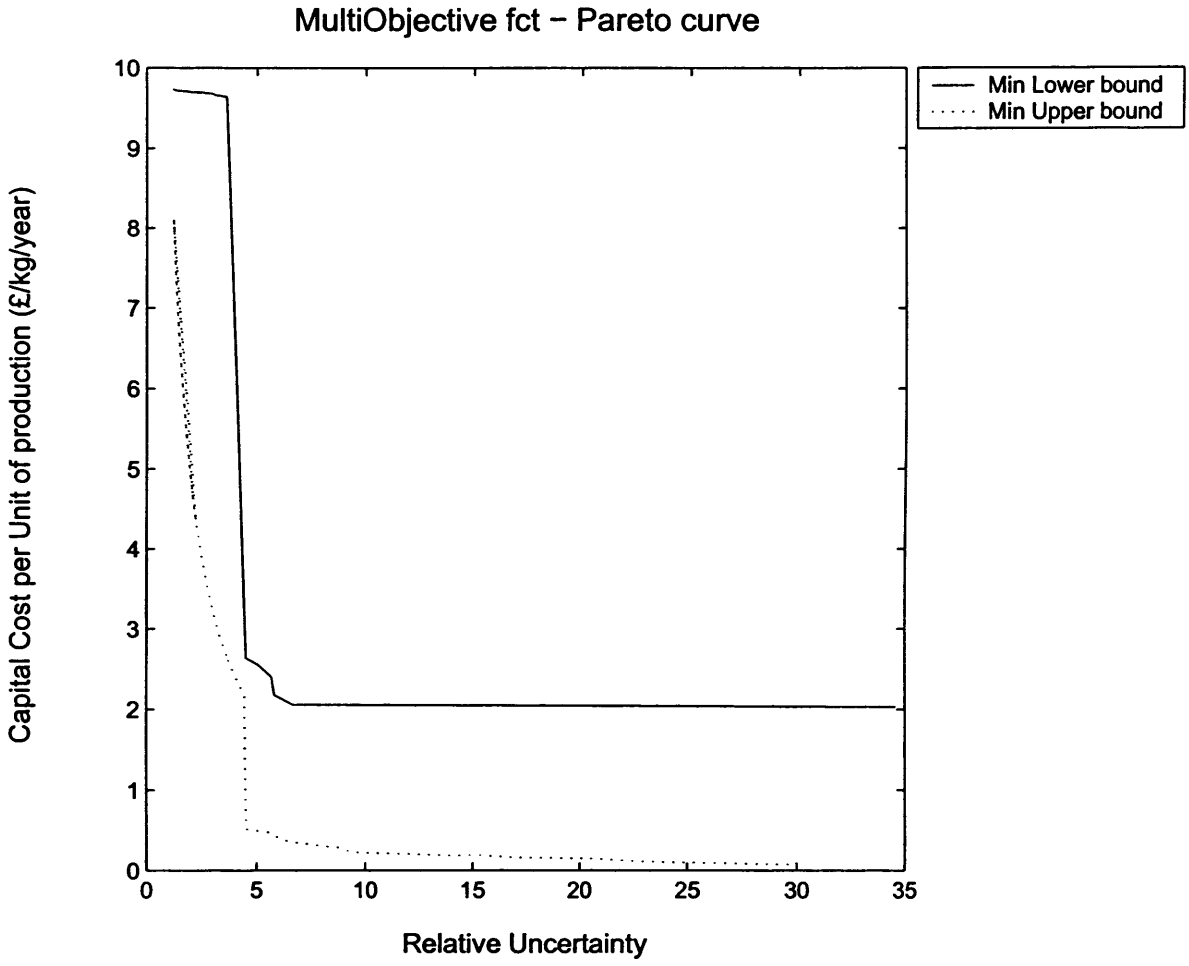

Fig. 5.19: Lowerbound and Upperbound pareto front - Mass transfer model

5.2.4 *Exhaustive Search (ES) versus Multiobjective Simulated Annealing (MOSA)*

The graph 5.20 represents a comparison between an exhaustive search or totally random search of 10,000 iterations with a MOSA of 2500

iterations

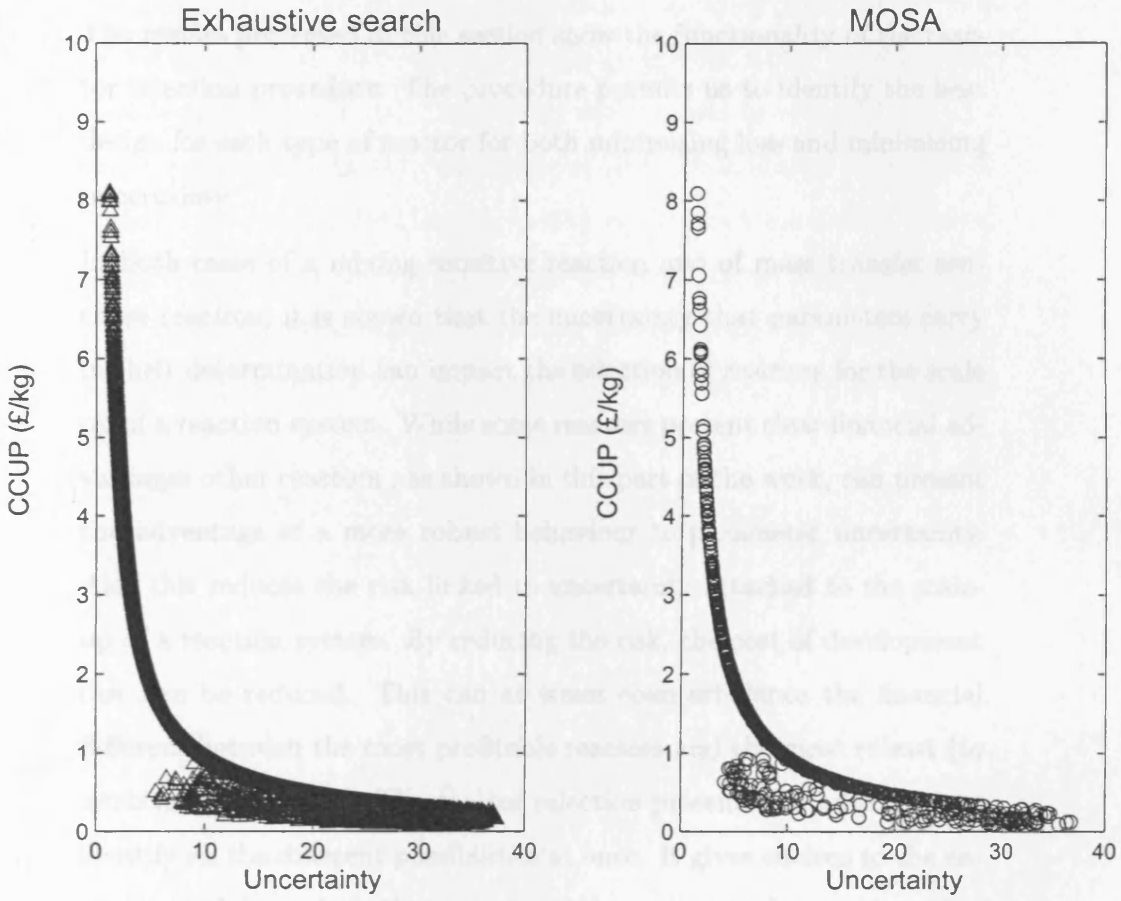

Fig. 5.20: Exhaustive search space Versus MOSA search space

It can be seen that the number of points minimising both the uncertainty and the Capital Cost per Unit of Production (CCUP) achieved with MOSA is equivalent to the number of points achieved with the exhaustive search though the number of iterations necessary to achieve this result was almost 4 times less than for the exhaustive search. MOSA is faster and less 'greedy' with regards to the number of function evaluations (iterations) necessary.

5.2.5 Conclusion

The results presented in this section show the functionality of the reactor selection procedure. The procedure permits us to identify the best design for each type of reactor for both minimising loss and minimising uncertainty.

In both cases of a mixing sensitive reaction and of mass transfer sensitive reaction, it is shown that the uncertainty that parameters carry in their determination can impact the selection of reactors for the scale up of a reaction system. While some reactors present clear financial advantages other reactors , as shown in this part of the work, can present the advantage of a more robust behaviour to parameter uncertainty. Also this reduces the risk linked to uncertainty attached to the scale-up of a reaction system. By reducing the risk, the cost of development can also be reduced. This can at times counterbalance the financial different between the most profitable reactors and the most robust (to uncertainty) reactors. The reactor selection presents the advantage to identify all the different possibilities at once. It gives choices to the engineers with regards to the project and the various and numerous other factors impacting the project, for example the life time of a project. If a project has a short life time but presents a profit advantages in its immediate implementation, then the engineer might favour reactors robust to uncertainty to maximise time to market and profit and vice versa.

Also from the features that they provide they contribute a great deal to learning-before-doing and present the engineer with fundamental thoughts regarding the influencing factor in the scale-up. For exam-

ple with regards to the influence that some parameters have on the reaction system the engineer can decide that these parameters have to be determined with extreme accuracy or that a few experimental data would be sufficient. This allows the engineer to organise and prioritise scale-up tasks e.g. gathering of data for a kinetic parameters. It also provides a better understanding of the reactor/reaction system and permits us to forecast the difficulties encountered during scale-up. Also by fully participating in learning before doing this novel reactor selection procedure reduces the amount of necessary work shortening scaling-up time and therefore time to market.

6. ADVANTAGES AND IMPROVEMENTS

Throughout the development of this reactor selection procedure special attention has been given to the adaptability of the procedure. The genericity of the procedure is articulated around the three constituent parts of the procedure i.e. Mathematical model - FAST : Sensitivity analysis - MOSA - Optimisation. Each of this three elements can be adapted to select different types of processes.

6.1 Mathematical Models

As shown in 1.9, the mathematical model represents the core element of the selection procedure. The model is used to evaluate the characteristics of all the possible types of process equipment in our case, the various types of reactor. Also, the model has to include within its definition variables which will permit us to identify different types of equipment, ϵ or Energy dissipation rate for the micromixing model and *kla* for the case of the mass transfer model. Other variables, identified through the degree of freedom (see A.4C.4) will have to be selected, when possible, to help to further refine the selection of reactors/processes through the identification of the design within the type of reactors/processes selected.

6.2 Optimiser and Sensitivity Analysis

An adaptable procedure can be seen as a type of generic procedure whose methods self-adjust based upon the state of its runtime environment. Also, the control mechanisms of this adaptable reactor selection procedure is realised using generic procedures. This sort of reflective architecture would enables us to write a dynamically adaptable software system in highly flexible, extensive, readable and maintainable way.

6.2.1 Genericity

In this work the reactor procedure has been applied to two different type of reaction system i.e. mass transfer sensitive reaction (semi-batch and continuous). The two generic elements - sensitivity analysis (FAST) and optimisation (SA and MOSA) - of the automated reactor selection framework have been developed such as to permit the handling of simple and complex mathematical models regarding the number of variables treated. The FAST sensitivity analysis was purposely chosen to permit the treatment of a large number of variables while carrying a global sensitivity analysis (see 3.2). Also, when considering the very many and various types of optimisation carried out with simulated annealing, it can be considered as a generic combinatorial approximation algorithm.

The selection criteria on which the automated reactor selection lie are also generic as the impact of uncertainty is fundamental to the implementation of new processes in any industry [45] and probably even more in the pharmaceutical industry [172].

6.2.2 Adaptability

As explained in 4.2.4 the optimiser - simulated annealing and multiobjective simulated annealing - use a general automated cooling schedule [187, 90]. This feature allows the tuning of the different parameter to be self-adaptive to the optimisation problem treated. It is nevertheless to be understood that the speed of the SA/MOSA in achieving solutions still relies on the following parameters which might require some adjustment with regards to the type of cases considered [187, 90]:

$N_{standardeviation}$: Number of iterations or function evaluations used to determine the standard deviation of the cost distribution

$N_{iteration}$: Maximal number of iterations or function evaluations per temperature reduction

$N_{acceptance}$: Specified number of acceptances $N_{acceptance} = 0.4N_{iteration}$ as recommended by van Laarhoven and Aarts [106, 187]

λ : A typical value for λ is 0.7 [90], it represents the fraction value taken of the standard deviation σ see 4.2.4.

Φ : Fraction of the total number of solutions in constituting the pareto front see 4.2.4

k : $k = \frac{-3}{lnP}$ k is computed assuming a normal cost distribution and selecting a temperature high enough to accept with probability P a configuration whose cost is three times the standard deviation $\sigma 1$ of the cost distribution and the standard deviation $sigma2$ of the uncertainty distribution.

The fact that the cooling schedule adjusts itself over the cost distribution and the uncertainty distribution makes the algorithm straight

forward to implement, easy to use and therefore to maintain.

6.3 Further improvement

6.3.1 Heat transfer and Multiphase phase modeling

The procedure could be extended to include heat transfer by either using the pathway used by Baldyga et al. [24] and then modeling the mathematical model implemented in this work or by using the model developed by Lai et al. which uses energy dissipation rate in the modeling of near-wall turbulent heat fluxes [108, 107]. Another development would be to include a selection for mixing sensitive reaction for laminar flow through the model developed by Baldyga et al. [26] For the case of multiphase mixing sensitive reaction Brilman et al. propose an adjustment to the micromixing model developed by Baldyga et al. [42].

6.3.2 The use of Computational Fluid Dynamics (CFD) within the reactor selection

Reactor engineering demands expertise in various fields ranging from chemistry, kinetics, catalysis to reaction engineering, fluid dynamic, mixing, heat and mass transfer. Various tools for modeling of chemical kinetics have been developed and are used in practice [34]. Quite sophisticated models and theories are available, e.g. see chapter 2, to predict the heat and mass transfer.

CFD deals with the solution of fluid dynamic equations on digital computers. CFD requires relatively few restrictive assumptions and gives a complete description of flow field for all variables. Though CFD

does not replace experimental testing, such a technique can be used to reduce the necessary experiments and to interpret the experimental results with more confidence [156].

Design engineers use CFD models for two purposes : 'design' models, which attempt to provide a quantitative relationship between the hardware and performance, and 'learning' models, which provide a basic understanding of different underlying processes. Equipment designers would like to have computational flow models, which could predict what could or would happen as a result of a specific design, thereby steering the design in promising directions. This would allow the evaluation of new design concepts, which often get sidelined because of the lack of resources (experimental facilities, time, funding, etc.) to test them [157]. Having the capability to make a priori predictions of the process performance, with just the knowledge of geometry and operating parameter, would be on the 'wish list' of any designer [157].

Following this thought, it is easy to see how beneficial it would be to couple a CFD tool to the procedure that has been developed in this project. The procedure developed in this project aimed at narrowing the choice of reactor available to carry out reaction scale-up and defined what the 'best' reactor for the scale-up of a reaction. CFD would not provide an efficient tool for this as the time required for the development of a CFD model can be extensive [84] or difficult to develop e.g. Jet-loop reactor [13]. Also while CFD packages for single-phase system have been used for optimising the operation and control of existing processes in the chemical industry, their use is limited for systems containing reactive and/or multiphase flows. Without the use of simulation tools, the plant's engineer's ability to visualise process phenomena is limited

and optimising operation is made more difficult and time-consuming [47].

On the other hand CFD, if linked to the selection procedure developed in this project, could provide useful information in the more detail design of the reactor and potentially in the selection when the selection comes down to selecting a type of reactor from only one other possibility, particularly if the choice given by the selection procedure shows little differences in the performance of the two reactors, CFD could then be used to further the selection and distinguished which reactor will present the best properties for the reaction system considered.

Flowsheet modeling software can analyse the operation of complete plants. To make the models tractable, simplified hydrodynamic models with reduced reaction sets can be used for the individual chemical reactors [178, 85, 48]. On the other end of the spectrum, specialised software exists to model complex chemistry. Such software can handle stiff (i.e. those with a large difference in time-scales) reaction sets with hundreds of surface and volumetric reactions, but the software is neither suitable to model complete processes nor able to take into account the hydrodynamics of the reactor [13]. In between these two extremes falls CFD software, which can model both chemical reactions and the link with reactor hydrodynamics dynamics. CFD software is nevertheless generally used to model individual plant components, and not the whole process at once. When tied to flow-sheet-modeling software, however, it can provide more accurate flow-field data (averaged velocities or temperatures) about unit operations than the simplified assumptions normally used for input [13, 14]. The current limitations of CFD packages are as follow ;

Commercially available CFD tools cannot or do not [47]:

1. use available computational horsepower (e.g., parallel computing), as well as they should
2. use leading edge numerical methods (e.g. adaptive gridding, solution-driven grid refinement) or theoretical methods
3. include available submodels of key subprocesses (e.g., crystal nucleation and growth), or submodels are not coupled properly (i.e., turbulence and chemistry)
4. have a common chemical engineering infrastructure to allow linking to programs common in the chemical processing industries (e.g., physical and chemical properties data base)

By linking the procedure hereby develop to a CFD software to further refine the design of reactors selected by the reactor selection, the third argument of the above list will be supplied and this improved reactor selection procedure will permit us to further narrow the uncertainty in the reactor final design.

6.4 Conclusion

In this part of the thesis report we have looked at the advantage brought by the reactor selection procedure. The major advantages of the procedure is that it is a generic and a self-adaptive procedure, bringing therefore ease of use. Potential improvement which could be brought have also been looked at under the form of widening the scope of the reactor selection from mass transfer and mixing to heat transfer and looking at tackling multiphase reaction systems. It was shown that the

foundation of the work done has been laid for upgrade e.g. micromixing models have been developed for multiphase system. Therefore only new models would have to be implemented, the rest of the reactor selection procedure remaining the same. Finally the use of CFD in the pharmaceutical industry was discussed and the advantage of coupling it with this reactor selection discussed. Given that CFD can be a time and labour intensive tool it was recommended that the use of CFD was kept to final stages of the reactor selection.

7. CONCLUSION

During the Research and Development stage of a chemical process, plant design requires special attention. Scale-up procedures are part of the integrated process development. The challenge is to find the optimum between the chemistry, engineering design, the EHS (Environment, Hygiene and Safety) compliance and economic factors. The iterative process requires concept discrimination at the early stage of the process development. A direct transfer from laboratory scale to the industrial scale is rarely feasible.

Generally, one or several scales between the laboratory and the industrial process may be used. Thus, various intermediate expressions to the full scale are used, bench scale, mini-pilot plant, pilot plant, quarter scale, demonstration unit, and these often vary from one company to another [67].

Process development requires a good understanding of the chemical system in terms of kinetics, thermodynamics, hydrodynamics and product properties. As economic factors become more and more important, the priority rises for other aspects such as product quality, EHS compliance.

Along side new priorities, the margin for errors and uncertainty gets restricted by the nature of the industry itself. The pharmaceutical industry is held to very strict guidelines and rules. The making of a

drugs brings with its process and necessity of elimination of uncertainty and the unknown.

Therefore, the aim of the procedure developed here is to address these issues. First by studying scale-up through mathematical models the engineer gives a new dimension to the scale-up study. Many different options and conditions can be evaluated. The pace of a computer presents undeniable advantages alongside pilot plant trials. Also, 'What if...' cases can be studied without, for example, the safety and planning necessary for the realisation of a plant trial.

The procedure is also developed to tackle issues that are generally treated in order but never simultaneously. With the reactor selection procedure, an opportunity is given for the engineer to look at the problem with different angles of approach as the reactor procedure searches for solutions to reduce the level of uncertainty and maximise profits simultaneously.

Another interesting aspect of the reactor selection is its genericity, adaptability and automaticity. It is self-tuned and therefore brings the possibility to be applicable to numerous cases. The procedure also responds to the regulators guidelines which specifies that in assessing the suitability of a given piece of equipment, it is usually insufficient to rely solely upon the representations of the equipment supplier, or upon experience in producing some other product. Sound theoretical and practical engineering principles and considerations are a first step in the assessment. This process provides engineers with a new method of developing products and processes taking all variables into account.

In this work a computerised procedure that uses evolutionary algo-

rithms for solving multi-objective problems was developed to facilitate scale-up of drugs. The novelty of the procedure is its ability to tackle difficulties simultaneously, offering the advantage of parallel evaluation of the impact that various problems can have on a reaction system scale-up. Also uncertainty within the system is considered along financial aspects of the scale-up process. The engineer uses the procedure to address issues simultaneously such as reducing uncertainty and increasing profit and is given a range of options for solution. The decision remains in the hand of the engineer who then disposes of a quantitative evaluation of the qualitative aspect of scale-up that uncertainty can represent.

L'imaginaire est ce qui tend à devenir réel.

André Breton

L'avenir c'est ce qui dépasse la main tendue.

Louis Aragon

APPENDIX

A. MICROMIXING MODEL - SEMI-BATCH OPERATION : OBJECTIVE FUNCTION DESCRIPTION

This micromixing model is presented by Baldyga et al. [23]. It also include aspects presented by Samant et al. [171].

A.1 List of parameters involved

a	:	Ratio of feed volume to reactor volume (-)
A	:	Life of the plant (Years)
B	:	Number of batches achieved per day (Batch/day)
C	:	Capital Cost of the reactor per Year (£/year)
d	:	Diameter of the agitator (m)
D	:	Diameter of the reactor Vessel (m)
Dam	:	Micromixing time (-)
e	:	Price of 1 kWatt (/Watt.h)
ξ	:	Ratio between the diameter of the agitator and the diameter of the reactor vessel (-)
E	:	Engulfment rate (s^1)
ϵ	:	Energy dissipation rate (m^2/s^3
f	:	Self-engulfment factor - this factor is used to model the engulfment

within the fluid elements (self-engulfment) which does not contribute to the growth of the micromixed region (-)

fat : Feed addition time (s) ; Represents the time the feed is added to the reactor

F : Feed rate (m^3/s)

k_j : Reaction constant (s^{-1})

k_{max} : Maximum Reaction constant (s^{-1})

L : Level of filling of reactant A in the reactor (%)

M_i : Molecular weight of the fluid element (g/mol)

M_x : Average Molecular weight of the fluid element (g/mol)

M_y : Average molecular weight of the fluid element environment (g/mol)

N : Agitator speed (rps : rotation per second)

N_f : Number of feed ports (-)

N_p : Agitator power number (-)

N_q : Agitator pumping number (-)

N_{Re} : Impeller Reynolds number (-)

p : Number of production days per year (Days per year)

P : Product sales price ($£/m^3$)

P_{dC} : Product distribution of targeted product C relative to B consumed (-)

φ : φ = V/Vo with V : Volume of the micromixed region and V0 : volume of the micromixed region at t=0

P_u : Power delivered by the motor (Watt)

Q : Mixing index

R_B : Reactant B purchase price ($£/m^3$)

R_A : Reactant A purchase price ($£/m^3$)

R_j : Reaction rate (s^{-1})

t_d : Reaction time of a drop of reactant B (s)

t_m : Micromixing time (s)

Torque	:	Torque given by the motor (N.m)
t_r	:	Reaction time (s)
t_s	:	Mesomixing time (s)
u	:	Velocity of the fluid within the reactor (m/s)
V	:	Volume of the reactor content (m^3)
V_a	:	Volume of reactant A (m^3)
W	:	Working hours per day (h/day)
x	:	Composition of the fluid element as mole fraction (-)
y	:	Composition of the fluid element environment as mole fraction (-)
ν	:	Kinematic viscosity (m^2/s)
ν_i	:	Stoichiometric coefficient of constituent i (-)
$\nu_{Tot,j}$	:	Sum of the different stoichiometric coefficient for reaction j (-)
ω	:	Speed of the motor (rad/s)

A.2 Micromixing model - semi-batch operation : Equations

Rate of change of composition of component i in the growing fluid elements

$$\frac{dx_i}{dt} = \frac{1}{t_m}\frac{M_x}{M_y}(y_i - x_i)\left[1 - \varphi e^{\frac{-t_d}{t_s}}\right] + \sum_{j=1}^{r}(\nu_{i,j} - x_i\nu_{Tot,j})\,R_j \qquad (s^{-1}) \tag{A.1}$$

t_d is being reinitialised after each addition of constituent B

$$\frac{t_d}{dt} = 1 \quad \text{and} \quad t_d(0) = 0 \qquad (-) \tag{A.2}$$

Engulfment rate

$$E = \frac{1}{t_m} \qquad (s^{-1}) \tag{A.3}$$

Self-engulfment factor

$$\frac{d\varphi}{dt} = \left[1 - \varphi e^{\frac{-Q\,t_d}{Damt_r}}\right] \qquad (-) \qquad (A.4)$$

Volumetric expansion of micromixed fluid elements - Dimensionless form $\varphi = \frac{V}{V0}$

$$\frac{d\varphi}{dt} = E\varphi f \qquad (-) \quad \text{and} \quad \varphi(0) = 1 \qquad (A.5)$$

Charateristic mesomixing time

$$t_s = 2\left(\frac{F}{\pi u \epsilon N_f}\right) \qquad (s) \qquad (A.6)$$

Damköler number for micromixing

$$Dam = \frac{t_m}{t_r} \qquad (-) \qquad (A.7)$$

Mixing index

$$Q = \frac{t_m}{t_s} \qquad (-) \qquad (A.8)$$

Characteristic micromixing time

$$t_m = \left(\frac{12}{log(2)}\right)\left(\frac{\nu}{\epsilon}\right)^{0.5} \qquad (s) \qquad (A.9)$$

Reaction time

$$t_r = \frac{1}{k_{max}} \qquad (s) \qquad (A.10)$$

Algebraic sum of the stochiometric coefficients of the components in reaction j

$$\nu_{Tot(j)} = \sum \nu_j \qquad (-) \qquad (A.11)$$

Reaction rates = rate of reaction j per mole of reacting mixture of composition x

$$R_j = k_j \prod \left(x_i^{order(j)}\right) \qquad (s^{-1}) \qquad (A.12)$$

Average Molecular Weights for fluid element within the reaction zone

$$M_x = \sum (M_i x_i) \qquad (g/mol) \tag{A.13}$$

Average Molecular Weights for fluid element in the environment of the reaction zone

$$M_y = \sum (M_i y_i) \qquad (g/mol) \tag{A.14}$$

Product distribution

$$P_{dC} = \frac{\text{C produced}}{\text{B reacted}} \qquad (-) \tag{A.15}$$

Influence of the feed addition time on the reactor volume

$$F = \frac{aV}{\text{fat}} \qquad (m^3/s) \tag{A.16}$$

Number of batches done per day

$$B = \frac{3600W}{t} \qquad (-) \qquad \text{i.e. (number of batches / number of working hours per day)} \tag{A.17}$$

Capital cost of the reactor

$$C = 14595 + 13418 \left(\frac{V}{L}\right)^{0.661} \qquad (£) \tag{A.18}$$

Ratio of the agitator diameter to the reactor vessel

$$\xi = \frac{D}{d} \qquad (m) \tag{A.19}$$

Agitator Reynolds number

$$N_{Re} = \frac{Nd^2}{\nu} \qquad (-) \tag{A.20}$$

Product distribution of C relative to B consumed

$$P_{dC} = f(\text{a},\epsilon,\text{t},\text{u},\text{V}) \qquad (-) \tag{A.21}$$

Power needed by the motor

$$P_u = \text{Torque}\ \omega \qquad (Watt) \tag{A.22}$$

Rotational speed of the agitator

$$\omega = 2\pi N \qquad (s^{-}1) \tag{A.23}$$

Velocity of the liquid within the reactor

$$u = 2^{1/2} N_p^{1/2} N_q^{-1/2} N d \qquad (m/s^{-1}) \tag{A.24}$$

Volume of the reactor vessel

$$\frac{V}{l} = \frac{\pi}{4} D^3 \qquad (m^3) \quad \text{(assuming vessel height H = D)} \tag{A.25}$$

Volume of the content of the reactor

$$V = V_a + Ft \qquad (m^3) \tag{A.26}$$

A.3 Micromixing model - semibatch operation : List of parameters with fixed values

Period of running of the project

$$A = 2 \qquad (years) \tag{A.27}$$

Torque given by the motor

$$\text{Torque} = 3 \qquad (N.m) \tag{A.28}$$

Price of 1 Watt-hours

$$e = 0.01 \qquad (£/Watt - hours) \tag{A.29}$$

Ratio agitator diameter to vessel diameter

$$\xi = 1/3 \qquad (-) \tag{A.30}$$

Power number of the agitator

$$N_p = 0.35 \qquad (-) \tag{A.31}$$

Pumping number of the agitator

$$N_q = 2 \qquad (-) \tag{A.32}$$

Days of operation per year

$$p = 350 \qquad (days) \tag{A.33}$$

Sales price of product

$$P = 5500 \qquad (£/m^3) \tag{A.34}$$

Purchase price of reactant A

$$R_A = 300 \qquad (£/m^3) \tag{A.35}$$

Purchase price of reactant B

$$R_B = 200 \qquad (£/m^3) \tag{A.36}$$

Working hours per day

$$W = 8 \qquad (hours/day) \tag{A.37}$$

Filling level of the reactor vessel

$$L = 50 \qquad (\%) \tag{A.38}$$

Kinematic viscosity

$$\nu = 2.10^{-6} \qquad (m^2/s) \tag{A.39}$$

Reaction constant

$$k_j = [250\ 250] \qquad (s^{-1}) \tag{A.40}$$

Highest reaction constant

$$k_{max} = 250 \qquad (s^{-}1) \tag{A.41}$$

Molecular weight of each component i.e. A,B,C,D

$$M = [1000\ 60\ 1060\ 1120] \qquad (g/mol) \tag{A.42}$$

Stochiometric coefficient of the reactions 1 and 2

$$\nu_{ij} = [1\ 1\ 0][1\ 1\ 0] \qquad (-) \tag{A.43}$$

Number of feed ports in the reactor vessel

$$N_f = 1 \qquad (-) \tag{A.44}$$

A.4 Micromixing model - semibatch operation : Degree of freedom

Number of variables : 49

Number of equations : 44

Degree of freedom : 5

B. MICROMIXING MODEL - CONTINUOUS OPERATION : OBJECTIVE FUNCTION DESCRIPTION

B.1 List of parameters involved

E	:	Engulfment rate (s^{-1})
ϵ	:	Energy dissipation rate (m^2/s^3)
F	:	Feed flowrate (m^3/h)
k_j	:	Reaction constant (s^{-1})
k_{max}	:	Maximum Reaction constant (s^{-1})
Λ_C	:	Integrale concentration scale (m)
M_i	:	Molecular weight of the fluid element (g/mol)
M_x	:	Average Molecular weight of the fluid element (g/mol)
M_y	:	Average molecular weight of the fluid element environment (g/mol)
p	:	Number of production days per year (Days per year)
P	:	Product sales price (£/m^3)
P_{dC}	:	Product distribution of targeted product C relative to B consumed (-)
Q_i	:	Volume flowrate of i (m^3/s)
R_B	:	Reactant B purchase price (£/m^3)
R_A	:	Reactant A purchase price (£/m^3)
R_j	:	Reaction rate (s^{-1})

t_m	:	Micromixing time (s)
τ_S	:	Time scale for dissipation of segregation in inertial-convective sub-range (s)
u	:	Velocity of the fluid within the reactor (m/s)
W	:	Working hours per day (h/day)
x	:	Composition of the fluid element as mole fraction (-)
y	:	Composition of the fluid element environment as mole fraction (-)
X_i	:	Volume fraction of micromixed fluid (-)
X_u	:	Volume fraction of large spots of reagent (-)
ν	:	Kinematic viscosity (m^2/s)
ν_i	:	Stochiometric coefficient of constituent i (-)
$\nu_{Tot,j}$	:	Sum of the different stochiometric coefficient for reaction j (-)

B.2 Micromixing model - continuous operation : Equations

Engulfment rate

$$E = \frac{1}{t_m} \qquad (s^{-1}) \tag{B.1}$$

Characteristic micromixing time

$$t_m = \left(\frac{12}{log(2)}\right)\left(\frac{\nu}{\epsilon}\right)^{0.5} \qquad (s) \tag{B.2}$$

Rate of change of composition of component i in the growing fluid elements

$$\frac{dx_i}{dt} = \frac{1}{t_m}\frac{M_x}{M_y}\left(1 - \left(\frac{X_i}{X_u}\right)\right) + \sum_{j=1}^{r}\left(\nu_{i,j} - x_i\nu_{Tot,j}\right)R_j \qquad (-) \tag{B.3}$$

The fluid containing reagent is not distributed uniformly (because mesomixing is not ideal) but rather concentrated in large spots of the

size within the inertial-convective subrange of turbulence. Denoting by X_u the local volume fraction of such spots, one gets the micromixing equations in the form :

$$\frac{dX_i}{dt} = EX_i\left(1 - \frac{X_i}{X_u}\right) \qquad (-) \qquad \text{(B.4)}$$

Evolution of the volume fraction X_u is described by the mesomixing equation:

$$\frac{dX_u}{dt} = X_u\frac{X_u\left(1 - X_u\right)}{\tau_S} \qquad (-) \qquad \text{(B.5)}$$

τ_S is the time constant for the inertial-convertive mixing. As shown by Baldyga et al. [23], the time constant, τ_S, can be calculated from :

$$\tau_S = A\frac{\Lambda_C^{2/3}}{\epsilon^{1/3}} \text{with,} \qquad A \approx 1.2[25] \qquad (s) \qquad \text{(B.6)}$$

where :

$$\frac{d\Lambda_C}{dt} = C\epsilon^{1/3}\Lambda_C^{1/3} \text{with initial condition :} \Lambda_C\left(0\right) = \Lambda_{C0} = \sqrt{\frac{Q_i}{\pi u}} \qquad (m/s) \qquad \text{(B.7)}$$

Algebraic sum of the stochiometric coefficients of the components in reaction j

$$\nu_{Tot(j)} = \sum \nu_{ij} \qquad (-) \qquad \text{(B.8)}$$

Reaction rates = rate of reaction j per mole of reacting mixture of composition x

$$R_j = k_j \prod \left(x_i^{order(j)}\right) \qquad (s^{-1}) \qquad \text{(B.9)}$$

Average Molecular Weights for fluid element within the reaction zone

$$M_x = \sum \left(M_i x_i\right) \qquad (g/mol) \qquad \text{(B.10)}$$

Average Molecular Weights for fluid element in the environment of the reaction zone

$$M_y = \sum (M_i y_i) \qquad (g/mol) \tag{B.11}$$

Product distribution

$$P_{dC} = \frac{\text{C produced}}{\text{B reacted}} \qquad (-) \tag{B.12}$$

Feed in m^3/h

$$F = Qf/3600 \qquad (m^3/h) \tag{B.13}$$

Product distribution of C relative to B consumed

$$P_{dC} = f(\epsilon,\text{t},\text{u}) \qquad (-) \tag{B.14}$$

B.3 Micromixing model - continuous operation : List of parameters with fixed values

Feed flowrate

$$F = 1 \qquad (m^3/h) \tag{B.15}$$

Days of operation per year

$$p = 200 \qquad (days) \tag{B.16}$$

Sales price of product

$$P = 45000 \qquad (£/m^3) \tag{B.17}$$

Purchase price of reactant A

$$R_A = 1000 \qquad (£/m^3) \tag{B.18}$$

Purchase price of reactant B

$$R_B = 1000 \qquad (£/m^3) \tag{B.19}$$

Working hours per day

$$W = 24 \qquad (hours/day) \tag{B.20}$$

Reaction constant

$$k_j = [250\ 250] \qquad (s^{-1}) \tag{B.21}$$

Highest reaction constant

$$k_{max} = 250 \qquad (s^{-1}) \tag{B.22}$$

Molecular weight of each component i.e. A,B,C,D

$$M = [1000\ 60\ 1060\ 1120] \qquad (g/mol) \tag{B.23}$$

Stochiometric coefficient of the reactions 1 and 2

$$\nu_{ij} = [1\ 1\ 0][1\ 1\ 0] \qquad (-) \tag{B.24}$$

Kinematic viscosity

$$\nu = 2.10^6 \qquad (m^2/s) \tag{B.25}$$

B.4 Micromixing model - continuous operation : Degree of freedom

Number of variables : 27

Number of equations : 25

Degree of freedom : 2

C. OBJECTIVE FUNCTION DESCRIPTION

In this section we present the mass transfer model that we developed to simulate a mass transfer sensitive reaction [135, 185].

C.1 List of parameters involved

ab	:	G/L interfacial area per unit volume of mixture (m^2/m^3))
$C_{l(RhL*)}$	:	Liquid concentration of RhL* (mol/m^3)
$C_{l(IPA)}$	:	Liquid concentration of IPA as Isopropanone (mol/m^3)
$C_{l(RhL*H)}$	:	Liquid concentration of RhL*H (mol/m^3)
$C_{l(Acetone)}$	:	Liquid concentration of Acetone (mol/m^3)
$C_{l(Sub)}$	:	Liquid concentration of Sub as Substrate (mol/m^3)
$C_{l(SIM)}$	:	Liquid concentration of SIM as S-Intermediate (mol/m^3)
$C_{l(RIM)}$	:	Liquid concentration of RIM as R-Intermediate (mol/m^3)
$C_{l(R-SubH)}$	:	Liquid concentration of R-SubH (mol/m^3)
$C_{l(S-SubH)}$	:	Liquid concentration of S-SubH (mol/m^3)
$C_{g(RhL*)}$	:	concentration of RhL* (mol/m^3)
$C_{g(IPA)}$	:	Gas concentration of IPA as Isopropanone (mol/m^3)
$C_{g(RhL*H)}$	:	Gas concentration of RhL*H (mol/m^3)
$C_{g(Acetone)}$	:	Gas concentration of Acetone (mol/m^3)
$C_{g(Sub)}$	:	Gas concentration of Sub as Substrate (mol/m^3)
$C_{g(SIM)}$	:	Gas concentration of SIM as S-Intermediate (mol/m^3)

$C_{g(RIM)}$: Gas concentration of RIM as R-Intermediate (mol/m^3)

$C_{g(R-SubH)}$ Gas concentration of R-SubH (mol/m^3)

$C_{g(S-SubH)}$ Gas concentration of S-SubH (mol/m^3)

db : mean diameter of bubble (m)

D : Diffusivity of gas in liquid of fluid within the reactor (cm^2/s)

ϵ : Energy dissipation rate (cm^2/s^3)

$GHup$: Gas hold-up (−)

k_1 : reaction constant for reaction 1 (−)

k_2 : reaction constant for reaction 2 (−)

k_3 : reaction constant for reaction 3 (−)

k_4 : reaction constant for reaction 4 (−)

k_5 : reaction constant for reaction 5 (−)

k_6 : reaction constant for reaction 6 (−)

k_7 : reaction constant for reaction 7 (−)

k_8 : reaction constant for reaction 8 (−)

k_9 : reaction constant for reaction 9 (−)

k_{10} : reaction constant for reaction 10 (−)

K_H : Henry's constant - dimensionless (-)

k_l : Overall Mass transfer coefficient based on liquid-side concentration differential (m/s^{-1})

k_la : Overall Mass transfer coefficient per unit volume of the G/L mixture (s^{-1})

μ : liquid kinematic viscosity (cm^2/s)

MW_{IPA} : Molecular weight of IPA (-)

$\dot{N}_{IPA,l\rightarrow g}$: Molar flow of IPA removed from the liquid mixture (mol/s^{-1})

$Pcritical_{acetone}$ used to calculate $Pvap_{IPA}$ value found in [148] (bar)

$Pvap_{acetone}$ vapour pressure of acetone in the reaction system (bar)

$Pvap_{IPA}$: vapour pressure of IPA as Isopropanol in the reaction system (bar)

P_{total}	:	Total pressure inside the reactor (bar)
r_1	:	reaction rate for reaction 1 ($-$)
r_2	:	reaction rate for reaction 2 ($-$)
r_3	:	reaction rate for reaction 3 ($-$)
r_4	:	reaction rate for reaction 4 ($-$)
r_5	:	reaction rate for reaction 5 ($-$)
r_6	:	reaction rate for reaction 6 ($-$)
r_7	:	reaction rate for reaction 7 ($-$)
r_8	:	reaction rate for reaction 8 ($-$)
r_9	:	reaction rate for reaction 9 ($-$)
r_{10}	:	reaction rate for reaction 10 ($-$)
ρ_{IPA}	:	Density of IPA (kg/m^3)
R	:	Ideal gas law constant ($8.205.10^{-5} m^3.atm/mol.K$)
T_{kelvin}	:	Temperature (K)
$\dot{V}_{g,acetone}$	:	Flowrate of gaseous acetone inside the reactor (m^3/s)
$\dot{V}_{g,IPA}$	:	Flowrate of gaseous IPA inside the reactor (m^3/s)
$\dot{V}_{g,N_2}$	:	Flowrate of nitrogen inside the reactor (m^3/s)
$\dot{V}_{g,total}$	:	Flowrate of gas inside the reactor (m^3/s)
V	:	volume total (m^3)
V_g	:	Total gas volume (m^3)
V_l	:	Total liquid volume (m^3)
x	:	coefficient used in formula to calculate P_{vap_j} ($-$) see [148]

C.2 Mass transfer model - batch operation : Equations

Reaction rate of each reaction of the reaction system:

$$r_1 = k_1 [RhL*] [IPA] \quad \text{(C.1)}$$

$$r_2 = k_2 [RhL*H] [Acetone] \quad \text{(C.2)}$$

$$r_3 = k_3 [RhL*H] [Sub] \quad \text{(C.3)}$$

$$r_4 = k_4 [SIM]$$

$$r_5 = k_5 [RhL*H] [Sub] \quad \text{(C.4)}$$

$$r_6 = k_6 [RIM]$$

$$r_7 = k_7 [SIM]$$

$$r_8 = k_8 [RhL*] [S - SubH] \quad \text{(C.5)}$$

$$r_9 = k_9 [RIM] \quad \text{(C.6)}$$

$$r_{10} = k_{10} [RhL*] [R - SubH] \quad \text{(C.7)}$$

Amount of gas leaving the gas phase is constituted of nitrogen, IPA and acetone and is expressed by :

$$\dot{V}_g = \dot{V}_{g,N_2} + \dot{V}_{g,IPA} + \dot{V}_{g,acetone} \qquad \left(m^3/s\right) \quad \text{(C.8)}$$

From Raoult's law

$$\frac{x_{IPA} Pvap_{IPA}}{P_{total}} = \frac{\dot{n_{g,IPA}}}{\dot{n_{total}}} \quad \text{(C.9)}$$

$$\dot{n_{g,total}} = \dot{n_{N_2}} + g, \dot{n_{IPA}} + g, \dot{n_{acetone}} \quad \text{(C.10)}$$

Number of mole of IPA gas is expressed by :

$$\dot{n_{g,IPA}} = \left(\frac{Pvap_{IPA}}{P_{total} - Pvap_{IPA}} \right) \dot{n_{N_2}} \quad \text{(C.11)}$$

Applying the ideal gas law :

$$PV = nRT \tag{C.12}$$

Volume IPA gas is expressed by :

$$\dot{V}_{g,IPA} = \left(\frac{Pvap_{IPA}}{P_{tot} - Pvap_{IPA}}\right)\dot{V}_{g,N_2} \qquad \left(m^3/s\right) \tag{C.13}$$

The amount of IPA present in the gas phase is in equilibrium with the liquid phase, if the steady state is considered, and correspond to the total flowrate of gas through the reaction system and is expressed by :

$$\dot{N}_{IPA,l\rightarrow g} = \dot{V}_{g,total}C_{g(IPA)} \qquad (mol/s) \tag{C.14}$$

The concentration of IPA in the gas phase corresponds to the vapour pressure of IPA in the gas phase following the law of ideal gas and Raoult's law :

$$C_{g(IPA)} = x_{IPA}\frac{Pvap_{IPA}}{R_{kelvin}T} \qquad \left(mol/m^3\right) \tag{C.15}$$

List of equation for mass-transfer of each component [131] :
Equations for the liquid phase :

$$\frac{d\left(V_l C_{l(RhL*)}\right)}{dt} = V_l * \sum_{n=1}^{j} \nu_{j,RhL*} r_{j,RhL*} \qquad \left(mol/m^3\right) \tag{C.16}$$

$$\frac{d\left(V_l C_{l(IPA)}\right)}{dt} = V_l * \sum_{n=1}^{j} \nu_{j,IPA} r_{j,IPA} - \dot{N}_{IPA,l\rightarrow g} \qquad \left(mol/m^3\right) \tag{C.17}$$

$$\frac{d\left(V_l C_{l(RhL*H)}\right)}{dt} = V_l * \sum_{n=1}^{j} \nu_{j,RhL*H} r_{j,RhL*H} \qquad \left(mol/m^3\right) \tag{C.18}$$

$$\frac{d\left(V_l C_{l(Acetone)}\right)}{dt} = (k_l a V)\left(\frac{C_{g(Acetone)}}{K_H} - C_{l(Acetone)}\right) \tag{C.19}$$

$$+V_l * \sum_{n=1}^{j} \nu_{j,Acetone} r_{j,Acetone} \quad \left(mol/m^3\right) \quad \text{(C.20)}$$

$$\frac{d\left(V_l C_{l(Sub)}\right)}{dt} = V_l * \sum_{n=1}^{j} \nu_{j,Sub} r_{j,Sub} \quad \left(mol/m^3\right) \quad \text{(C.21)}$$

$$\frac{d\left(V_l C_{l(SIM)}\right)}{dt} = V_l * \sum_{n=1}^{j} \nu_{j,SIM} r_{j,SIM} \quad \left(mol/m^3\right) \quad \text{(C.22)}$$

$$\frac{d\left(V_l C_{l(RIM)}\right)}{dt} = V_l * \sum_{n=1}^{j} \nu_{j,RhL*} r_{j,RIM} \quad \left(mol/m^3\right) \quad \text{(C.23)}$$

$$\frac{d\left(V_l C_{l(S-SubH)}\right)}{dt} = V_l * \sum_{n=1}^{j} \nu_{j,S-SubH} r_{j,SSubH} \quad \left(mol/m^3\right) \quad \text{(C.24)}$$

$$\frac{d\left(V_l C_{l(R-SubH)}\right)}{dt} = V_l * \sum_{n=1}^{j} \nu_{j,RhL*} r_{j,RSubH} \quad \left(mol/m^3\right) \quad \text{(C.25)}$$

Equations for the gas phase :

$$\frac{d\left(V_g C_{g(RhL*)}\right)}{dt} = 0 \quad \left(mol/m^3\right) \quad \text{(C.26)}$$

$$\frac{d\left(V_g C_{g(IPA)}\right)}{dt} = \dot{N}_{IPA,l\rightarrow g} - \dot{V}_g C_{g(IPA)} \quad \left(mol/m^3\right) \quad \text{(C.27)}$$

$$\frac{d\left(V_g C_{g(RhL*H)}\right)}{dt} = 0 \quad \left(mol/m^3\right) \quad \text{(C.28)}$$

$$\frac{d\left(V_g C_{g(Acetone)}\right)}{dt} = -\left(k_l a V\right)\left(\frac{C_{g(Acetone)}}{K_H} - C_{l(Acetone)}\right) \quad \text{(C.29)}$$

$$-\dot{V}_{g,total} C_{g(Acetone)} \quad \left(mol/m^3\right) \quad \text{(C.30)}$$

$$\frac{d\left(V_g C_{g(Sub)}\right)}{dt} = 0 \quad \left(mol/m^3\right) \quad \text{(C.31)}$$

$$\frac{d\left(V_g C_{g(SIM)}\right)}{dt} = 0 \quad \left(mol/m^3\right) \quad \text{(C.32)}$$

$$\frac{d\left(V_g C_{g(RIM)}\right)}{dt} = 0 \quad \left(mol/m^3\right) \quad \text{(C.33)}$$

$$\frac{d\left(V_g C_{g(S-SubH)}\right)}{dt} = 0 \quad \left(mol/m^3\right) \quad \text{(C.34)}$$

$$\frac{d\left(V_g C_{g(R-SubH)}\right)}{dt} = 0 \qquad \left(mol/m^3\right) \tag{C.35}$$

The volume of liquid IPA removed can be expressed by :

$$\frac{dV_l}{dt} = \dot{N}_{IPA,l\rightarrow g}\frac{MW_{IPA}}{\rho_{IPA}} \qquad \left(m^3/s\right) \tag{C.36}$$

and the volume flowrate of gas IPA removed is expressed by :

$$\dot{V}_{g,IPA_{l\rightarrow g}} = \dot{N}_{IPA,l\rightarrow g}\frac{RT}{P_{total}} \qquad \left(m^3/s\right) \tag{C.37}$$

The vapour pressure of IPA is obtained by [148]:

$$\begin{aligned} Pvap_{IPA} &= \left(e^{\frac{1}{1-x}}\left(-8.17\right)x + \left(-9.43.10^{-2}\right)x^{1.5} + \left(-8.1\right)x^3 + \left(7.85\right)x^6\right) \text{Pcritical} \\ x &= \left(1 - \left(\frac{T_{kelvin}}{508.3}\right)\right) \end{aligned} \tag{C.38}$$

The local volumetric mass transfer coefficient on the bubble surface is expressed by:

$$k_l a = kl * ab \qquad \left(s^{-1}\right) \tag{C.39}$$

The mass transfer coefficient $k_l a$ can be linked to the energy dissipation in the system by:

$$k_l = 0.4 * \left(\frac{\mu}{D}\right)^{\left(-\frac{2}{3}\right)}(\epsilon\mu)^{\left(\frac{1}{4}\right)} \qquad (cm/min) \tag{C.40}$$

The local specific area of bubble is determined by:

$$ab = \frac{6}{db}\,GHup \qquad \left(m^2/m^3\right) \tag{C.41}$$

The Gas hold-up of the reactor is determined by:

$$GHup = \frac{Vg}{V} \qquad (-) \tag{C.42}$$

The total volume of the reactor is:

$$V = V_g + V_l \qquad \left(m^3\right) \tag{C.43}$$

The total volume of the reactor is:

$$x = 1 - \frac{T_{kelvin}}{508.3} \qquad (-) \tag{C.44}$$

Change of volume of gas within the reactor versus time is equal to zero:

$$\frac{dV_g}{dt} = 0 \qquad \left(m^3.s^{-1}\right) \tag{C.45}$$

C.3 List of parameters with fixed values

Reaction constant of each reaction constituting the reaction system

$$k_1 = 78.2 \quad (s^-1) \tag{C.46}$$

$$k_2 = 2423.1 \quad (s^-1) \tag{C.47}$$

$$k_3 = 85740.7 \quad (s^-1) \tag{C.48}$$

$$k_4 = 7988.0 \quad (s^-1) \tag{C.49}$$

$$k_5 = 23695.4 \quad (s^-1) \tag{C.50}$$

$$k_6 = 69.9 \quad (s^-1) \tag{C.51}$$

$$k_7 = 96518.1 \quad (s^-1) \tag{C.52}$$

$$k_8 = 853061.9 \quad (s^-1) \tag{C.53}$$

$$k_9 = 18.5 \quad (s^-1) \tag{C.54}$$

$$k_{10} = 67349.2 \quad (s^-1) \tag{C.55}$$

Diffusivity of gas into liquid :

$$D = 0 \qquad \left(m^2.s^{-1}\right) \tag{C.56}$$

liquid kinetic viscosity :

$$\mu = 1E-3 \qquad \left(cm^2.s^{-1}\right) \tag{C.57}$$

Henry's constant :

$$K_H = 0.0478 \qquad (-) \tag{C.58}$$

C.4 Mass transfer model - batch operation : Degree of freedom

Number of variables : 64

Number of equations : 47 (equations) + 12 (Fixed parameters)

Degree of freedom : 5

D. FAST: MATHEMATICAL FORMULATION

Let's consider the general mathematical model (see [55])

$$Y = F(X) \tag{D.1}$$

where $X = x_i, i = 1, ..., m$ is a vector of model input parameters $Y = y_j, j = 1, ..., n$ is a vector of model outputs and F is an operator acting on X.

The ensemble mean for the model output y_j is given by :

$$< y_j >= \int ... \int y_j (x_1, ..x_m)\ p(x_1, ..., x_m)\ dx_1 ... dx_m \tag{D.2}$$

Where p is the m-dimensional probability density function for X. The central idea of the FAST method is to convert the above integral over the m-dimensional space of input parameters into a one-dimensional integral over a certain search variable s [55, 120]:

$$< y_j >= \lim_{T \to \infty} \frac{1}{2T} \int_{-T}^{T} y [x_1(s), ..., x_m(s)]\, ds \tag{D.3}$$

It is done by assigning a frequency w_i to each input parameters x_i and using the transformation [55, 120]

$$x_i = G_i [\sin(\omega_i s)] \tag{D.4}$$

In our case the following transformation is used, as it was shown to outperforms the transformation used by McRae et al. and Cukier et al. see([170]).

$$x_i = \bar{x_i} \left(1 + \frac{\bar{\nu_i}}{\pi} \arcsin\left(\sin\left(\omega_i\, s + \varphi_i\right)\right) \right) \tag{D.5}$$

and,

$$\bar{\nu_i} = \frac{x_{i_{max}} - x_{i_{min}}}{x_{i_{max}} + x_{imin}} \tag{D.6}$$

with,

x_i : Model input parameter on which the sensitivity analysis is carried out on

$\bar{x_i}$: Mean value of the model input parameter over the interval considered

$\bar{\nu_i}$: nominal value of input parameter

under the assumption that the following conditions are satisfied :

1. The input parameters are assumed to be uncorrelated, i.e. their probability density functions are independent

$$p\left(x_1, ..., x_m\right) = \prod_{i=1}^{m} p_i\left(x_i\right) \tag{D.7}$$

2. The frequency set $\{\omega_i\}$ is incommensurate, i.e.,

$$\sum_{i=1}^{m} \gamma_i \omega_i = 0, \tag{D.8}$$

Where the values γ_i are arbitrary integers;

3. The functions G_i are chosen so that the arc length, ds, is proportional to $p(x_1, ..., x_m)\, dx_i$ for all i

The transformation function (see equation D.5) describes a search curve that samples the parameter space in a manner consistent with the statistics expressed by $p(x_1, ..., x_m)$. Specifying one value of search variable s specifies all values of the parameter $x_1, x_2, ..., x_m$. As s varies from $-\infty$ to $+\infty$ all possible x_i values are obtained via equation D.5.

The parametric curve defined by equation D.5 is termed as the search curve, and s is varied, the curve from equation D.5 traces out a space filling curve in the parameter space. If it were possible to use an incommensurable frequency set, the curve would never close upon itself and would pass arbitrarily close to every point in the parameter space. This result is a consequence of Weyl's theorem. When integer frequencies are used, it is not possible to obtain a truly incommensurate frequency set and the search curves take on the appearance of multi-dimensional Lissajous curves. The use of higher frequencies results in successively longer search curves. Two examples are shown in fig D.1 and D.2. The length of the search curve and the identity of sample points is considerably greater in the second case i.e. example D.2. Practical consideration dictate that an integer rather than an incommensurate frequency set must be used. This introduces two types of error :

- The search curve is no longer space-filling, i.e. it does not pass arbitrarily close to any point in the x-space, see figure D.2
- The fundamental harmonics used to described the set $\{x_i\}$ will have harmonics that interfere with one or another. However, the

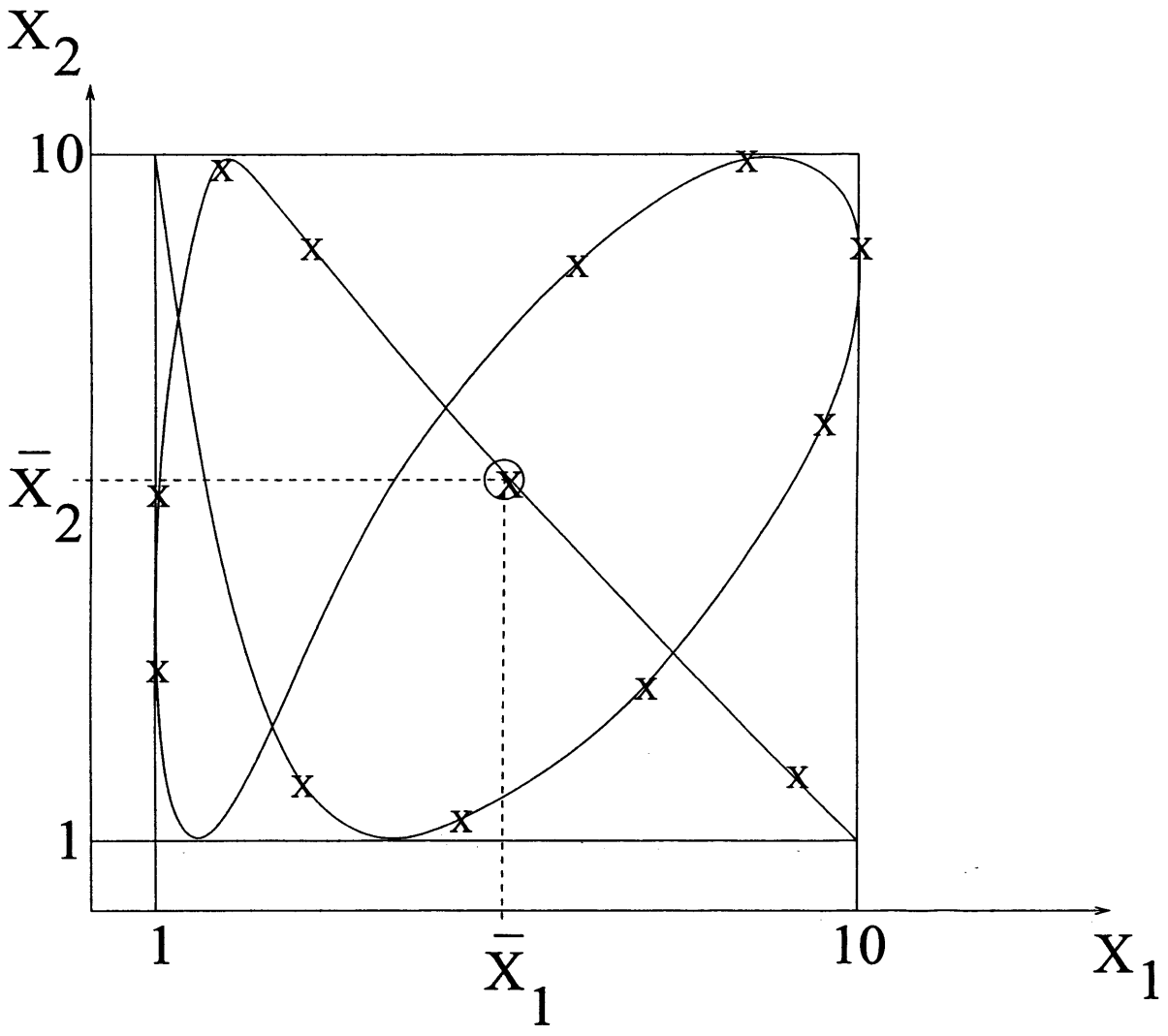

Fig. D.1: Search curve with frequencies $\omega_1 = 3; \omega_2 = 5$

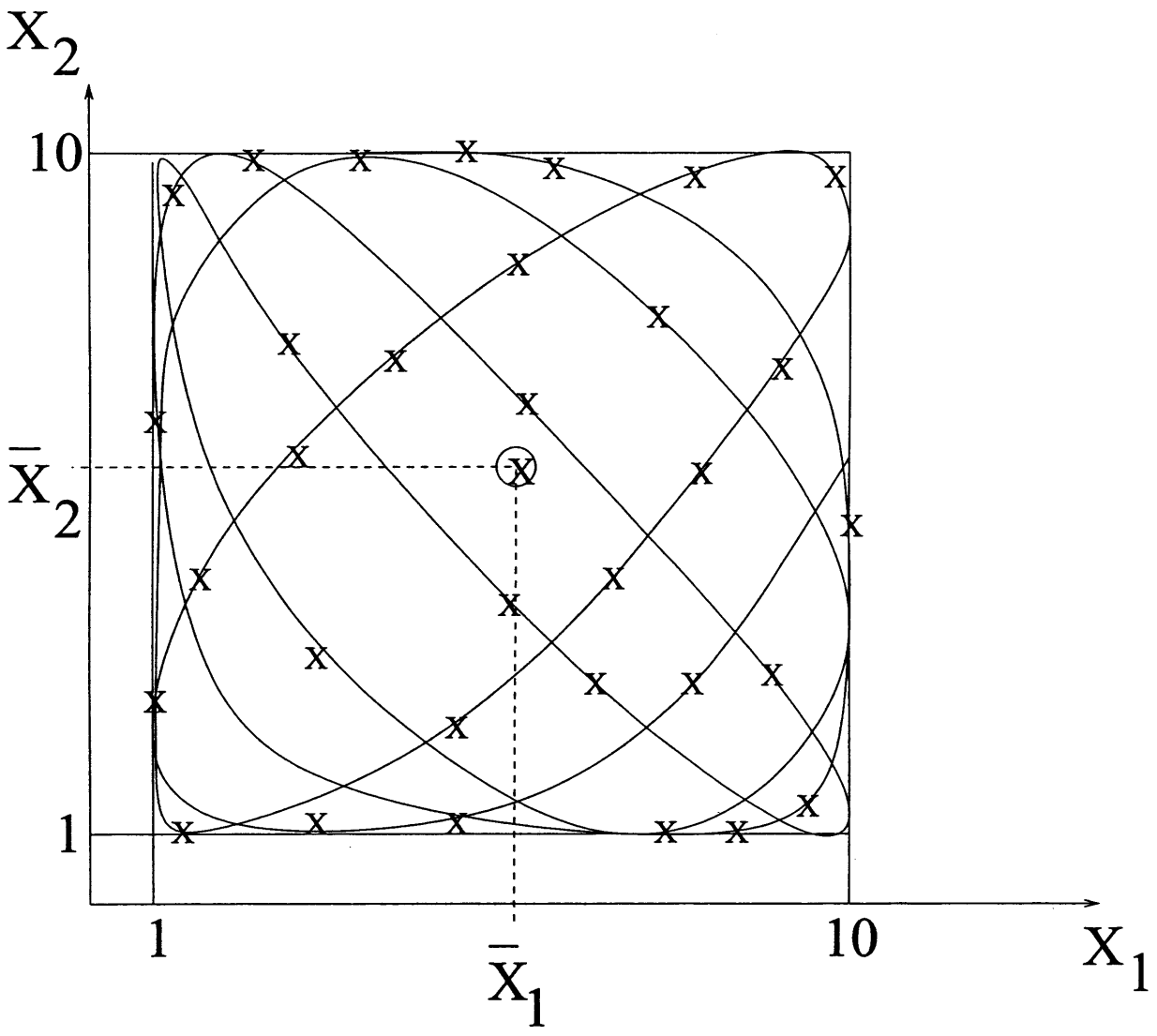

Fig. D.2: Search curve with frequencies $\omega_1 = 11; \omega_2 = 13$

differences between $\bar{x_i}$ and $< x >$ for a well chosen integer frequency set can be made arbitrarily small [174, 56].

These errors resulting in differences between the integrals D.2 and D.3 can be made arbitrarily small by a proper choice of the integer frequency set [55].

The use of integer frequencies in the transformation D.5 implies that the input parameters x_i and in turn the model outputs y_i are periodic in s on the interval $[-\pi, +\pi]$, i.e., $x_i(s) = x_i(s + 2\pi)$ and $y_i(s) = y_i(s + 2\pi)$. The model outputs can thus be Fourier analysed to obtain their Fourier coefficients as follow [120, 52]:

$$A_k^{(j)} = \frac{1}{2\pi} \int_{-\pi}^{\pi} y_j [x_1(s), ..., x_m(s)] \cos(ks)\, ds \quad k = 0, 1, 2, ... \tag{D.9}$$

$$B_k^{(j)} = \frac{1}{2\pi} \int_{-\pi}^{\pi} y_j [x_1(s), ..., x_m(s)] \sin(ks)\, ds \quad k = 0, 1, 2, ... \tag{D.10}$$

The mean value $< y_j >$ and the variance σ_j^2 of the model output y_j can be written in terms of Fourier coefficients according to Parseval's theorem [120]:

$$< y_j >= \sqrt{2\left[A_0^{(j)}\right]} \tag{D.11}$$

$$\sigma_j^2 =< y_j^2 >= 2 \sum_{\substack{k=-\infty \\ k \neq 0}}^{\infty} \left[\left(A_k^{(j)}\right)^2 + \left(B_k^{(j)}\right)^2 \right] \tag{D.12}$$

The total variance does not identify the contributions of the individual parameters to σ_j^2. Also, the *partial variances* are introduced by selecting from all the Fourier coefficients those corresponding to the

fundamental frequency ω_i and its harmonics $p\omega_i (k = p\omega_i, p = 1, 2, ...)$. These coefficients express the contribution of the ith input parameter variation into the total variance $sigma_j^2$ of the model output :

$$-\sigma_{j/i}^2 = 2\sum_{p=1}^{\infty}\left[\left(A_{p\omega_i}^{(j)}\right)^2 + \left(B_{p\omega_i}^{(j)}\right)^2\right] \tag{D.13}$$

The normalised sensitivity measure, the partial variance $S_{j/i}$, is then defined by the ratio of the above variance due to uncertainty of the ith parameter to the total variance :

$$S_{j/i} = \frac{\sigma_{j/i}^2}{\sigma_j^2} \tag{D.14}$$

It is apparent that the sum $\sum_{i=1}^{m} S_{j/i}$ or the partial variances will not equal unity because $\sigma_{j/i}^2$ in the numerator of equation D.14 involves only the sum of the squares of the Fourier coefficients of the fundamental and all harmonics of the ith frequency ω_i. The total variance σ_j^2 can be written as the following sum :

$$\sigma_j^2 = 2\sum_{i=1}^{m}\sigma_{j/i}^2 + \sum_{i=2}^{m}\sum_{l=1}^{i-1}\sigma_{j/il}^2 \sum_{i=3}^{m}\sum_{l=2}^{i-1}\sum_{k=1}^{l-1}\sigma_{j/ilk}^2 + ..., \tag{D.15}$$

where the second and further terms contain increasingly more detailed information about the coupling of sensitivity among larger and larger groups of parameter uncertainties. For example, a part of total variance of the jth model output related to the couple effect of uncertainties in ith and lth parameters can be expressed as the following *coupled partial variance* [120] :

$$S_{j/il} = \frac{\sigma_{j/il}^2}{\sigma_j^2} \tag{D.16}$$

$$S_{j/il} = \frac{2}{\sigma_j^2} \sum_{p=1}^{\infty} \sum_{q=1}^{\infty} \left[\left(A^{(j)}_{p\omega_i + q\omega_l} \right)^2 + \left(B^{(j)}_{p\omega_i + q\omega_l} \right)^2 \right] \quad \text{(D.17)}$$

When coupled partial variances are large, it is difficult to separate the effect of one input parameter from that of the other.

D.0.1 Computer implementation

Application of the FAST method requires the numerical evaluation of the Fourier coefficients (Equations D.9). This in turn requires the model output y_i to be evaluated as the search variable s ranges over $[-\pi; \pi]$. Restricting the frequency set to odd integers reduces the range of s to the interval $[\frac{-\pi}{2}; \frac{\pi}{2}]$ since it is possible to use the symmetry relations for the output functions. The model is solved for r sampling points uniformly spaced along the search curve throughout the range $[\frac{-\pi}{2}; \frac{\pi}{2}]$:

$$s = \frac{\pi}{2} \frac{2l - r - 1}{r}, \quad l = 1, 2, ..., r. \quad \text{(D.18)}$$

Each value of the search variable s is related to the input parameters x_i by the transformation see equation D.5. The Fourier coefficients may be now written in the finite difference form using a numerical quadratic technique [120] :

$$A_k^{(j)} = 0 \quad \text{for k odd,} \quad \text{(D.19)}$$

$$A_k^{(j)} = \frac{1}{2q+1} \left[y_{<j>,0} + \sum_{l=1}^{q} (y_{<j>,l} + y_{<j>,-l}) \cos \frac{\pi k l}{2q+1} \right] \quad \text{for k even,} \quad \text{(D.20)}$$

$$B_k^{(j)} = 0 \quad \text{for k even,} \quad \text{(D.21)}$$

$$B_k^{(j)} = \frac{1}{2q+1} \left[\sum_{l=1}^{q} (y_{<j>,l} + y_{<j>,-l}) \sin \frac{\pi k l}{2q+1} \right] \quad \text{for k odd,} \quad \text{(D.22)}$$

where $y_{<j>}$ replace y_j for notational purposes and the number of sampling point is presented for convenience as :

$$r = 2q + 1 \quad \text{(q - an integer)} \tag{D.23}$$

The number of sampling points r that must be taken can be related to the maximum frequency ω_{max} of the frequency set using the Nyquist criterion :

$$r \geq N\omega_{max} + 1, \tag{D.24}$$

where N is the maximum number of the Fourier coefficients that may be retained in calculating the partial variances without interference between the assigned frequencies [120]. In general, the interference between the higher harmonics will be eliminated when [120]:

$$N < \omega_{min} - 1 \tag{D.25}$$

Larger values of r are numerically desirable for reasons of accuracy, although smaller values are desirable for reasons of computing economy. The minimum value $N = 2$ is usually sufficient in practice because the magnitude of the higher-order terms in the Fourier series tends to decrease rapidly [120].

The final working equations for partial variances and coupled partial variances then become :

$$S_{j/i} = \frac{2}{\sigma_j^2}\left[\left(B_{1\omega_i}^{(j)}\right)^2 + \left(A_{2\omega_i}^{(j)}\right)^2\right], \tag{D.26}$$

$$S_{j/i} = \frac{2}{\sigma_j^2}\left[\left(A^{(j)}_{\omega_i+\omega_l}\right)^2 + \left(A^{(j)}_{2(\omega_i+\omega_l)}\right)^2 + \left(B^{(j)}_{2\omega_i+\omega_l}\right)^2 + \left(B^{(j)}_{\omega_i+2\omega_l}\right)^2\right] \quad \text{(D.27)}$$

The selection of a frequency set is made in accordance with the number of input parameters to be analysed m with the aid of the recursive algorithm described by Cukier et al. [55] :

$$\omega_1 = \Omega_m \quad , \omega_i = \omega_{i-1} + d_{m+1-i} \quad i = 2, ..., m. \quad \text{(D.28)}$$

Values of the coefficients Ω_m and d_m assumed in the present implementation after McRae et al. [120]are listed in table D.1 together with the minimum number of model solutions r required for calculation of partial variances.

The number r determined by condition (D.24) with $N = 2$ depends on the assumed frequency set and strongly grows with the number of input parameters m to be analysed as can be seen in table D.1.

Tab. D.1: Parameters used in calculating frequency sets free of interference to fourth order

Number of input parameters m	Ω_m	d_m	Number of model solutions r
1	0	4	-
2	3	8	15
3	1	6	27
4	5	10	47
5	11	20	79
6	1	22	99
7	17	32	175
8	23	40	251
9	19	38	323
10	25	26	411
11	41	56	495
12	31	62	587
13	23	46	695
14	87	76	915
15	87	96	1027

BIBLIOGRAPHY

[1] L.E.K Achenie and L.T. Biegler. Algorithmic synthesis of chemical reactor networks using mathematical programming. *Industrial & Engineering Chemistry Fundamentals*, 25(4):621–627, Nov 1986.

[2] L.E.K Achenie and L.T. Biegler. A superstructure based approach to chemical reactor network synthesis. *Computers and Chemical Engineering*, 14(1):23–40, Jan 1990.

[3] H.E.A. van den Akken. Coherent structures in multiphase flows. *Powder Technology*, 100(2-3):123–136, Dec 1 1998.

[4] M.H. Al-Dahhan, F. Larachi, M.P. Dudukovic, and A. Laurent. High-pressure trickle bed reactors : a review. *Industrial and Engineering Chemistry Research*, 36(8):3292–3314, Aug 1997.

[5] J. Anderson. A survey of multiobjective optimisation in engineering design. http://www.machine.ikp.liu.se/staff/johan/files/ikp-r-1097.pdf, 2000.

[6] N.G. Anderson. *Practical process research and development.* Academic press, ISBN-0120594757, first edition, 2000.

[7] W. Angst, J.R. Bourne, and R.N. Sharma. Mixing and fast chemical reaction - V. *Chemical Engineering Science*, 37(8):1259–1264, 1982.

[8] W. Angst, J.R.Bourne, and R.N. Sharma. Mixing and fast chemical reaction - IV. *Chemical Engineering Science*, 37(4):585–590, 1982.

[9] W. Angst, J.R.Bourne, and R.N. Sharma. Mixing and fast chemical reaction - VI. extension of the reaction zone. *Chemical Engineering Science*, 38(7):999–1003, 1983.

[10] R. Aris. Studies in optimization-I, the optimum design of adiabatic reactors with several beds. *Chemical Engineering Science*, 8(12):243–252, 1960a.

[11] R. Aris. Studies in optimization-II, the optimum temperature gradients in tubular reactors. *Chemical Engineering Science*, 8(13):18–29, 1960b.

[12] J.H. Atherton and K.J. Carpenter. *Process development physicochemical concepts.* Oxford Science Publications, first edition, 1995.

[13] A. Bakker, A.H. Haidari, and E.M. Marshall. Design reactors via CFD. *Chemical Engineering Progress*, 97(12):30–39, Dec 2001.

[14] A. Bakker, A.H. Haidari, and L.M. Oshinowo. Realize greater benefits from CFD. *Chemical Engineering Progress*, 97(3):45–53, Mar 2001.

[15] S. Balakrishna and L.T. Biegler. A constructive targeting approach for the synthesis of isothermal reactor network. *Industry and Engineering Chemical Research*, 31(1):300–312, Jan 1992.

[16] J. Baldyga. Turbulent mixer model with application to homogeneous instantaneous chemical reactions. *Chemical Engineering Science*, 44(5):1175–1182, 1989.

[17] J. Baldyga and J.R. Bourne. A fluid mechanical approach to turbulent mixing and chemical reaction. *Chemical Engineering Communication*, 29(2):293–305, 1984.

[18] J. Baldyga and J.R. Bourne. Micromixing in inhomogeneous turbulence. *Chemical Engineering Science*, 43(1):107–112, 1988.

[19] J. Baldyga and J.R. Bourne. Simplification of micromixing calculations. *Chemical Engineer Journal and The Biochemical Enginnering Journal*, 42(2):83–101, Nov 1989.

[20] J. Baldyga and J.R. Bourne. Interactions between mixing on various scales in stirred tank reactor. *Chemical Engineering Science*, 47(8):1839, Jun 1992.

[21] J. Baldyga, J.R. Bourne, B.Dubuis, A.W. Etchells, R.V. Gholap, and B. Zimmerman. Jet reactor scale-up for mixing controlled reactions. *Chemical Engineering Research and Design*, 73(A5):497–502, Jul 1995.

[22] J. Baldyga, J.R. Bourne, and R.V. Gholap. The influence of viscosity on mixing in jet reactors. *Chemical Engineering Science*, 50(12):1877–1880, Jun 1995.

[23] J. Baldyga, J.R. Bourne, and S.J. Hearn. Interaction between mixing on various scales. *Chemical Engineering Science*, 52(4):457–466, Feb 1997.

[24] J. Baldyga, J.R. Bourne, and B. Walker. Non-isothermal micromixing in turbulent liquids: theory and experiment. *The Canadian Journal of Chemical Engineering*, 76(3):641–649, Jun 1998.

[25] J. Baldyga, M. Henczka, and L. Makowski. Effect of mixing

on parallel chemical reactions in a continuous-flow stirred-tank reactor. *Chemical Engineering Research and design*, 79(A8):895–900, Nov 2001.

[26] J. Baldyga, A. Rozen, and F. Mostert. A model of laminar micromixing with application to parallel chemical reactions. *Chemical Engineering Journal*, 69(1):7–20, Feb 1998.

[27] H. Bandemer. *Modelling Uncertain Data.* Akademie Verlag, ISBN-3055015789, first edition, 1992.

[28] S. Banerjee, D. Scott, and E. Rhodes. Mass turbulent to falling wavy liquid films in turbulent flow. *Industrial & Engineering Chemistry fundamentals*, 1(10):340–354, October 1968.

[29] A. Barozza, F. Velardi, and M. Fornaroli. Thermochemical scale-up of a mesylation reaction. *Organic Process research and Development*, 7(4):599–608, Jul-Aug 2003.

[30] S. Bartlett. The A to Z of british medicines research. The association of the British Pharmaceutical Industry - ABPI - www.abpi.org.uk, May 2002.

[31] P.I. Barton. *The Modelling and Simulation of Discrete/Continuous Processes.* PhD thesis, University of London, 1992.

[32] R.J. Berger, E.H. Stitt, G.B. Marin, F. Kapteijn, and J.A. Moulijn. Chemical reaction kinetics in practice. *CaTTech*, 5(1):30–60, 2001.

[33] J. Blacker and J. Martin. Development of some large scale catalytic asymetric reactions. *Asymetric Catalysis on Industrial*

Scale: Challenges, approaches and solutions, first(Wiley):201–216, ISBN-3527306315 2004.

[34] D. Blackmond. Riding the reaction. *Chemistry in Britain*, 6(4):65–74, April 2002.

[35] D.G. Blackmond. Kinetic aspects of nonlinear effects in asymmetric catalysis. *ACCOUNTS OF CHEMICAL RESEARCH*, 33(6):402–411, Jun 2000.

[36] G. Boothroyd and P. Dewhurst. Product design for manufacture and assembly. *Manufacturing Engineering*, 100(4):42–46, Apr 1988.

[37] J.R. Bourne. Mixing on the molecular scale (micromixing). *Chemical Engineering Science*, 38(1):5–8, 1983.

[38] J.R. Bourne. Mixing and the selectivity of chemical reactions. *Organic Process Research and Development*, 7(4):471–508, Jul-Aug 2003.

[39] J.R. Bourne and P. Dell'Ava. Micro-mixing and macro-mixing in stirred tank reactors of different sizes. *Chemical Engineering Research and Design*, 65(2):390–394, Jun 1987.

[40] J.R. Bourne and C.P. Hilber. The productivity of micromixing-controlled reactions : effect of feed distribution in stirred tanks. *Chemical Engineering Research and Design*, 68(1):51–56, Jan 1990.

[41] J.R. Bourne and P. Rys. Mixing effect in the bromination of resorcin. *Chemical Engineering Science*, 38(3):54–63, 1977.

[42] D.W.F. Brilman, R. Antink, W.P.M. van Swaaij, and G.F. Versteeg. Experimental study of the effect of bubbles, drops, and

particles on the product distribution for a mixing sensitive, parallel-consecutive reaction system. *Chemical Engineering Science*, 54(13-14):2325–2337, Juk 1999.

[43] A.B. Bulsari and H. Saxen. Implementation of a chemical reactor selection expert system in an artificial neural network. *Engineering Applications of Artificial Intelligence*, 5(2):113–119, Mar 1992.

[44] K.J. Carpenter. Chemical engineering aspects of fine chemicals manufacture. *Chemical Engineering Science*, 56(2):305–322, Jan 2001.

[45] J.E. Carrillo and C. Gaimon. A framework for process change. *IEEE Transactions on Engineering Management*, 49(4):409–427, Nov 2002.

[46] J-C. Charpentier. Mass transfer rates in gas-liquid absorbers and reactors. *Advances in Chemical Engineering*, 11(2):210–228, Feb 1981.

[47] Chemical Industry and US department of Energy. Technology roadmap for computational fluid dynamics. http://www.chemicalvision2020.org/pdfs/compfluid.pdf, January 1999.

[48] J. Chern and F.G. Helfferich. Effective kinetic modelling of multistep homogeneous reactions. *American Institute of Chemical Engineering journal*, 36(8):1200–1208, Aug 1990.

[49] C.A. Coello Coello. A comprehensive survey of evolutionary-based multiobjective optimisation techniques.

http://www.lania.mx/ ccoello/EMOO/EMOObib.html, October 1999.

[50] C.A. Coello Coello. *Evolutionary Algorithm for Solving Multi-objective Problems.* Kluwer Academis Publishers, ISBN-0306467623, first edition, 2002.

[51] G. Cole and B. Bennett. *Pharmaceutical production : an engineering guide.* Institution of Chemical Engineers, ISBN-0852954409, first edition, 2003.

[52] D.C. Collins and R. Avissar. An evaluation with the Fourier Amplitude Sensitivity Test (FAST) of which land surface parameters are os greatest importance in atmospheric modeling. *Journal of climate*, 7(5):1994, May 1994.

[53] S. Corrsin. The isotropic turbulent mixer. part ii. arbitrary schmidt number. *A.I.Ch.E. Journal*, 10(7):56–71, 1964.

[54] R.I. Cukier, C.M. Fortuin, K.E. Shuler, A.G. Petschek, and J.H. Schaibly. Study of the sensitivity of coupled reaction system to uncertainties in rate coefficients. I theory. *The Journal of Chemical Physics*, 8(1):52–73, 1973.

[55] R.I. Cukier, H.B. Levine, and K.E. Shuler. Non-linear sensitivity analysis of multiparameter model systems. *The Journal of Computational Physics*, 26(12):234–247, Nov-Dec 1978.

[56] R.I. Cukier, J.H. Schaibly, and K.E. Shuler. Study of the sensitivity of coupled reaction system to uncertainties in rate coefficients. III analysis of the approximations. *The Journal of Chemical Physics*, 3(4):104–111, 1975.

[57] P.V Danckwerts. *Gas-Liquid reations.* McGraw-Hill, ISBN-007015287, first edition, 1970.

[58] J.T. Davies. The effects of surface films in damping eddies at a free surface of a turbulent liquid. *Proceedings of the Royal Society of London. Series A, Mathematical and Physical Sciences*, 290(6):328–337, 1966.

[59] K. Deb. Nonlinear goal programming using multi-objective genetic algorithms. *Journal of the Operational Research Society*, 52(3):291–302, March 2001.

[60] W-D. Deckwer. *Bubble column reactors.* Wiley, ISBN-0471918113, first edition, 1992.

[61] J.A. Dimasi and R.W. Hansen H.G. Grabowski. The price of innovation: new estimates of drug development costs. *Journal of Health Economics*, 22(2):151–185, Mar 2003.

[62] L.K. Doraiswamy. *Organic Synthesis Engineering.* OXFORD University Press, ISBN-0-19-509689-4, first edition, 2001.

[63] L. Duckstein, A. Goicoechea, and E. Parent. *Applied Mathemathics and Computation - Special issue on multicriterions decision-making with enginnering applications.* Elsevier Science Publishing Co. Inc., ISSN-00963003, first edition, 1993.

[64] J.A. Dyer and K.L. Mulholland. Prevent pollution via better reactor design and operation. *Chemical Engineering Progress*, 94(2):61–66, Feb 1998.

[65] A. Eiben and J.S. Smith. *Introduction to evolutionary computing.* Spinger-Verlag Berlin, ISBN-3540401849, first edition, 2003.

[66] P. Engrand. A multi-objective optimization approach based on simulated annealing and its application to nuclear fueal management. *Proceedinds of ICONE 5 : 5th International Conference On Nuclear Engineering*, Nice(France):416–423, 1997.

[67] J-P Euzen, P. Trambouze, and J-P Wauquier. *Scale-up methodology for chemical processes.* Gulf publishing, ISBN-0884151883, first edition, 1993.

[68] L.-S. Fan, G.Q. Yang, D.J. Lee, K. Tsuchiya, and X.K. Luo. Some aspects of high-pressure phenomena of bubbles in liquid and liquid-solid suspensions. *Chemical Engineering Science*, 54(21):4681–4709, Nov 1999.

[69] D.D. Fontaine, P.L. Havens, G.E. Blau, and P.M. Tillotson. The role of sensitivity analysis in groundwater risk modeling for pesticides. *Weed Technology*, 6(3):716–724, Jul-Sep 1992.

[70] Foods and Drugs Administration. Guidelines on general principles of process validation. http://www.fda.gov/cder/guidance/pv.htm, September 2003.

[71] R.O. Fox. Computational methods for turbulent reacting flows in the chemical process industry. *Revue de l'institut Francais du petrole*, 51(2):215–243, Mar-Apr 1996.

[72] E.S. Fraga and A. Žilinskas. Experience with hybrid evolutionary/local optimization for process design. In I.C. Parmee, editor, *Adaptive Computing in Design and Manufacture V*, pages 53–64. Springer-Verlag, 2002.

[73] E.S. Gaddis. Mass tansfer in gas-liquid contactors. *Chemical engineering and processing*, 38(4-6):503–510, Sep 1999.

[74] D. Gerwin. A theory of innovation processes for computer-aided manufacturing technology. *IEEE Transactions on Engineering Management*, 35(2):90–100, May 1988.

[75] L.P.P.P. van Ginneken and R.H.J.M. Otten. *The annealing algorithm.* Kluwer Academic Publishers, ISBN-0792390229, first edition, 1989.

[76] D. Glasser, D. Hildebrandt, and C. Crowe. A geometric approach to steady flow reactors: The attainable region and optimization in concentration space. *Industrial and Engineering Chemistry Research*, 26(9):1803–1810, Sep 1987.

[77] D. Glasser, D. Hildebrandt, and C. Crowe. Geometry of the attainable region generated by reaction and mixing - with and without constraint. *Industrial and Engineering Chemistry Research*, 29(1):49–58, Jan 1990.

[78] A. Goicoechea, D.R. Hansen, and L. Duckstein. *Multiobjective decision analysis with engineering and business applications.* John Wiley and Sons, ISBN-0471064017, first edition, 1982.

[79] D. Goldberg. *Genetic Algorithms in search, Optimisation and Machine Learning.* Addison-Wesley Reading MA, ISBN-0201157675, first edition, 1995.

[80] A. Green. *3rd International Conference on Process intensification for the chemical industry.* BHR group Conference Series, ISBN-186058215, first edition, 1999.

[81] P.J. Hanratty and B. Joseph. Decision-making in chemical engineering and expert sustem : Application of the analytic hierarchy

process to reactor slection. *Computers and Chemical engineering*, 16(9):849–860, Sep 1992.

[82] P.J. Hanratty, B. Joseph, and M.P. Dudukovic. Knowledge representation and reasoning in the presence of uncertainty in an expert system for laboratory reactor selection. *Industrial and Engineering Chemistry Research*, 31(1):228–238, Jan 1992.

[83] G.J. Harmsen and A.P. Hinderink. *We want less: process intensification by process synthesis methods / 3rd International Conference on Process Intensification for the Chemical Indusrty.* BHR Group Conference Series, ISBN-186058215, first edition, 1999.

[84] C.K. Harris, D. Roekaerts, F.J.J. Rosendal, F.G.J. Buitendijk, Ph. Daskopoulos, A.J.N. Vreenegoor, and H. Wang. Computational fluid dynamics for chemical reactor engineering. *Industrial Engineering Science*, 51(10):1569–1594, May 1996.

[85] F.G. Helfferich. Systematic approach to elucidation of multistep reaction network. *Journal of Physical Chemistry*, 93(18):6676–6681, Sep 7 1989.

[86] K.B. Hendricks and V.R. Singhal. Delays in new product introductions and the market value of the firms: The consequences of being late to the market. *Management Science*, 43(4):422–436, Apr 1997.

[87] S. Higgins. Comment. *Chemistry in Britain*, 11(October):1, 10 2003.

[88] R. Hooke and T.A. Jeeves. 'direct search' solution of numerical and statistical problem. *ACM - Association for Computing Machinery*, 8(2):46–56, 1961.

[89] J.R. Hopper. Pollution prevention through reactor design. *Industrial pollution prevention handbook*, 1995.

[90] M.D. Huang, F. Romeo, and A. Sangiovanni-Vincentelli. An efficient general cooling schedule for simulated annealing. *IEEE International Conference of Computer Aided Design, Santa Xlara, California, pp. 381-384*, pages 617–632, 1986.

[91] M. Iansiti. From technological potential to product performance: an empirical analysis. *Research Policy*, 26(3):345–365, Oct 1997.

[92] ISPE. ISPE baseline pharmaceutical engineering guides. http://www.ispe.org/guides8.html, June 2001.

[93] R. Jacobs and W. Jansweijer. A knowledge-based system for reactor selection. *Computers and Chemical Engineering*, 24(8):1781–1801, Sep 1 2000.

[94] D.F. Jones and M. Tamiz S.K. Mirrazavi. Multi-objective meta-heuristics : An overview of the current state-of-the-art. *European Journal of Operational Research*, 137(1):1–9, Feb 16 2002.

[95] F. Kastanek, J. Zahradnik, J. Kratochvil, J. Cermak, and D.H. Sharp(Translator). *Chemical reactors for gas-liquid systems.* Ellis Horwood series in Chemical Engineering, ISBN-0131273906, first edition, 1992.

[96] V.L. Kelkar and K.M. Ng. Screening multiphase reactors for non-isothermal multiple reactions. *American Institute of Chemical Engineering*, 46(2):389–406, Feb 2000.

[97] C.T. Kelley. *Iterative methods for optimization.* SIAM - Society for Industrial and Applied Mathematics, ISBN-0898714338, first edition, 1999.

[98] E.H. Kessler. Tightening the belt: methods for reducing development costs associated with new product innovation. *Journal of engineering and technology management*, 17(1):59–92, Mar 2000.

[99] E.H. Kessler and P.E. Bierly. Is faster really better ? an empirical test of the implications of innovation speed. *IEEE Transactions on Engineering Management*, 49(1):2–12, Feb 2002.

[100] E.H. Kessler and A.K. Chakrabarti. Speeding up the pace of new product development. *Journal of Product Innovation Management*, 16(3):231–247, May 1999.

[101] K.E. Kinnear Jr. Generality and difficulty in genetic programming: Evolving a sort. *Proceedings of the 5th International Conference on Genetic Algorithms*, 5:345–357, 1993.

[102] S. Kirkpatrick, C.D. Gelatt, and M.P. Vecchi. Optimisation by simulated annealing. *Science*, 220(4598):671–680, 2001.

[103] A.C. Kokossis and C.C. Floudas. Optimisation of complex reactor networks - I-isothermal operation. *Chemical Engineering Science*, 45(3):595–614, 1990.

[104] A.C. Kokossis and C.C. Floudas. Optimisation of complex reactor networks - II-non-isothermal operation. *Chemical Engineering Science*, 49(7):1037–1051, Apr 1990.

[105] N. Kunzle, JW. Soler, and Baiker A. Continuous enantioselectivity hydrogenation in fixed-bed reactor: towards process intensification. *Catalysis today*, 79(1-4):503–509, Apr 30 2003.

[106] P.J.M. Laarhoven and E.H.L. Aart. *Simulated Annealing : Theory and Application.* Kluwer Academic Publishers, ISBN-9027725136, first edition, 1987.

[107] Y.G. Lai and R.M.C. So. Near-wall modeling of turbulent heat fluxes. *International journal of heat and mass transfer*, 33(7):1429–1440, Jul 1990.

[108] Y.G. Lai and R.M.C. So. On near-wall turbulent-flow modeling. *Journal of fluid mechanics*, 221:641–673, Dec 1990.

[109] A. Lakshamanan and L.T. Biegler. Synthesis of optimal chemical reactor network. *Industry and Enginnering Chemistry Research*, 35(4):1344–1353, Apr 1996.

[110] J.C. Lamont and D.S. Scott. An eddy cell model of mass transfer into the surface of a turbulent liquid. *American Institute of Chemical Engineering*, 4(3):314–324, March 1970.

[111] S. Lee and G. Robinson. *Process development - Fine chemicals from grams to kilograms.* Oxford Science Publications, first edition, 1995.

[112] S. Lee and Y.P. Tsui. Succeed at gas/liquid contacting. *Chemical Engineering Progress*, 95(7):23–49, Jul 1999.

[113] M. Lesieur. *Turbulence in Fluids: stochastic and numerical modeling.* Kluwer Academic Publishers, first edition, 1990.

[114] M. Levin. *Pharmaceutical process scale-up.* Drugs and the pharmaceutical sciences, ISBN-0824706250, volume 118 edition, 2002.

[115] D.M. Levins and J.R. Glastonbury. Application of kolmogoroff's theory to particle-liquid mass transfer in agitated vessels. *Chemical Engineering Science*, 27(11):137–148, Nov 1972.

[116] S-Y. Li, M-Y. Wu, and J. Zhu. A practical simulated anneàling program and its application to quantitative cbed pattern matching. *Ultramiscroscopy*, 83(1-2):103–109, May 2000.

[117] P. Linke and A.C. Kokossis. On the robust application of stochastic optimisation technology for the synthesis of reaction/separation systems. *Computers and Chemical Engineering*, 27(5):733–758, May 2003.

[118] Y.C. Lu and S.Mohanty. Sensitivity analysis of complex, proposed geologic waste disposal system using the fourier amplitude test method. *Reliability Engineering and System Safety*, 72(3):275–291, Jun 2001.

[119] K.I.M. McKinnon. Convergence of the nelder-mead simplex method to a non stationary point. *SIAM Journal on optimisation*, 9(1):148–158, Dec 1999.

[120] G.J. McRae, J.W. Tilden, and J.H. Seinfeld. Global sensitivity analysis - a computational implementation of the Fourier Amplitude Sensitivity Test (FAST). *Computers & Chemical Engineering*, 6(1):15–25 1982, 1982.

[121] V.L. Mehta and A. Kokossis. New generation toll for multiphase reaction system : a validated systematique methodology for novelty and design automation. *Computers and Chemical Engineering*, 22(Suppl.):S119–S126, Suppl. S 1998.

[122] V.L. Mehta and A.C. Kokossis. Non-isothermal synthesis of homogeneous and multiphase reactor networks. *American Institute of Chemical Engineering*, 46(11):2256–2273, Nov 2000.

[123] A. Mersmann. Gas-liquid reactors. *Internatinal Chemical Engineering*, 3(3):45–78, 1991.

[124] N. Metropolis, A. Rosenbluth, A. Teller, and E. Teller. Equation

of state calculations by fast computing machines. *Journal of Chemical Physics*, 1953.

[125] K.M. Miettinen. *Non-linear Multiobjective Optimization.* Kluwer International series, ISBN-0792382781, first edition, 1999.

[126] T. Minahan. Attack cost at its roots. *Purchasing*, 3(7):45–53, Jul 1997.

[127] D. Mitra, F. Romeo, and A. Sangiovanni-Vincentelli. Convergence and finite-time behavior of simulated annealing. *Advances in Applied Probability*, 18(3):747–771, Sep 1986.

[128] S. Nagata. *Mixing : principles and applications.* Wiley, first edition, 1975.

[129] O. Nagel, B. Hegner, and H. Kurten. Criteria for the selection and design of gas/liquid reactors. *International Chemical Engineering*, 21(8):203–215, Jun 1981.

[130] D. Nardin. Trends and opportunities with modern buss loop reactor technology. *Chemspec Europe 95 BACS Symposium*, pages 87–92, 1995.

[131] E.B. Nauman. *Chemical reactor design, optimization, and scale-up.* McGraw-Hill Professional Engineering, ISBN-0071377530, first edition, 2002.

[132] J.A. Nelder and R. Mead. A simplex method for function minimisation. *Computer Journal*, 7(9):34–44, August 1965.

[133] R. Nelson. The role of knowledge in R&D efficiency. *Quaterly journal of economics*, 8(3):345–356, 1982.

[134] D.Y.C. Ng and D.W.T Rippin. The effect of incomplete mixing on

conversion in homogeneous reactions. *Proceedings of Third Symposium on Chemical Reaction Engineering*, 6(1):212–225, 1965.

[135] R. Noyori and S. Hashigushi. Asymetric transfer hydrogenation catalyzed by chiral ruthenium complexes. *Accounts of Chemical Research*, 37(2):79–85, Nov 1997.

[136] E. Otto. Productivity improvement : from a multipurpose to a single-product unit and from batch to continous production. *Chimia*, 54(12):721–723, 2000.

[137] P. Oxley, C. Brechtelsbauer, F. Ricard, N. Lewis, and C. Ramshaw. Evaluation of spinning disk reactor technology for the manufacture of pharmaceuticals. *Industrial & Engineering Chemistry Research*, 39(7):2175–2182, Jul 2000.

[138] L. Painton and U. Diwekar. Synthesizing optimal design configurations for a brayton cycle power plant. *Computers in Chemical Engineering*, 18(5):369–381, May 1994.

[139] L. Painton and U. Diwekar. Stochastic annealing for synthesis under uncertainty. *European Journal of Operational Research*, 83(3):489–502, Jun 22 1995.

[140] C.C. Pantelides. An advanced tool for process modelling, simulation and optimisation. Presented at CHEMPUTERS EUROPE III, frankfurt, October 2002.

[141] S.R. Patil and H.C. Frey. Identification and review of sensitivity analysis methods. Proceedings of workshop on Sensitivity Analysis Methods - Department of Civil Engineering, North Carolina State University, 2001. http://www.ce.ncsu.edu/risk/abstracts/frey.html.

[142] E.L. Paul and F.J. Muzzio. Mixing as a tool for pollution prevention in reactive system. *Industrial pollution prevention handbook*, 1995.

[143] C.J. Pereira. Environmentally friendly processes. *Chemical Engineering Science*, 54(13-14):1959–1973, Jul 1999.

[144] R.H. Perry and D.W. Green. *Perry's Chemical Engineering Handbook.* McGraw-Hill, ISBN-0071159827, seventh edition, 1998.

[145] Author's personal notes. Course on the development of pharmaceutical products by: GlaxoSmithkline, AstraZenecca, Pfizer & Celltech. Liverpool University - Department of Chemistry - Professor Stanley Roberts, February 2001.

[146] G.P. Pisano. Learning before doing in the development of new process technology. *Research Policy*, 25(7):1097–1119, Oct 1996.

[147] G.P. Pisano. *The development factory.* Harvard Business School Press - Boston Massachusetts, ISBN-087584-650-5, first edition, 1997.

[148] B. Poling, J.M. Prausnitz, and J.P. O'Connell. *The properties of gases and liquids.* McGraw-Hill education, ISBN-0070116822, fifth edition, 2000.

[149] S.B. Pope. Lagrangian pdf methods for turbulent flow. *Annual review of fluid mechanics*, 26:23–63, 1994.

[150] E. Poupaert and Y. Deville. Simulated annealing with estimated temparature. *AI Communications*, 13(1):19–26, 2000.

[151] B.D. Prasher. Gas absorption into a turbulent liquid. *Chemical Engineering Science*, 28(6):65–78, 1973.

[152] B.D. Prasher and A.L. Fricke. Mass transfer at a free gas-liquid interface in turbulent thin films. *Industrial & Engineering Chemistry Process Design and Development*, 4(12):156–172, 1974.

[153] B.D. Prasher and G.B. Wills. Mass transfer in an agitated vessel. *Industrial & Engineering Chemistry Process Design and Development*, 3(5):146–161, May 1973.

[154] B.D. Prasher and G.B. Wills. Mass transfer in an agitated vessel. *Industrial & Engineering Chemistry Process Design and Development*, 3(3):178–189, 1973.

[155] H. Rabitz, M. Kramer, and D. Dacol. Sensitivity analysis in chemical kinetics. *Annual review of physical chemistry*, 34:419–461, 1983.

[156] V.V. Ranade. Computational fluid dynamics for reactor engineering. *Reviews in Chemical engineering*, 11(3):229–289, 1995.

[157] V.V. Ranade and J.B. Joshi. Computational fluid dynamics for designing process equipment : Expectations, current status and path forward. *Industrial Engineering and Chemistry Research*, 46(6):1115–1128, Mar 2003.

[158] C. Reeves. *Modern Heuristic Techniques for Combinatorial Problems.* McGraw-Hill, ISBN-0077092392, first edition, 1995.

[159] F. Reif. *Fundamentals of Statistical and Thermal Physics.* Harvard Business School Press - Boston Massachusetts, ISBN-0070518009, first edition, 1965.

[160] O. Repič. *Principles of process research and chemical development in the pharmaceutical industry.* Wiley-Interscience, ISBN-0471165166, first edition, 1998.

[161] A. Roessler and P. Rys. Selectivity of mixture masked reactions - contact sensitivity determines product distribution. *Chemie in unserer zeit*, 35(5):314–323, Oct 2001.

[162] W.C. Rooney and L.T. Biegler. Incorporation joint confidence regions into design under uncertainty. *Computers & Chemical Engineering*, 23(10):1563–1575, Dec 1999.

[163] W.C. Rooney and L.T. Biegler. Optimal process design with parameter uncertainty and process variability. *American Institute of Chemical Engineering*, 49(2):438–449, Feb 2003.

[164] R.F. Rosensweig. Idealised theory for turbulent mixing in vessels. *A.I.Ch.E. Journal*, 10(9):89–102, 1964.

[165] JM. Rousseaux, L. Falk, H. Muhr, and E. Plasari. Micromixing efficiency of a novel sliding-surface mixing device. *American Institute of Chemical Engineers*, 45(10):1999, Oct 1999.

[166] R.A Rutenbar. Simulated annealing algorithms : An overview. *IEEE circuits and devices magazine*, 5(1):19–26, Jan 1989.

[167] T.L. Saaty. *The analytic hierarchy process.* RWS publication, ISBN-0962031720, second edition, 1990.

[168] A. Saltelli and R. Bolado. An alternative way to compute Fourier Amplitude Sensitivity Test (FAST). *Computational Statistics and Data Analysis*, 26(4):445–460, Feb 6 1998.

[169] A. Saltelli, K. Chan, and E.M. Scott. *Sensitivity Analysis.* Wi-

ley series in Probability and Statistics, ISBN-0471998923, first edition, 2000.

[170] A. Saltelli, S. Tarantola, and K.P-S. Chan. A quantitative model-independent method for global sensitivity analysis of model output. *Technometrics*, 41(1):39–56, Feb 1999.

[171] K.D. Samant and K.M. Ng. Development of liquid-phase agitated reactors : synthesis, simulation and scale-up. *American Institute of Chemical Engineers*, 45(11):2371–2391, Nov 1999.

[172] F.M. Santos. The coevolution of firms and their knowledge environment: Insights from the pharmaceutical industry. *Technological Forecasting & Social Change*, 70(7):687–715, Sep 2003.

[173] A. Satelli, S. Tarantola, and F. Campolongo. Sensitivity analysis as an ingredient of modelling. *Statistical Science*, 15(4):377–395, Nov 2000.

[174] J.H. Schaibly and K.E. Shuler. Study of the sensitivity of coupled reaction system to uncertainties in rate coefficients. II. *The Journal of Chemical Physics*, 8(1):84–98, 1973.

[175] G. Schembecker, T. Droge, U. Westhaus, and K. Simrock. Readpert - development, selection and design of chemical reactors. *Computers and Chemical Engineering*, 34(3):317–322, Jun 1995.

[176] P. Sharratt. Environmental criteria in design. *Computers and Chemical Engineering*, 23(10):1469–1475, Dec 1999.

[177] Claudia Martins da Silva and Evaristo Chalbaud Biscaia, Jr. Multi-objective dynamic optimization of semi-batch polymerization processes. *Macromolecular symposia*, 45(1):231–245, May 2004.

[178] D. Singh, K.D. Samant, and KM Ng. Design of homogeneous biphasic catalytic processes. *American Institute of Chemical Engineering journal*, 48(9):1991–2005, Sep 2002.

[179] I.M. Sobol. Quasi-monte-carlo methods. *Progress in Nuclear Energy*, 24(1-3):55–61, 1990.

[180] I.M. Sobol. Sensitivity analysis for non-linear mathematical models. *Mathematical Modeling & Computational Experiment*, 1(1):178–192, 1993.

[181] G. Stalk. Time - the next source of competitive advantage. *Harvard Business Review*, 66(4):41–51, Jul-Aug 1988.

[182] M.A. Steffens, E.S. Fraga, and I.D.L. Bogle. Multicriteria process synthesis for generating sustainable and economic bioprocesses. *Computers & Chemical Engineering*, 23(10):1455–1467, Dec 1 1999.

[183] F. Stoessel and O. Ubrich. Safety assessment and optimization of semi-batch reactions by calorimetry. *Journal of Thermal Analysis and Calorimetry*, 64(1):61–74, 2001.

[184] J. Stonebraker. How bayer makes decisions to develop new drugs. *Interphase*, 6, 200.

[185] X. Sun, G. Manos, J. Blacker, J. Martin, and A. Gavriilidis. Asymetric transfer hydrogenation of acetophenone with 1r,2s-aminoindanol/pentamethylcyclopentadienylrhodium catalyst. *Organic process research & development*, 8(6):909–914, Nov-Dec 2004.

[186] S. Sundaresan. Modeling the hydrodynamics of multiphase flow

reactors : Current status and challenges. *American Institute of Chemical Engineering*, 46(6):1102–1105, Jun 2000.

[187] A. Suppapitnarm, K.A. Seffen, G.T. Parks, and P.J. Clarkson. A simulated algorithm for multiobjective optimization. *Engineering Optimization*, 33(1):59–85, 2000.

[188] S. Tarantola, A. Saltelli, and K. Chan. Sensitivity analysis of model ouput : Variance-based methods make the difference. In *Proceeding of the 1997 Winter Simulation Conference*, 1997.

[189] G.B. Tatterson. *Scale-up and design of industrial mixing processes.* McGraw-Hill, ISBN-0070629390, first edition, 1994.

[190] G.B. Tatterson. Success in multiphase mixing. *Chemical Processing*, 10(4):56–61, Apr 1999.

[191] D. Thoenes. *Chemical Reactor Development : from laboratory synthesis to industrial production.* Kluwer Academic Publisher, ISBN-07923302770, first edition, 1994.

[192] S.H. Thomke. Modes of experimentation: an innovation process - and competitive - variable. *Research Policy*, 27(3):315–332, Jul 1998.

[193] M. Thompson. Application of multi objective evolutionary algorithms to analogue filter tuning. *Evolutionary Multicriterion Optimisazion, Procedings, Lecture Notes in Computer Science*, 1993(3):546–559, 2001.

[194] H. Tominaga and M. Tamaki. *Chemical Reaction and Reactor Design.* John Wiley and Sons, Ltd, ISBN-0471977926, first edition, 1997.

[195] V. Torczon. *Multi-Directional search : A direct search algorithm for parallel machines.* PhD thesis, Department of Mathematical Science, Rice University, Houston, Texas, May 1989.

[196] V. Torczon. On the convergence of pattern search algorithms. *SIAM Journal on Optimisation*, 7(1):1–25, Feb 1997.

[197] K.T. Ulrich and S.D. Eppinger. *Product design and development.* McGraw-Hill Higher Education, ISBN-007229647, second edition, 2000.

[198] E.L. Ulungu, J. Teghem, P.H. Fortemps, and D. Tuyttens. MOSA method : A tool for solving multiobjective conbinatorial problem. *Journal of Multicriteria Decision Analysis*, 8(2):23–45, 1999.

[199] A. Varma, M. Morbidelli, and H. Wu. *Parametric Sensitivity in Chemical Systems.* Cambridge series in Chemical Engineering, ISBN-0521621712, first edition, 1999.

[200] E.S. Venkataramani, F. Vaidya, W. Olsen, and S.C. Wittmer. Create drugs, not waste. *Chemtech*, 22(11):674–679, Nov 1992.

[201] E.S. Venkatarami. Pollution prevention in the pharmaceutical industry. *Industrial pollution prevention handbook*, 1995.

[202] J. Villermaux. Mixing effects on complex chemical reactions in a stirred reactor. *Reviews in Chemical Engineering*, 7(1):51–108, 1991.

[203] J. Villermaux. The role of energy dissipation in contacting and mixing devices. *Chemical Engineering Technology*, 11(7):45–57, Jul 1998.

[204] J. Villermaux and L. Falk. A generalised mixing model for ini-

tial contacting of reactive fluids. *Chemical Engineering Science*, 49(24B):5127–5140, 1994.

[205] J. Villermaux and L. Falk. Recent advances in modelling micromixing and chemical reaction. *Revue de l'institut Francais du petrole*, 51(2):205–213, Mar-Apr 1996.

[206] A. Wheeler. Reaction rates and selectivity in catalysts pores. *Advances in Catalysis*, 3(7):75–82, 1951.

[207] S.R. White. Concepts of scale in simulated annealing. *American Institute Proceedings*, 122:245–286, 1984.

[208] H.A.K Whitney. The more pharmacy changes, the more it remains the same. *Drug intelligence & clinical pharmacy*, 22(10):797–797, Oct 1988.

[209] H. Wiederkehr. Examples of process improvements in the fine chemicals industry. *Chemical Engineering Science*, 43(8):1783–1791, 1988.

[210] J.H. Worstell. Succeed at reactor scale-up. *Chemical Engineering Progress*, 96(6):55–60, Jun 2000.

[211] M.H. Wright. Direct search methods : once scorned, now respectable. *Numerical analysis*, 1995.

[212] Y. Yang and L. Shi. Integrating environmental impact minimization into conceptual chemical process design - a process systems engineering review. *Computers & Chemical Engineering*, 24(2-7):1409–1419, Jul 15 2000.

[213] J.G. Yates. Effects of temperature and pressure on gas-solid fluidization. *Chemical Engineering Science*, 51(2):167–205, Jan 1996.

[214] A.K.Y. Yee, A.K. Ray, and G.P. Rangaia. Multiobjective optimisation of an industrial styrene reactor. *Computers & Chemical Engineering*, 27(1):111–130, Jan 15 2003.

[215] J. Zhang and R. Smith. Design and optimisation of batch and semi-batch reactors. *Chemical Engineering Science*, 59(2):459–478, Jan 2004.